

This file is part of the following work:

Schlaefer, Jodie Anne (2020) *Determining the population structures of cubozoan jellyfishes with biophysical modelling*. PhD Thesis, James Cook University.

Access to this file is available from:

<https://doi.org/10.25903/8mz3%2D7n45>

Copyright © 2020 Jodie Anne Schlaefer.

The author has certified to JCU that they have made a reasonable effort to gain permission and acknowledge the owners of any third party copyright material included in this document. If you believe that this is not the case, please email

researchonline@jcu.edu.au

Determining the population structures of cubozoan jellyfishes with biophysical modelling

Thesis submitted by
Jodie Anne Schlaefer
B. Sc. (Hons.) James Cook University

in March 2020

For the degree of Doctor of Philosophy
in the College of Science and Engineering
James Cook University
Townsville, Queensland, Australia



Acknowledgements

A lot of people have helped me during my PhD candidature. I am so grateful for the guidance and encouragement that I received from my supervisors Mike Kingsford and Eric Wolanski. I appreciate that you always found time to give me feedback and advice. To Mike, thank you for helping me see the forest through the trees. Eric, thank you for ensuring that I kept the physics in mind.

I am thankful for the financial support of the Australian Lions Foundation, James Cook University, the ARC Centre of Excellence for Coral Reef Studies, TropWATER and the Estuarine and Coastal Sciences Association.

My PhD research involved numerous field trips to collect both data and jellyfish. A special thank you to Mark O'Callaghan for teaching me the logistics of field work at James Cook University, and for your willingness to help when things did not go to plan. Mike and Mark are excellent boat drivers, thank you both for your hard work during the hot days at Weipa and the many late nights spent jellyfishing at Magnetic Island. I would also like to thank Queensland Boating and Fisheries Patrol for letting us work out of their boat shed at Evans Landing, Weipa. I greatly appreciate the numerous volunteers who gave up their time to help with the Magnetic Island trips. Additionally, I would like to thank Ben Lawes, Simon Wever and Andrew Thompson for their help in setting up and running the jellyfish lab at MARFU where I ran experiments with the jellyfish we brought back from Magnetic Island.

My PhD also involved a lot of biophysical modelling. I am grateful to Eric for his tutelage in the application of the biophysical model used in Chapter 2. I am indebted to the immensely talented Jonathan Lambrechts. Jonathan got the SLIM model, which I used in Chapter 4, working during a visit to James Cook University. His help was instrumental because progress on setting up the model had stalled prior to his visit.

I really appreciated the kindness of Shreya Yadav who trusted me with her unpublished data on the swim speeds of box jellyfish. The data made a significant contribution to Chapter 3 and informed the modelling in Chapter 4. Likewise, I appreciate the generosity of Steve Lewis who gave me access to his current meter data. His data invaluablely allowed me to confidently validate the currents simulated in Chapter 4.

Thank you to the past and present members of the Reef Ocean and Ecology Lab. I would particularly like to thank Chris Mooney for his advice on working with jellyfish, Tiffany Sih for her encouragement during the early stages of my PhD and my compatriot Ky Hartog-Burnett.

During my candidature, I worked as a tutor and research assistant at James Cook University to help support myself financially. While working in these roles, I was lucky enough to be mentored by Orpha Bellwood, Alana Grech and Severine Choukroun.

I thank my friends in Townsville and further afield for their humour and support. I would especially like to acknowledge my fellow post-graduate students Vanessa Haller-Bull and Sivee Chawla.

Finally, I would like to say a big thank you to my family in Canberra and Townsville. Mum, Dad, David and Jason, I knew encouragement was only a phone call away. Patting Lizzie dog was always therapeutic, even when she pushed me off the couch. To my teammate and beautiful partner Laura, thank you for making me laugh when I was stressed. I am so grateful for your comfort and understanding and I am very much looking forward to spending weekends with you again.

Statement of the Contribution of Others

SUPERVISION AND EDITORIAL SUPPORT

Professor Michael Kingsford (primary supervisor), James Cook University (JCU)

Professor Eric Wolanski (secondary supervisor), JCU

FINANCIAL SUPPORT

Australian Postgraduate Award

Australian Lions Foundation – research grant

JCU – ER Walker Bequest Bursary

JCU Graduate Research School – research funding

Estuarine & Coastal Sciences Association – Charles Boyden Award

The Centre for Tropical Water and Aquatic Ecosystem Research (TropWATER) – conference travel grant

ARC Centre of Excellence for Coral Reef Studies – symposium travel allocations

RESEARCH ASSISTANCE

Professor Michael Kingsford, JCU

Professor Eric Wolanski, JCU

Mr Mark O’Callaghan, JCU

Dr Jonathan Lambrechts, Université catholique de Louvain

FACILITIES

Queensland Boating and Fisheries Patrol, Evans Landing, Weipa

Marine and Aquaculture Research Facilities Unit (MARFU), JCU

DATA CONTRIBUTION

Ms Shreya Yadav, University of Hawai’i at Mānoa – swim speed data (Chapter 3)

Dr Stephen Lewis, TropWATER – current meter data (Chapter 4, Appendix II)

OPEN SOURCE MATERIALS UTILIZED

Beaman RJ (2017) High-resolution depth model for the Great Barrier Reef – 30 m.
<https://doi.org/10.4225/25/5a207b36022d2> – bathymetry data (Chapter 4, Appendix II)

eReefs GBR 4 – tide, current and wind speed data (Chapter 4, Appendix II)

Queensland Government, Maritime Safety Queensland – tide data (Chapter 4, Appendix II)

Integration & Application Network Symbol Libraries – symbols used in Fig 2.2, Fig 3.2 and Fig 3.3

Executive summary

Cubozoan jellyfishes inhabit estuarine and coastal systems used by humans. The order Cubozoa includes the highly venomous box jellyfish *Chironex fleckeri* and the infamous Irukandji jellyfishes. Managing the risks posed by these dangerous species is complicated by the high spatial and temporal variability in abundance that is characteristic of cubozoan medusae. Further, cubozoan medusae are highly mobile and they have an advanced sensory system which includes image forming eyes. They orient within their environment by swimming in reaction to environmental cues, with the strongest evidence provided for reactions to visual stimuli. Cubozoan species are understudied despite the threat they pose to humans and their interesting biology. Consequently, ecological data on cubozoans are rare and the spatial scales of connectivity between cubozoan mesopopulations (called stocks in a fisheries context) are poorly understood. Biophysical models couple hydrodynamic and behavioural models, allowing for the behaviour of organisms to be considered in investigations of their population structure. Given the sensory and mobility capabilities of cubomedusae, biophysical models are apt tools for studying the population structures of cubozoans.

The broad objective of this PhD was to determine the spatial scales separating cubozoan stocks, and the scales separating local populations within stocks. Field sampling and laboratory experiments were conducted to gather data on the spatial distribution and behaviour of medusae from two cubozoan species with different swimming capabilities and suites of behaviour: the box jellyfish *C. fleckeri* (Chapter 2), and the non-venomous *Copula sivickisi* (Chapter 3). These behavioural data informed biophysical models which were applied to determine the structure of a *C. fleckeri* population inhabiting a system that is physically partially closed (Port Musgrave, a semi enclosed estuarine bay on Cape York Peninsula, Queensland Australia; Chapter 2), and of a *C. sivickisi* population inhabiting an open system exposed to coastal currents (Magnetic Island, an island 8 km from mainland Queensland, Australia; Chapter 4).

The population of *C. fleckeri* in the semi-enclosed estuarine bay of Port Musgrave was possibly a stock, and the swimming of medusae generated significant local substructure (Chapter 2). *C. fleckeri* medusae were observed in the field at Port Musgrave. The medusae swam up and down parallel to the shore in waters < 0.5 m deep. Medusae ranging in size from 4 to 12 cm width had an average measured swim speed ($5.3 \pm 3.5 \text{ cm s}^{-1}$ SD) nearly double the measured average nearshore current speed ($2.7 \pm 2.4 \text{ cm s}^{-1}$ SD). Medusae in the field deviated their course to avoid

observers who stood to block their paths. These and other ecological data were used to parameterise a biophysical model of *C. fleckeri* movements in Port Musgrave. When medusae were modelled to swim directionally, aggregations of medusae formed local populations in nearshore waters at scales of hundreds of meters. At the bay scale, no medusae modelled as passive were lost from the mouth of Port Musgrave in the 14-day model runs, and < 2.5% of swimming medusae were lost. Additionally, a literature search revealed that the pelagic early life history stages of *C. fleckeri* (zygotes, blastulae, planulae larvae and juvenile medusae) have characteristics that would limit dispersal (e.g. negative buoyancy, stickiness and fast growth). Therefore, both the simulated retentive currents within Port Musgrave and the biological characteristics of *C. fleckeri* would limit the potential for *C. fleckeri* to leave Port Musgrave at any life stage. Further modelling suggested that the persistence of the Port Musgrave population was not threatened by short-lived river floods flowing into the bay as the salinity range within shallow, nearshore waters remained habitable. The biophysical modelling results suggested that the population of *C. fleckeri* inhabiting Port Musgrave represented a stock that exported few *C. fleckeri* to near-by populations outside the bay. *C. fleckeri* populations inhabiting similar, nearby semi enclosed estuarine bays likely represent other stocks.

The observed distribution of *C. sivickisi* medusae in the open bays of Magnetic Island was largely restricted to reefal habitat, and the observed behaviours of medusae were likely critical to maintaining this restricted distribution (Chapter 3). Underwater jellyfish camera units (JCams) were used to map the distribution of medusae in relation to depth and reefal habitat, dominated by *Sargassum* sp. algae and coral. Medusae were significantly more abundant at shallow (≤ 4.1 m) and mid-depth (4.2 to 7 m) sites with high to moderate reefal habitat availability, compared to deep (≥ 7.1) sites where sand was the dominant substratum and reefal habitat was either scarcely available or absent. A bay scale JCam survey revealed medusae were absent from sites off the ends of bands of reefal habitat less than 2 km long, suggesting their distribution was restricted to the bands. *C. sivickisi* medusae swam competently in laboratory swim trials. Medusae ≤ 1 cm wide swam at maximum sustainable speeds ($4.9 \text{ cm s}^{-1} \pm 4.4$ SD) equivalent to or faster than most of the local current speeds measured in the shallow waters (median = 2.6 cm s^{-1}) where medusae were most abundant. Further, greater than 40% of the medusae tested in the swim trials attached to the flow tank with the sticky pads on the apex of their bells to avoid being pushed back by the flow. *C. sivickisi* medusae also displayed preferential habitat selection. They were found adjacent to reefs near the bottom of the water column in depth stratified plankton tows,

and they quickly attached to *Sargassum* upon encountering it in a habitat choice experiment. Finally, *C. sivickisi* medusae observed in the laboratory were more active at night than during the day, confirming the species is nocturnal. Medusae could feasibly maintain positions on reefs by attaching to habitat and swimming against currents, thereby restricting dispersal.

In Chapter 4, the behavioural component of a biophysical model was built around the behavioural data collected in Chapter 3. Modelling (Chapter 4) supported the hypothesis developed from observations of *C. sivickisi* medusae (Chapter 3), that the behaviour of the medusae was critical to maintaining their restricted distribution on fringing reef habitat. The modelled bay-scale distribution of medusae only matched the observed distribution (bay-scale JCam survey, Chapter 3) when model medusae selectively attached to the habitat to avoid strong currents. Population mapping with JCam revealed that the Magnetic Island population of *C. sivickisi* extends along the entire east coast of the island. Further biophysical modelling provided strong evidence that the island population represented a stock with considerable substructure. Medusae modelled to attach to habitat in strong currents were able to maintain positions on the islands fringing reef for the duration of the *C. sivickisi* medusae season. Exchange of medusae between adjacent bays was predicted in the model, but only at the scale of a few kilometres. There was limited potential for model medusae from the Magnetic Island population to emigrate to a mainland population. The few model medusae lost from Magnetic Island reefs were projected to be advected into open water and away from the mainland. The model results, therefore, suggest that emigrants from Magnetic Island are unlikely to contribute to medium scale connectivity or to potential population 'founder effects' at scales of tens to hundreds of kilometres. The simulated export of medusae from the island population to Middle Reef was insubstantial, and medusae were absent from Middle Reef in JCam surveys. Consequently, Middle Reef was unlikely to act as a steppingstone between island and mainland populations. Incipient speciation (where isolated and genetically distinct stocks retain morphological similarities and reproductive compatibility) may be common within the cosmopolitan distribution of *C. sivickisi* given the small scales of connectivity simulated for the Magnetic Island stock.

In summary, complex behaviours were documented in both *C. fleckeri* and *C. sivickisi* medusae. The swim speeds of large and small cubozoans were measured and found to equal or exceed the local current speeds, especially in the nearshore waters where the medusae were observed to be most abundant. Medusae modelled to swim were projected to maintain connected local populations at small (hundreds of meters) spatial

scales. Model results also suggested that cubozoan stocks were isolated at medium (tens of kilometres) spatial scales in both a physically partially closed and a physically open system. In the model system that was partially closed, a combination of retentive currents and medusae swimming facilitated the isolation of the stock. In contrast, in the modelled open system, the sophisticated behaviours of medusae counteracted the dispersive currents to restrict the dispersal of medusae. Biophysical models were useful in determining the spatial scales of connectivity in cubozoan stocks. Genetic analyses could be carried out in future work to corroborate the modelled scales of stock differentiation. Further, little is known about the spatial and temporal abundance patterns of Irukandji species, and the novel JCam technology used in this thesis could be applied to fill this knowledge gap. Given the predicted small spatial scales of cubozoan stocks, local conditions could have a great effect on the abundance of cubomedusae, partially explaining the high variability in abundance characteristic of cubomedusae. Future research could look deeper into the causes of variability in cubomedusae abundance and provide management relevant outputs such as near real time or forecasted sting risk assessments. Historically, jellyfish populations have been generally considered open, with genetically well mixed populations covering hundreds to thousands of kilometres. The scales of cubozoan stock differentiation revealed in this thesis suggest that populations of estuarine/coastal cubozoans are closed at much smaller spatial scales. The paradigm of open jellyfish populations should, therefore, be revised.

Table of contents

Acknowledgements		iii
Statement of the Contribution of Others		v
Executive summary		vi
List of tables		xi
List of figures		xii
Thesis outputs		xvii
Chapter 1	General introduction	1
Chapter 2	Swimming behaviour can maintain localised jellyfish (<i>Chironex fleckeri</i> : Cubozoa) populations	13
Chapter 3	Behavioural maintenance of highly localised jellyfish (<i>Copula sivickisi</i> , Class Cubozoa) populations	44
Chapter 4	Behavioural and oceanographic isolation of an island-based jellyfish (<i>Copula sivickisi</i> , Class Cubozoa) population	77
Chapter 5	General discussion	104
References		115
Appendix I	Chapter 2 supplement	132
Appendix II	Chapter 4 supplement	137
Appendix III	Experimental validation of the relationships between cubozoan statolith elemental chemistry and salinity and temperature	146

List of tables

Table 1.1.	Examples of the behaviours documented in medusae from different cubozoan species, and the methods used to ascertain the behaviours	6
Table 1.2.	Examples of published swim speeds of cubomedusae. The sizes of the tested medusae are presented as either Bell Diameter (BD) or InterPedalial Distance (IPD). The methods used to determine the swim speeds are indicated. NP = Not Provided	9
Table 2.1.	Modelled scenarios and results. The tidal forcing, the modelled behaviour of the <i>Chironex fleckeri</i> medusae (A, B or C; Fig. 2.2), the simulated discharge from the Wenlock and Ducie rivers (0 m ³ s ⁻¹ for the 'No flood' scenarios, 1000 m ³ s ⁻¹ from each river for the 'Flood' scenarios), the diffusion coefficient (kx), the duration of the model run and the percentage of modelled medusae remaining in Boxes 1 and 2 (see Fig. 2.1d,e), and in Port Musgrave are shown. Medusae are passive in behavioural model A. Behavioural model B includes 3 behaviours: swimming back and forth, parallel to shore, swimming to shore and avoiding beaching. Behavioural model C includes an additional avoidance behaviour, where model medusae perform a 180° turn when they encounter mangroves at bay edges.	22
Table 2.2.	Sensitivity analysis (SA) scenarios and results. All sensitivity analysis scenarios had the same hydrodynamic forcings (average tide and wind, and no river outflow). 25000 behaviour C medusae were seeded from Red Beach and another site on the opposite side of the bay, respectively (Fig. 2.1d,e). The parametrisation of the C set of behaviours for simulated <i>Chironex fleckeri</i> medusae was sequentially altered. The C set includes 4 behaviours: swimming back and forth, parallel to shore, swimming to shore, avoiding beaching and performing a 180° turn upon encountering mangroves at bay edges (Fig. 2.2). The width of the behaviour band (BB) and the modelled swimming speed of the <i>C. fleckeri</i> medusae in the SA scenarios are indicated. The percentage of modelled medusae remaining in Boxes 1 and 2 (see Fig. 2.1d,e), and in Port Musgrave at the end of the 14 day runs are shown	23
Table 2.3.	Examples of maximum recorded speeds of jellyfishes (Max. speed). The size of medusae refers to the size reported in the relevant reference and is presented as either interpedalial distance (IPD), bell diameter (BD) or diagonal bell width (DBW). Method: method used to measure speed	36
Table 3.1.	Definitions of the behaviours observed in the temporal variation in behaviour experiment (experiment 1)	50
Table 3.2.	The results of the one-way ANOVA performed to test the effect of substrate on <i>Copula sivickisi</i> medusae corrected search times (SearchTime _{corrected}) in the habitat choice experiment (experiment 2). The source of variation (source), mean sum-of-squares (MS), degrees of freedom (df), F-value (<i>F</i>), and <i>P</i> -value (<i>P</i>) are shown	61

- Table 3.3.** Results from the Linear Mixed effects Model (LMM) analysis performed on the 2015 JCam survey data to test the effects of depth (shallow, mid and deep; encompassing habitat availability) on the abundance of *Copula sivickisi*. The degrees of freedom (df), t ratio and *P*-value (*P*) from the Tukey's test for each pairwise comparison have been shown, along with the effect size (Hedge's *g*) 65
- Table 4.1.** Descriptions of the base and dependent models of *Copula Sivickisi* medusae behaviour. The behaviour of medusae in the base model was determined by the time of day (day or night) and the location of medusae in relation to reefal habitat. An additional behaviour was added to the dependent model where medusae only swam at night if the current speed at their location was less than a predefined cut off (6, 7.5 or 9 cm s⁻¹). When medusae swam in the base or dependent model, their speed was either set to their maximum sustainable (U_{sust} ; 2.45 cm s⁻¹) or maximum (U_{crit} ; 4.9 cm s⁻¹) swim speed 85

List of figures

- Fig. 1.1.** A diagrammatic representation of a tiered population structure on an idealised coastline (line with polka dot fill). The disconnected mesopopulations/stocks (stocks 1 to 3; dashed lines) are nested within the metapopulation (solid line) and connected local populations (e.g. L1 and L2; dashed and dotted lines) are nested within the stocks. Taken from Kingsford and Mooney (2014) 2
- Fig. 2.1.** Study site. (a) Australia; (b) detailed view of the west coast of Cape York Peninsula, which contains multiple estuarine systems including Port Musgrave; (c) bathymetry of Port Musgrave. The number of *Chironex fleckeri* remaining nearshore in the biophysical modelling scenarios were counted in (d) Box 1 on the west side of the bay (adjacent to Red Beach) and (e) Box 2 on the east side of the bay. Medusae were seeded from the locations marked by the red circles 17
- Fig. 2.2.** Schematic of the *Chironex fleckeri* medusae behaviours included in the biophysical model. Red arrows: behaviours in the Y direction; blue arrows: behaviours in the X direction. Solid arrows: swimming behaviours included in Behaviour B (swimming back and forth, parallel to shore, in the Y direction, and swimming to shore and avoiding beaching in the X direction); Dashed arrows: additional behaviour included in Behaviour C (avoidance behaviour, with a directional reversal of 180° in the Y direction). Behaviours were only carried out if medusae were within the behavioural band, as denoted by the blank dashed line 20
- Fig. 2.3.** (a) Velocity of an individual observed *Chironex fleckeri* medusa through time, showing the current velocity (C), the velocity over ground (OG) and the velocity through the water (TW). (b) Average (\pm SE) velocity through water of observed medusae grouped by interpedalial distance (IPD). The number of medusae in each size class are shown above the error bars 26

- Fig. 2.4.** Modelled velocity field at Red Beach (see Fig. 2.1d) at peak ebb tide. Velocities were reported from the ends of the transect shown with the pink line 28
- Fig. 2.5.** Number of *Chironex fleckeri* medusae per grid cell with (a) Behaviour A (passive; scenario 2), (b) Behaviour B (scenario 5) and (c) Behaviour C (scenario 8) at the end of the model runs. Behavioural model B includes 3 behaviours: swimming back and forth, parallel to shore, swimming to shore and avoiding beaching (Fig. 2.2). Behavioural model C includes an additional avoidance behaviour, where model medusae perform a 180° turn when they encounter mangroves at bay edges. Runs lasted for 14 d after the particles had been released from the seed locations (see Fig. 2.1d,e). The model was forced with average tides. No freshwater outflow from the rivers were included (i.e. ‘no flood’; Table 2.1). Depth contours are indicated 30
- Fig. 2.6.** Proportion of simulated *Chironex fleckeri* medusae remaining near shore through time for the modelling scenarios listed in Table 2.1. A 24 h running average was performed on the raw data to remove tidal variability. Scenario numbers are shown. (a) Retention in Box 1 (see Fig. 2.1d), no flood scenarios; (b) Box 1, flood scenarios; (c) retention in Box 2 (see Fig. 2.1e), no flood scenarios; (d) Box 2, flood scenarios. For the no flood scenarios, the 2 lines for each behavioural category show the range of proportions obtained among the different tidal forcings. Medusae are passive in behavioural model A. Behavioural model B includes 3 behaviours: swimming back and forth, parallel to shore, swimming to shore and avoiding beaching (Fig. 2.2). Behavioural model C includes an additional avoidance behaviour, where model medusae perform a 180° turn when they encounter mangroves at bay edges. Active medusae (Behaviours B and C) swam at 5.3 cm s⁻¹ (average) and performed the prescribed behaviours within a 275 m band from shore 31
- Fig. 2.7.** Proportion of simulated *Chironex fleckeri* medusae (behaviour C) remaining near shore through time in the sensitivity analysis (SA) modelling scenarios listed in Table 2.2. A 24 h running average was performed on the raw data to remove tidal variability. In the first row, the retention in (a) Box 1 (see Fig. 2.1d) and (b) Box 2 (see Fig. 2.1e) is shown for scenarios SA1 to SA3 where medusae perform the prescribed behaviours in a 165 m band from shore. In the second row, the retention in (c) Box 1 and (d) Box 2 is shown for scenarios SA4 to SA6 where there is a 275 m band from shore. In the third row, the retention in (e) Box 1 and (f) Box 2 is shown for scenarios SA7 to SA9 where there is a 550 m band from shore. The C behavioural set includes 4 behaviours: swimming back and forth, parallel to shore, swimming to shore, avoiding beaching and performing a 180° turn upon encountering mangroves at bay edges (Fig. 2.2) 33
- Fig. 2.8.** Simulated salinity within Port Musgrave at peak ebb tide after 5 d of flooding at a rate of 1000 m³ s⁻¹ from both the Wenlock and Ducie Rivers. Depth contours are indicated 34

- Fig. 3.1.** The study region. a) Australia, the North Queensland coastline. The locations of panes a and b are indicated by the grey boxes. b) Magnetic Island. The locations of Middle Reef (MR), Picnic Bay (PB), Nelly Bay (NB), Geoffrey Bay (GB), Alma Bay (AIB), Arthur Bay (ArB) and Florence Bay (FB) are shown. The extents of panes c and d are indicated by the dark grey and light grey boxes, respectively. The designs of the c) 2015 and d) 2016 Jellyfish Camera unit (JCam) surveys. The white squares mark the locations of the sampled sites. The bathymetry of NB and GB is shown, the color bar indicates the depth (m). Depths > 10 m are shown in black. In all panes, land is filled with a hatch pattern. Reefs are filled with solid grey in panes a and b, and they are outlined in black and filled with dots in panes c and d 47
- Fig. 3.2.** Diagrammatic representation of the tank set up in experiment 2, the habitat choice experiment 52
- Fig. 3.3.** Jellyfish Camera unit (JCam) design. A diagram of a deployed JCam, with labelled components. A close up photograph of a JCam is provided in the insert 54
- Fig. 3.4.** Results from experiment 1, the temporal variation in behaviour experiment. The estimated proportions \pm 95% confidence interval (CI) of *Copula sivickisi* medusae performing active (swimming, feeding or mating) versus passive (attached or bobbing) behaviours during the day and at night. Shown are the pooled data from a) the five adult trials and b) the five juvenile trials 58
- Fig. 3.5.** Results from experiment 1, the temporal variation in behaviour experiment. The average percentage + SE of *Copula sivickisi* medusae performing each passive (attached and bobbing; closed, grey symbols) and active (swimming, feeding and mating; open black symbols) behaviour at each day time (white background) and night time (grey background) observation. The results from a) the five adult trials, and b) the five juvenile trials are shown 60
- Fig. 3.6.** Results from experiment 2, the habitat choice experiment. The cumulative number of *Copula sivickisi* medusae that attached to the different substrates (empty tank control, sand, *Sargassum Sp.* algae and *Montipora sp.* coral rubble) through time. The corrected search times ($\text{SearchTime}_{\text{corrected}}$) of the medusae are shown 61
- Fig. 3.7.** Results from the habitat choice experiment (experiment 2). The average corrected number of times ($\text{Count}_{\text{corrected}} \pm \text{SE}$) *Copula sivickisi* medusae were counted in each of the four substrate quadrants. For the medusae that attached to a substrate, average counts are shown for the period before they attached to a) the tank control, b) the sand, c) the *Sargassum sp.* algae or d) the *Montipora sp.* coral rubble. Average counts over the entire trial period have been shown for e) the medusae that never attached to a substrate. The dashed lines show the maximum extent of the y-axis in panes a, b and c. The numbers of attached (per habitat) and unattached medusae are shown; total n = 50 62
- Fig. 3.8.** a) Abundance of *Copula sivickisi* medusae among depth strata estimated by JCam; Geoffrey Bay, 2015. $N_{\text{max}} \pm \text{SE}$ is presented for shallow (≤ 4.1 m), mid (4.2 to 7 m) and deep (≥ 7.1 m) strata. The pie

charts show the proportion of the four sites sampled per depth that had the different categories of reef habitat (*Sargassum* sp. algae and coral) availability. The post-hoc analysis groupings (a or b) and the number of sites averaged per depth are indicated. Total n = 45. b) Surface current speeds, from drogues, above each depth stratum. Current speeds greater than the upper quartile plus 1.5 times the interquartile range have been shown as outliers. The number of drogue deployments per depth is indicated; total n = 95. The overlaid lines show the greatest sprint (U_{sprint}) and the average critical (U_{crit}) swim speeds of the *C. sivickisi* medusae from the swimming trials

64

Fig. 3.9. The longshore abundance of *Copula sivickisi* medusae estimated by JCam; Nelly Bay and Geoffrey Bay, 2016. The average $N_{\text{max}} + \text{SE}$ is shown by site for each of the four sampling trips (panes a to d). The sites are in sequential order on the x-axis, from the southern most site in Nelly Bay to the northern most site in Geoffrey Bay (Fig. 3.1). The y-axis of pane b is split; the extent of the lower section matches the full extent of the other panes. n(1) indicates the sites where N_{max} could only be determined for one replicate; total n = 77. The exact values of high SEs have been provided in text. The background has been shaded dark grey where reefal habitat (*Sargassum* sp. algae and coral) was present at both replicates within the site, and habitat availability was high in at least one of the replicates. It has been shaded light grey where habitat was present at both replicates in either moderate or low availability. The diagonal stripes indicate where the habitat was entirely absent

66

Fig. 4.1. Biophysical model development, validation and application. a) The model domain (white line with black border), and the bathymetry of the modelled region. The color bar indicates the depth (m). Depths > 180 m are shown in black. The inset shows the location of the model domain (grey polygon) in Queensland, and its scale in relation to Australia. The location of pane b is indicated by the grey box. b) The instruments used to validate the hydrodynamic simulations in the Townsville (TSV)/Magnetic Island (M. Isl.) region. The white dots mark the locations of the current meters at Cleveland Bay (CB), Middle Reef (MR), Geoffrey Bay (GB) and Orchard Rocks (OR). The white triangle marks the location of the tide gauge at the Port of Townsville (POT). The locations of panes c and d are indicated by the dark and light grey boxes respectively. Reefs from OR to MR are shown in black. c) and d) The seed locations (white) and reefal habitats (black outline; identified from satellite images and validated with JCam footage) used in the behavioural retention and connectivity analyses respectively. The variable resolution SLIM mesh is shown in c and d. Land is filled with a hatch pattern in panes a and b, and filled grey in panes c and d

82

Fig. 4.2. The study region. a) The Townsville coast and Magnetic Island. The location of a is shown on a map of Australia (star). The rectangle shows the extent of b. b) The JCam survey design covering Middle Reef (MR), Picnic Bay (PB), Geoffrey Bay (GB), Alma Bay (AB), Alma North (AN), Arthur Bay (ArB) and Florence Bay (FB). The white dots show the sites where the JCams were deployed within each location. The white triangles show the sites in Nelly Bay (NB; * no JCams were deployed in NB) and GB where the modelled currents were extracted for inclusion in Fig. 4.3. Land is filled grey and reefs are filled black in both panes

86

- Fig. 4.3.** Results of the behavioural retention analysis. The simulated currents experienced by medusae (i.e. half the depth averaged current) at sites in a) Nelly Bay (NB) and b) Geoffrey Bay (GB). The sites are marked in Fig. 4.2. The lengths of the sticks indicate the current speed and the sticks are oriented in the direction the current flowed to. The reference stick in a) shows the stick length for a speed of U_{crit} . c) The average percentage of *Copula sivickisi* medusae remaining in NB and GB through time as simulated with the passive (dashed and dotted line; light grey band) and base models. Base model medusae were modelled to swim at either U_{crit} (solid line; dark grey band) or U_{sust} (dashed line; grey band). The bands underlying each line indicate the range of percentages simulated among the five replicate model runs. The circles at the top of the figure, and the vertical lines running down from them, show when there was a full (white) or new (grey) moon 91
- Fig. 4.4.** Results of the behavioural retention analysis. The average percentage of *Copula sivickisi* medusae remaining in Nelly Bay and Geoffrey Bay through time as simulated with the dependent model. Model medusae were modelled to swim at either a) U_{crit} or b) U_{sust} , and to attach to habitat at current speed cut offs of 6 (solid line; dark grey band), 7.5 (dashed line; grey band), and 9 $cm\ s^{-1}$ (dashed and dotted line; light grey band). The bands underlying each line indicate the range of percentages simulated among the five replicate model runs. The circles at the top of the figure, and the vertical lines running down from them, show when there was a full (white) or new (grey) moon 93
- Fig. 4.5.** The abundance of *Copula sivickisi* medusae estimated by JCam. The average $N_{max} \pm SE$ is shown by location. Locations are: Middle Reef (MR), Picnic Bay (PB), Geoffrey Bay (GB), Nelly Bay (NB), Alma Bay (AB), Alma North (AN), Arthur Bay (ArB) and Florence Bay (FB; Fig. 4.2). The number of sites averaged per location are indicated; total $n = 70$ 94
- Fig. 4.6.** A connectivity matrix showing the relative connectivity between source/from and sink/to detection zones over the entire 2017 medusae season. The detection zones have been pooled by the reefs/bays identified on the x and y axes. Locations are: Middle Reef (MR), Picnic Bay (PB), Geoffrey Bay (GB), Nelly Bay (NB), Alma Bay (AB), Alma North (AN), Arthur Bay (ArB) and Florence Bay (FB; Fig. 4.2). The matrix shows the result from one of five replicate model runs (dependent model, swim speed = $U_{crit} = 4.9\ cm\ s^{-1}$, attach at cut off of 6 $cm\ s^{-1}$). The yellow dashed line indicates the transect of the connectivity matrices shown in Fig. 4.7, where the blue triangle shows the position of the focal detection zone 95
- Fig. 4.7.** The average relative connectivity $\pm SE$ of the modelled detection zones with a zone in mid Nelly Bay (NB), as indicated in Fig. 4.6. The relative connectivity is plotted with distance along the near continuous habitat band starting from Middle Reef (MR). The position of the focal detection zone is shown by the blue triangle; the connectivity at this position is indicative of the level of within zone retention. The locations/extents of the different reefs/bays are indicated by the identifiers along the top of the figure. Locations are: MR, Picnic Bay (PB), Geoffrey Bay (GB), NB, Alma Bay (AB), Alma North (AN), Arthur Bay (ArB) and Florence Bay (FB; Fig. 4.2). $n = 5$ replicate model runs (dependent model, swim speed = $U_{crit} = 4.9\ cm\ s^{-1}$, attach at cut off of 6 $cm\ s^{-1}$) 96

Fig. 4.8. Positions of all adult medusae lost from Magnetic Island habitat over the entire 2017 *Copula sivickisi* medusae season, representing < 1% of the total number of simulated medusae released (dependent model, swim speed = $U_{crit} = 4.9 \text{ cm s}^{-1}$, attach at cut off of 6 cm s^{-1}). The plotted plumes, therefore, show the maximum extent of the export of adult *C. sivickisi* medusae from Magnetic Island. The sequential colours, from yellow to blue, distinguish the results of the five replicate model runs. Land is filled with a hatch pattern and reefs are shown in black 97

Thesis outputs

PUBLICATIONS

Chapter 2

Schlaefer JA, Wolanski E, Kingsford MJ (2018) Swimming behaviour can maintain localised jellyfish (*Chironex fleckeri*: Cubozoa) populations. Mar Ecol Prog Ser 591: 287-302. <https://doi.org/10.3354/meps12305>

Author contributions: All authors contributed to the study conception and design.

Schlaefer conducted the field sampling with assistance from Kingsford. **Schlaefer** and Wolanski developed and applied the biophysical model. **Schlaefer** analysed the model outputs with assistance from Wolanski and Kingsford. **Schlaefer** developed the figures and tables and wrote the first draft of the manuscript. **Schlaefer** revised the manuscript with editorial support from Wolanski and Kingsford.

Chapter 3

Schlaefer JA, Wolanski E, Yadav S, Kingsford MJ (2020) Behavioural maintenance of highly localised jellyfish (*Copula sivickisi*, Class Cubozoa) populations. Mar Biol 167. <https://doi.org/10.1007/s00227-020-3646-6>

Author contributions: All authors contributed to the study conception and design.

Schlaefer and Yadav conducted the field sampling with assistance from Kingsford. **Schlaefer** analysed the video footage. Yadav designed and conducted the swim trials with assistance from Kingsford. **Schlaefer** conducted additional swim trials following Yadav's design. **Schlaefer** designed and conducted all other laboratory experiments with advice from Kingsford. **Schlaefer** analysed the data with assistance from Kingsford. **Schlaefer** developed the figures and tables and wrote the first draft of the manuscript. **Schlaefer** revised the manuscript with editorial support from Wolanski, Yadav and Kingsford.

Chapter 4

Schlaefer JA, Wolanski E, Lambrechts J, Kingsford MJ (in review) Behavioural and oceanographic isolation of an island-based jellyfish (*Copula sivickisi*, Class Cubozoa) population. Target journal: Sci Rep

Author contributions: **Schlaefer**, Wolanski and Kingsford contributed to the study conception and design. **Schlaefer** conducted the field sampling with assistance from Kingsford. **Schlaefer** and Lambrechts developed the biophysical model. **Schlaefer** applied the model and analysed the model outputs. **Schlaefer** developed the figures and tables and wrote the first draft of the manuscript. **Schlaefer** revised the manuscript with editorial support from Wolanski and Kingsford.

Appendix III

Morrissey SJ, **Schlaefer JA**, Kingsford MJ (2020) Experimental validation of the relationships between cubozoan statolith elemental chemistry and salinity and temperature. J Exp Mar Biol Ecol 527. <https://doi.org/10.1016/j.jembe.2020.151375>

Author contributions: All authors contributed to the study conception and design. **Schlaefer** conducted the field sampling and experiments with assistance from Kingsford. Morrissey performed the elemental chemistry analysis with assistance from Kingsford. Morrissey developed the figures and tables and wrote the first draft of the manuscript. Morrissey revised the manuscript with editorial support from **Schlaefer** and Kingsford.

CONFERENCE PRESENTATIONS

Kingsford MJ, Mooney C, **Schlaefer JA** (2019) Ecology and population connectivity of the cubozoan *Copula sivickisi* in northern Australia. 6th International Jellyfish Bloom Symposium, Cape Town, South Africa

Schlaefer JA, Yadav S, Lambrechts J, Wolanski E, Kingsford MJ (2018) Limited connectivity between local jellyfish (*Copula sivickisi*, Class Cubozoa) populations. AMSA Canyons to Coasts

Schlaefer JA, Wolanski E, Lambrechts J, Kingsford MJ (2018) Limited connectivity between two adjacent populations of the jellyfish *Chironex fleckeri*. ECSA 57: Changing Estuaries, Coasts and Shelf Systems - Diverse Threats and Opportunities, Perth, WA, Australia

Schlaefer JA, Wolanski E, Kingsford MJ (2016) Swimming behaviour can maintain localised *Chironex fleckeri* populations. 5th International Jellyfish Bloom Symposium, Barcelona, Spain

Chapter 1.

General introduction

The population structures of living things are influenced by their cumulative movements across all life stages (i.e. propagules, larvae, juveniles and adults). Populations are often structured in tiers (Fig. 1.1; Sinclair, 1988). The biogeographic range of a species may be composed of one or more metapopulations (a population of populations; Sinclair, 1988; Kingsford and Battershill, 1998). In turn, metapopulations may be made up of a collection of largely disconnected mesopopulations/stocks, which can be further divided into connected local populations (Kingsford and Battershill, 1998; Kingsford et al., 2000). As robust stocks are essentially self-contained units, the biomass within stocks is chiefly determined by intrinsic factors such as mortality, growth, reproduction and self-recruitment, and populations are generally considered 'closed' at the scale of stocks (Sinclair, 1988). In contrast, 'open' populations are well mixed, lacking discernible stocks over large spatial scales (Roughgarden et al., 1985).

In aquatic species, biological, geographic and/or hydrodynamic mechanisms interact to isolate stocks or connect local populations. Biological mechanisms include species characteristics that effect their exposure and vulnerability to dispersive currents. The duration of the pelagic larval stage in species with bipartite life cycles, the timing of spawning and the swimming capabilities and behaviours of different life stages are examples of such characteristics. Comparing the epifaunal mollusc species *Adalaria proxima* and *Goniodoris nodosa* provides a specific example of how biological factors can influence the spatial scales of stocks. The lecithotrophic larvae of *A. proxima* only remain in the pelagic for 1 to 2 days before metamorphosing, and *A. proxima* stocks in the northern British Isles were found to be separated by less than ten kilometres (Todd, 1998). In contrast, no isolated stocks of *G. nodosa* were identified within a 1,600 km zone in the northern British Isles. *G. nodosa* have planktotrophic larvae which can remain in the pelagic for up to 3 months, during which they are potentially exposed to dispersive currents (Todd, 1998).

The physical settings of species habitats determine the geographic and hydrodynamic mechanisms of isolation or connectivity. For example, the current regimes of sheltered coastal bays are generally less dispersive than the currents in open waters.

Additionally, some bays are more sheltered than others, depending on factors such as their orientation in relation to the prevailing wind direction and how open they are to

the ocean (e.g. Critchell et al. 2015). The tidepool copepod *Tigriopus californicus* inhabits geographically isolated supralittoral tidepools and stocks can be separated by less than 12 kilometres even though all life stages of *T. californicus* are free swimming (Burton and Lee, 1994).

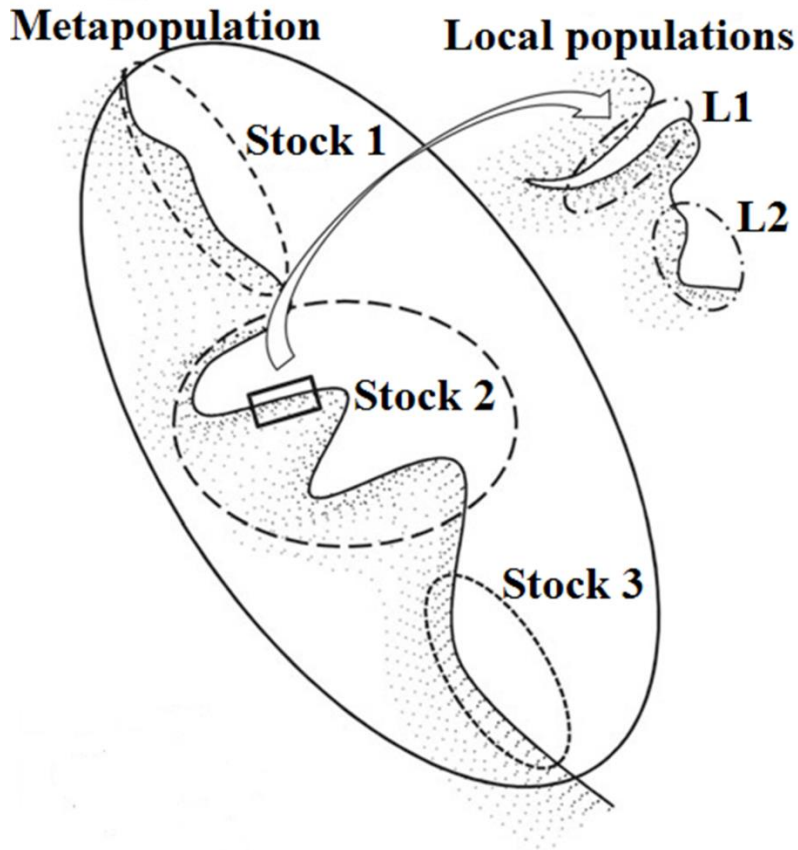


Fig. 1.1. A diagrammatic representation of a tiered population structure on an idealised coastline (line with polka dot fill). The disconnected mesopopulations/stocks (stocks 1 to 3, dashed lines) are nested within the metapopulation (solid line) and connected local populations (e.g. L1 and L2, dashed and dotted lines) are nested within the stocks. From Kingsford and Mooney (2014).

Aquatic taxa generally have a bipartite lifecycle which includes a dispersive pelagic larval stage. Historically, there used to be a consensus that taxa with pelagic larvae have open populations at scales matching the thousands of kilometres spanned by large scale ocean currents (e.g. Roughgarden et al., 1985; Scheltema, 1988). This paradigm has been challenged over the past two decades, and taxa with pelagic larvae are now generally thought to have populations that are primarily closed at spatial scales much smaller than thousands of kilometres (e.g. Todd, 1998; Jones et

al., 1999; Cowen et al., 2000). In contrast, jellyfish populations are still widely considered open. Jellyfish are classified in the phylum Cnidaria. They are a morphologically diverse group found throughout the aquatic ecosystems of the world, from the deep sea to inland lakes. Jellyfish have been understudied as they have historically been perceived as socioeconomically and ecologically unimportant. They can also be difficult to study as their abundance can vary greatly in space and time, and their gelatinous bodies can be destroyed in the trawl sampling commonly conducted in fisheries science. Most jellyfishes have a bipartite lifecycle, with sessile polyps that produce free swimming larvae or medusae. The polyps of jellyfish in the class Scyphozoa successively strobilate larval medusae called ephyrae. In contrast, the polyps of jellyfish in the classes Cubozoa and Hydrozoa typically metamorphose into or laterally bud juvenile medusae, respectively. Most of the published studies on population structures in jellyfish have focused on scyphozoan species. The poor swimming ephyrae of scyphozoans can be carried hundreds of kilometres by ocean currents, connecting disjointed populations (e.g. Barz et al., 2006; Chen et al., 2014). Scyphozoans with bipartite life histories have been found to have populations that are genetically well mixed over thousands of kilometres (e.g. *Chrysaora melanaster* in the Bering Sea; Dawson et al., 2015). Further, the lifecycles of some scyphozoan jellyfishes lack a polyp phase (e.g. *Pelagia noctiluca* and *Periphylla* spp.). The entire lifecycles of these holoplanktonic species are completed in the plankton; their planula larvae develop into ephyrae which develop into medusae. Populations of holoplanktonic jellyfish have been found to be genetically well mixed over thousands of kilometres, although discrete populations have been differentiated across ocean basins (Stopar et al., 2010; Miller et al., 2012; Glynn et al., 2016; Abboud et al., 2018).

Emergent evidence from scyphozoans is challenging the paradigm of open jellyfish populations, and this parallels the rejection of the paradigm of open populations for broader aquatic taxa. There are numerous published examples of scyphozoan populations containing substructure at surprisingly small spatial scales. For example, medusae of the scyphozoan *Catostylus mosaicus* have been found to swim strongly to maintain positions away from the mouths of the estuaries they inhabit, reducing the potential for expatriation from the estuaries (Pitt and Kingsford, 2000). Pitt and Kingsford (2000) investigated abundance and recruitment patterns in *C. mosaicus* populations inhabiting different estuarine bays along the coast of New South Wales, Australia, separated by tens to hundreds of kilometres. The demographics of the populations varied greatly suggesting the estuaries represented separate stocks.

These findings were later corroborated with genetics which revealed the populations inhabiting each of the bays were distinct (Dawson, 2005). Similarly, distinct populations of *Aurelia aurita* have been identified in lakes and sounds in southern England separated by tens of kilometres (Dawson et al., 2015), and incipient species of *Mastigias papua* have been identified in marine lakes in Palau, also separated by tens of kilometres (Dawson and Hamner, 2005). More broadly, Abboud et al. (2018) conducted a global analysis of the scales of genetic structuring in 1 hydrozoan genera and 15 scyphozoan genera. They found that taxa with bipartite life cycles tended to have structured populations with genetically distinct units separated by tens to hundreds of kilometres, and they identified genetic structuring at spatial scales as small as 3 km (e.g. *Cassiopea* from Indonesia).

Less is known about the population structures of cubozoan jellyfishes. There are two orders in the class Cubozoa: Carybdeida and Chirodropida. Carybdeids have one tentacle per pedalia, and the family includes the infamous Irukandji jellyfishes. In contrast, chirodropids have multiple tentacles per pedalia. The potentially lethal box jellyfish *Chironex fleckeri* is an example of a chirodropid. Venomous cubozoans represent a significant risk to the health and safety of water users, particularly in tropical waters (Fenner, 2005). Additionally, the publicity surrounding envenomation's can negatively affect the tourism industry by deterring tourists (Gershwin et al. 2010). The class Cubozoa has a low species diversity compared to the class Scyphozoa; there are around 50 accepted cubozoan species (Kingsford and Mooney, 2014), and hundreds of recognised scyphozoans (<https://www.marinespecies.org>). However, new cubozoan species are described regularly (e.g. *Meteorona kishinouyei*; Toshino et al. 2015). Elucidating the taxonomy of Cubozoa is an active area of research complicated by the cryptic nature of cubozoan polyps and the morphological similarity of cubomedusae in some genera (e.g. Bentlage et al., 2010; Lawley et al., 2016; Acevedo et al., 2019). Collecting ecological data on cubozoans is further complicated by the high spatial and temporal variability in abundance that is characteristic of cubomedusae. The dynamics of populations can be influenced by drivers at the spatial scale of stocks given stock biomass is determined by internal factors (Sinclair, 1988). Accordingly, the observed high variability in cubomedusae abundance could be a symptom of local factors influencing stocks that are isolated at relatively small spatial scales (e.g. Pitt and Kingsford, 2000). Improving our knowledge of how cubozoan populations are structured may, therefore, advance our understanding of the variability in cubomedusae abundance. Stakeholders could then manage the risks of

envenomation's from dangerous species based on a well-founded understanding of cubomedusae dynamics.

Cubozoan jellyfishes inhabit tropical and temperate latitudes in the Pacific, Atlantic and Indian Oceans. The tropical western Pacific is a hotspot of cubozoan biodiversity (Kingsford and Mooney, 2014). The distributions of cubozoan species cover a range of spatial scales. For example, *Alatina alata* has a circumtropical distribution (Lawley et al., 2016) and *Copula sivickisi* is found throughout the Pacific (e.g. Australia, Vietnam, Japan, New Zealand, Hawaii; Kingsford and Mooney, 2014) and in the Indian Ocean (West Sumatra; Lewis et al., 2008). In contrast, *Carybdea arborifera* and *Chirodropus palmatus* are endemic to Hawaii and Saint Helena, respectively (Kingsford and Mooney, 2014). Within these distributions, most cubozoans inhabit neritic systems, however some species appear to be oceanic (Kingsford and Mooney, 2014). The neritic environments inhabited by most cubozoans have different levels of physical openness. At the closed end of this spectrum, *Tripedalia cystophora* live among mangrove roots in mangrove channels (Stewart, 1996). Intermediately, *C. fleckeri* are found in numerous habitats ranging in physical openness from semi-enclosed mangrove creeks and estuarine bays to open beaches (Kingsford and Mooney, 2014). Other cubozoans, such as *Carukia barnesi* and *C. sivickisi*, inhabit reefs which can be relatively exposed (Kingsford et al., 2012). Wolanski (2017) asserted that across the spectrum from physically closed to physically open systems, population closure increasingly relies on the behaviour of species. Therefore, within the habitats of neritic cubozoans with exposures ranging from closed to open, the behaviours of cubomedusae will likely become increasingly important for the structuring of their populations.

The estuarine, coastal and reefal environments inhabited by cubozoans also tend to be spatially complex. The sticky water effect and current shear can weaken the currents in spatially complex systems. The sticky water effect describes when a current is diverted around a sheltered area, thereby reducing the current speed and increasing retention within the area (Andutta et al., 2012). Current shear describes how the current speed tends to decrease with proximity to a physical boundary (Fischer et al., 1979; Davies and Lawrence, 1994). The edges of mangrove creeks, the shores of estuarine bays and reef tops are examples of boundaries in neritic environments.

Cubomedusae capably navigate through these spatially complex environments. However, behavioural data are only available for a select few cubozoan species (Table

1.1). All cubomedusae poses a sophisticated visual system made up of four sensory clubs (rhopalium), each containing six eyes. Two of these eyes (the upper and lower lens eyes) are image forming, and the remaining four (pairs of slit and pit eyes) are simple ocelli (Coates and Theobald, 2003; Nilsson et al., 2005). Obstacle avoidance appears to be widespread among cubozoan species (Table 1.1). Interestingly, the strength of the avoidance response may be linked to the spatial complexity of the environment that the medusae inhabits (Garm et al., 2007). *T. cystophora* medusae swim between prop roots in mangrove creeks and *Chiropsella bronzie* medusae inhabit coastal marine waters which contain fewer obstacles comparatively. Garm et al. (2007) subjected *T. cystophora* and *C. bronzie* medusae to duplicate obstacle avoidance experiments, and the *T. cystophora* displayed a stronger response to the obstacles. Relatedly, cubomedusae appear to have species-specific sets of behaviour adapted to suit their environments. For example, *C. sivickisi* medusae are nocturnal and they uniquely have sticky pads on the tops of their bells which they use to adhere to hard surfaces when they are inactive (Hartwick, 1991b; Garm et al., 2012). The eyes of *C. sivickisi* medusae are also adapted to low light levels, and they can see the flashes given off by bioluminescent plankton at night (Garm et al., 2016). While hunting, *C. sivickisi* medusae may find areas of high prey density by swimming toward bioluminescent flashes (Garm et al., 2016). As stock boundaries are influenced by the movements of animals, knowledge of the full set of behaviours exhibited by medusae is integral to understanding cubozoan population structures and dynamics.

Table 1.1. Behaviours documented in medusae from different cubozoan species, and the methods used to ascertain the behaviours.

Behaviour	Species (order)	Method	Study
Obstacle avoidance	<i>Carybdea rastonii</i> (Carybdeida)	Field observations (SCUBA) and laboratory experiments	Matsumoto (1995)
	<i>Chironex fleckeri</i> (Chirodropida)	Laboratory experiments	Hamner et al. (1995)
	<i>Chiropsella bronzie</i> (Chirodropida)	Laboratory experiments	Garm et al. (2007)
	<i>Tripedalia cystophora</i> (Carybdeida)	Laboratory experiments	Garm et al. (2007)

Table 1.1. Continued.

Behaviour	Species (order)	Method	Study
Maintain positions near the shore	<i>C. rastonii</i>	Field observations (SCUBA)	Matsumoto (1995)
	<i>C. fleckeri</i>	Opportunistic sampling (e.g. Surf Life Saver plankton tows and verbal records)	Kingsford et al. (2012)
		Electronic tagging	Gordon and Seymour (2009)
Diel activity - nocturnal	<i>Copula sivickisi</i> (Carybdeida)	Field observations (SCUBA)	Hartwick (1991b)
		Field sampling (plankton tows and SCUBA) and laboratory experiments	Garm et al. (2012)
Attach to substrate	<i>C. sivickisi</i>	Laboratory observations	Hartwick (1991b)
		Laboratory experiments	Garm et al. (2012)
Swim toward bioluminescent plankton	<i>C. sivickisi</i>	Laboratory experiments	Garm et al. (2016)
Diel activity - diurnal	<i>T. cystophora</i>	Field sampling (snorkel and SCUBA) and laboratory experiments	Garm et al. (2012)
Maintain positions in light shafts	<i>T. cystophora</i>	Field observations (snorkel)	Stewart (1996)
		Laboratory experiments	Buskey (2003)
		Laboratory experiments and in field video recordings	Garm and Bielecki (2008)
Orient via the mangrove canopy	<i>T. cystophora</i>	Eye orientation measurements, optical modelling and in field experiments	Garm et al. (2011)

Cubomedusae are also strong swimmers but data on the swimming capabilities of cubomedusae are relatively rare (but see Table 1.2). Cubozoans swim via jet propulsion, where they expand their bell to take in water and then contract it to expel the water, propelling them forward (Shorten et al., 2005). Although, larger medusae may transition to a hybrid jetting/rowing method of propulsion (Colin et al., 2013). While the swim speed of cubozoans tends to increase with size, even small cubomedusae are exceptional swimmers (Shorten et al., 2005; Garm et al., 2007; Colin et al., 2013). To the authors knowledge, all published measures of cubozoan swim speed have been made in a laboratory setting and over short time scales. Hamner et al. (1995) did observe *C. fleckeri* medusae in the field, but they only estimated their swim speeds, and they were only able to watch the medusae for 5 to 10 minutes. Consequently, there are no data available on the sustained swimming capabilities of cubomedusae. Gordon and Seymour (2009) used electronic tags to track the movements of 12 *C. fleckeri* medusae for 10 to 38 hours. The medusae travelled hundreds of metres to kilometres while being tracked; however, the currents they were traversing were not measured so their swim speeds could not be determined. Gordon and Seymour (2009) noted that medusae were capable of swimming against the currents but tended to travel with the currents when the flow was high. Cubomedusae could potentially maintain relatively fast swim speeds for long time periods as they are highly efficient swimmers. Medusae expend less energy per meter travelled compared to other swimming animals by utilising a passive energy recapture mechanism (Gemmell et al., 2013). Further, the jetting motion of cubomedusae is more efficient than the rowing motion of most scyphomedusae as it takes greater advantage of the mechanism (Gemmell et al., 2018). The sustained swimming abilities of cubomedusae would influence their dispersal potential, and thereby the distances separating cubozoan stocks.

Table 1.2. Published data on the swim speeds of cubomedusae. The sizes of the tested medusae are presented as either Bell Diameter (BD) or InterPedalial Distance (IPD). The methods used to determine the swim speeds are indicated. NP = Not Provided.

Species (order)	Size in cm (n)	Speed (cm s ⁻¹)	Method	Study
<i>Tripedalia cystophora</i> (Carybdeida)	0.8 – 1.2 BD (NP)	max: 3 – 4 against current in tank, range: 1 – 1.5	rheotaxis measurements in a flow tank	Garm et al. (2007)
	0.9 – 1.1 BD (12)	avg: 0.61 – 0.75 against current in kreisel, avg: 0.11 (centre) and 1.54 (outer edge)	digital video analysis of rheotaxis in a kreisel	Buskey (2003)
<i>Chiropsella bronzie</i> (Chirodropida)	0.5 – 5.6 IPD (7)	avg: 1.2 – 7.1 max: 3.1 – 11.4	digital video analysis	Colin et al. (2013)
	0.5 – 6.1 BD (4)	avg: 1.2 – 7.4 max: 3.5 – 11.0	digital video analysis	Gemmell et al. (2018)
	3 – 5 BD (NP)	max: 7 – 8 against current in tank, range: 1 – 1.5	rheotaxis measurements in a flow tank	Garm et al. (2007)
<i>Chiropsalmus</i> sp. (Chirodropida)	1.5 – 6.5 BD (9)	2.3 – 6.7	digital video analysis	Shorten et al. (2005)
<i>Chironex fleckeri</i> (Chirodropida)	1.3 – 10 BD (37)	0.9 – 7.6	measured in still water after visual disturbance	Hamner et al. (1995)
	NP (20)	≤ 8	measured in still water after mechanical disturbance	
	> 10 BD (3)	10 – 20	field estimate	
	2.0 to 16 IPD (4)	avg: 2.5 – 5.7 max: 4.7 – 11.5	digital video analysis	Colin et al. (2013)
	2.1 – 14.2 BD (4)	avg: 2.4 – 5.7 max: 4.9 – 11.7	digital video analysis	Gemmell et al. (2018)
	4.5 to 10 BD (7)	3.6 to 11.5	digital video analysis	Shorten et al. (2005)

The dispersal of the pelagic (i.e. gametes, zygotes, blastula, embryo sacs, planulae larvae and juvenile medusae) early life history stages of cubozoans could also determine the distances separating cubozoan stocks; however, characteristics that limit the potential for dispersal are seemingly widespread among cubozoan early life history stages. It is likely that all species in the order Carybdeida are ovoviviparous, meaning the fertilization of eggs occurs internally (Bentlage et al., 2010). The eggs of carybdeids are, therefore, not dispersed in the water column pre-fertilization. The carybdeid *C. sivickisi* produces sticky embryo sacs which they may attach to reefal habitat selectively (Hartwick, 1991b). Other carybdeids (*T. cystophora*, Werner et al., 1971; *Tripedalia binata*, Toshino et al., 2017) have been found to release mature, free-swimming planulae larvae or negatively buoyant fertilized eggs (*Carukia barnesi*, Courtney et al. 2016; *Malo maxima*, Underwood et al. 2018). Carybdeida planulae larvae generally settle on the bottom quickly, so the potential for them to be exposed to dispersive currents is limited (e.g. *T. binata* planulae settle 2 to 4 days after release, Toshino et al. 2017). Members of the order Chirodopida release their gametes into the water column and fertilization occurs externally (Bentlage et al., 2010). Post-fertilization, the zygotes, blastula and planulae of chirodopids may have limited exposure to currents. The chirodopid *C. fleckeri* produced zygotes and blastula that were negatively buoyant and adhered to surfaces (Hartwick, 1991a). Further, *C. fleckeri* planulae emerged within 12 to 24 hours of fertilization and settled within 24 hours (Hartwick, 1991a). Additionally, the juvenile cubozoan medusae that emerge from polyps are nearly fully formed (e.g. Werner et al., 1971; Straehler-Pohl and Jarms, 2005), and they grow quickly (Toshino et al., 2014). Cubomedusae, therefore, may gain competence in swimming quickly, especially compared to the underdeveloped (Straehler-Pohl and Jarms, 2010) scyphozoan ephyrae which can disperse hundreds of kilometres in ocean currents (Barz et al., 2006; Chen et al., 2014). Cubozoan populations may be subdivided at surprisingly small spatial scales given the small scales of differentiation identified in scyphozoan populations with less competent juveniles.

Stock differentiation at small spatial scales is likely in cubozoan species given: (1) the small scales of stock differentiation reported in scyphozoans with bipartite life histories analogous to cubozoans, (2) the complexity of habitats inhabited by cubozoans, (3) the associated complex behaviours and strong swimming abilities of cubomedusae, (4) the limited dispersal potential of cubozoan early life history stages, and (5) the presumed greater swimming ability of newly metamorphosed cubozoan juveniles compared to

the ephyrae larvae of scyphozoans. However, there are limited data on the scales of stock differentiation in cubozoan species.

Stock differentiation has been documented at relatively large spatial scales in cubozoans. The sensory systems of cubomedusae include four bassanite crystals called statoliths. Mooney and Kingsford (2017) extracted statoliths from *C. fleckeri*, *C. sivickisi* and, *C. barnesi* medusae taken from different populations across Northern Australia, and they compared the shapes of the statoliths between locations and within species. Significant differences were found in the statoliths of *C. fleckeri* and *C. sivickisi* medusae from populations separated by hundreds of kilometres. Mooney and Kingsford (2016a) similarly found significant differences in the elemental chemistry of statoliths from *C. fleckeri* medusae collected from populations separated by hundreds of kilometres. Statolith shape and elemental chemistry are likely affected by the surrounding environment (Secor et al., 1995; Bath et al., 2000; Cadrin, 2010), and shape could be heritable (Cadrin, 2010). Therefore, the cubomedusae with significantly different statolith shapes/chemistry were likely from separate, genetically isolated stocks which experienced different environmental conditions (Mooney and Kingsford 2016a, 2017). Importantly, Mooney and Kingsford (2016a, 2017) also found evidence of divisions in *C. fleckeri* stocks at smaller spatial scales; they found significant differences in the statoliths of *C. fleckeri* medusae collected from different sites within regions, and the sites were separated by a minimum of a few kilometres. The behaviour of the *C. fleckeri* medusae tracked in the tagging study conducted by Gordon and Seymour (2009) also suggested that *C. fleckeri* could maintain stocks separated by only small spatial scales. The tracked medusae tended to stay within the coastal or estuarine environments they were tagged in despite traveling hundreds of meters to kilometres within a day. Some tracked medusae even returned to their release locations.

More research is required to build a comprehensive understanding of cubozoan population structures. Numerous techniques have been used to investigate the structures of jellyfish populations including: statolith morphometrics (Mooney and Kingsford, 2017) and elemental chemistry (Mooney and Kingsford, 2016a), demographics (e.g. Pitt and Kingsford, 2000), genetics (e.g. Glynn et al., 2015) and biophysical modelling (e.g. Chen et al., 2014). Some studies have used a multidisciplinary approach, combining genetic analyses with biophysical modelling (e.g. Dawson et al., 2005; Lee et al., 2013). Biophysical modelling is unique among the listed techniques. In addition to elucidating population structures, the models allow

users to identify the causal biological, geographic and hydrodynamic mechanisms that shape the structures (e.g. Fossette et al., 2015).

Biophysical modelling has not yet been applied to investigate the population structures of cubozoan species. The strong swimming and orientation abilities documented in cubomedusae would need to be accurately represented in biophysical models before the movements, and thereby the population structures, of cubozoans could be simulated accurately. However, the data needed to produce an accurate behavioural model have not yet been collected for most cubozoans (Table 1.1, Table 1.2, Kingsford and Mooney, 2014).

The broad objective of this PhD was to improve our understanding of how cubozoan populations are structured. This was principally achieved by collecting data on the behaviours and swimming capabilities of cubomedusae and incorporating these data into biophysical models of their movements. The research focused on medusae from two species of cubozoans inhabiting environments with different levels of physical openness. Further, the two species differed greatly in size and behaviour. The specific aims, by chapter, were to:

Chapter 2. determine if the population of the large, venoms box jellyfish *C. fleckeri* inhabiting Port Musgrave, a semi enclosed estuarine bay in Queensland, Australia, represents a stock with substructure.

Chapter 3. quantify the behaviours and swimming capabilities of medusae from the small, non-venomous cubozoan *C. sivickisi*, and elucidate their related distribution on a reef fringing the relatively exposed/open nearshore island Magnetic Island, Queensland, Australia.

Chapter 4. determine if the *C. sivickisi* population inhabiting Magnetic Island, which lies 8 km offshore of the mainland, represents a structured stock that is isolated from any mainland populations.

Chapter 2.

Swimming behaviour can maintain localised jellyfish (*Chironex fleckeri*: Cubozoa) populations

INTRODUCTION

Most cubozoan jellyfishes inhabit coastal or reefal waters in the tropics, putting them in close proximity to humans. This is particularly true for chirodropids such as *Chironex fleckeri*, which is only found close to shore in a few metres of water (Gordon and Seymour 2009, Kingsford and Mooney 2014). *C. fleckeri* and the Irukandji jellyfishes have extremely potent venom and stings can be fatal (Fenner 2005). Additionally, publicity following stinging events can cause a drop in tourism revenue (Gershwin et al. 2010). Despite the threat they pose to humans, cubozoans are an understudied taxa and we know little about their population ecology (Kingsford and Mooney 2014).

Cubozoans have a bipartite life history, with a benthic polyp phase and a pelagic medusa phase. *C. fleckeri* polyps are thought to reside in estuaries during the dry season and metamorphose into medusae with the onset of the wet season (Hartwick 1991a). Polyps may also inhabit coastal waters (Mooney and Kingsford 2012). The presence of medusae is highly seasonal (Gordon and Seymour 2012, Kingsford and Mooney 2014), with metamorphosis from polyps occurring throughout the medusae season (Gordon and Seymour 2012). As medusae are pelagic and highly mobile, they have a greater potential for dispersal than the earlier life history stages (from the zygotes to the recently metamorphosed juvenile medusae; Hartwick 1991a).

Scales of connection between cubozoan populations within their geographic ranges are unknown. A metapopulation often corresponds with the biogeographic range of the species (Sinclair 1988, Kingsford and Battershill 1998) and is made up of a collection of mesopopulations (often called 'stocks' in a fisheries context; Kingsford et al. 2000). In turn, stocks can be made up of connected 'local populations' (Kingsford and Battershill 1998). It is assumed that robust stocks have limited exchange among them and that the size of these stocks would largely depend on intrinsic factors such as reproductive output, recruitment, growth and mortality (Sinclair 1988).

For *C. fleckeri*, there may be one or more metapopulations in the species biogeographic range, which includes South east Asia and Northern Australia (Bentlage

et al. 2009). The identity of stocks is yet to be determined, but *C. fleckeri* medusae inhabit spatially complex regions, including winding coastlines, nearshore islands, estuaries and embayments. In these environments, oceanographic processes such as trapping in shallow waters and the limited flushing of bays have the potential to keep populations of medusae separate from each other (e.g. Pitt and Kingsford 2000, Mooney and Kingsford 2016a, 2017). Such processes, in combination with the high mobility of medusae (Gordon and Seymour 2009), may limit immigration and emigration between populations. Mooney and Kingsford (2016a, 2017) recently presented evidence that the elemental signatures and shapes of statoliths in *C. fleckeri* medusae varied at spatial scales of tens to hundreds of kilometres. They concluded that local populations and even stocks may be divided at surprisingly small spatial scales. An understanding of behavioural ecology and local oceanography would help to explain these patterns.

Other approaches have been used to determine levels of connectivity among population units of jellyfishes including demographics (e.g. Pitt and Kingsford 2000), genetics (e.g. Dawson 2005, Glynn et al. 2015, van Walraven et al. 2016) and biophysical modelling (e.g. Johnson et al. 2005, Barz et al. 2006, Chen et al. 2014, Wei et al. 2015). Each of these techniques, individually or in combination, can assist in estimating connectivity in ecological and evolutionary time. Marine biophysical models couple hydrodynamic and behavioural models. They are increasingly being used to examine the connections between populations (e.g. Bode et al. 2019, Swearer et al. 2019). Biophysical models of jellyfish have largely simulated medusae as passive medusae (e.g. Moon et al. 2010) or with only simple vertical migration behaviours (e.g. Berline et al. 2013, Wei et al. 2015, Wu and Xu 2016). Medusae have rarely been modelled with horizontal swimming behaviour. Notably, Fossette et al. (2015) modelled *Rhizostoma octopus* with horizontal swimming behaviour and demonstrated that this behaviour was integral to the maintenance of blooms.

The inclusion of behaviour is critical if the organisms being modelled have the capacity to influence their dispersion (Simpson et al. 2013, Wolanski and Kingsford 2014, Fossette et al. 2015); this is certainly the case for *C. fleckeri* medusae as they are highly mobile and have sophisticated sensory systems. *C. fleckeri* are the largest cubozoans in the world (Kingsford and Mooney 2014). They have sensory receptors including statocysts for balance and complex eyes that enable orientation (Coates and Theobald 2003, Nilsson et al. 2005). Hamner et al. (1995) demonstrated avoidance behaviour in *C. fleckeri*, where medusae swam away from black objects placed at the

ends of tanks and manoeuvred around black pipes distributed throughout tanks. Medusae ranging in size from 4.5 to 10 cm bell diameter have been recorded swimming at velocities ranging from 3.6 to 11.5 cm s⁻¹ in a laboratory setting (Shorten et al. 2005). Colin et al. (2013) analysed video of four *C. fleckeri* medusae, with interpedalial distances of 2 to 16 cm; the medusae swam at maximum speeds of 5 to 12 cm s⁻¹. Furthermore, medusae ranging in size from 9 to 17.5 cm interpedalial distance have been recorded travelling hundreds of metres to kilometres within a day in the wild, and there is some evidence from tagged individuals that they stay within tens to hundreds of metres from the shore (Gordon and Seymour 2009).

There is, however, an inherent risk associated with living in shallow coastal waters, namely rapid decreases in salinity from local runoff. The sensitivity of *C. fleckeri* to low salinities has been demonstrated in several studies. Hartwick (1991a) documented the collapse of a population of *C. fleckeri* polyps which coincided with the arrival of freshwater runoff following heavy rain. Kingsford et al. (2012) sampled cubozoan medusae over three seasons and found *C. fleckeri* medusae were rare or absent when riverine discharge was high. Mooney and Kingsford (2016b) demonstrated experimentally that *C. fleckeri* medusae were incapacitated at salinities between 21 and 16 Practical Salinity Units (PSU), and the medusae mortality rate was greater than 50% at salinities less than 16 PSU. Further, Llewellyn et al. (2016) attracted medusae to lights and recorded their occurrence over 5 years. In the summer months, *C. fleckeri* were never recorded at salinities below 25.2 PSU, although monsoonal rains periodically reduced the salinity to as low as 17.7 PSU. Freshwater pulses, therefore, may affect the size and persistence of *C. fleckeri* populations.

The objective of this study was to apply a biophysical model to determine if *C. fleckeri* medusae can maintain localised populations at medium (tens kilometres) to small (hundreds of metres) spatial scales. The specific aims were to: (1) quantify the swimming speed and behaviour of medusae in relation to the currents, obstacles and the shoreline; (2) generate a biophysical model to determine the importance of medusae mobility in maintaining localised populations; (3) sequentially vary the parameters in the biological component of the biophysical model to verify the reliability of the modelling results; (4) determine the threat that pulses of fresh water from storm events can pose to populations of medusae, and identify strategies medusae could use to survive such events.

MATERIALS AND METHODS

Study site

The study site was Port Musgrave, Cape York Peninsula. Port Musgrave is a ~ 17 x 21 km shallow bay, with a maximum depth of ~ 12 m (Fig. 2.1 c). The bay is semi-enclosed, with a narrow ~ 3.5 km mouth which, along with many other bays, opens into the Gulf of Carpentaria in the tropical north of Australia. Behavioural studies of *Chironex fleckeri* were done at Red Beach Mapoon within Port Musgrave (12°01'7.43"S, 141°54'17.78"E).

Swimming velocity and behaviour of jellyfish

The swimming speed and behaviour of *C. fleckeri* was determined for medusae ranging in size from 4 to 12 cm interpedalial distance. Observations on a total of 22 jellyfish were made from 12 to 14 December 2015 at a sandy beach near mangrove habitat when the tide was high; medusae were in shallow water < 0.5 m deep. Swimming speeds were determined by placing the weighted end of a transect tape near each medusa without disturbing it. An observer then walked parallel and slightly behind the medusa, with a separation distance of approximately 3 m. None of the medusae overtly reacted to the presence of the observer. The tape was used to measure the distance travelled in 30 s intervals for 2 to 10 minutes. Medusae generally swam parallel to the edge of the beach. Trials were discontinued after a minimum of 2 minutes when jellyfish disappeared due to poor visibility or, in one case, when a medusa veered seaward into water over one metre deep. The mean current velocity was then determined by measuring the distance a natural float (e.g. submerged leaf or seagrass fragment) travelled through time ($n = 2$ medusa⁻¹). The swimming orientation of the medusa with respect to the current and the beach was noted. The swimming velocity over ground was determined from the swim speed and orientation. The velocity through water was calculated by subtracting the current velocity from the velocity over ground when the medusae swam with the current and calculated by adding the current velocity if they swam against it.

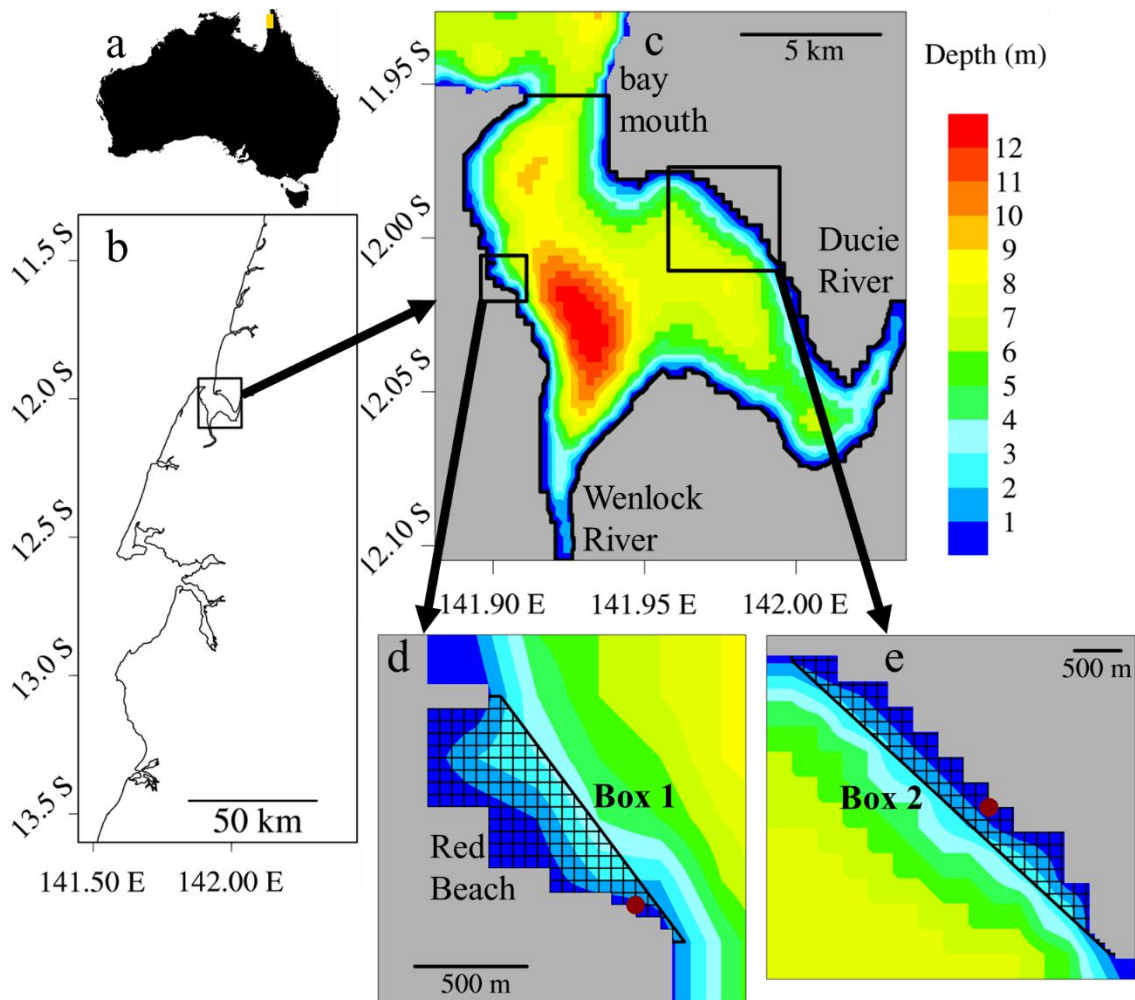


Fig. 2.1. Study site. (a) Australia; (b) detailed view of the west coast of Cape York Peninsula, which contains multiple estuarine systems including Port Musgrave; (c) bathymetry of Port Musgrave. The number of *Chironex fleckeri* remaining nearshore in the biophysical modelling scenarios were counted in (d) Box 1 on the west side of the bay (adjacent to Red Beach) and (e) Box 2 on the east side of the bay. Medusae were seeded from the locations marked by the red circles

The avoidance behaviour of *C. fleckeri* medusae was investigated experimentally using medusae ranging in size from 3 to 11 cm interpedalial distance. *C. fleckeri* were observed from 14 to 16 December 2016. There were two treatments in the design: (1) with obstruction and (2) a control without an obstruction. For treatment 1, the paths of seven medusae were obstructed by an observer who stood 2 to 6 m in front of them. The observer estimated the distance at which the medusa performed an avoidance manoeuvre and the angle of deviation. For treatment 2, seven unobstructed medusae were observed to determine natural deviations in swimming direction. These medusae were observed for up to 6 minutes and the distance they travelled in a straight course

was estimated. A course was considered straight if it deviated $\leq 20^\circ$ from the initial heading.

Biophysical modelling

The biophysical model of Port Musgrave consisted of a hydrodynamic model coupled with a dispersion model that incorporated medusae swimming behaviour. The hydrodynamic model of Wolanski and Kingsford (2014) was used to simulate the circulation in Port Musgrave. It is a two dimensional (depth-averaged) finite-difference model which solves the Navier-Stokes equations (Black et al. 1991). Two dimensional depth averaged models realistically recreate observed currents in shallow, vertically well mixed waters (Lambrechts et al. 2008). The waters of Port Musgrave are shallow and vertically well mixed in dry conditions (Wolanski et al. 1986, present study), justifying the use of a two-dimensional model to simulate the currents in the bay. The Port Musgrave region gets little rain in the dry season (May to November), which intersects the start of the *C. fleckeri* season in northern Australia (October to April). Wolanski (1986) measured vertical temperature and salinity profiles at different stations in Port Musgrave during the dry season and found the bay waters were well mixed. In this study, a Conductivity Data Logger (HOBO U24-002-C) was similarly used to measure vertical temperature and salinity profiles in Port Musgrave at the beginning of the wet season (15 and 16 December 2016). There had been little rain in the watershed in the week preceding the salinity measurements. The profiles were measured along a transect from Red Beach, across the middle of the bay and to the other side, and the waters were found to be well mixed at each of the sampled locations along the transect (see results).

The model was forced with tides and wind. The mouth of the bay was the seaward open boundary. Port Musgrave faces the Gulf of Carpentaria where the longshore currents in coastal waters are weak (Wolanski 1993); further, the mouth of Port Musgrave is narrow. I assumed, therefore, that the longshore currents in the gulf have little influence in Port Musgrave. Port Musgrave has mixed semi-diurnal tides that alternated between spring (12 December 2015), average (waxing crescent moon, 17 December 2015), and neap (19 December 2015) phases. These three tidal scenarios were reconstructed from the predictions of the software AusTide 2015 version 1.10.1 and forced at the seaward open boundary. The average wind measured at Weipa Airport (12°40'40.08"S, 141°55'14.88"E ~ 70 km from Port Musgrave) over 10 jellyfish

seasons (from 2005/06 to 2014/15) was $2.63 \text{ m s}^{-1} \pm 1.92 \text{ SD}$ and the average wind direction was from the east (89.14°). These average conditions were imposed as a constant wind to force all model scenarios. I ran models with and without a wind shadow area on the leeward side of the bay (east). As wind shadow had little effect on the dispersion of medusae, wind shadow was not included in the scenarios presented in the study. The wind data were provided by the Australian Government Bureau of Meteorology.

The bathymetry data were derived from the Geoscience Australia, Australian Bathymetry and Topography 2009 data set which has a resolution of $\sim 250 \text{ m}$. A bi-linear interpolation was performed on the bathymetry data to increase the resolution to 55 m for use in the model. The hydrodynamic model had a time step of 2 s and the output was saved every 30 min and used to run the advection-dispersion model.

Medusae were seeded as particles in the advection-dispersion model. It was assumed that the medusae exported seaward out of Port Musgrave were unable to return to the bay. It was also assumed that the medusae that advected onto dry cells beached and died, though this is very conservative as the behaviour of medusae suggests that beaching is unlikely. Medusae were either set to be passive (behaviour A) or to swim according to assigned behaviours (behaviours B and C; Fig. 2.2). The behaviours were assigned using scalar fields. Separate fields were generated for behaviour in the X (perpendicular to the shore) and Y (parallel to the shore) directions. The value of each cell in the field designated the direction medusae would swim when in that cell. For behaviour B, medusae were made to swim back and forth in the Y direction, as they were observed doing at Red Beach. This was achieved by generating random numbers between 0 and 1 at each cell in the scalar field. If the number was < 0.5 the medusae were made to swim south, otherwise they swam north. In the X direction, medusae swam back toward the shore. This behaviour was included because a combination of prevailing currents and behaviour can disperse medusae hundreds of metres to kilometres within a day (Gordon and Seymour 2009). If medusae did not swim directionally toward the shore, they would be dispersed seaward into deeper waters where stronger currents persist (Appendix AI, Fig. AI.3), contradicting their observed distribution in predominantly shallow waters, less than a few hundred metres from the shore (Gordon and Seymour 2009, Kingsford and Mooney 2014). In the first line of wet cells, which surround the coastline, medusae were set to swim away from the shore to avoid beaching. A new condition was added to behaviour B to generate behaviour C. Medusae were seeded in small bays that had a U shape. For behaviour

C, when they reached the ends of these bays and encountered mangroves they were made to perform a 180° turn and swim back into the bays. This behaviour represents the avoidance response I document in this paper and our findings concur with the observations of Hamner et al. (1995) of *C. fleckeri* avoiding obstacles, with directional reversals of up to 180°. The responses I documented are also consistent with the considerable avoidance and orientation capabilities documented in other cubozoan species (Garm et al. 2007, 2011). Behaviours B and C were only carried out within the first 5 cells from shore, which corresponded to ~ 275 m. This is conservative given that Gordon and Seymour (2009) observed a medusa staying within 300 m of the shore over a 26 hour period (Appendix AI, Fig. AI.3).

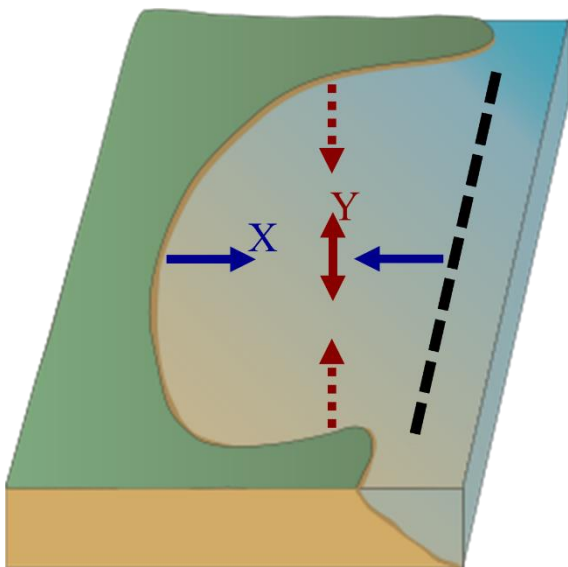


Fig. 2.2. Schematic of the *Chironex fleckeri* medusae behaviours included in the biophysical model. Red arrows: behaviours in the Y direction; blue arrows: behaviours in the X direction. Solid arrows: swimming behaviours included in Behaviour B (swimming back and forth, parallel to shore, in the Y direction, and swimming to shore and avoiding beaching in the X direction); Dashed arrows: additional behaviour included in Behaviour C (avoidance behaviour, with a directional reversal of 180° in the Y direction). Behaviours were only carried out if medusae were within the behavioural band, as denoted by the blank dashed line

The movement of medusae was calculated as the sum of three vectors: the water velocity, the swimming velocity, and a random diffusion vector representing horizontal turbulent mixing at sub-grid scales (Paris et al. 2002). The average swimming velocity through water calculated for the *C. fleckeri* observed in this study ($5.3 \text{ cm s}^{-1} \pm 3.5 \text{ SD}$) was used in the model as it best represents the swimming capabilities of medusae in

the size range sampled. The behaviour of medusae determined the swimming direction. The random diffusion vector was calculated as a Markov diffusion process, parameterized by the horizontal diffusion coefficient k_x , following Spagnol et al. (2002). The exact value of k_x is unknown. For a grid size of 55 m, $k_x \sim 0.02 - 0.17 \text{ m}^2 \text{ s}^{-1}$ (Okubo 1971, Wolanski 1992).

In scenarios 1 – 9 (listed in Table 2.1), all combinations of tide and behaviour were modelled to determine how patterns of dispersion vary by condition. Medusae were seeded from Red Beach where the biological data were collected, and from another site on the opposite side of the bay (Fig. 2.1 d, e). A total of 25,000 simulated medusae were seeded per site. The scenarios were run for 14 days to determine the degree to which jellyfish were retained within the system. No river discharge was simulated in these scenarios, which is realistic given the flow rates of the Wenlock and Ducie Rivers are often $< 10 \text{ m}^3 \text{ s}^{-1}$ for extended periods of time during the medusae season (Appendix AI, Fig. AI.1 and Fig. AI.2).

Relative importance of swim speed and the width of the behaviour band

The robustness of our outcomes from the model were tested with a sensitivity analysis (SA). A series of model scenarios (SA1 – SA9; Table 2.2) were run, each having the same hydrodynamic forcings of average tide and wind, and no river outflow. Run SA5 was the standard run, in which behaviour C medusae were set to swim at the average speed measured in the field and could implement a behavioural response within ~ 275 m from the shore, as in scenario 8 (Tables 2.1 and 2.2). The behavioural parameters in the other runs were changed as follows. One standard deviation was either added to or removed from the swim speed, making it 1.8 or 8.8 cm s^{-1} respectively. The width of the behaviour band was either 'halved' to three cells (~ 165 m) or doubled to ten cells (~ 550 m). All combinations of swim speed and behaviour band width were modelled. The sensitivity analysis runs are listed in Table 2.2 and they address specific aim 3 (see final paragraph of the Introduction). They were analysed separately from the model scenarios listed in Table 2.1, which address the specific aims 2 and 4.

Table 2.1. Modelled scenarios and results. The tidal forcing, the modelled behaviour of the *Chironex fleckeri* medusae (A, B or C; Fig. 2.2), the simulated discharge from the Wenlock and Ducie rivers ($0 \text{ m}^3\text{s}^{-1}$ for the 'No flood' scenarios, $1000 \text{ m}^3\text{s}^{-1}$ from each river for the 'Flood' scenarios), the diffusion coefficient (kx), the duration of the model run and the percentage of modelled medusae remaining in Boxes 1 and 2 (see Fig. 2.1d,e), and in Port Musgrave are shown. Medusae are passive in behavioural model A. Behavioural model B includes 3 behaviours: swimming back and forth, parallel to shore, swimming to shore and avoiding beaching. Behavioural model C includes an additional avoidance behaviour, where model medusae perform a 180° turn when they encounter mangroves at bay edges

Scenario no.	Tide	Behaviour	Discharge ($\text{m}^3 \text{ s}^{-1}$)	kx	Days	% Box 1	% Box 2	% bay
No flood								
1	Spring	A	0	0.02	14	2.3	0	100
2	Avg	A	0	0.02	14	1.1	0	100
3	Neap	A	0	0.02	14	3.2	0	100
4	Spring	B	0	0.17	14	65.4	0.6	94.8
5	Avg	B	0	0.17	14	73.2	0.5	97.6
6	Neap	B	0	0.17	14	68.3	0.6	99.0
7	Spring	C	0	0.17	14	60.8	89.0	95.7
8	Avg	C	0	0.17	14	68.3	81.6	98.4
9	Neap	C	0	0.17	14	63.4	84.7	99.6
Flood								
10	Avg	A	1000	1	5	1.1	7.1	79.2
11	Avg	C	1000	1	5	14.8	56.3	79.8

Table 2.2. Sensitivity analysis (SA) scenarios and results. All sensitivity analysis scenarios had the same hydrodynamic forcings (average tide and wind, and no river outflow). 25000 behaviour C medusae were seeded from Red Beach and another site on the opposite side of the bay, respectively (Fig. 2.1d,e). The parametrisation of the C set of behaviours for simulated *Chironex fleckeri* medusae was sequentially altered. The C set includes 4 behaviours: swimming back and forth, parallel to shore, swimming to shore, avoiding beaching and performing a 180° turn upon encountering mangroves at bay edges (Fig. 2.2). The width of the behaviour band (BB) and the modelled swimming speed of the *C. fleckeri* medusae in the SA scenarios are indicated. The percentage of modelled medusae remaining in Boxes 1 and 2 (see Fig. 2.1d,e), and in Port Musgrave at the end of the 14 day runs are shown

Scenario no.	BB width (m)	Speed (cm s ⁻¹)	% Box 1	% Box 2	% bay
SA1	165	1.8	4.3	0.9	99.5
SA2	165	5.3	3.2	1.3	99.0
SA3	165	8.8	7.1	3.6	99.6
SA4	275	1.8	24.3	10.7	97.1
SA5/Scenario 8	275	5.3	68.3	81.6	98.4
SA6	275	8.8	32.6	93.6	99.7
SA7	550	1.8	67.5	31.1	99.5
SA8	550	5.3	96.7	99.9	100
SA9	550	8.8	93.3	100	99.9

Fresh water pulse flood events

Port Musgrave is in tropical north Queensland and the region gets monsoonal rain in the wet season (December to April). The wet season overlaps with the northern *C. fleckeri* season (October to April). It was hypothesised that pulses of freshwater into the bay during the wet season would pose a threat to *C. fleckeri* medusae through increasing their seaward export and decreasing the salinity of the bay water. A decrease in salinity could be fatal given the sensitivity of *C. fleckeri* medusae to low salinities (Mooney and Kingsford 2016b).

To investigate these hypotheses, flood conditions were simulated in Port Musgrave in scenarios 10 and 11 (Table 2.1). The average tide and wind were used to force the hydrodynamic model. Freshwater pulses from the Wenlock and Ducie rivers, which

discharge into Port Musgrave, were added as current fluxes at open boundaries imposed where the model boundary intersected the rivers. Flow rate data for the Wenlock were recorded at Jacks Camp (12°24'32.5"S, 142°18'16.9"E; ~ 102 km from the river mouth) between March 1971 and May 1988. Flow rate data for the Ducie were recorded at Bertiehaugh (12°07'37.4"S, 142°22'31.6"E; ~ 55 km from the river mouth) between December 1968 and September 1988. These data were sourced from the Queensland Government water monitoring information portal (<https://water-monitoring.information.qld.gov.au/>). A discharge of 1000 m³s⁻¹ from both rivers for 5 days was identified as a realistic wet season flood event (Appendix AI, Fig. AI.1 and Fig. AI.2) and was simulated in the flood scenarios.

The seaward export of simulated *C. fleckeri* medusae under flood conditions was assessed by releasing passive and behaviour C medusae from both the east and west sides of Port Musgrave (Fig. 2.1). 25,000 simulated medusae were released per side and per behavioural model. During storm events that generate floods, there is greater capacity for diffusion given the increased turbulence in the system (Wolanski and Elliott 2015). Consequently, the horizontal diffusion coefficient, k_x , which was used to calculate the sub-grid scale diffusion of model medusae, was increased from 0.02/0.17 (dry conditions values; Okubo 1971, Wolanski 1992) to 1 m² s⁻¹ in the flood scenarios. The simulated medusae with behavioural set C were modelled to swim at the average speed within an approximately 275 m wide band adjacent to the shore.

The change in the salinity of the bay waters as the flood plumes moved into Port Musgrave was then modelled. Passive particles were continuously released from the open river boundaries over the 5-day runs. After 5 days, it was assumed that the middle of each river plume contained fresh water, with a salinity of 0 PSU, as demonstrated in the flood plumes of tropical estuaries following heavy river discharge (Chevalier et al. 2014). It was assumed that cells containing no simulated water particles had a salinity equal to the salinity measured at Red Beach in dry conditions. This measure was taken using a conductivity, temperature and depth device (CTD; Seabird SBE 19 Plus) on 16 December 2015, when the watershed had received little rain in the preceding week. The salinity was 35.57 PSU ± < 0.01 SD (n = 2). The salinity of the simulated flood plume was then assumed to increase linearly with decreasing particle concentration, from the particle concentration corresponding to 0 PSU to the absence of particles which was estimated to be 35.57 PSU.

The intrusion of flood plumes into estuarine/marine systems is a three-dimensional process which was modelled in two dimensions in this study. The fresh water from

river floods floats on the denser, more saline estuarine/marine waters, stratifying the water column (Wolanski and Elliott 2015). This breaks down the steady state in which two-dimensional models perform reliably (i.e. vertically well mixed waters). Two-dimensional models specifically cannot capture the buoyancy driven flow components which are generated by the density gradient in the stratified water column. The two-dimensional modelling of flood plumes presented in this study, therefore, could not fully capture the complexity of either the water flow in flood conditions or the development of the flood plume. The modelling results should be interpreted accordingly. This note of caution is reiterated in the discussion.

Data analysis

It was possible that the swimming speed of jellyfish would vary with size. Accordingly, the relationship between medusa interpedalial distance and average swim velocity through water was tested using a Spearman's rank correlation because the data did not meet the assumption of the Pearson's correlation of a bivariate normal distribution.

Retention on a medium spatial scale (i.e. whole bay) was compared between scenarios by counting the number of medusae remaining in Port Musgrave at the end of each of the model runs. Furthermore, retention on a small spatial scale was compared between scenarios by tracking the number of simulated jellyfish remaining in the small bays where they were seeded. The number of medusae remaining in water generally < 3 m deep were counted in Box 1 (~0.5 km²; Fig. 2.1 d) on the west side of the bay and Box 2 (~1.9 km²; Fig. 2.1 e) on the east side of the bay.

RESULTS

Observed swim velocity and behaviour

Observed *Chironex fleckeri* medusae swam at an average velocity through water of 5.3 cm s⁻¹ ± 3.5 SD while being tracked (167 time intervals for n = 22 jellyfish). The swim speeds of tracked individuals varied through time (e.g. Fig. 2.3 a), and medusae may have altered their speed to avoid hitting the bottom or the water surface. Overall, the swimming performance of the jellyfish was about two times faster than the average measured current velocity near the beach of 2.7 cm s⁻¹ ± 2.4 SD (n = 40). Current

speeds were low but varied from 0 to 10 cm s⁻¹. Current speeds along the beach varied according to an interaction between small waves (< 5 cm high) and minor deviations in the beach shape. Faster currents were ‘mini rips’ that generally only affected a few metres of beach.

There was a poor but significant negative correlation between medusa interpedalial distance and their average measured swim velocity through water (Spearman’s rank correlation, $r_s = -0.44$, $z_{(2)} = -2.03$, $P < 0.05$, $n = 22$). Medusae ranging in size from 4 to 8.5 cm interpedalial distance had an average swim velocity through water of 7.0 cm s⁻¹ ± 3.2 SD (Fig. 2.3 b). Larger medusae, ranging in size from 9 to 12 cm interpedalial distance, had a slower average swim velocity through water of 3.9 cm s⁻¹ ± 2.1 SD. The smallest individual observed in this study had an interpedalial distance of 4 cm and swam at a maximum speed of 6.5 cm s⁻¹. The fastest speed for an individual within a 30 second interval was 16.6 cm s⁻¹, recorded for a medusa with an interpedalial distance of 6 cm.

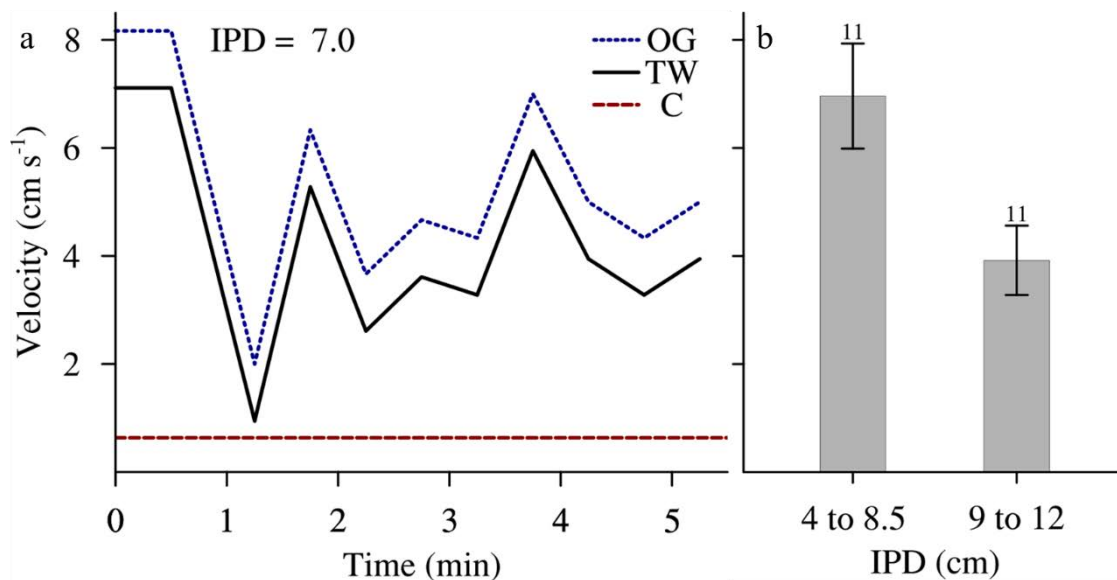


Fig. 2.3. (a) Velocity of an individual observed *Chironex fleckeri* medusa through time, showing the current velocity (C), the velocity over ground (OG) and the velocity through the water (TW). (b) Average (± SE) velocity through water of observed medusae grouped by interpedalial distance (IPD). The number of medusae in each size class are shown above the error bars

Of the 22 observed medusae, 21 initially tracked along the beach, 40.91% were swimming with the longshore current and 54.55% were swimming against it. Only one medusa (4.55%) was initially swimming perpendicular to the longshore current, away from shore.

Medusae performed avoidance manoeuvres when they encountered an obstruction (the observer). The average distance of response was of $1.4 \text{ m} \pm 0.4 \text{ SD}$ from the observer. Medusae altered their heading by an average of $83^\circ \pm 47 \text{ SD}$ (range 45° to 180°). In the control treatment, without an obstacle, observed medusae maintained a straight course parallel to the beach for an average distance of $8.1 \text{ m} \pm 5.6 \text{ SD}$.

Hydrodynamics of Port Musgrave

The hydrodynamic model revealed significant current shear, where the currents increased with distance from shore. For example, from Red Beach at peak ebb during the average tide, the simulated currents increased along a transect, from 0.5 cm s^{-1} 55 m from shore to 7.8 cm s^{-1} 550 m from shore (Fig. 2.4). The waters of Port Musgrave were measured at the beginning of the wet season, and found to be well mixed. In waters shallower than 5 m, the measured variation in temperature of the water column was $< 0.53 \text{ }^\circ\text{C}$ and salinity was $< 0.31 \text{ PSU}$. In waters greater than 5 m and to a depth of 10.8 m, the temperature varied by $< 0.27 \text{ }^\circ\text{C}$ and the salinity varied by $< 0.45 \text{ PSU}$. In dry conditions, the simulated tidally-averaged net circulation consisted of an inflow over the shallows and an outflow in the deeper waters around the axis of the bay. The simulated inflow took $\sim 10\text{-}14$ days to reach the headwaters. This same amount of water exits the bay in the deeper parts, which are typically three times the depth of the shallows. Because mass is conserved the outflow would take three times longer, $\sim 30\text{-}42$ days. Thus, in dry conditions, the simulated residence time of Port Musgrave is $\sim 40\text{-}56$ days.

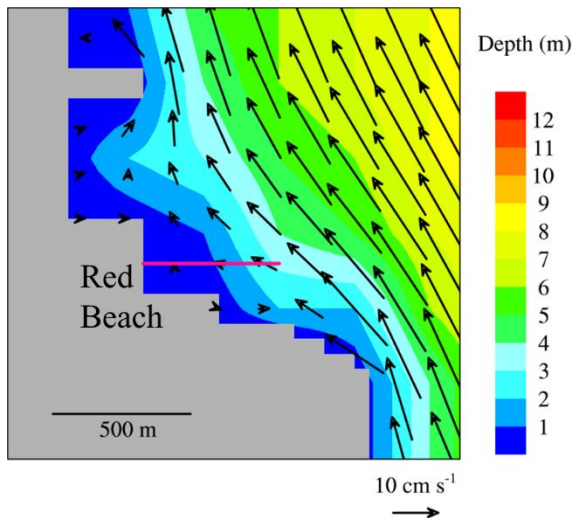


Fig. 2.4. Modelled velocity field at Red Beach (see Fig. 2.1d) at peak ebb tide. Velocities were reported from the ends of the transect shown with the pink line

Simulated retention – dry conditions

In all modelled behavioural scenarios, the net current transported some simulated medusae from the west side to the east side of Port Musgrave (Fig. 2.5). At both medium (kilometres) and small scales (i.e. individual beaches, tens to hundreds of metres) the tidal conditions made little difference to the level of retention. The numbers of simulated medusae remaining in Port Musgrave after 14 days were similar among the different tidal scenarios and similar numbers were retained in Boxes 1 and 2 through time (Fig. 2.6 a, c, Table 2.1).

At a spatial scale of tens of kilometres, no simulated medusae were lost from Port Musgrave after 14 days when they were treated as passive particles in dry conditions (no flood, behaviour A; scenarios 1-3; Table 2.1). Very low loss rates were found when behaviour was included: less than 5.2% of the behaviour B medusae were lost (scenarios 4-6) and $\leq 4.3\%$ of the behaviour C medusae were lost (scenarios 7-9).

At a smaller spatial scale (hundreds of metres), passive medusae (scenarios 1-3) were quickly advected away from the release points on both the west and east sides of the bay (Figs. 2.5 and 2.6 a, c). After 14 days, few were retained in Box 1 ($< 3.2\%$) and no medusae were in Box 2 (Table 2.1).

The behaviour of the simulated medusae had a great influence on near shore retention. On the west side of the bay $> 50\%$ of behaviour B medusae (scenarios 4-6) were initially advected out of Box 1, but they swam back into the small bay over the

course of a few days. At the end of 14 days, between 65.4 and 73.2% remained. In contrast, behaviour B medusae were quickly advected from Box 2 on the east side of the bay with only between 0.5 and 0.6% remaining after 14 days. The net current advected the medusae plume south and medusae were subsequently retained in high numbers at some sheltered locations on the jagged eastern coastline, < 5 km from Box 2. The addition of avoidance behaviour slightly decreased retention in Box 1. Again, over 50% of medusae (behaviour C, scenarios 7-9) were initially advected out of the Box but they quickly swam back in and between 60.8 and 68.3% remained after 14 days. The retention in Box 2 greatly improved when avoidance behaviour was included, with between 81.6 and 89% remaining at the end of the 14 day run.

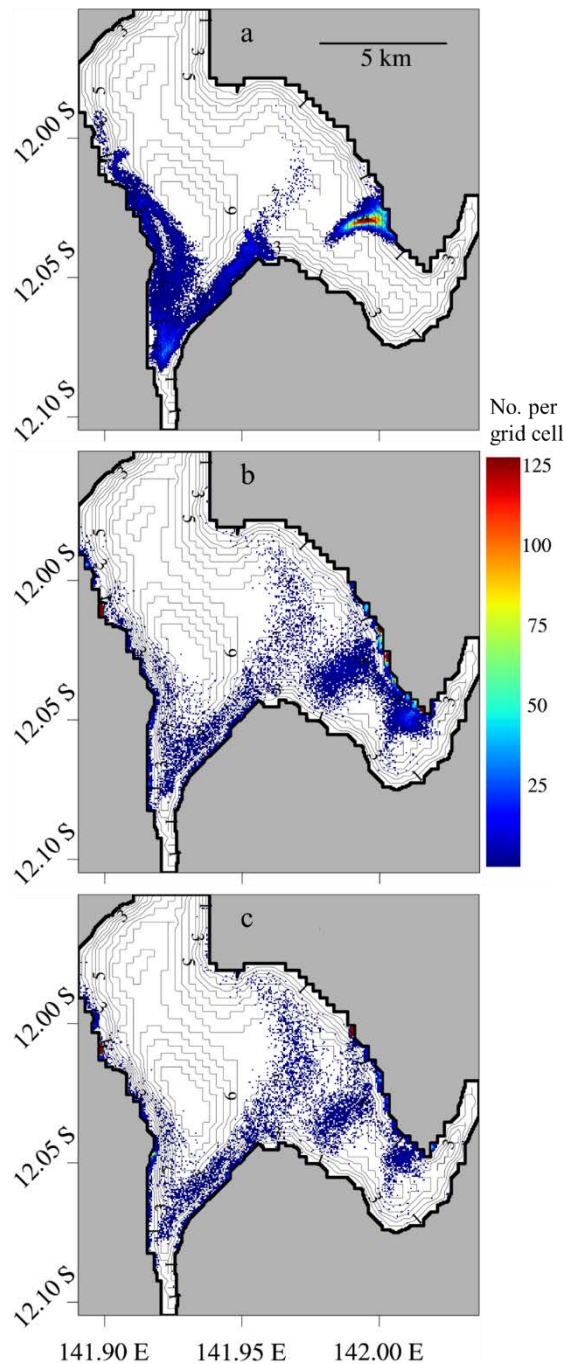


Fig. 2.5. Number of *Chironex fleckeri* medusae per grid cell with (a) Behaviour A (passive; scenario 2), (b) Behaviour B (scenario 5) and (c) Behaviour C (scenario 8) at the end of the model runs. Behavioural model B includes 3 behaviours: swimming back and forth, parallel to shore, swimming to shore and avoiding beaching (Fig. 2.2). Behavioural model C includes an additional avoidance behaviour, where model medusae perform a 180° turn when they encounter mangroves at bay edges. Runs lasted for 14 d after the particles had been released from the seed locations (see Fig. 2.1d,e). The model was forced with average tides. No freshwater outflow from the rivers were included (i.e. 'no flood'; Table 2.1). Depth contours are indicated

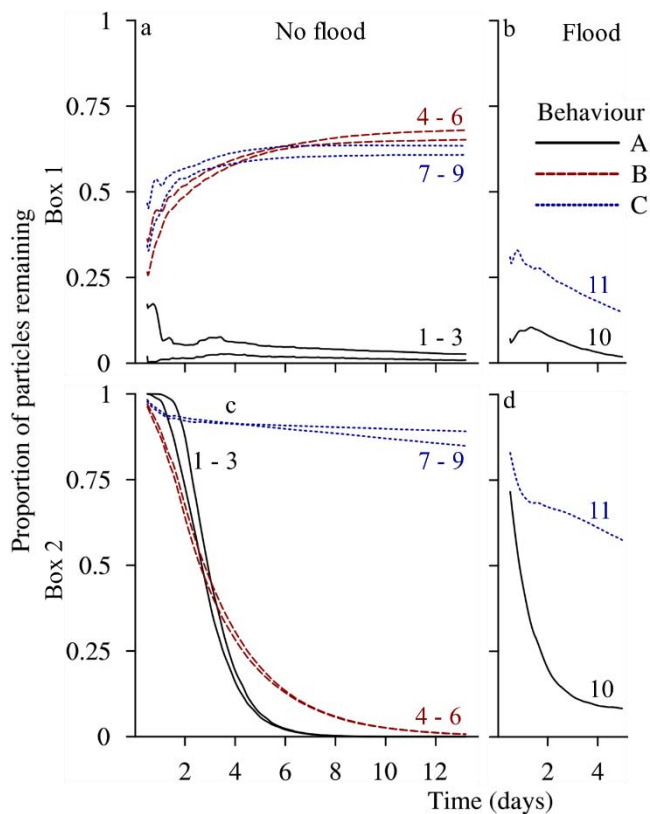


Fig. 2.6. Proportion of simulated *Chironex fleckeri* medusae remaining near shore through time for the modelling scenarios listed in Table 2.1. A 24 h running average was performed on the raw data to remove tidal variability. Scenario numbers are shown. (a) Retention in Box 1 (see Fig. 2.1d), no flood scenarios; (b) Box 1, flood scenarios; (c) retention in Box 2 (see Fig. 2.1e), no flood scenarios; (d) Box 2, flood scenarios. For the no flood scenarios, the 2 lines for each behavioural category show the range of proportions obtained among the different tidal forcings. Medusae are passive in behavioural model A. Behavioural model B includes 3 behaviours: swimming back and forth, parallel to shore, swimming to shore and avoiding beaching (Fig. 2.2). Behavioural model C includes an additional avoidance behaviour, where model medusae perform a 180° turn when they encounter mangroves at bay edges. Active medusae (Behaviours B and C) swam at 5.3 cm s⁻¹ (average) and performed the prescribed behaviours within a 275 m band from shore

Behavioural model sensitivity analysis

At the medium spatial scale of the whole bay, the simulated retention was > 97% in all scenarios (Table 2.2). At the small spatial (hundreds of meters, nearshore waters), retention of simulated medusae was high in the standard run (SA5), where medusae were set to swim at the average speed and make behavioural responses within an intermediate distance from shore (Fig. 2.7 c, d, Table 2.2). In Box 1, on the west side of the bay, 68.3% of medusae remained after 14 days. Retention was even higher in

Box 2, on the east side of the bay, where 81.6% of medusae remained, although medusae were slowly lost through time.

Reducing the behaviour band width and swim speed below the standard parameterisation was detrimental for retention. The number of simulated medusae remaining in nearshore waters declined through time when the behaviour band width was 165 m, the narrowest setting, irrespective of the swim speed (Fig. 2.7 a, b, SA1-SA3). Loss of medusae was rapid in these scenarios, with $\leq 7.1\%$ remaining in either Box after 14 days. The number of simulated medusae remaining near shore through time did stabilize when the behaviour band was at its narrowest and they swam at above average speed (SA3), although few medusae were retained (7.1% in Box 1 and 3.6% in Box 2). Numbers declined through time when medusae swam at below average speeds (SA1, SA4 and SA7), irrespective of the behaviour band width. The width of the behaviour band did affect the rate of loss, for example, only 24.3% of slow swimming medusae remained in Box 1 after 14 days when the behaviour band width was 275 m wide and 67.5% remained when it was 550 m wide.

Widening the behaviour band from 275 to 550 m (SA7-SA9) improved retention; for example, when the swim speed was average, widening the behaviour band improved retention in Box 1 by 28.4%. Near 100% retention was recorded in Box 2 when medusae swam at average or above average speed and the behaviour band was 550 m wide (SA8, SA9). Increasing the swim speed above the standard parameterisation (SA3, SA6 and SA9) was bad for the retention of medusae in Box 1 and only marginally improved the retention in Box 2. For instance, retention in Box 1 dropped from 68.3 to 32.6% when the behaviour band was 275 m wide and the swim speed was increased from average (SA5) to above average (SA6). In the same scenarios, medusae retention in Box 2 only increased from 81.6 to 93.6% with the increase in swim speed.

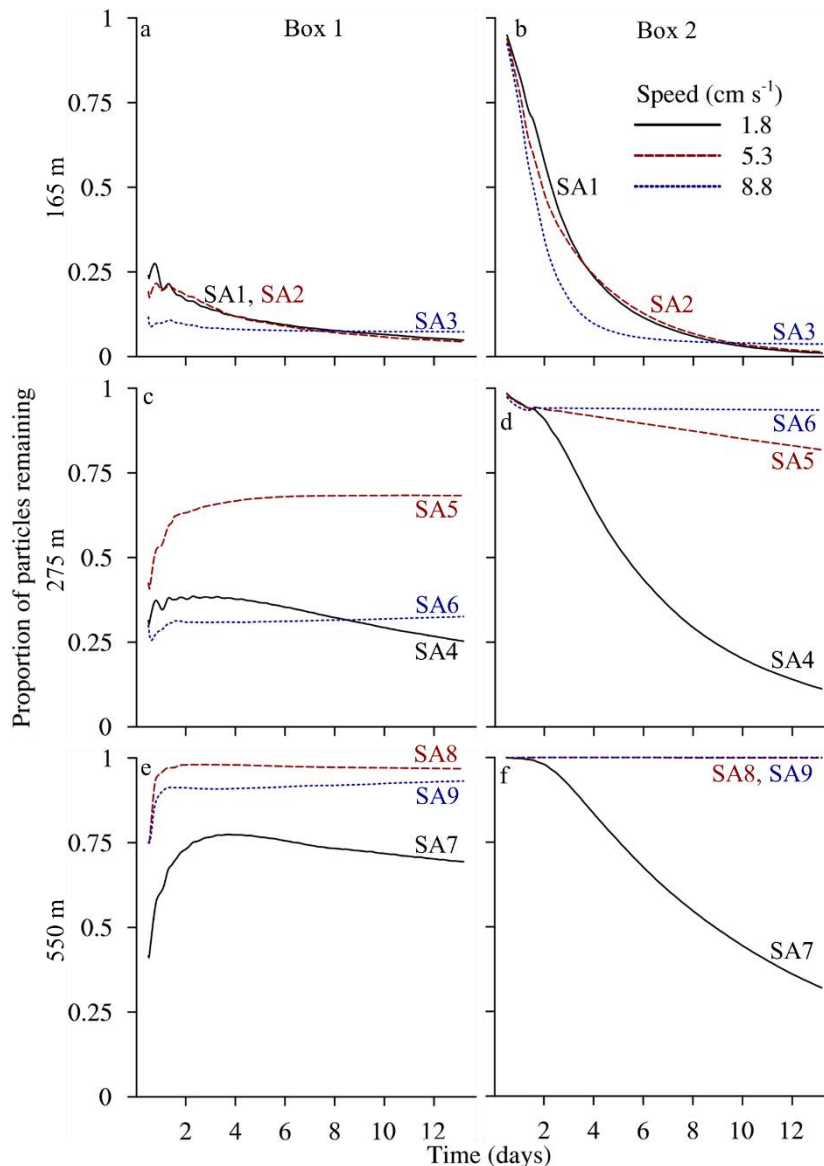


Fig. 2.7. Proportion of simulated *Chironex fleckeri* medusae (behaviour C) remaining near shore through time in the sensitivity analysis (SA) modelling scenarios listed in Table 2.2. A 24 h running average was performed on the raw data to remove tidal variability. In the first row, the retention in (a) Box 1 (see Fig. 2.1d) and (b) Box 2 (see Fig. 2.1e) is shown for scenarios SA1 to SA3 where medusae perform the prescribed behaviours in a 165 m band from shore. In the second row, the retention in (c) Box 1 and (d) Box 2 is shown for scenarios SA4 to SA6 where there is a 275 m band from shore. In the third row, the retention in (e) Box 1 and (f) Box 2 is shown for scenarios SA7 to SA9 where there is a 550 m band from shore. The C behavioural set includes 4 behaviours: swimming back and forth, parallel to shore, swimming to shore, avoiding beaching and performing a 180° turn upon encountering mangroves at bay edges (Fig. 2.2)

Simulated flood events; retention and refugia

During the strong flood, the salinity in a large proportion of Port Musgrave was reduced to < 21 PSU (Fig. 2.8). The salinity near the mouth of the bay, in the northern most region farthest from the rivers, was not reduced from the original bay salinity of 35.57 PSU. Additionally, the salinity in a band of shallow water adjacent to the coastline on each side of the bay remained above 21 PSU (i.e. above the threshold of risk to *C. fleckeri*) for the duration of the flood event. The additional volume of water and related transport resulted in a 20% reduction in the retention of both passive (dropped from 100 to 79.2%; scenarios 2 and 10, Table 2.1) and swimming medusae (dropped from 98.4 to 79.8%; scenarios 8 and 11) within Port Musgrave. Passive medusae were quickly advected from near shore waters on both the east and west sides of the bay (Fig. 2.6 b, d). Only 1.1% of the seeded medusae remained in Box 1 and 7.1% remained in Box 2 after 5 days. When behaviour was included medusae were still advected from near shore waters but, after the flood event, 14.8 and 56.3% remained in Boxes 1 and 2 respectively. The average salinity in Box 1 did not fall below 35.41 PSU at any time during the flood event and the average salinity in Box 2 did not fall below 35.57 PSU.

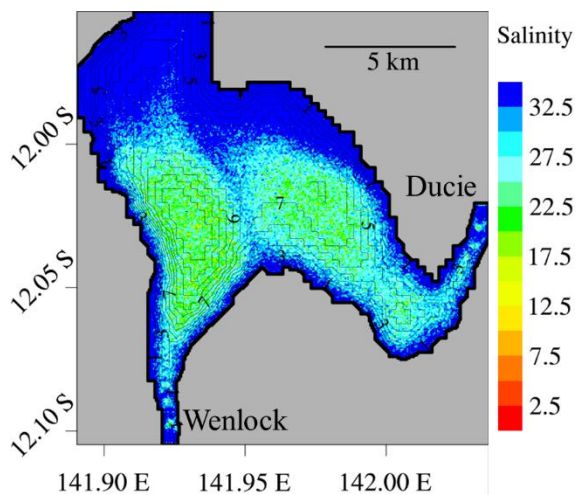


Fig. 2.8. Simulated salinity within Port Musgrave at peak ebb tide after 5 d of flooding at a rate of $1000 \text{ m}^3 \text{ s}^{-1}$ from both the Wenlock and Ducie Rivers. Depth contours are indicated

DISCUSSION

Swim speed

Chironex fleckeri medusae are strong swimmers. The maximum swim speed recorded in this study (16.6 cm s^{-1}) is among the fastest recorded for any jellyfish (Table 2.3). It is also greater than the fastest swimming speeds of *C. fleckeri* medusae reported by Shorten et al. (2005) and by Colin et al. (2013), of 11.5 cm s^{-1} and 12 cm s^{-1} respectively. Multiple methods have been used to measure the swim speeds of medusae over short time periods, including digital video analysis (Larson 1992, Shorten et al. 2005, Colin et al. 2013, Katija et al. 2015), flow tank experiments (Garm et al. 2007) and acoustic methods (Lee et al. 2010). In this study, simple distance over time measurements were made in the field over short periods. This technique is particularly useful for *C. fleckeri* medusae due to their extreme nearshore distribution and their tendency to swim parallel to the beach. Pitt and Kingsford (2000) also used this method for estimating the swim speed of *Catostylus mosaicus* in a shallow lake. Using electronic tags to track medusae has the potential to provide great insights into the swimming capabilities of jellyfishes over longer time periods (Fossette et al. 2016). For example, Moriarty et al. (2012) and Fossette et al. (2015) attached electronic tags to medusae and tracked their movements for 24 hours and 6 hours respectively; the swimming speeds of the medusae could be calculated in both studies because the local current speeds had been measured. Electronic tagging of jellyfishes has only recently been made possible due to the difficulties of attaching the tags to soft bodied invertebrates and tag retention is often a problem (Fossette et al. 2016).

Table 2.3. Examples of maximum recorded speeds of jellyfishes (Max. speed). The size of medusae refers to the size reported in the relevant reference and is presented as either interpedalial distance (IPD), bell diameter (BD) or diagonal bell width (DBW). Method: method used to measure speed.

Class	Species	Max speed (cm s⁻¹)	Size (cm)	Method	Reference
Cubozoa	<i>Chironex fleckeri</i>	12	16 IPD	Digital video analysis	Colin et al. 2013
	<i>Chiropsella bronzie</i>	12	5.6 IPD	Digital video analysis	Colin et al. 2013
	<i>C. fleckeri</i>	11.5	10 BD	Digital video analysis	Shorten et al. 2005
	<i>Chiropsalmus sp.</i>	6.7	4.5 BD	Digital video analysis	Shorten et al. 2005
	<i>Carybdea marsupialis</i>	5	3.3 DBW	Digital video analysis	Bordehore pers. comm
	<i>Tripedalia cystophora</i>	4 against 1.5 current	0.8 to 1.2 BD	Flow tank	Garm et al. 2007
Scyphozoa	<i>Nemopilema nomurai</i>	53	68 BD	Particle tracking velocimetry	Lee et al. 2010
	<i>Stomolophus meleagris</i>	15	Not reported	Observed in field	Shanks and Graham 1987
	<i>Phacellophora camtschatica</i>	10.2	25 to 45 BD	Electronic tags	Moriarty et al. 2012
	<i>Catostylus mosaicus</i>	10	> 14 BD	Observed in field	Pitt and Kingsford 2000
	<i>Linuche unguiculata</i>	8.3	1.4 to 2.2 BD	Digital video analysis	Larson 1992
	<i>Rhizostoma octopus</i>	8	30 to 40 BD	Electronic tags	Fossette et al. 2015
	<i>Cyanea capillata</i>	5.7	20 to 35 BD	Electronic tags	Moriarty et al. 2012
Hydrozoa	<i>Sarsia tubulosa</i>	4.1	0.8 BD	Digital video analysis	Katija et al. 2015

Medium scale retention

C. fleckeri medusae showed strong swimming behaviour and a preference to stay close to shore. These behaviours, and in some cases combined with favourable currents, resulted in a high level of retention at medium (tens of kilometres) and small (tens to hundreds of metres) spatial scales. It is likely, therefore, that the *C. fleckeri* population inhabiting Port Musgrave has little exchange with other similar estuaries and suitable habitats, and it represents a stock. I provided evidence that even medusae behaving as passive particles are unlikely to emigrate out of the system in dry conditions. The geographic configuration, flow regime and high residence time of Port Musgrave must play a large role in controlling the dynamics of the resident *C. fleckeri* population. Port Musgrave is a relatively closed system, with only a narrow connection to the Gulf of Carpentaria, and the flow into the bay from the Wenlock and Ducie Rivers is negligible for a large portion of the *C. fleckeri* medusae season. There are several estuaries and bays of similar size and geomorphology within the Gulf of Carpentaria and at other tropical locations in northern Australia and Oceania, thus our findings may have broad applicability. Like Port Musgrave, these bays have very long residence times that can limit the potential for dispersion and facilitate the genetic divergence of populations (e.g. 71 days in Nikko Bay, Palau; Golbuu et al. 2016). Genetically distinct populations of rainbow smelt *Osmerus mordax* have been found in bays along the northeastern coast of the USA that are geographically complex, with flow regimes that favour retention (Kovach et al. 2013). Bay scale population units have also been found in other jellyfish species. Pitt and Kingsford (2000) found significant variation in the abundance and recruitment of *C. mosaicus* in estuaries in New South Wales, Australia. This variation indicated that population regulation was occurring at the scale of individual bays, suggesting that the populations inhabiting the different bays were separate stocks (Kingsford et al. 2000, Pitt and Kingsford 2000). Further, *C. mosaicus* medusae have strong swimming abilities and could maintain positions in the upper reaches of estuaries where the advective forces are the weakest (Pitt and Kingsford 2000). These ecological data concurred with Dawson's (2005) conclusions that there were genetic differences among *C. mosaicus* populations inhabiting many of the same bays sampled by Pitt and Kingsford (2000). Similarly, great insights into the population structures of cubozoans could be gained through using genetic analyses to test clear predictions on population connectivity and spatial disjunctions that are generated from alternate methods (e.g. biophysical modelling; Dawson et al. 2005).

Near shore retention and patchiness

The behaviour of medusae facilitated retention near the shore and at small spatial scales (hundreds of metres) and the medusae inhabiting these areas may be quite insular from other local populations. I demonstrated that medusae are capable of swimming to overcome nearshore current speeds, so they can maintain positions in shallow waters adjacent to beaches. Ecologically, it would be beneficial for *C. fleckeri* medusae to remain close to shore as the prawns and fish they feed on are commonly found nearshore (Carrette et al. 2002). Directional swimming was needed for medusae to remain non-dispersed, in groups; such groupings could only be maintained in shallow water as the current speeds and resultant dispersive forces increased with distance from shore. Fossette et al. (2015) constructed a biophysical model of the dispersion of *Rhizostoma octopus* medusae in the Bay of Biscay, France, a much more open environment than the semi enclosed Port Musgrave. *R. octopus* medusae can form large blooms and Fossette et al. (2015) demonstrated that the counter current swimming of medusae facilitated the formation and maintenance of such blooms. While *C. fleckeri* and *R. octopus* behave in very different ways, the importance of horizontal swimming behaviour in maintaining groupings is clear for both species.

Within estuary residency has been demonstrated (e.g. *C. mosaicus*; Pitt and Kingsford 2000), but the extreme nearshore distribution of *C. fleckeri* appears to be unusual. Immigration and emigration occurs between local populations (Kingsford and Battershill 1998) and the potential for such exchange between the east and west sides of Port Musgrave was found in this study. In many of our scenarios, however, mixing between local populations was low. Gordon and Seymour (2012) counted the rings on the statoliths of *C. fleckeri* medusae. They assumed the rings were laid down daily and calculated that the age of the oldest sampled medusae was 78 days. The model in our study was run for 14 days in dry conditions which is only a portion of the medusae life span. Accordingly, more mixing could occur over an entire lifespan. Additionally, there may be multiple storms in a season and, as I demonstrated, these events increase the advective forces in the bay and so increase the potential for mixing between local populations. The increased potential for mixing may not be utilized if medusae utilize oceanographic refugia. There are other considerations for dispersal and connectivity. Hartwick (1991a) suggested that adult *C. fleckeri* may move upstream to spawn (Cubozoans are gonochoristic, Kingsford and Mooney 2014), so promoting further connectivity within an estuary, but there are no data on this.

Dispersion potential of early life history stages

In this study, I focused on the dispersion potential of *C. fleckeri* medusae and the evidence I provided was from medusae with interpedalial distances greater than 4 cm. Although I did not study earlier life stages, logically they are not able to swim as well as the recorded medusae. I did model medusae as passive particles and the high retention recorded in these scenarios suggests that earlier life history stages have a limited potential for dispersion. Furthermore, two kinds of evidence from the literature support our conclusion of low levels of emigration: the biological characteristics of the early life stages of *C. fleckeri* and the hydrodynamics of the polyp habitat, which are characterised by structural complexity and related 'sticky water' (sensu Wolanski 1994, Andutta et al. 2012). Hartwick (1991a) investigated the biological characteristics of *C. fleckeri* over the course of 11 years. He reared the early life stages in the laboratory and found that the zygotes and blastulae were negatively buoyant and have an adhesive coating, so they adhered to hard surfaces. These characteristics limit the amount of time that these stages spend in the water column, so reducing the potential for dispersion (Hartwick 1991a). The planulae larvae emerge from the blastulae and only remain in the water column for up to 24 hours before attaching to the substrate, where they metamorphose into creeping polyps (Hartwick 1991a). The creeping polyps become sessile, presumably after they find a suitable habitat (Hartwick 1991a). Cubozoans metamorphose from polyps into nearly fully formed medusae (Werner et al. 1971), unlike the ephyrae of scyphozoans (Straehler-Pohl and Jarms 2010) which have the potential to be transported hundreds of kilometres from polyp sources to medusae sinks (Barz et al. 2006, Chen et al. 2014). As they are nearly fully formed, newly detached medusae are capable of swimming and so could offer some resistance against advective currents. Indeed, newly detached *Carybdea marsupialis* medusae with diagonal bell widths as small as 0.05 cm can swim at speeds of around 1 cm s⁻¹ (C. Bordehore pers. comm.). Further, *C. fleckeri* medusae grow quickly, and so their swimming competence would similarly increase quickly. Gordon and Seymour (2012) recorded a large maximum growth rate for *C. fleckeri* medusae of ~ 3 mm d⁻¹. They constructed a Gompertz growth equation, and according to this equation a medusae could grow to 4 cm interpedalial distance (the size of the smallest individual observed in this study) in approximately 42 days. In our study, at 4 cm medusae were already capable of swimming faster than the mean current. Polyps are thought to reside in tidal estuaries (Hartwick 1991a), although their habitat may include other coastal zones (Mooney and Kingsford 2012) these are also characterised by 'sticky

water' habitats such as mangroves (Wolanski 2007). These habitats would facilitate retention due to low levels of flushing (Wolanski 2007). If juvenile medusae were flushed from the tidal estuaries they would enter Port Musgrave itself and, as demonstrated in our model of passive drift, the currents in the bay would still favour retention.

Impact of storms on population persistence

The *C. fleckeri* medusae season overlaps with the rainy season, so medusae will be affected by pulse storm events. A strong storm event was modelled, so the flow in most events would be smaller. Further, the two-dimensional flood plume modelling presented in this study would not have captured the full complexity of the water flow or the development of the flood plume given the three-dimensional buoyancy driven aspects of these processes (Wolanski and Elliott 2015). The strongest trends in the model results are discussed below, as they are likely valid despite the missed complexity. While the rate of flushing increased during the storm event, most medusae remained within the system. The salinity of the shallow nearshore waters preferred by medusae remained above 21 PSU, the threshold for incapacitation identified by Mooney and Kingsford (2016b) and, even in storm conditions, medusae behaviour facilitated nearshore retention. Medusae could also find refuge in the reaches of the bay farthest from the river mouths, where waters also had salinities above 21 PSU. If the bay was stratified during river floods, then medusae could find refuge from low salinities in deeper water. Although this type of stratification is typical of estuaries (Wolanski and Elliott 2015), no data on stratification during the wet season are available for Port Musgrave. The identified and assumed refugia suggest that population persistence in Port Musgrave is highly likely during freshwater events of high impact.

Reliability of results from biophysical modelling

The behaviours selected for inclusion in the biophysical model were well supported by field observations and evidence from the literature (Hamner et al. 1995, Garm et al. 2007, 2011, Gordon and Seymour 2009). However, the avoidance behaviour that could further facilitate retention (where medusae perform a 180° turn when they reach

mangrove habitat at the bay edges, included in the Behaviour C suite) was not necessary for the retention of medusae in the more sheltered bays on both the east and west sides of Port Musgrave, indicating that high levels of retention are likely with even simple behavioural responses. The results of the sensitivity analysis demonstrated that the modelling outputs were robust, despite major alterations to the behavioural components of the biophysical model. While considerable nearshore retention was recorded in the standard run, widening the behaviour band did improve retention. The swim speed used in the standard run was conservative given the swimming capabilities of *C. fleckeri* medusae that were discussed previously. The retention-related effects of increasing the swim speed were dependent on small scale geography (tens to hundreds of metres). Medusae performed the prescribed behaviours within a set distance from shore (the distance depended on the sensitivity analysis scenario). In the other direction, parallel to shore, in the bay enclosed by Box 1, the band was narrower at the bay edges than at the centre because of the concavity of the bay. Consequently, when medusae performed a 180° turn at the bay edges, they could turn into an area beyond the behaviour band where they acted as passive particles, exaggerating the risk of loss when the swim speed was increased. This edge effect did not influence the retention of medusae in box 2 because the bay was comparatively less concave. Future biophysical modelling studies investigating the population structure of *C. fleckeri* should consider increasing the complexity of the behavioural model to include swim speeds that vary in relation to current speeds to avoid similar edge effects.

***C. fleckeri* population substructure**

This study is a contribution to the growing body of evidence that *C. fleckeri* stocks are only separated by spatial scales of tens to hundreds of kilometres. Recently, Mooney and Kingsford (2016a) found significant differences in the geochemical compositions of *C. fleckeri* statoliths from medusae collected at different regions, separated by hundreds of kilometres. Differences were even found among some sites, separated by only a few kilometres (Mooney and Kingsford 2016a). They also found that the shapes of *C. fleckeri* statoliths varied on scales of tens to hundreds of kilometres (Mooney and Kingsford 2017).

Conclusions

Chironex fleckeri medusae were capable of swimming at velocities that greatly exceeded the current velocities in the nearshore waters where they are commonly found. The current regime and high residence time of waters in estuarine bays may assist in the retention of medusae when their swimming ability at small interpedalial distances is weak. Because few medusae may emigrate from estuarine bays, the populations within the bays may constitute stocks. The strong swimming behaviour of medusae provided evidence that medusae can maintain localised populations at spatial scales as small as hundreds of metres. Furthermore, the behavioural preference of medusae to remain very close to shore would allow them to survive during storm events, and related freshwater pulses, where survivable salinities would be found nearshore and perhaps in deep water high salinity refugia. Our findings concur with a growing body of evidence that local populations of *C. fleckeri* may have minimal connectivity and that stocks may often be at the scale of estuaries and bays. I predict that population genetics will reflect this conclusion.

CHAPTER SUMMARY

The potentially lethal *Chironex fleckeri* (Class Cubozoa) inhabits estuarine and nearshore coastal waters in the western Pacific. The spatial scales of connectivity between *C. fleckeri* populations are poorly understood. Biophysical modelling of Port Musgrave, a 17 × 21 km shallow bay in tropical Australia, was used to investigate the potential for connections between populations separated by medium (10s of km) to small (100s of m) spatial scales. I measured the swimming speeds and orientations of medusae ranging in size from 4 to 12 cm interpedalial distance (the distance between two adjacent corners on the bell of the medusae). Medusae swam longshore at average speeds ($5.3 \pm 3.5 \text{ cm s}^{-1}$ SD) that exceeded the local average current speeds ($2.7 \pm 2.4 \text{ cm s}^{-1}$). These and other ecological data were used to parameterise the biophysical model. No medusae modelled as passive were advected from the bay in 14 d; < 2.5% of swimming medusae were lost. When medusae swam directionally, a high percentage aggregated in shallow waters within 10s to 100s of m of the seeding locations. Newly metamorphosed medusae are likely to be retained in the bay through a combination of 'sticky water' (i.e. water with reduced current speeds, reduced through diversion around obstacles) in shallow complex habitats and favourable currents. *C. fleckeri* are vulnerable to low salinities; however, modelling a strong flood

revealed higher salinity refugia in shallow water. As there was high retention within the system, I conclude that populations of *C. fleckeri* inhabiting shallow, semi-enclosed estuarine bays possibly represent stocks. Within these stocks, swimming and favourable currents may minimise connectivity and maintain populations at multiple spatial scales.

Chapter 3.

Behavioural maintenance of highly localised jellyfish (*Copula sivickisi*, Class Cubozoa) populations

INTRODUCTION

The behaviour of organisms can influence how their populations are structured. Marine organisms generally have a hierarchy of recognisable population structures (Kingsford and Battershill 1998; Sinclair 1988). The broadest distinction in the hierarchy is the geographic range of a species, which often equates to a metapopulation. The metapopulation can be further divided into a series of mesopopulations (also known as stocks) which are largely self-contained. Local populations with strong connectivity may also be identified within a stock. Because the scales and structure of stocks are determined by the movement of animals between locations, data on the behaviour and mobility of animals in relation to local currents are crucial to understanding the population dynamics of species. Connectivity may be influenced by the combined effects of oceanographic transport and the behaviour of larvae, juveniles and adults (e.g. Chapter 2; Freiwald 2012; Chin et al. 2013; Wolanski 2017; Williamson et al. 2016).

The medusae of jellyfish in the class Cubozoa generally have strong swimming and orientation abilities, and so they may have great capacity to influence the structuring of their populations. *Chironex fleckeri* is the largest cubozoan species (Kingsford and Mooney 2014), and their swim speed is amongst the fastest recorded for any jellyfish (16.6 cm s^{-1} ; Chapter 2). The swim speeds of smaller species have been investigated in laboratory settings and were also found to be considerable (*Chiropsella bronzie*, 12 cm s^{-1} , Colin et al. 2013; *Chiropsalmus sp.*, 6.7 cm s^{-1} , Shorten et al. 2005; *Tripedalia cystophora*, 4 cm s^{-1} against a 1.5 cm s^{-1} current, Garm et al. 2007). Further, cubozoan medusae are nearly fully formed after they metamorphose from polyps (Werner et al. 1971) so cubomedusae can likely swim well and influence their dispersion soon after metamorphosis. Cubozoans also have sophisticated visual systems. They have four rhopalia and each contains two image forming eyes, similar in structure to the eyes of vertebrates and cephalopods (Nilsson et al. 2005). Given the sophistication of their

visual system, it is unsurprising that cubozoan species exhibit an array of visually guided behaviours including: obstacle avoidance (*C. fleckeri*, Chapter 2, Hamner et al. 1995; *T. cystophora*, Garm et al. 2007; *Carybdaea rastonii*, Matsumoto 1995; *C. bronzie*, Garm et al. 2007), navigating via terrestrial cues (*T. cystophora*, Garm et al. 2011), and orienting toward prey species (*Copula sivickisi*, Garm et al. 2016; *T. cystophora*, Buskey 2003, Garm and Bielecki 2008, Stewart 1996).

The species-specific data required to evaluate how behaviour might influence the structuring of populations are largely lacking for cubozoan species. The cubozoan *C. sivickisi* (formerly known as *Carybdea sivickisi*) has a cosmopolitan distribution and is one of the better studied species in the class. A complex suite of behaviours has been observed in *C. sivickisi* medusae. They have adhesive pads on the apex of their bells which they can use to attach to substrates (Hartwick 1991b). The species is nocturnal; SCUBA divers have observed *C. sivickisi* foraging at night in the wild (Hartwick 1991b) and extensive plankton tows in daylight hours have previously yielded no *C. sivickisi* medusae (Garm et al. 2012). Further, in laboratory experiments, medusae attached themselves to the sides of their tanks during the day and were actively swimming, foraging and mating in the water column at night (Garm et al. 2012). *Copula sivickisi* also seem to preferentially attach to favourable substrata. In a laboratory experiment, when given a choice between coral, stone, red algae, sea grass and the tank control, most medusae attached to the undersides of hard structures (coral or stone) or seagrass (Garm et al. 2012). SCUBA divers have also observed *C. sivickisi* medusae swimming close to and adhering to the benthic macroalgae *Sargassum spp.* and *Colpomenia spp.* in the wild (Hartwick 1991b). The habitat associations of *C. sivickisi* and how these preferences influence patterns of distribution have rarely been addressed in the literature; data on their associations in the wild are especially lacking. Together, the behaviours exhibited by *C. sivickisi* medusae have the potential to greatly influence their dispersal and population structure.

Copula sivickisi has a broad distribution, inhabiting nearshore waters in the Pacific and Indian Oceans at tropical to temperate latitudes (Kingsford and Mooney 2014). The substructure of the metapopulation(s) inhabiting this broad distribution is largely unknown. However, Mooney and Kingsford (2017) analysed the shapes of *C. sivickisi* statoliths taken from medusae from three different locations on the East Australian coast, separated by hundreds of kilometres. Twenty statoliths were analysed per location and their shapes differed significantly between locations, suggesting that the populations inhabiting the locations were separate stocks. Further divisions may exist

within these stocks, but data have not been collected at sufficiently small spatial scales to distinguish these divisions. Collecting data to assess cubozoan population structures can be difficult as the abundance of cubozoans can vary greatly spatially and temporally (Kingsford and Mooney 2014). Many cubozoan medusae are photopositive and night lighting, where a light is used as an attractant, has been utilized to sample cubomedusae (Kingsford and Mooney 2014). Further, digital cameras mounted to jetties have effectively been used to monitor the presence of relatively large photopositive cubomedusae (*C. fleckeri* and *Morbakka spp.*) attracted to the field of view by strong lights (Llewellyn et al. 2016). I developed a similar system in which an underwater camera and light were paired to record the abundance of smaller cubomedusae.

The overall objective of this study was to elucidate the fine scale spatial structure of a *C. sivickisi* population inhabiting a fringing reef, and to determine the importance of behaviour (namely diel cyclic behaviours, attachment to habitat and swimming) in maintaining this structure. I specifically aimed to: (1) expand on previous laboratory experiments examining the behaviour of *C. sivickisi* medusae through time, (2) experimentally determine their habitat preferences in a fringing reef environment, (3) perform depth stratified plankton tows in day and night hours to investigate how wild *C. sivickisi* medusae are vertically distributed in the water column through time, (4) deploy underwater jellyfish cameras (JCams) to investigate the habitat use, and related geographic distribution, of a population of *C. sivickisi* medusae on a fringing reef and, (5) quantify the swimming ability of *C. sivickisi* medusae and compare it with the speeds of currents measured in their natural habitat.

MATERIALS AND METHODS

***Copula sivickisi* collection and care**

Copula sivickisi medusae were collected at night from September to November of 2012 and 2016 from Geoffrey Bay (19°9'12.67''S, 146°51'52.38''E) and Nelly Bay (19°9'50.37''S, 146°51'3.43''E) on the eastern side of Magnetic Island (Fig. 3.1a, b). The island lies on the central section of the Great Barrier Reef, approximately 8 km from the coast of Townsville, Queensland, Australia. Bays on the eastern side of Magnetic Island contain fringing reefs that are dominated by *Sargassum sp.* algae and coral species.

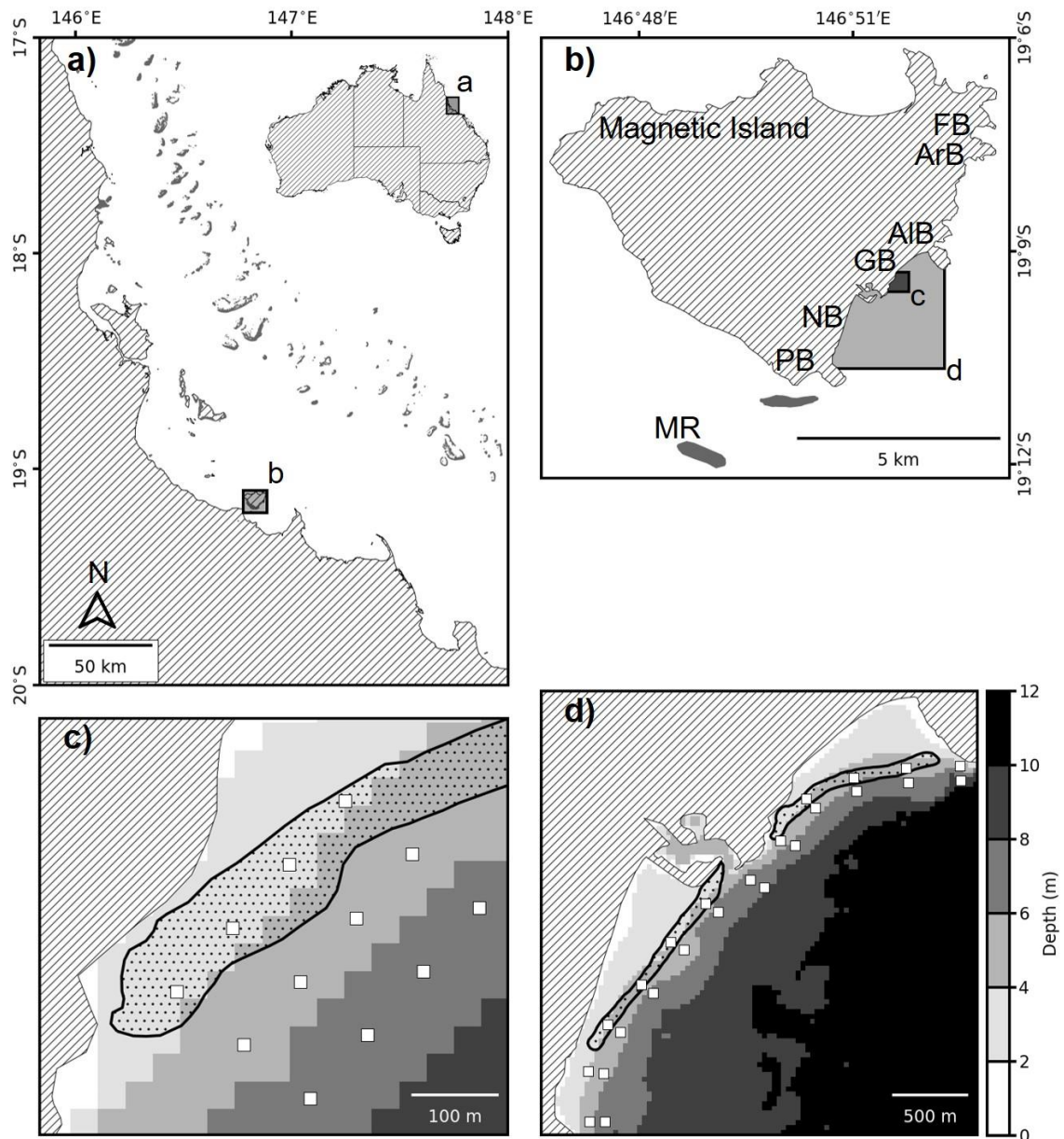


Fig. 3.1. The study region. a) Australia, the North Queensland coastline. The locations of panes a and b are indicated by the grey boxes. b) Magnetic Island. The locations of Middle Reef (MR), Picnic Bay (PB), Nelly Bay (NB), Geoffrey Bay (GB), Alma Bay (AIB), Arthur Bay (ArB) and Florence Bay (FB) are shown. The extents of panes c and d are indicated by the dark grey and light grey boxes, respectively. The designs of the c) 2015 and d) 2016 Jellyfish Camera unit (JCam) surveys. The white squares mark the locations of the sampled sites. The bathymetry of NB and GB is shown, the color bar indicates the depth (m). Depths > 10 m are shown in black. In all panes, land is filled with a hatch pattern. Reefs are filled with solid grey in panes a and b, and they are outlined in black and filled with dots in panes c and d

The *C. sivickisi* medusae were collected using light attraction. In 2012, a 1000-watt light (Alpha Diving Products diving flood light; cool white light) was placed within the top 2 to 4 m's of the water column for at least 30 minutes and the attracted medusae were gathered from the surface with pool scoop nets (rectangular mesh size: 1 × 2 mm). The medusae were transported back to a temperature controlled wet lab at James Cook University. The indirect sunlight in the lab gave the medusae a light/dark cycle of approximately 12:12 h. The physical characteristics of the water column were measured during flood and ebb tides on 15 November 2012 using a conductivity, temperature and depth device (CTD; Seabird SBE 19 Plus). The water column was vertically well mixed. The average water temperature ranged from 26.7°C on flood tide to 26.9°C on ebb tide. The temperature in the lab was set to 26°C, near the measured average. The average water salinity ranged from 36.0 PSU on flood tide to 36.1 PSU on ebb tide. The salinity in the lab was maintained at approximately 36 PSU.

In 2016, weighted lights (Intova action video lights, 640 Lumens, 120° beam angle; 6000 K to 6500 K cool white light) were submerged in 1.5 to 5 m of water for up to 1.5 hours; medusae aggregated around the lights and were collected by snorkelers with pool scoop nets. They were transported back to JCU and fed plankton that had been caught from the collection site on the night of capture. Medusae were held in an artificially lit, temperature controlled wet lab. The lights were set to turn on at 06:45 and off at 18:45, giving the medusae a light dark cycle of 12:12 h. The temperature was again set at 26°C and the salinity was maintained at approximately 36 PSU.

In both years, medusae (size range: 1 to 10 mm InterPedalial Distance; IPD) were kept in 100 L holding tanks (depth = 47 cm, radius = 28 cm) and half water changes were performed daily. Medusae were fed *Artemia* nauplii daily after the night of capture. The *Artemia* nauplii were hatched in brackish water without an enrichment medium. While cubomedusae can live on a diet of *Artemia*, it may be nutritionally deficient (Acevedo et al. 2013). Consequently, fresh medusae were caught on a weekly or bi-weekly basis for use in experiments to avoid confounding holding effects. All experiments were performed within two weeks of capture and the condition of the medusae did not deteriorate in this time.

Laboratory experiments

Experiment 1 – Temporal variation in behaviour

The behaviour of *C. sivickisi* medusae was monitored through time. In each trial, medusae were transferred from the holding tanks into a 25 L (depth = 35 cm, radius = 14 cm) bucket at 15:00. Live *Artemia* nauplii were then added to the bucket. The number of medusae performing predefined behaviours (Table 3.1) was recorded after a 1 hour acclimation period. Observations were made every half an hour between 16:00 and 21:30. The room light was shut off at 18:45, which corresponded to the normal time of dusk in the region during the *C. sivickisi* season (September to November). Therefore, in each trial, six day time observations (16:00 to 18:30) were made under a fluorescent light that recreated the tropical blue sky light spectrum (SYLVANIA F36W/T8 Aquastar; colour temperature = 10000 K) and six night time observations (19:00 to 21:30) were made in darkness under a fluorescent light with a red filter (SYLVANIA F36W/RED). Garm et al. (2012) used red fluorescent light to film *C. sivickisi* at night and concluded that the medusae performed natural behaviours in the tanks, suggesting that the red light did not disrupt their natural activity pattern. In our study, adults were observed in five trials, each with five males and five females, and juveniles were observed in five trials, each with ten juvenile medusae.

All statistical analyses were performed in R version 3.4.3 (R Core Team, 2017). I tested the null hypothesis that the relative proportions of active and inactive behaviours performed by *C. sivickisi* medusae were independent of the time of day. Separate tests of this hypothesis were done for the adult and juvenile trials. Firstly, the data in each trial were pooled by time (day or night) and behaviour (active: swimming, feeding and mating; inactive: attached and bobbing) to produce a 2x2 contingency table for each trial. Therefore, a set of five contingency tables were generated from the adult trials and a set of five were generated from the juvenile trials. Repeated test of independence needed to be performed on the contingency table sets so, ideally, the Cochran-Mantel-Haenszel (CMH) test (Mantel and Haenszel 1959; Cochran 1954) would be used (McDonald 2014). The assumptions of the CMH test were assessed following McDonald (2014). The adult set of contingency tables met the assumptions, so a CMH test was performed. The juvenile set did not meet the assumptions so separate Fishers Exact Tests of Independence were performed on each contingency table in the set. The Bonferroni correction was applied to control the familywise error

rate. The critical value was reduced from 0.05 to 0.01 (0.05/5) because 5 individual tests were performed.

Table 3.1. Definitions of the behaviours observed in the temporal variation in behaviour experiment (experiment 1)

Behaviour	Definition
Attached	When a medusa attached to the side or bottom of the tank using the pads on its bell. Their tentacles were either withdrawn inside the bell or lying motionless outside of the bell.
Bobbing	When a medusa was upright, pulsing and maintaining its position in a single location.
Swimming	When a medusa was actively swimming through the water column or against the sides of the tank with its tentacles not fully extended. Tentacle lengths shorter than 2 bell lengths (BL).
Feeding	Characteristic feeding behaviour. When a medusa sank down through the water column with its tentacles extended, and returned to the surface to repeat the behaviour (Garm et al. 2012). Tentacle lengths greater than or equal to 2 BL.
Mating	Characteristic “wedding dance” mating behaviour where the male medusa attached his tentacles to the female’s tentacles to pull her around (Lewis and Long 2005).

Experiment 2 - Habitat choice

The searching and attachment behaviour of *C. sivickisi* medusae was examined in a habitat choice experiment. The behaviour of medusae was compared over three habitats and one control as follows. Tufts of *Sargassum* and a fragment of dead coral rubble (*Montipora sp.*) were gathered from the sites of *C. sivickisi* collection. The natural substrates were placed into a 9 L rectangular tank (length = 28.5 cm, width = 18.5 cm, depth = 17 cm) with sand (Ki-Carma double washed sand) so each substrate took up approximately one quarter of the bottom of the tank (Fig. 3.2). The natural substrates and the sand were chosen for inclusion in this experiment as they were the predominant substrates at the sites of *C. sivickisi* collection. The final quarter was left empty as a control. Black shade cloth was wrapped around the sides of the tank to obscure the observer from the medusae’s view. In each trial, an individual medusa was taken from the holding tank and placed in the centre of the experiment tank. The behaviour of the medusa (attached or swimming; Table 3.1) and the quadrat they were in were recorded every 15 seconds for ten minutes. The number of times the medusa

was recorded in each quadrat was summed ($\text{Count}_{\text{observed}}$). The *Sargassum* tended to overhang the boundaries of its quarter and the fragment of coral rubble did not fill its entire quarter. Multiple birdseye view photos of the tank were taken, and the proportions of the bottom covered by each substrate ($\text{Prop}_{\text{cover}}$) were determined from the photos using the image analysis software ImageJ version 1.51j8. These proportions were used to correct the $\text{Count}_{\text{observed}}$ data to account for the greater/lesser areas covered by the different substratum. The corrected data ($\text{Count}_{\text{corrected}}$) were calculated following the formula:

$$\text{Count}_{\text{corrected}} = \text{Count}_{\text{observed}} \times \frac{0.25}{\text{Prop}_{\text{cover}}} \quad (1)$$

Fifty medusae were trialled in daylight hours, between 10:00 and 18:00, when they were most likely to be inactive. Thirty nine of the 50 trialled medusae attached to a substrate within the 10-minute period. The search time was calculated as the time it took these medusae to attach to a substrate ($\text{SearchTime}_{\text{observed}}$). Once attached, most medusae remained attached for the duration of the trial. However, four medusae attached to more than one substrate during the trial period. The time it took these medusae to find the substrate they spent the most time on was taken as the search time. The search time data were corrected ($\text{SearchTime}_{\text{corrected}}$) following the formula:

$$\text{SearchTime}_{\text{corrected}} = \text{SearchTime}_{\text{observed}} \times \frac{\text{Prop}_{\text{cover}}}{0.25} \quad (2)$$

A one-way ANOVA was performed on the $\text{SearchTime}_{\text{corrected}}$ data to test if the search times for the 39 *C. sivickisi* medusae that attached to substrates differed significantly between the substrates. The *Montipora sp.* coral rubble was excluded from this analysis as only one medusa attached to it. The ANOVA had an unbalanced design; 14 medusae attached to the tank control, 14 attached to the sand, and 10 attached to the *Sargassum*. $\text{SearchTime}_{\text{corrected}}$ data were \log_{10} transformed to satisfy the ANOVA assumptions of normality and homogeneity of variance. After the transformation, the residuals were normally distributed (Shapiro-Wilk test, $W = 0.95$, $P = 0.09$) and the variance in search times did not differ significantly between substrates (Levene's test, $F(2,35) = 0.47$, $P = 0.63$).

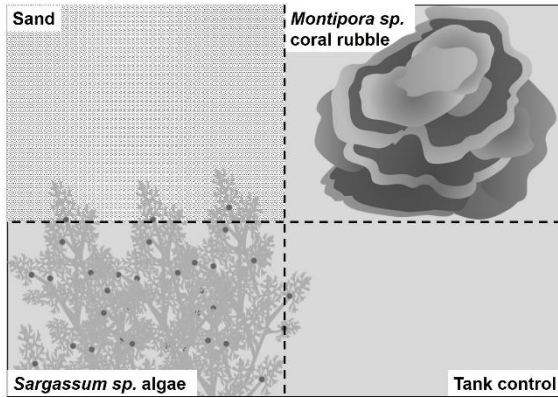


Fig. 3.2. Diagrammatic representation of the tank set up in experiment 2, the habitat choice experiment

Experiment 3 - Swimming speeds

The swimming abilities of *C. sivickisi* medusae were tested against increasing water velocities in a swimming chamber (length = 45.5 cm, width = 25 cm, depth = 6.5 cm), following the U-crit method of Brett (1964). The design of the chamber was based on the swim chamber of Stobutzki and Bellwood (1994). The water speed within the chamber was controlled by multi-turn gate valves and calibrated by measuring how fast food dye moved through the chamber. A total of 41 medusae (23 males, 18 females), ranging in size from 4 to 11 mm, were trialled. Each medusa was acclimated in the swimming lane in a 1 cm s^{-1} current for 5 minutes before the start of each trial. The water speed was then increased to 3 cm s^{-1} for 5 minutes, and subsequently increased by 3 cm s^{-1} (speed increment, U_{ii}) every 5 minutes (trial interval, T_{ii}) up to a speed of 18 cm s^{-1} . This was done to simulate the strengthening of a current with a rising tide. The range of speeds used matched current speeds measured near the site of *C. sivickisi* collection (see results section, 'Swimming speeds (Experiment 3) and drogue deployments'). The trial was suspended once the medusa became fatigued. A medusa was considered fatigued if it was being pressed against the end of the tank by the current, or if it attached itself to the tank via the adhesive pads on its bell. The highest velocity maintained for a whole T_{ii} (U_i) and the time elapsed at fatigue (T_i) were used to calculate the maximum swim speeds (U_{crit}) of the *C. sivickisi* medusae based on the U_{crit} formula from Brett (1964):

$$U_{crit} = U_i + U_{ii} \times \frac{T_i}{T_{ii}} \quad (3)$$

The sprint swim speed (U_{sprint}) was defined as the maximum speed a medusa could perform in a burst and was calculated as the highest speed a medusa swam against for at least half of a T_{ii} (i.e. ≥ 2.5 minutes).

Vertical distribution

The vertical distribution of *C. sivickisi* in the water column was examined in the wild during the day and at night to determine if the nocturnal behaviour of medusae produced diel changes in their distribution. Depth stratified plankton tows were performed in Geoffrey Bay and Nelly Bay, in day (15:50 – 18:30 h) and night (19:30-21:50 h) hours. Tows were performed in all states of the tide (high, ebb, low, flood). A 320 μm mesh net with a circular mouth, 75 cm in diameter, was towed slowly (0.25 to 0.93 m s^{-1}) for 5 to 10 minutes and a flow meter attached to the net recorded the distance travelled in each tow. Water volumes between 60 and 120 m^3 were sampled in the tows and the measure of *C. sivickisi* medusae abundance was accordingly standardized to the number recorded per 100 m^3 . The neuston layer was skimmed in the shallow tows. The bottom 1 m of the water column, corresponding to depths between 2 and 7 m, was sampled with diver-controlled deep tows. Each bay, depth and time combination was sampled twice per day over three non-consecutive days, from 8 October 2014 to 7 November 2014. A total of 48 tows were therefore performed, with 12 replicates per depth and time combination. No statistical analyses were performed on these data due to the absence of *C. sivickisi* medusae in most tow samples.

Horizontal distribution

The geographic distribution of *C. sivickisi* was determined over two bays (Geoffrey Bay and Nelly Bay) on the eastern coast of Magnetic Island over two medusae seasons (2015 and 2016). Their distribution was mapped using underwater jellyfish camera units (JCams, Fig. 3.3) which consisted of GoPro's (models 3 and 3+) or SJ Cam's (model 4000) paired with underwater lights (Intova action video lights). Medusae were attracted to the light and recorded by the video camera. The video cameras were set to record at 1080 p resolution, with a frame rate of 30 frames per second. The JCam units were deployed in 30-minute intervals, in organised grid patterns. The maximum number of medusae in any single frame of video during the 30-minute deployment

period (N_{max}) was used as the measure of medusae abundance; this is the convention when managing potential repeat counts (Cappo et al. 2004).

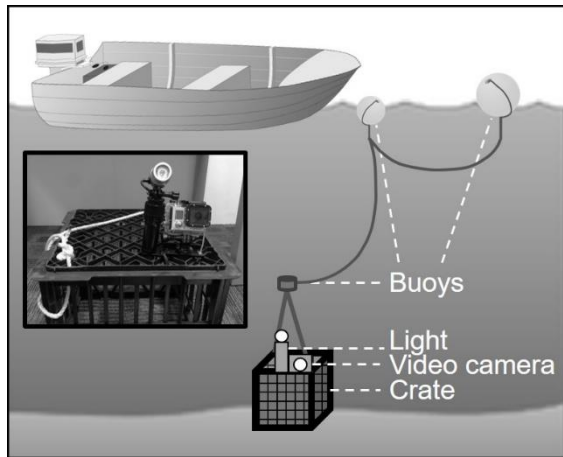


Fig. 3.3. Jellyfish Camera unit (JCam) design. A diagram of a deployed JCam, with labelled components. A close up photograph of a JCam is provided in the insert

The availability of fringing reef habitat at each of the mapped sites was also qualitatively determined from the JCam footage to investigate the link between medusae abundance and habitat availability. *Sargassum* and coral dominated the fringing reef habitat. The habitat availability at a site was classified as high if reefal habitat took up greater than 66% of the substrate in still images from the JCam footage recorded at the site. The habitat availability was classified as moderate if between 66% and 33% of the substrate was covered by reef and it was classified as low if less than 33% of the substrate was covered. Finally, the habitat availability was classified as absent at a site if no *Sargassum* or coral were visible in any of the stills extracted from the JCam footage.

A small-scale grid was sampled in Geoffrey Bay in 2015 to determine the habitat and depth usage of *C. sivickisi* medusae in the bay at a fine spatial scale (Fig. 3.1c). The grid had 12 sites; the GPS locations of the sites were predetermined from satellite imagery to guide the night field sampling. The sites were separated from each other by 100 m and set out in a 3 x 4 pattern, so the grid covered a 300 x 400 m (0.12 km²) area. The three grid rows corresponded to three distinct depth strata (≤ 4.1 m, 4.2 to 7 m, ≥ 7.1 m) and were set at incremental distances from a band of fringing reef habitat that was dense enough to be visible from the satellite images. The shallowest sampling row lay within the visible habitat band, the mid depth row lay just outside of

the band (range: 35 to 70 m from band) and the deepest row was set far from the band (range: 124 to 168 m from band). The placement of the sites in relation to reef habitat was later ground-truthed from the JCam footage. The grid was sampled four times over four non-consecutive nights, from the 1st of October to the 3rd of September.

A Linear Mixed effects Model (LMM) was used to test for the effect of depth (which encompassed habitat availability) on the abundance of *C. sivickisi* medusae. N_{max} could not be determined for 3 of the 48 deployments so the LMM design was balanced by replacing the missing data with the N_{max} averaged over the matching depth and sampling trip. Depth was treated as a fixed factor. Sites were nested within depths, and so they were treated as a random effect. Further, repeated measures were taken at each site on four separate trips that were completed at random times, so trip number was treated as an additional crossed random effect. Multiple intercept/slope candidate models were trialled. The candidate models which included slopes all displayed a singular fit, suggesting they were overfit and had poor power for hypothesis testing (Matuschek et al. 2017). The intercept only candidate model had the lowest Bayesian Information Criterion (BIC) score (28.18) and did not have a singular fit. When model selection criterion indicate that it is appropriate, excluding the slopes of random effects in LMM's can yield higher power models without inflating the Type I error rate (Matuschek et al. 2017). The intercept only model was therefore used, and it had the form:

$$\log_{10}(N_{max} + 1) \sim depth + 1|trip + 1|site \quad (4)$$

Importantly, the exclusion of the slopes necessitated the assumption that the effect of depth remained constant across the nested sites and the different trips. A log base 10 transformation was performed on the $N_{max} + 1$ data to improve the normality and homoscedasticity of the model residuals. An ANOVA was performed on the LMM followed by a post-hoc Tukey's multiple comparison of least square means. The effect size of the pairwise comparisons was measured with Hedges' g , corrected for the small sample size (< 50 ; Durlak 2009). The difference between means is considered large if the effect size is ≥ 0.8 (Cohen 1988).

In 2016, a larger grid, spanning both Geoffrey Bay and Nelly Bay, was sampled to investigate the fidelity of *C. sivickisi* medusae to fringing reef habitat, and the related potential extent of the local population. The grid tracked the bands of fringing reef habitat located in the bays and was extended beyond the edges of the bands (Fig 3.1d). The grid had 12 sites, with two replicate locations per site, and the GPS

locations of the replicates were again predetermined from satellite imagery. The sites were separated from each other by 350 m in the longshore direction. The replicates within sites were separated by 100 m in the cross-shelf direction. The 2 x 12 grid therefore covered an approximate area of 100 x 3,850 m (0.385 km²). In the post-hoc analysis of the 2015 JCam results, the shallow and mid-depth rows were grouped together, and they were both grouped separately from the deep row where *C. sivickisi* medusae were rare (see results section, 'Horizontal distribution'). Consequently, when a site in the 2016 grid was adjacent to dense fringing reef habitat, the GPS locations of the replicates in the site were set to mirror the placement of the shallow and mid-depth sites in 2015. The shallower replicate was placed on the habitat dense enough to be visible from the satellite images and the deeper replicate was placed just outside of the dense habitat (range: 38 to 109 m from habitat). Sites that lay away from the visible habitat were placed along the same longshore contour as the habitat. Again, the placement of the sites in relation to habitat was ground-truthed from the JCam footage post sampling. The depths of the shallower row of replicates ranged from 1.3 to 7.8 m, and the depths of the deeper row ranged from 4.8 to 11.6 m. The whole grid was sampled three times over six non-consecutive nights, from the 27th of September to the 31st of October.

The grid was then expanded to determine the extent of the horizontal distribution of medusae. Additional sampling was conducted on the 3rd of November and the 9th of November. Six sites (three in Geoffrey Bay and three in Nelly Bay) which intersected dense fringing reef habitat were sampled for a fourth time. Additional sites in Alma Bay (19°8'54.99''S, 146°52'10.84''E; n = 5), to the north east of Geoffrey Bay, and Middle Reef (19°11'47.67''S, 146°48'49.86''E; n = 5), south west of Magnetic Island, were each sampled once (Fig. 3.1b).

Drogue deployments

Current speeds in waters inhabited by medusae were measured using drogues. The drogues consisted of two A4 sized acetate sheets placed one on top of the other and tied together with fishing line to form a thicker, more robust A4 rectangle. The joined sheets were weighed down by small fishing sinkers. The sheets were tied to 1 m long ropes with two small buoys on the end, chosen to reduce wind drag. A small strobe light (GLO-TOOB™ AAA) was also attached to each drogue so they could be recovered at night. A total of 95 drogue deployments were done at sites on the eastern

coast of Magnetic Island in September, October and November of 2015, 2016 and 2017. Drogues were dropped in Geoffrey Bay, Nelly Bay, Alma Bay, Middle Reef, Picnic Bay (19°11'6.81''S, 146°50'7.26''E), Florence Bay (19°7'19.71''S, 146°52'43.48''E) and Arthur Bay (19°7'44.81''S, 146°52'36.62''E; Fig. 3.1b). Deployments were made at the surface over water depths corresponding to the rows of the 2015 JCam deployments (≤ 4.1 m, 4.2 to 7 m, ≥ 7.1 m). Drogues were left to drift for 10 minutes, and the mean current speeds and directions of drift were calculated from the GPS points taken at deployment and pick up. Drogues were deployed in all states of the tide (high, ebb, low, flood) and at spring and neap tides. Drogues could only be tracked in winds of less than 15 knots (7.72 m s^{-1}).

Note, all measures of variation presented in the results section are ± 1 standard error unless otherwise specified.

RESULTS

Laboratory experiments

Experiment 1 – Temporal variation in behaviour

Copula sivickisi adult and juvenile medusae were most active at night. The relative proportions of medusae performing active (swimming, feeding and mating) and inactive (attached and bobbing) behaviours changed significantly with the time of day for both adults and juveniles (adults: Cochran-Mantel-Haenszel test, $\chi^2 = 23.80$, $df = 1$, $P < 0.001$, Fig. 3.4a; juveniles: $P < 0.01$ for 4 of 5 Fishers Exact Tests of Independence, Fig. 3.4b). Pooling all trials (adults and juveniles), there was a 30% increase in active behaviour from day to night and a 60% decrease in inactive behaviour. The change was more pronounced in the juveniles than the adults.

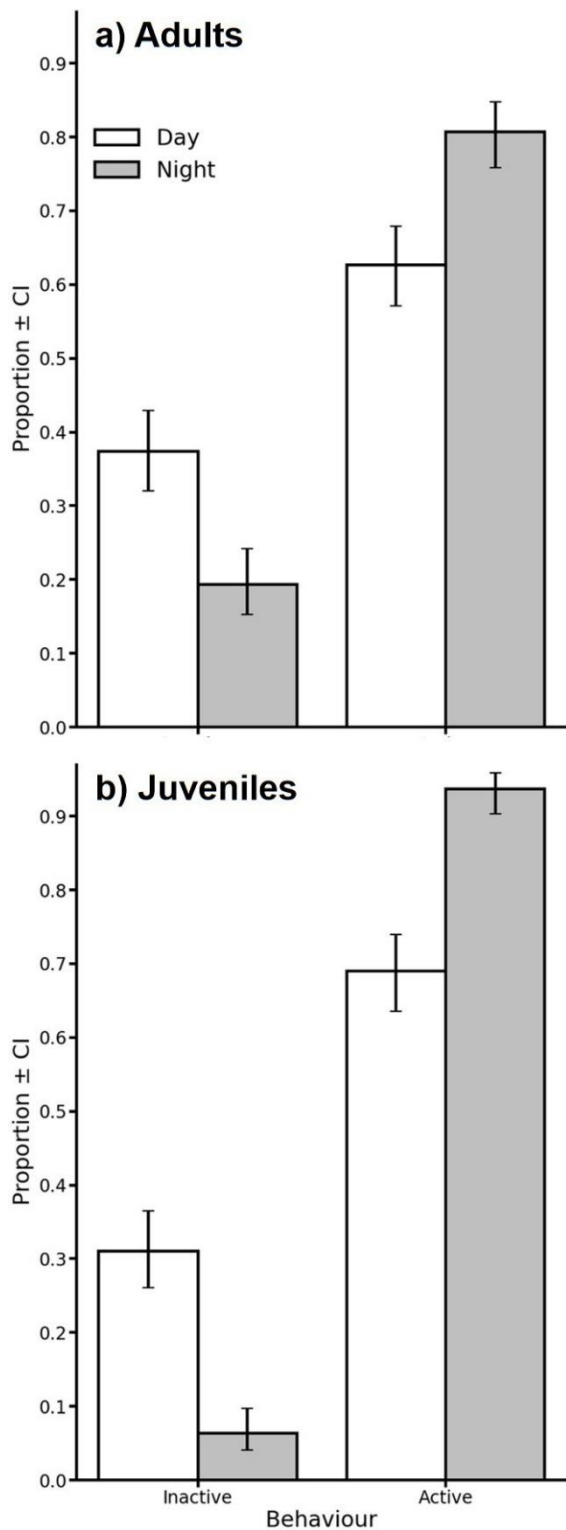


Fig. 3.4. Results from experiment 1, the temporal variation in behaviour experiment. The estimated proportions \pm 95% confidence interval (CI) of *Copula sivickisi* medusae performing active (swimming, feeding or mating) versus passive (attached or bobbing) behaviours during the day and at night. Shown are the pooled data from a) the five adult trials and b) the five juvenile trials

Analyses by hour indicated contrasting patterns of activity between day and night for adults and juveniles. Adult medusae were observed actively mating more and feeding more at night, which coincided with a reduction in the number of medusae that were swimming (Fig. 3.5a). Medusae were observed to mate almost exclusively at night; the greatest incidence was recorded at 20:00, when an average of $20\% \pm 6.3$ of adult medusae were observed performing the characteristic 'wedding dance' mating behaviour (Table 3.1). There was a trend for feeding in adult medusae to increase toward dusk and stay high at night, with the percentage feeding remaining around 60%. Increases in the percentage of adult medusae feeding were mirrored by reductions in the percentage swimming; an average of only $13.3\% \pm 6.3$ of adult medusae swam at night.

Conversely, in the juvenile trials, the increase in activity at night was driven by an increase in the incidence of swimming, and not feeding (Fig. 3.5b). Feeding peaked in the hour before lights out and remained high at the first night time observation. Feeding levels then nearly returned to where they had been before the peak. Comparatively, the percentage of juvenile medusae swimming nearly doubled from an average of $27.7\% \pm 7.0$ in day light hours to an average of $54.7\% \pm 15.5$ at night.

Night-time reductions in the observed frequency of inactive behaviours occurred in both the adult and the juvenile trials. The average percentage of medusae attached dropped by approximately 10% from day ($27.7\% \pm 5.9$) to night ($16.7\% \pm 4.5$) in the adult trials, and it dropped by 13% (from $19.3\% \pm 4.9$ to $6.3\% \pm 2.4$) in the juvenile trials. The bobbing behaviour was not observed after 19:45 at night in any of the adult trials and it was not recorded in any of the night time observations in the juvenile trials.

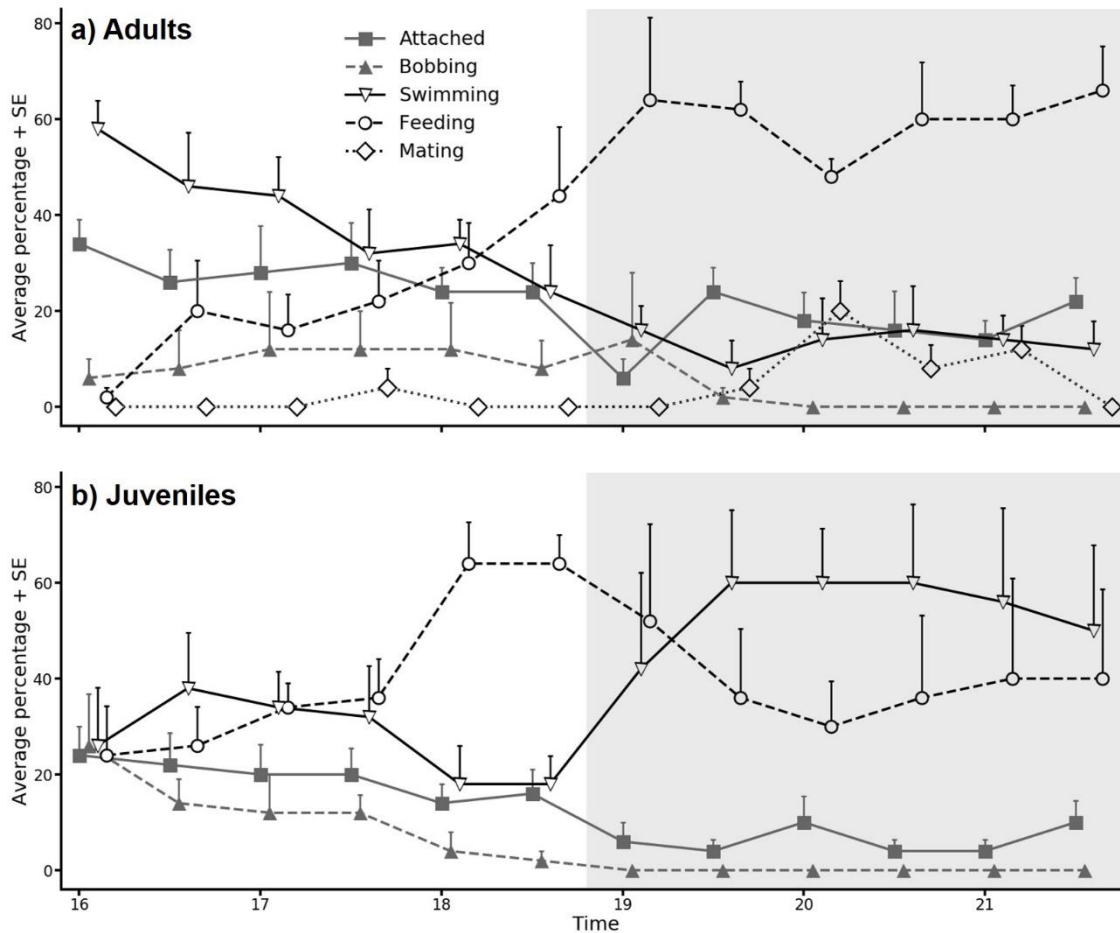


Fig. 3.5. Results from experiment 1, the temporal variation in behaviour experiment. The average percentage + SE of *Copula sivickisi* medusae performing each passive (attached and bobbing; closed, grey symbols) and active (swimming, feeding and mating; open black symbols) behaviour at each day time (white background) and night time (grey background) observation. The results from a) the five adult trials, and b) the five juvenile trials are shown

Experiment 2 – Habitat choice

Copula sivickisi Medusae showed a preference for *Sargassum sp.* algae over the other substrates in the habitat choice experiment. Eight of the ten (80%) medusae that attached to the *Sargassum* had corrected search times less than or equal to 1 min 38 s (Fig. 3.6). Medusae generally took much longer to attach to the other substrata; the majority of the medusae that attached to the tank control (10 of 14; 71%) and to the sand (10 of 14; 71%) had corrected search times longer than 1 min 38 s. On average, medusae attached to the *Sargassum* ($\text{SearchTime}_{\text{corrected}} = 1 \text{ min } 42 \text{ s} \pm 24 \text{ s}$) 1.6 times faster than they attached to both the tank control ($2 \text{ min } 49 \text{ s} \pm 29 \text{ s}$) and the sand substrates ($2 \text{ min } 40 \text{ s} \pm 23 \text{ s}$). However, this difference was not statistically significant

(Table 3.2). Only one medusa attached to the dead *Montipora sp.* coral rubble, and it had a relatively long corrected search time of 6 min 55 s.

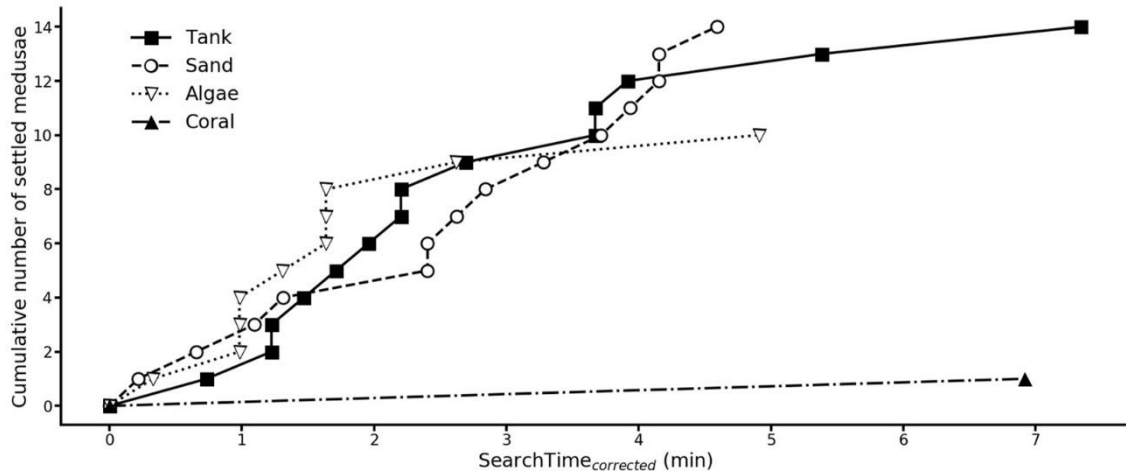


Fig. 3.6. Results from experiment 2, the habitat choice experiment. The cumulative number of *Copula sivickisi* medusae that attached to the different substrates (empty tank control, sand, *Sargassum Sp.* algae and *Montipora sp.* coral rubble) through time. The corrected search times ($\text{SearchTime}_{\text{corrected}}$) of the medusae are shown

Table 3.2. The results of the one-way ANOVA performed to test the effect of substrate on *Copula sivickisi* medusae corrected search times ($\text{SearchTime}_{\text{corrected}}$) in the habitat choice experiment (experiment 2). The source of variation (source), mean sum-of-squares (MS), degrees of freedom (df), F-value (F), and P -value (P) are shown

Source	MS	df	F	P
Substrate	0.17	2	1.62	0.21
Residual	0.11	35		

The *C. sivickisi* medusae that encountered the *Sargassum* and remained in contact with it for a short time tended to attach to the algae quickly (Fig. 3.7c). The medusae that attached to the algae, therefore, spent little time in the other substrate quadrants before attaching. In contrast, the medusae that attached to the tank (Fig. 3.7a) and to the sand (Fig. 3.7b) spent more time searching before they chose to attach; they spent considerable time in both the tank and sand quadrants, and generally had little contact with the algae (average $\text{Count}_{\text{corrected}} < 1$). The medusa that attached to the *Montipora* coral rubble was only counted in the sand quadrant and the coral quadrant in the period before it attached (Fig. 3.7d). Further, 11 of the 50 medusae trialled in

experiment 2 did not attach to any substrate (Fig. 3.7e). These medusae had nearly 5 times as much exposure to the tank control and sand quadrants compared to the algal quadrant. They were also counted in the coral quadrant more than twice as many times as they were counted in the algal quadrant.

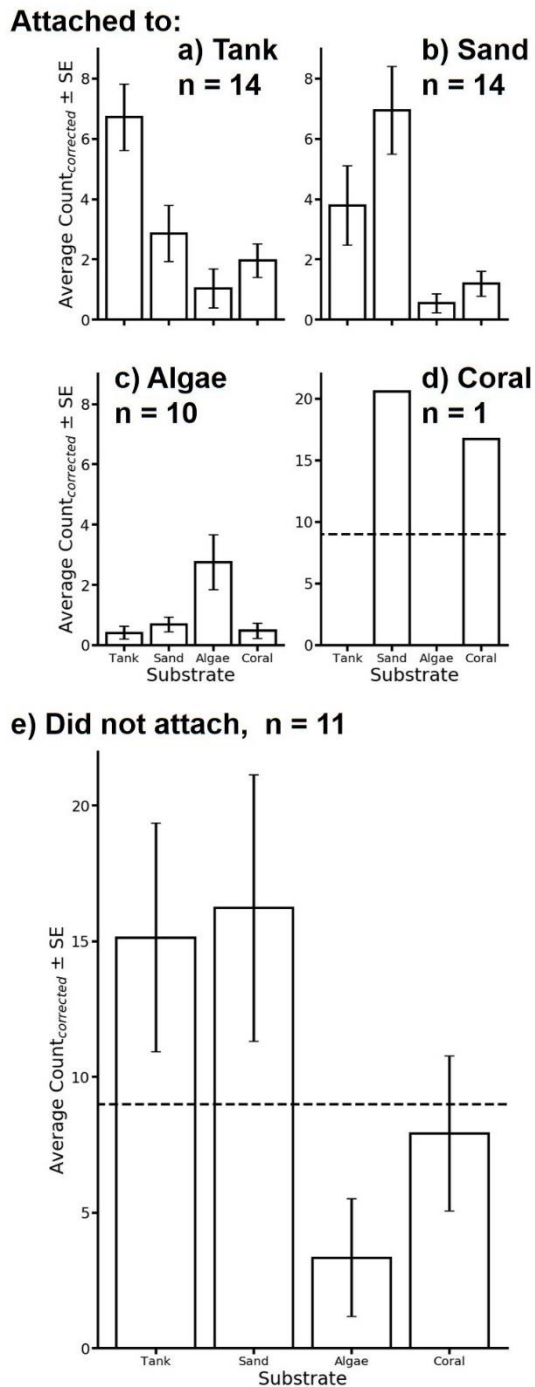


Fig. 3.7. Results from the habitat choice experiment (experiment 2). The average corrected number of times ($\text{Count}_{\text{corrected}} \pm \text{SE}$) *Copula sivickisi* medusae were counted

in each of the four substrate quadrants. For the medusae that attached to a substrate, average counts are shown for the period before they attached to a) the tank control, b) the sand, c) the *Sargassum sp.* algae or d) the *Montipora sp.* coral rubble. Average counts over the entire trial period have been shown for e) the medusae that never attached to a substrate. The dashed lines show the maximum extent of the y-axis in panes a, b and c. The numbers of attached (per habitat) and unattached medusae are shown; total n = 50

Vertical distribution

The vertical distribution of *C. sivickisi* medusae varied greatly with depth and time of day. *Copula sivickisi* medusae were almost exclusively found within 1 m of the bottom at night (average depth = 4.0 m \pm 0.4); an average abundance of 3.7 medusae per 100 m³ \pm 2.1 was recorded in the night time, near bottom tows (n = 12 tows). No medusae were caught near the bottom during the day. A single *C. sivickisi* medusa was caught at the surface during the day. Accordingly, a low average abundance was recorded in the surface day tows (0.1 medusae per 100 m³ \pm 0.1; n = 12 tows). No medusae were collected at the surface at night.

Horizontal distribution

The abundance of *C. sivickisi* medusae in the small-scale grid in Geoffrey Bay differed significantly with depth/habitat availability (ANOVA, $F(2,42)$, $P < 0.001$; Fig. 3.8a). *Copula sivickisi* medusae were most abundant at sites in the shallowest depth stratum, which all had high *Sargassum* density and/or coral cover. There was a trend for medusae to be less abundant at the mid depths where habitat availability was moderate or high, but the difference between shallow and mid-depths was not significant (Table 3.3). Medusae were rare in the deepest stratum where habitat availability was either low or absent. The abundance of *C. sivickisi* medusae at the deep sites was 11 and 7 times less than the abundances at the shallow and mid-depth sites respectively; these differences were large (effect size, Hedges' $g \geq 0.8$) and statistically significant. Depth accounted for 38.6% of the variability in medusae abundance.

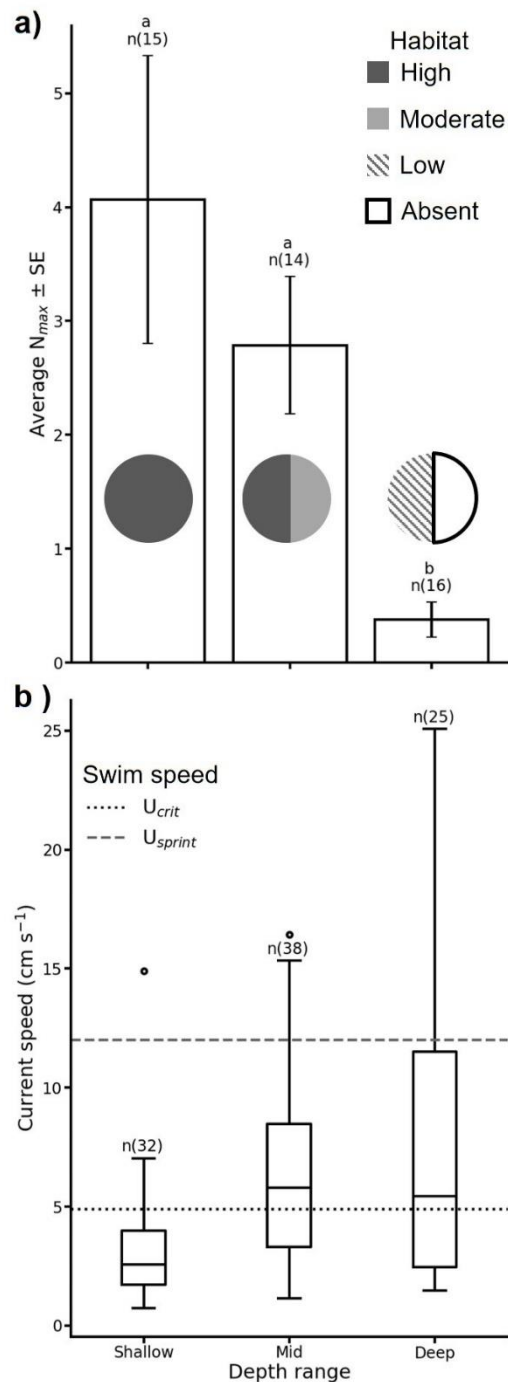


Fig. 3.8. a) Abundance of *Copula sivickisi* medusae among depth strata estimated by JCam; Geoffrey Bay, 2015. $N_{max} \pm SE$ is presented for shallow (≤ 4.1 m), mid (4.2 to 7 m) and deep (≥ 7.1 m) strata. The pie charts show the proportion of the four sites sampled per depth that had the different categories of reef habitat (*Sargassum* sp. algae and coral) availability. The post-hoc analysis groupings (a or b) and the number of sites averaged per depth are indicated. Total $n = 45$. b) Surface current speeds, from drogues, above each depth stratum. Current speeds greater than the upper quartile plus 1.5 times the interquartile range have been shown as outliers. The number of drogue deployments per depth is indicated; total $n = 95$. The overlaid lines show the greatest sprint (U_{sprint}) and the average critical (U_{crit}) swim speeds of the *C. sivickisi* medusae from the swimming trials

Table 3.3. Results from the Linear Mixed effects Model (LMM) analysis performed on the 2015 JCam survey data to test the effects of depth (shallow, mid and deep; encompassing habitat availability) on the abundance of *Copula sivickisi*. The degrees of freedom (df), t ratio and *P*-value (*P*) from the Tukey's test for each pairwise comparison have been shown, along with the effect size (Hedge's *g*)

Pairwise	df	t ratio	<i>P</i>	Hedges' <i>g</i>
Shallow - Mid	9	-0.49	0.88	0.31
Shallow - Deep	9	-6.18	< 0.001	1.01
Mid - Deep	9	-5.68	< 0.001	1.41

The population of *C. sivickisi* medusae inhabiting Nelly Bay and Geoffrey Bay was largely restricted to reef habitat. *Copula sivickisi* medusae were almost always present, and often highly abundant, at sites in the 2016 sampling grid where the habitat availability was high in at least one replicate (Fig. 3.9). Medusae were absent at two of the three sites where there was no reefal habitat and they were rare at the third (Fig. 3.9a-c). A JCam recorded a single medusa attaching to a leaf of *Sargassum*, further indicating that medusae interact with algae.

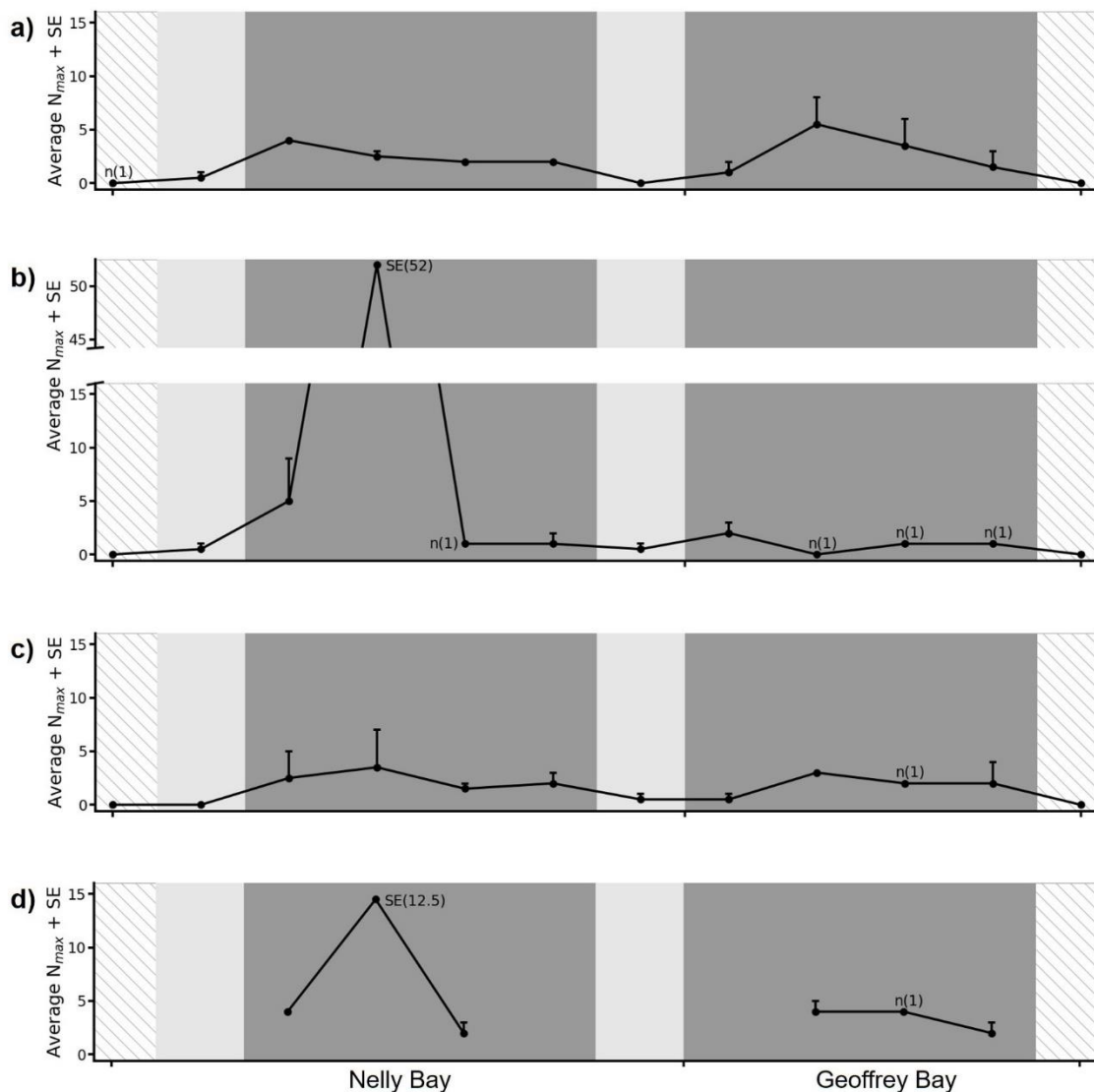


Fig. 3.9. The longshore abundance of *Copula sivickisi* medusae estimated by JCam; Nelly Bay and Geoffrey Bay, 2016. The average $N_{max} + SE$ is shown by site for each of the four sampling trips (panes a to d). The sites are in sequential order on the x-axis, from the southern most site in Nelly Bay to the northern most site in Geoffrey Bay (Fig. 3.1). The y-axis of pane b is split; the extent of the lower section matches the full extent of the other panes. n(1) indicates the sites where N_{max} could only be determined for one replicate; total $n = 77$. The exact values of high SEs have been provided in text. The background has been shaded dark grey where reefal habitat (*Sargassum sp.* algae and coral) was present at both replicates within the site, and habitat availability was high in at least one of the replicates. It has been shaded light grey where habitat was present at both replicates in either moderate or low availability. The diagonal stripes indicate where the habitat was entirely absent

Sampling at two other locations indicated that the presence of reef habitat did not guarantee the presence of medusae. All sampled sites within Alma Bay and Middle Reef had either high or moderate reef availability. *Copula sivickisi* medusae were

present in Alma Bay in moderate abundance ($N_{\max} = 1.6 \pm 0.5$, $n = 5$) and were absent from Middle reef ($n = 5$). Alma Bay is relatively sheltered while Middle Reef lies in open water (Fig. 3.1b).

Swimming speeds (Experiment 3) and drogue deployments

The *C. sivickisi* medusae swam at speeds comparable to the surface currents measured in the field. The greatest burst swim speed sustained by a medusa for more than half of a trial interval (U_{sprint}) was 12 cm s^{-1} (Fig. 3.8b). However, only 15% of medusae tested reached this speed. The average maximum swim speed of the trialled medusae (U_{crit}) was $4.9 \text{ cm s}^{-1} \pm 4.4$ standard deviation (SD). There was high variation in U_{crit} over the full size range of medusae, as indicated by the high SD around the average U_{crit} . Seventeen of the 41 medusae were observed attaching to a side of the tank during their trial to avoid being washed backwards; 13 attached in slow currents $\leq 3 \text{ cm s}^{-1}$ and four attached in faster currents $\geq 6 \text{ cm s}^{-1}$.

The surface current speeds increased with total depth of the water column (Fig. 3.8b). The weakest currents were generally measured by the drogues deployed above depths equivalent to the shallow sites in the 2015 JCam survey. The greatest U_{sprint} of the trialled *C. sivickisi* medusae was faster than all but one of the shallow water current measurements. The U_{crit} of the medusae exceeded most of the shallow water surface current speeds and was approximately double the median. The greatest U_{sprint} of the medusae exceeded most of the surface current speeds measured by the drogues that were deployed in waters with total depths equivalent to the mid and deep sites. The U_{crit} of the *C. sivickisi* medusae was slower than a majority of the mid and deep surface currents; although, U_{crit} was approximately 85% of the median speed measured at mid depths and 90% of the deep-water median. The direction of the currents as measured by the drogues was highly variable. It changed as a function of the release depth and location (i.e. within a bay, near a point, or in open water), and the state of the tide (rising, falling, high, low).

DISCUSSION

Copula sivickisi medusae inhabited shallow/mid depth reefs where *Sargassum* sp. algae and coral was abundant and current speeds were low. Where structured habitats were lacking, *C. sivickisi* medusae were rare or absent. Complex diel behaviour, where they were most active at night, combined with active swimming and a near substratum distribution suggested that dispersal from local populations would be low under normal conditions.

Temporal variation in behaviour

The diurnal activity pattern of *C. sivickisi* medusae recorded in the laboratory and in the wild (plankton tows) affirms the species is nocturnal. In the present study, medusae were detected in the night time plankton tows and were practically absent from the day time tows. Garm et al. (2012) also conducted day and night plankton tows, although their nets were drawn up vertically through the water column (approximately 5 m deep), starting at different depths. They similarly found *C. sivickisi* medusae were present in the night samples and absent from the day samples. Further, I observed major diel behavioural shifts in the laboratory, where the level of activity increased from day to night over the scale of hours. In contrast, Garm et al. (2012) recorded behavioural shifts over the scale of minutes in their experiments. For example, in an experiment where Garm et al. (2012) turned a light on at night, all of the observed medusae stopped swimming and attached themselves to the tank within 30 minutes of the introduction of the light. The differences in day time and night time activity levels reported in the present study were also less pronounced than those reported by Garm et al. (2012). Near 100% of the medusae observed by Garm et al. (2012) were attached in day light hours and an average activity level of greater than 70% was maintained in all night time hours. In the present study, greater than 60% of adult medusae were still active during the day on average, and the percentage increased to above 80% at night.

It is possible that there were some tank artefacts that influenced behaviour. Medusae were observed swimming and feeding in the tank during the day. In the wild, *C. sivickisi* medusae may hunt planktonic crustaceans at night by swimming to areas of high prey density, guided by the flashes given off when bioluminescent dinoflagellates (e.g. *Pyrocystis noctiluca*) contact zooplankton (Garm et al. 2016).

Bioluminescent flashes were observed during the night sampling in the present study. The *C. sivickisi* medusae I kept in the laboratory were fed *Artemia* nauplii, which are not bioluminescent. Consequently, the medusae that hunted in the tank at night would not have been guided by the flashes they associate with their normal prey. During the day, the orange colour of the *Artemia* would have contrasted against the white walls of the tank. This contrast may have triggered a feeding response in the *C. sivickisi* medusae. Contrast has been found to guide the behaviour of the cubozoan *T. cystophora* (Garm et al. 2013).

Habitat choice

Copula sivickisi medusae displayed a preference for *Sargassum* and avoided coral in experiment 2. SCUBA divers have previously observed *C. sivickisi* medusae swimming near and attaching to macroalgae (*Sargassum spp.* and *Colpomenia spp.*) in the wild (Hartwick 1991b). Similarly, medusae were captured swimming close to and attaching to *Sargassum* in the Jellyfish Camera Unit (JCam) footage. Contrastingly, the underside of coral was the preferred habitat of *C. sivickisi* medusae in the habitat choice experiment conducted by Garm et al. (2012). Few medusae attached to the calcified red alga *Gracilaria sp.* in the same experiment. The association between *C. sivickisi* medusae and fringing reef habitat revealed in the JCam surveys was most likely driven by a preference for *Sargassum* and not coral.

Swimming speeds

Copula sivickisi medusae are capable swimmers. The average maximum swim speed of the medusae (4.9 cm s^{-1}) exceeded most of the surface current speeds measured in the shallow waters they inhabit. Further, they could swim much faster in bursts (12 cm s^{-1}). They were also collected within one meter of the bottom in the stratified plankton tows, where the currents would be expected to be weaker than the surface currents due to current shear (Davies and Lawrence 1994).

The swim speeds of other cubomedusae in the size range of *C. sivickisi* medusae ($< 1 \text{ cm}$ InterPedalial Distances; IPD) have been measured and are comparable to the speeds measured in the present study. *Chiropsella bronzie* medusae with IPD's less than 1 cm were recorded swimming at maximum speeds of approximately 3 cm s^{-1}

(Colin et al. 2013). Garm et al. (2007) measured *T. cystophora* medusae ranging in size from 0.8 to 1.2 cm Bell Diameter (BD) swimming at maximum speeds of 3 to 4 cm s⁻¹ against a 1 to 1.5 cm s⁻¹ current in a flow chamber. Adding the highest speed and current measurements, the *T. cystophora* medusae could have been swimming at maximum speeds of up to 5.5 cm s⁻¹, similar to the presented maximum swim speed of *C. sivickisi* medusae. Larger cubomedusae have been recorded swimming at faster speeds. Colin et al. (2013) recorded a *C. bronzie* medusa with an IPD of 5.6 cm swimming at a maximum speed of approximately 12 cm s⁻¹. Garm et al. (2007) additionally reported *C. bronzie* with 3 to 5 cm BD's swimming at maximum speeds of 9.5 cm s⁻¹. *Chironex fleckeri* medusae ranging in size from 4 to 12 cm IPD have been measured swimming at speeds of up to 16.6 cm s⁻¹ in bursts in the wild (Chapter 2). Increases in cubomedusae swimming performance with size have been reported previously (Colin et al. 2013; Shorten et al. 2005; Bordehore pers comm; Garm et al. 2007). Schlaefer et al. (Chapter 2) found the opposite relationship but this was likely due to the observed wild medusae not swimming at their greatest capacity.

The formula used to determine the maximum swim speed of *C. sivickisi* medusae in the present study was developed for fish larvae (Brett 1964). To the authors knowledge, no such formula has been defined that directly relates to jellyfish. Jellyfish medusae have been found to travel more energetically efficiently than other swimming organisms, expending less energy per meter travelled (Gemmell et al. 2013). Further, compared to medusae that swim by rowing, the jetting propulsion of cubomedusae is significantly greater at utilizing the passive energy recapture mechanism that partially enables the energetically inexpensive transport of jellyfish (Gemmell et al. 2018). Despite the efficiency of cubomedusae swimming, the maximum speeds of *C. sivickisi* medusae determined from the fish larvae method matched the reported maximums of similarly sized cubomedusae derived from alternate techniques (rheotaxis measurements in a flow tank, Garm et al. 2007; digital video analysis, Colin et al. 2013). This suggests that the fish larvae method provided a true representation of the swimming capabilities of *C. sivickisi* medusae.

JCams

The JCams used to map the distribution of *C. sivickisi* medusae proved to be highly effective at detecting the small medusae in enough detail to positively identify the species. *C. sivickisi* medusae have been observed by SCUBA divers in their natural

environment (Hartwick 1991b) but such observations are rare and efforts to observe *C. sivickisi* in the wild have previously yielded no medusae (e.g. Garm et al. 2012). Cameras have already been used to detect larger jellyfish, but from above the water (Llewellyn et al. 2016). The JCam system presented here is novel because it used lights underwater. The technique allowed for the simultaneous sampling of medusae over relatively large areas. It was also cost effective; each unit was relatively inexpensive (~ \$500 AUD). However, the presence of the light likely affected the behaviour of the medusae, so their natural behaviours could not be inferred from the JCam footage. To observe the natural behaviours of medusae, the camera field of view could be illuminated by a red light imperceptible to the medusae. The medusae could be attracted by additional lights simulating the intermittent bioluminescent flashes from dinoflagellates that purportedly guide hunting in *C. sivickisi* medusae (Garm et al. 2016).

The quality of the JCam footage varied based on several factors including the placement of the JCam on the substratum, the position of the camera in relation to the light and the presence of dense plankton and algae in the field of view. Some of the footage was also unusable due to instrument failure (i.e. the camera or light malfunctioning or shutting off before the end of the 30-minute deployment); though loss of samples from JCam failure was < 9%. Therefore, it is recommended that the mapping of the distribution of cubomedusae with JCams or similar technology is done with high enough replication to account for the loss of replicates.

Behavioural maintenance of distribution

Mapping the distribution of *C. sivickisi* medusae revealed that they were generally only found at sites where the availability of fringing reef habitat, rich in *Sargassum*, was moderate to high. Moreover, areas of reef that had lower habitat availability generally had less medusae. The behaviour of *C. sivickisi* medusae is likely critical to maintaining their observed distribution on fringing reef habitat. Certainly, many of the behaviours performed by *C. sivickisi* medusae have the potential to limit their dispersion including limiting their activity, attaching to hard substrates and staying near the bottom of the water column.

Copula sivickisi medusae are only active for a portion of the day due to their diurnal activity pattern, limiting their exposure to dispersive currents. Even when medusae are

active at night, the swim trial results suggest it is unlikely that they would swim against dispersive currents for extended periods. In the trials, some medusae attached to the tank when exposed to currents speeds of 6 cm s^{-1} or greater for less than a trial interval (5 minutes). Wild medusae could rationally attach to reefal habitat to avoid being flushed away in strong currents and then remain attached until the currents weakened. *Copula sivickisi* medusae have been observed attaching to reef structures such as *Sargassum*, red algae, hard coral and stone (present study; Garm et al. 2012; Hartwick 1991b). Medusae were also found to maintain positions near the bottom of the water column where they would not have to swim far to find a surface to attach to. Further, medusae near the bottom would likely experience currents weakened from current shear (Davies and Lawrence 1994) and they could counteract dispersion by swimming into the weakened currents. Numerous *C. sivickisi* medusae exhibited rheotaxis in the swim trials, swimming directly into the current for minutes at a time. The cubozoans *C. bronzie* and *T. cystophora* have previously exhibited rheotaxis in a laboratory setting (Garm et al. 2007) and the scyphozoan *Rhizostoma octopus* has been documented swimming counter to the mean current direction in the wild (Fossette et al. 2015). While some insight was gained from the swim trials, more research is required to determine the maximum swimming duration of *C. sivickisi* medusae and the strategies they utilise to prevent expatriation. They are small, have transparent bodies, and are inactive during the day. Further laboratory experiments would likely be required to elucidate the behaviour of *C. sivickisi* medusae in currents because of the extreme difficulty in observing them in their natural environment.

Other cubozoan species have been found to perform behaviours that enable the maintenance of distribution patterns. *Tripedalia cystophora* medusae are most commonly found at the fringes of mangroves; they maintain positions in this preferred habitat by using their specialised eyes to peer up through the water surface to detect and navigate the mangrove canopy (Garm et al. 2011). *Chironex fleckeri* medusae inhabit estuarine and nearshore coastal waters. They are highly mobile and often swim longshore, and possibly toward the shore, to maintain their nearshore distribution and local populations (Chapter 2). Like the reefal habitat inhabited by *C. sivickisi*, the mangroves, estuaries and coasts inhabited by other cubozoans are characterised by 'sticky water', where complex structures reduce flow and facilitate retention (Andutta et al. 2012).

Maintaining positions near fringing reef habitat may have numerous advantages for *C. sivickisi* medusae, in addition to providing a refuge from dispersive currents. The

reefal structures (e.g. algal tufts and hard coral) may provide some protection against predators, as has been shown for other reef species (e.g. fishes; Hixon and Beets 1993). There may also be important reproductive benefits. The convergence of medusae to a thin band of reef would put them near potential mates and provide an abundance of structures and niches to attach their sticky embryo sacs to (Hartwick 1991b).

Population structure

The absence of medusae from sites off the fringing reef habitat band that were devoid of *Sargassum* and coral suggests that the *C. sivickisi* medusae inhabiting Nelly Bay and Geoffrey Bay represent a local population. In addition to their swimming/attachment behaviour, the reproductive behaviour of *C. sivickisi* medusae may assist in maintaining this restricted distribution. *Copula sivickisi* gametes are not dispersed via broadcast spawning because medusae have internal fertilization (Lewis and Long 2005), and the medusae may selectively attach their embryo sacs to reefal habitat (Hartwick 1991b). The early life history stages of *C. sivickisi* medusae are also seemingly adapted to limit dispersion. The planula larvae that arise from the embryos can attach to hard surfaces (Hartwick 1991b). Once settled, they develop into sessile polyps. The medusae that bud from cubozoan polyps are nearly fully formed (Werner et al. 1971), and could possibly swim competently to counteract dispersion soon after metamorphosis. The swimming capabilities of newly metamorphosed medusae have not been assessed, and this would be an interesting avenue for future research.

The spatial extent of the stock that the identified local population belongs to is still unknown. Mooney and Kingsford (2017) collected statoliths from *C. sivickisi* medusae inhabiting locations on the east Australian coast that were separated by hundreds of kilometres. They found that the shapes of the statoliths differed significantly by location, suggesting that the *C. sivickisi* stocks had a maximum extent of hundreds of kilometres. The potential for stock differentiation to occur at much smaller spatial scales is great given the non-dispersive reproductive behaviour of *C. sivickisi* medusae, the stickiness of *C. sivickisi* at all life stages, and the demonstrated strong swimming abilities of medusae > 4 mm IPD. *Copula sivickisi* medusae were absent from Middle Reef which had suitable habitat but is relatively exposed, given its location between Magnetic Island and mainland Australia. This suggests that the island population could be isolated from any mainland *C. sivickisi* populations. A separation

of Magnetic Island and mainland stocks has been reported for the larger cubozoan *C. fleckeri*. The statolith elemental chemistry of *C. fleckeri* medusae caught from the island and the adjacent mainland differed significantly indicating that the medusae had experienced different environmental conditions and were, therefore, from separate stocks (Mooney and Kingsford 2016a).

The seemingly poor dispersal potential of *C. sivickisi* contradicts the expansive extent of the metapopulation. The *C. sivickisi* phenotype has been recognised throughout the Pacific and in the Indian Ocean (Kingsford and Mooney 2014; Lewis et al. 2008). Such a cosmopolitan distribution is rare in cubozoan species and, given their poor dispersal abilities, it suggests a long geological history where range expansion occurred with the movements of tectonic plates (i.e. vicariance theory). It is highly likely that medusae from many locations within the metapopulation are genetically distinct enough to be recognised as incipient species (i.e. genetically distinct but morphologically similar with reproductive compatibility). Populations of scyphozoans inhabiting environmentally similar systems have diverged into incipient species through genetic isolation (*Mastigias* sp., Dawson and Hamner 2005; *Catostylus mosaicus*, Dawson 2005). Further, Schroth et al. (2002) found that different environmental conditions drove divergent selection and speciation in the cosmopolitan scyphozoan jellyfish genus *Aurelia* (moon jelly). There is great capacity for similar divergent selection across the tropical and temperate latitudes inhabited by *C. sivickisi*. However, speciation may be comparatively slower in cubozoans given the low number of described species (pers comm). Populations of the cubozoan *Carybdea marsupialis* from coastal locations across the Mediterranean, covering hundreds of kilometres, were found to represent populations of the same species as they were genetically and morphologically similar (Acevedo et al. 2019). The population genetics of species in the more pelagic cubozoan genus *Alatina* were also recently analysed; the species in the genus likely represent a single species with a pantropical distribution (Lawley et al. 2016). Similar analyses are currently being conducted for the *Copula* genus (pers comm). Genetic analyses have been combined with biophysical modelling (hydrodynamic models coupled with models of plant/animal behaviour) to effectively identified population structures in other jellyfish (e.g. Dawson et al. 2005). Similar analyses could help to elucidate the hierarchical structure of *C. sivickisi* populations, given the complex behaviour of medusae.

Storms and the attachment of polyps to drifting *Sargassum* could provide mechanisms for increasing the scales of connectivity between *C. sivickisi* populations or for

facilitating speciation. Medusae may not be able to maintain their positions on reefal habitat in extreme weather events, and adrift medusae could be transported by the currents. Further, the *Sargassum* species that *C. sivickisi* are associated with are annuals that shed the sporophyte seasonally. The loss of algal cover peaks in spring (Kingsford 1992, 1993), coinciding with the presence of *C. sivickisi* medusae at Magnetic Island. While medusae are likely to detach from drifting algae, as has been found for other invertebrate species (Kingsford and Choat 1985), the embryo sacs, planula larvae and polyps of *C. sivickisi* medusae could remain attached. Drifting macroalgae can travel for kilometres (Baring et al. 2018) transporting any attached fauna with it. To survive, the *C. sivickisi* would need to metamorphose into medusae before the drifting algae is washed onto the shore or into the open sea. Expatriated *C. sivickisi* could establish new populations or connect existing ones. The founder effect may affect a new population if the number of founding members is low, providing a method for speciation (Mayr 1954).

Conclusions

I have provided strong evidence that the behaviour of *C. sivickisi* medusae is likely to minimise dispersal from local populations. Medusae were most active at night, were found close to the substratum and could swim at speeds comparable to the current speeds measured at the depths they inhabit. The new JCam technology was highly effective in mapping the distribution of *C. sivickisi* medusae. The medusae were most abundant in shallow/mid depth waters with fringing reef habitat. The swimming ability of medusae and their restriction to bands of habitat suggests that the population of *C. sivickisi* medusae inhabiting Geoffrey Bay and Nelly Bay represents a local population. While the spatial extent of *C. sivickisi* stocks is unknown, the island population may be relatively isolated from any mainland populations. Despite the apparently limited dispersion potential of *C. sivickisi* at all life stages, *C. sivickisi* is a cosmopolitan species. This discrepancy suggests a long geologic history and I predict a level of incipient speciation within the species' cosmopolitan distribution.

CHAPTER SUMMARY

The medusae of cubozoan jellyfishes have sophisticated behaviours and are strong swimmers. Therefore, they have the potential to influence their distribution and connectivity among populations. I used ecological and behavioural data in combination with local oceanography to estimate the potential for medusae of the cubozoan *Copula sivickisi* to disperse from local populations at scales of hundreds of meters to kilometres. The distribution of *C. sivickisi* was mapped on a fringing reef at Magnetic Island, Queensland, Australia, with underwater jellyfish camera units (JCams). The availability of reef habitat, dominated by *Sargassum* sp. algae and coral, had a significant effect on the abundance of medusae. Medusae were 11 to 7 times more abundant at shallow (≤ 4.1 m) and mid-depth (4.2 to 7 m) sites with high to moderate habitat availability, compared to deep sites (≥ 7.1 m) where habitat availability was low. Further, medusae were absent at sites far from suitable habitat, both alongshore and in deeper water. Medusae displayed preferential habitat selection. They were found low in the water column near reefs in depth stratified plankton tows and they preferentially attached to *Sargassum* in a habitat choice experiment. The swimming speeds of *C. sivickisi* medusae were determined experimentally and were equivalent to or faster than most of the current speeds measured where populations occur. The results suggested that medusae can attach to habitat and swim against currents to maintain positions on reefs, thereby restricting dispersal. Incipient speciation is highly likely within the species cosmopolitan distribution.

Chapter 4.

Behavioural and oceanographic isolation of an island-based jellyfish (*Copula sivickisi*, Class Cubozoa) population

INTRODUCTION

The dynamics of populations are underpinned by their structures. The geographic ranges of marine species are generally inhabited by partite metapopulations composed of mesopopulations/stocks which are largely self-contained (Sinclair, 1988; Kingsford and Battershill, 1998). Stocks may be further divided into connected local populations (Kingsford and Battershill, 1998). As stocks are isolated, their population dynamics are principally determined by intrinsic factors such as growth, reproduction and self-recruitment (Sinclair, 1988). The stocks of aquatic species range in size from whole ocean basins to individual rivers, islands or bays. Currents and/or swimming can transport individuals long distances, connecting distant population units (e.g. Williamson et al., 2016). In contrast, species may inhabit systems with retentive currents and/or may limit dispersion through biological mechanisms (e.g. the box jellyfish *Chironex fleckeri*, Chapter 2; the tidepool copepod *Tigriopus californicus*, Burton 1997).

The distributions of cubozoan species cover a range of spatial scales; however, information on how populations within these distributions are structured is generally lacking. The class Cubozoa contains the venomous the box jellyfish, including the infamous Irukandji jellyfishes. The oceanic *Alatina alata* (encompassing the junior synonyms *Alatina moseri* and *Alatina mordens*) is unique among the cubozoans as *A. alata* medusae have been found at great depths in open water, and the species is thought to maintain a worldwide metapopulation through the dispersal of medusae and encysted planulae (Bentlage et al., 2010; Lawley et al., 2016). In contrast, most cubozoans inhabit nearshore estuarine and/or coastal waters (Kingsford and Mooney, 2014). The habitats fringing estuarine and coastal systems (e.g. mangroves, and rocky and coral reefs) are often highly structured. Complex eddy fields can be generated as currents flow past/through the biotic and abiotic structures within these habitats, thereby producing a zone of increased retention which can act as a refuge from strong currents (the sticky water effect; Wolanski, 1994). Further, cubozoan medusae

metamorphose from polyps nearly fully formed (Werner et al., 1971) and quickly grow (Gordon and Seymour, 2012; Toshino et al., 2014) to have strong swimming and orientation abilities (e.g. Chapter 2; Chapter 3; Garm et al., 2007). There is growing evidence that the dispersal of estuarine/coastal cubozoans is limited by their complex environment and behavioural responses. Accordingly, stocks may form at relatively small spatial scales within the metapopulations of estuarine/coastal cubozoans. Mooney and Kingsford (2017) investigated the scales of stock differentiation in three estuarine and coastal cubozoan species by analysing the shapes of cubomedusae statoliths. They collected *C. fleckeri*, *Copula sivickisi* and *Carukia barnesi* medusae from different locations in Queensland, Australia, separated by hundreds of kilometres. The shapes of the statoliths from two of the three surveyed species (*C. fleckeri* and *C. sivickisi*) differed significantly between locations, suggesting the populations inhabiting the locations represented separate stocks.

Small spatial scales of separation have been identified between *C. fleckeri* stocks. Significant differences have been found in the shapes and microchemistry of *C. fleckeri* statoliths from medusae collected at sites separated by only tens of kilometres (Mooney and Kingsford, 2016a; Mooney and Kingsford, 2017). Further, a *C. fleckeri* stock was found to have a distribution restricted to Port Musgrave, a semi enclosed estuarine bay in far north Queensland, Australia. The bays retentive currents made it unlikely that *C. fleckeri* would leave the bay at any life stage (Chapter 2). The bay-scale stock had substructure as swimming medusae formed local populations in nearshore waters at scales of hundreds of meters.

The data required to assess population structures at a fine spatial scale are lacking for other cubozoan species. The *C. sivickisi* metapopulation covers tropical and temperate latitudes in the Pacific and Indian Oceans (Lewis et al., 2008; Kingsford and Mooney, 2014). While this expansive distribution suggests broad dispersal and connectivity, the ecology and behaviour of *C. sivickisi* suggests that stocks are likely to be separated by relatively small spatial scales. *C. sivickisi* are seemingly adapted to limit dispersion at all life stages. *C. sivickisi* males directly transfer spermatophores to ovoviviparous females (Lewis and Long, 2005) so gametes are not released into the water column. Rather, females produce sticky embryo sacs, which they may selectively attach to the substrate (Hartwick, 1991b). The embryos develop into planula larvae which can also attach to surfaces (Hartwick, 1991b) before they adhere permanently and develop into sessile polyps. *C. sivickisi* medusae are strong swimmers (Chapter 3) and they have an array of sophisticated behaviours. The medusae have sticky pads on the apex of

their bells (Hartwick, 1991b) which they use to preferentially attach to substrates (Chapter 3; Garm et al., 2012). *C. sivickisi* medusae are also largely nocturnal (Hartwick, 1991b; Garm et al., 2012). When they are inactive, they may attach to substrates to rest and to avoid being expatriated from preferred habitats (Chapter 3).

In chapter 3, *C. sivickisi* medusae were predominantly found in shallow water in association with *Sargassum sp.* algae and hard coral. Their distribution was determined to be largely restricted to bands of reef which spanned 4 km across the two surveyed bays at Magnetic Island, Queensland, Australia. Magnetic Island lies 8 km from the mainland. Given the observed restricted distribution and the poor dispersal potential of *C. sivickisi*, it was predicted that the Magnetic Island population was isolated from any mainland *C. sivickisi* populations. However, stock differentiation techniques have not been applied at a sufficiently small scale to test this prediction.

Few stock differentiation techniques have been applied to *C. sivickisi*. Numerous techniques have been used to successfully differentiate stocks at relatively small spatial scales in other jellyfish species including: demographics (e.g. Pitt and Kingsford, 2000), genetics (e.g. Dawson et al., 2015), biogeochemistry (e.g. Mooney and Kingsford, 2016a) and biophysical modelling (e.g. Chapter 2). Uniquely, biophysical modelling gives information on both the scales and mechanisms of stock separation, and the technique is increasingly being applied to examine stock dynamics (e.g. Hinrichsen et al., 2011). Biophysical modelling is particularly useful when the behaviour of the focal organism has the potential to greatly influence its dispersal (Wolanski, 2017), which is true for *C. sivickisi* medusae.

The objective of this study was to determine the population structure of the *C. sivickisi* inhabiting Magnetic Island. The extent of the population was mapped with underwater Jellyfish Camera units (JCams; Chapter 3) and a biophysical model was applied to: (1) explore the role of *C. sivickisi* medusae behaviour in restricting their distribution to shallow reefs, (2) ascertain the interconnectedness of reefs and bays at Magnetic Island and, (3) determine if the island population represented a stock that was isolated from any mainland populations.

MATERIALS AND METHODS

Study site

Magnetic Island lies in the central area of the Great Barrier Reef (GBR) Marine Park. The currents in the GBR system are largely driven by the jets of the South Equatorial Current (SEC) which flow westward across the coral sea and collide with the outer reefs of the GBR (Kessler and Cravatte, 2013). In the central GBR, the North Caledonian Jet (NCJ) from the SEC generally diverges around the Queensland plateau before meeting the outer reefs (Kessler and Cravatte, 2013). In addition to these regional scale forcings, the waters within the GBR system are shallow (< 200 m) so winds can force currents at a local scale (Luick et al., 2007).

Behavioural retention

In 2016, the distribution of *Copula sivickisi* medusae in Nelly Bay and Geoffrey Bay of Magnetic Island was found to be largely restricted to shallow bands of fringing reef habitat dominated by *Sargassum sp.* algae and coral (Chapter 3). In this chapter, a biophysical model was used to investigate the role of behaviour in maintaining the observed restricted distribution.

Biophysical model

The Second-generation Louvain-la-Neuve Ice-ocean Model (SLIM; Lambrechts et al., 2008) was used to model the nearshore retention of *C. sivickisi* medusae in Nelly Bay and Geoffrey Bay. The two-dimensional depth averaged version of SLIM was used because the waters of interest were shallow (< 20 m deep) and vertically well mixed, like other waters in the Great Barrier Reef (GBR) lagoon (Luick et al., 2007). The two-dimensional version of SLIM has previously been used to accurately simulate the hydrodynamics of shallow systems that are well mixed (Lambrechts et al., 2008) and partially mixed (Pham Van et al., 2016). In SLIM, the shallow-water equations are discretised and solved in space with a second order discontinuous Gerlerkin finite element method and in time with a second order implicit Runge-Kutta method (Lambrechts et al., 2008). The dissipation due to bottom friction was calculated with a Chezy-Manning scheme, and the bottom friction was calculated according to the

Chezy-Manning-Strickler formulation. The turbulent velocity was calculated with a Smagorinsky scheme.

The unstructured mesh of SLIM allowed for the inclusion of regional and local scale forcings. The model domain extended westward into the coral sea (Fig 4.1a). The northern boundary of the model was approximately set in the middle of the Queensland Plateau, above the latitude where the southern divergence of NCJ typically meets the GBR (Kessler and Cravatte, 2013). The southern extent of the domain was far to the south of Magnetic Island to avoid confounding errors from the open boundary forcing. The model was forced with tides and currents at the open boundary, and with wind over the entire domain. The values of these forcings were interpolated to the SLIM boundary/grid from eReefs GBR 4, a heavily cross-checked regional scale model of the hydrodynamics of the GBR system and the adjoining coral sea (Herzfeld et al. 2016). The introduction of the open boundary forcings was buffered by: (1) situating the model boundary 10 km from the 200 m isobath and setting all depths in the model bathymetry > 200 m to 200 m, and (2) ramping the input up over 48-hours. The model bathymetry was derived from an open source high resolution (30 m) depth model of the GBR (Beaman 2017). Erroneous deep nearshore holes in the depth model had to be corrected before it could be used in SLIM (Appendix II, Fig. AII.1).

The model mesh was made finer near coasts and over reefs and coarser in open water, prioritizing the allocation of computational power (Fig. 4.1c d). As an indication of the model resolution and the related computational requirements, the mesh was composed of 74, 438 triangles and the side lengths of the triangles ranged from 30 m to 7.5 km. There were, therefore, 223,314 degrees of freedom by field (sea surface elevation, and zonal and meridional current components). The sea surface elevation simulated in SLIM was validated against a local tide gauge and the simulated currents were validated against current meters at 4 sites at or near Magnetic Island (Fig 4.1b; Appendix II, Fig. AII.2, Table AII.1). The hydrodynamic fields were saved every 15 minutes.

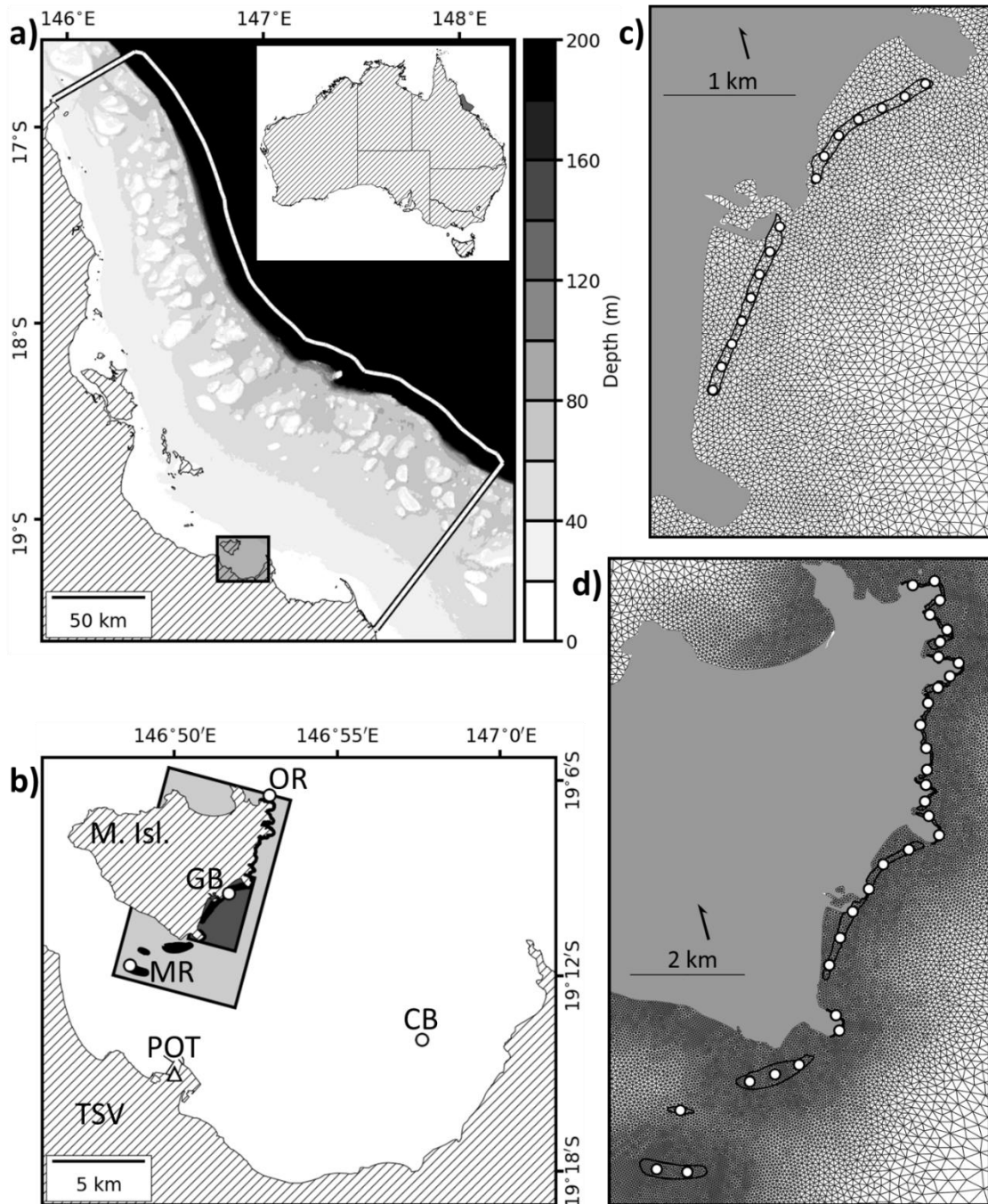


Fig. 4.1. Biophysical model development, validation and application. a) The model domain (white line with black border), and the bathymetry of the modelled region. The color bar indicates the depth (m). Depths > 180 m are shown in black. The inset shows the location of the model domain (grey polygon) in Queensland, and its scale in relation to Australia. The location of pane b is indicated by the grey box. b) The instruments used to validate the hydrodynamic simulations in the Townsville (TSV)/Magnetic Island (M. Isl.) region. The white dots mark the locations of the current meters at Cleveland Bay (CB), Middle Reef (MR), Geoffrey Bay (GB) and Orchard Rocks (OR). The white triangle marks the location of the tide gauge at the Port of Townsville (POT). The locations of panes c and d are indicated by the dark and light grey boxes respectively. Reefs from OR to MR are shown in black. c) and d) The seed locations (white) and reefal habitats (black outline; identified from satellite images and

validated with JCam footage) used in the behavioural retention and connectivity analyses respectively. The variable resolution SLIM mesh is shown in c and d. Land is filled with a hatch pattern in panes a and b, and filled grey in panes c and d

The dispersion of medusae was simulated by coupling the hydrodynamic output with two candidate models (base and dependent) of the behaviour of *C. sivickisi* medusae. An Okubo scheme (Okubo, 1971) was used to model the horizontal diffusion (K_h) of medusae from sub-mesh scale turbulent mixing as a function of the local mesh size (l) following de Broye et al. (2010):

$$K_h = \alpha \times l^{1.15} \quad (1)$$

The value of the coefficient α was set to $2 \times 10^{-4} \text{ m}^{0.85} \text{ s}^{-1}$, derived directly from Okubo (1971). The dispersal of passive particles released from a single location in Nelly Bay, Magnetic Island was analysed through time to determine the resulting effective diffusivity (combined sub-mesh and mesh scale diffusivity). Measures of the diameter of the passive particle plume were taken as the plume spread from the initial seed location. The effective diffusivity was estimated to be $< 20 \text{ m}^2 \text{ s}^{-1}$. Appropriately, this is less than the value of $25 \text{ m}^2 \text{ s}^{-1}$ that Hrycik et al. (2013) calculated for the more exposed Northumberland Strait, Canada.

The behavioural models were developed from the results of Chapter 3 and from data sourced from the literature. In both models, the behaviour of medusae changed with position in relation to reefal habitat (on/off) and with time of day (day/night; Table 4.1). The extent of the reefal habitat in Nelly Bay and Geoffrey Bay in 2016 was determined from historic satellite images sourced from Google Earth (version 7.3.2.5491). Where possible, the presence of reefal habitat was later validated with JCam footage (Chapter 3). Medusae were classified as 'on habitat' if they lay within 100 m of the midlines of the historic habitat bands and were classified as 'off habitat' if they were greater than 100 m from the midlines. The *C. sivickisi* medusae were modelled to be nocturnal, i.e. they were inactive during the day and active at night (Chapter 3; Garm et al., 2012). Between 07:00 and 18:57 was considered daytime and between 19:00 and 06:57 was considered night time, corresponding to the normal time of sunrise and sunset in the region during the *C. sivickisi* season (September to November). Medusae were re-assigned behaviours every 3 minutes.

The two models had the same day time behaviour; medusae on habitat during the day attached themselves to the habitat (Chapter 3; Garm et al. 2012) and were therefore

not affected by the current, while the medusae off habitat had no directional swimming cues. In the base model, medusae on habitat at night were made to swim toward the habitat midline (Chapter 3; Garm et al. 2012) regardless of the current speed and, again, medusae off habitat had no directional swimming cues. For swimming medusae, the direction of swimming was calculated as the direction of the shortest line that could be drawn from the medusa's position to the habitat midline. A current speed dependent attachment behaviour was added to generate the dependent model. A dependent model medusa on habitat at night would only swim if the current speed at its position was less than a predefined cut off (Chapter 3). If the current speed equalled or exceeded the cut off, the medusa would attach itself to habitat, thereby becoming immovable. In both candidate behavioural models, and in all times and positions, medusae unattached to habitat were assumed to stay close to the bottom of the water column. Some current shear (where the surface currents are faster than the currents near the bottom) would be expected, even in shallow water (Fischer et al., 1979; Davies and Lawrence, 1994), and so only half of the current velocities simulated in SLIM were applied to near bottom medusae. When the medusae swam in both models, their speed was either set to their calculated maximum swim speed (U_{crit} ; 4.9 cm s^{-1} ; Chapter 3) or the maximum speed they could sustain without signs of fatigue (U_{sust} ; 2.45 cm s^{-1}), estimated to be half U_{crit} (Fisher and Wilson, 2004). The inclusion of each component of the behavioural models is justified in detail in Appendix II (Table All.2).

Runs and analysis

Scenarios with different parameterisations of the two candidate models were performed to examine the effects of swim speed and selective attachment to habitat on the retention of *C. sivickisi* medusae. Two base model scenarios were simulated, where medusae were modelled to swim at U_{sust} and U_{crit} respectively. The dependent model was parameterised with all combinations of the two swim speeds and three different attachment to habitat current speed cut offs (6, 7.5 and 9 cm s^{-1} ; Chapter 3). 6 dependent model scenarios were therefore simulated in total. Further, medusae were modelled as passive in a control scenario to determine the level of retention without behaviour.

Table 4.1. Descriptions of the base and dependent models of *Copula Sivickisi* medusae behaviour. The behaviour of medusae in the base model was determined by the time of day (day or night) and the location of medusae in relation to reefal habitat. An additional behaviour was added to the dependent model where medusae only swam at night if the current speed at their location was less than a predefined cut off (6, 7.5 or 9 cm s⁻¹). When medusae swam in the base or dependent model, their speed was either set to their maximum sustainable (U_{sust} ; 2.45 cm s⁻¹) or maximum (U_{crit} ; 4.9 cm s⁻¹) swim speed

	Day (07:00 to 20:57)	Night (21:00 to 06:57)	
On habitat	Base = dependent Attached to habitat.	Base Near bottom. Unattached with cue to swim horizontally to the centre of the habitat band.	Dependent Current speed < cut off: Near bottom. Unattached with cue to swim horizontally to the centre of the habitat band. Current speed ≥ cut off: Attached to habitat.
Off habitat	Base = dependent Near Bottom. Unattached with no horizontal swimming cues.	Base = dependent Near bottom. Unattached with no horizontal swimming cues.	

In all candidate models/parameterisations, *C. sivickisi* medusae were released from the previously identified historic bands of reefal habitat in Nelly Bay and Geoffrey Bay (Fig. 4.1c). They were released from 15 locations spaced along the bands at 200 m intervals. 1000 medusae were released per location; 15,000 were released in total. Medusae were released simultaneously at mid night on 17 September 2016, the first full moon of the 2016 *C. sivickisi* season. The release was timed to coincide with a full moon because *C. sivickisi* medusae at Magnetic Island have been found to metamorphose from polyps within the four days following either a full or new moon (unpublished data). No mortality was included. The runs ended after 30 days, approximately the length of one lunar cycle, allowing for the assessment of retention under spring and neap tides. Five replicate runs were performed per candidate model/parameterisation. The number of medusae remaining in the bays was counted through time.

Population structure

Mapping the population

The geographic extent of the *C. sivickisi* population inhabiting the east coast of Magnetic Island was mapped as the first step in elucidating the structure of the island population. The mapping was done in the 2017 medusae season with underwater Jellyfish Camera units (JCam's, Chapter 3; Fig. 4.2b). The photopositive *C. sivickisi* medusae were attracted to the light on each JCam and recorded by the adjacent camera in 30-minute deployments. Following established methods for managing potential repeat counts (Cappo et al., 2004), the abundance of medusae was measured by counting the maximum number of medusae in any single frame of video during the deployment period (Nmax).

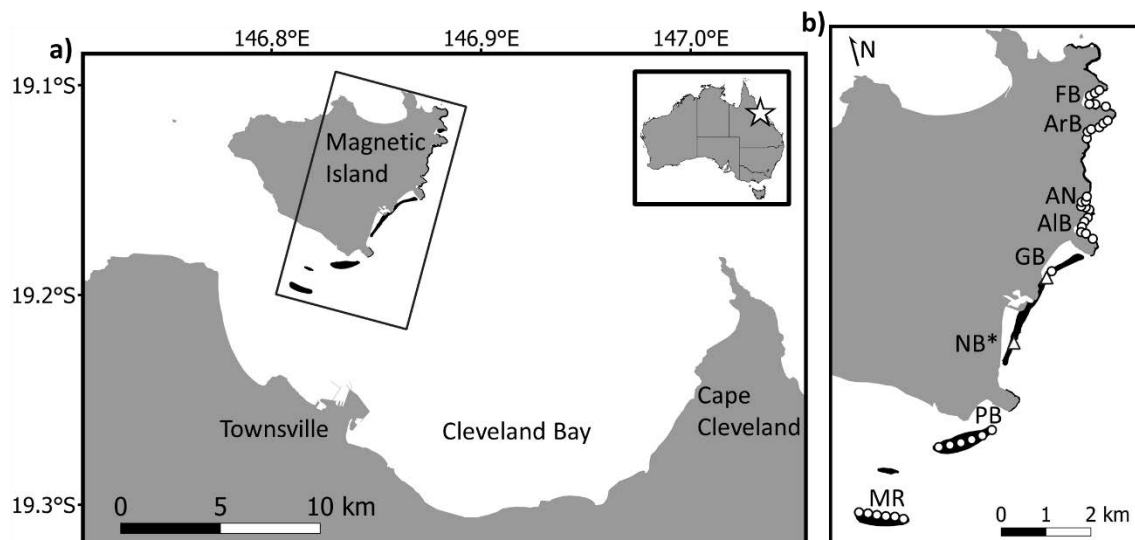


Fig. 4.2. The study region. a) The Townsville coast and Magnetic Island. The location of a is shown on a map of Australia (star). The rectangle shows the extent of b. b) The JCam survey design covering Middle Reef (MR), Picnic Bay (PB), Geoffrey Bay (GB), Alma Bay (AB), Alma North (AN), Arthur Bay (ArB) and Florence Bay (FB). The white dots show the sites where the JCam's were deployed within each location. The white triangles show the sites in Nelly Bay (NB; * no JCam's were deployed in NB) and GB where the modelled currents were extracted for inclusion in Fig. 4.3. Land is filled grey and reefs are filled black in both panes

JCam's were deployed at sites on reefal habitat along the east coast in Picnic Bay (6 sites), Geoffrey Bay (2 sites randomly placed near the *C. sivickisi* hotspot identified in chapter 3), Alma Bay (6 sites), Alma north (6 sites), Arthur Bay (6 sites) and Florence

Bay (6 sites). Further, Middle Reef lies approximately 3 km to the south west of Magnetic Island, between the island and the mainland and could potentially act as a bridge between the Magnetic Island *C. sivickisi* population and any mainland populations. JCamS were also deployed at 6 sites on Middle Reef to explore this possibility. The coordinates of the sites were pre-determined from Google Earth satellite images to guide the night time sampling. Darkened patches in the images were assumed to correspond to reefs and the presence of reefal habitat at the sites was later confirmed from the JCam footage. Each bay/reef, excluding Geoffrey Bay, was sampled two times over six non-consecutive nights from the 25th of September to the 30th of October. The sites within Geoffrey Bay were sampled in each of the 6 trips to confirm the presence of *C. sivickisi* medusae throughout the sampling period.

Connectivity analysis

Biophysical modelling was used to determine the inter bay/reefal connectedness of the *C. sivickisi* population on the east coast of Magnetic Island, and to investigate if the island population was isolated from any mainland stocks. SLIM was again used to model the movements of *C. sivickisi* medusae in the waters off the eastern coast of Magnetic Island and the surrounding region. The hydrodynamic component of the model had the same set up as previously described for the behavioural retention analysis, and the outputs were validated in the same way (Appendix II, Fig. AII.2, Table AII.1). For the behavioural component, the dependent model parameterised with medusae swimming at U_{crit} and attaching to habitat at night at a current speed cut off of 6 cm s^{-1} best fit the high retention documented in Chapter 3. This behavioural model/parameterisation combination was, therefore, selected for use in the connectivity analysis.

C. sivickisi medusae were seeded along and slightly beyond the identified east coast distribution (Fig. 4.1d). As part of assessing the potential for Middle Reef to act as a bridge between the island and mainland populations, medusae were also seeded from Middle Reef despite their absence from the reef in the JCam population survey (see results section 'Population structure'). The 'on habitat' bands in the behavioural model were extended to cover reefal habitat from Middle Reef to north of Florence Bay. Historic satellite images from Google Earth were again used to extrapolate the distribution of reefal habitat in the 2017 *C. sivickisi* season, and the extrapolated distribution was validated with JCam footage where possible. Medusae were seeded

on the five nights leading up to and including each of the 5 new or full moons (unpublished data) within the 2017 *C. sivickisi* medusae season, and so they were seeded on 25 nights in total. On each seed night, 200 medusae were released from each of the 32 seed locations on the hour over 12 night-time hours from 19:00 to 06:00. This ensured medusae were released in all states of the tide following Grech et al. (2016). Two thousand four hundred medusae were released from each seed location on each seed night, and 1,920,000 were released over the entire season. Natural mortality was added to the behavioural model to simulate the exponential attrition of medusae that would likely occur throughout the season. The instantaneous mortality rate ($z = 0.135 \text{ day}^{-1}$) was calculated from unpublished catch curves of *C. sivickisi* medusae and used to estimate the natural mortality following Ricker (1975):

$$N_t = N_0 \times e^{-z \times t} \quad (2)$$

Where the number of medusae alive at time t (N_t) was a function of the initial number of medusae (N_0), z and t . All remaining medusae were killed at 56 days, the maximum age of *C. sivickisi* medusae estimated from unpublished demographic data (unpublished data). An Okubo scheme, with a coefficient (α) derived directly from Okubo (1917), was again used to model the diffusion of medusae by turbulent mixing at a sub-mesh scale.

A measure of relative connectivity was generated to assess the levels of self-seeding and inter bay/reefal connectivity in the Magnetic Island *C. sivickisi* population. The 'on habitat' zones in the behavioural model (100 m buffer around habitat midlines) were divided into 32 detection zones, around the 32 seed locations. The detection zones had an average area of $0.08 \text{ km}^2 \pm 4 \times 10^{-3}$ (range: 0.04 km^2 to 0.13 km^2). The instances of unique connections (from source seed location to sink detection zone) made by adult medusae within and between zones were counted throughout the season. Medusae were considered adults 25 days post release because *C. sivickisi* medusae $> 5 \text{ mm}$ in diameter (half their maximum size; Kingsford and Mooney, 2014) are generally sexually mature (Lewis and Long, 2005), and *C. sivickisi* medusae would take around 25 days to grow to 5 mm (unpublished data). To generate the measure of relative connectivity, a log base 10 transformation was performed on the counts +1 data, and the transformed data was scaled from 0 (no connections) to 1 (most connections). Further, the potential for connectivity between the island and mainland populations was assessed by tracking the positions of all adult medusae lost from habitat at/near Magnetic Island through time. The combined trajectories showed the maximum extent of the emigration plume from the Magnetic Island population.

Importantly, medusae seeded from Middle Reef were excluded from this analysis because of the absence of *C. sivickisi* medusae at Middle Reef in the JCam survey and the demonstrated unlikelihood of Magnetic Island medusae successfully emigrating from the island to Middle Reef (see results section 'Population structure').

Note, all measures of variation presented in the results section are ± 1 standard error unless otherwise specified.

RESULTS

Behavioural retention

There was greater retention of simulated *C. sivickisi* medusae in Nelly Bay and Geoffrey Bay when the medusae swam compared to when they were passive (Fig. 4.3, 4.4). Medusae were released on the 17 September 2016, into the strong currents that followed the 16 September spring tide (Fig. 4.3a, b). In the passive model runs, $95.1\% \pm 0.1$ of the medusae were expatriated from the bays by these strong currents within four days of their release (Fig. 4.3c). A majority of the medusae left in the bays after four days were expatriated through time, with near zero remaining toward the end of the 30-day model run. Flood and ebb tides brought medusae in and out of the bays, causing small, regular fluctuations in the numbers of medusae counted within the bays.

There was greater retention of simulated medusae when they were modelled with the base set of behaviours, swimming at night irrespective of the current. However, during the initial period of strong currents, the base model medusae were lost at a similar rate ($95.8\% \pm 0.1$) to the medusae in the passive scenarios (Fig. 4.3c). In moderate currents, the number of base model medusae in the bays fluctuated amid diel cycles of accumulation and loss. The numbers increased during the day as medusae retained in tidal eddies were brought into the bays with the incoming tide and subsequently attached to habitat. The numbers decreased at night as the swimming medusae were expatriated by currents faster than their swimming speeds. These diel cycles occurred from the 9th to 16th day after release when the medusae swam at U_{crit} and from the 9th to 20th day after release when they swam at U_{sust} . In contrast, the number of medusae in the bays increased when the currents were weak. In weakened currents, the medusae transported back into the bays with tidal eddies during incoming tides were able to swim faster than the currents at night, and so maintained their positions on the

habitat. For example, there was a period of weakened currents which lasted from the 16th to the 23rd day after the initial release of medusae, around the neap tide which occurred 21 days after the release. When the base model medusae swam at U_{crit} , the percentage in the bays increased nearly 5-fold from $3.8\% \pm 0.1$ at the start of the period, to $18.0\% \pm 0.2$ at the end. The number of medusae in the bays increased at a slower rate when they swam at the slower U_{sust} . In the same period of weakened currents, the percentage of medusae in the bays in the U_{sust} runs started at a comparable $3.0\% \pm 0.1$ but only doubled to $6.2\% \pm 0.1$ by the end. However, the percentages of base model medusae retained in the bays in the U_{crit} and U_{sust} scenarios similarly approached zero at the end of the 30-day runs. There were strong currents around the spring tide which occurred 29 days after the initial release of medusae which expatriated the medusae swimming at night.

Retention was greatest when the simulated medusae's behavioural set included the current speed dependent attachment behaviour. In contrast to the base model, the more biologically realistic dependent model simulated much greater within bay retention than the passive model during the initial period of strong currents ($> 24\%$ in all scenarios; Fig. 4.3c, Fig. 4.4). The percentage of medusae remaining in the bays after 30 days did not approach zero in any of the dependent model scenarios, the average percentage remaining ranged from 10.2 ± 0.2 to $82.4\% \pm 0.7$. Greater retention was recorded in the dependent model scenarios with a lower attachment speed cut off and the higher swim speed. For example, in the set of scenarios where the medusae swam at U_{sust} , an average of over 5 times more medusae were retained at the end of the 30-day runs when they attached at current speeds $\geq 6 \text{ cm s}^{-1}$ (56.0 ± 0.4) compared to when they attached at speeds $\geq 9 \text{ cm s}^{-1}$ (10.2 ± 0.2). Further, in the pair of scenarios where medusae attached at current speeds $\geq 9 \text{ cm s}^{-1}$, the retention nearly quadrupled when the swim speed was increased from U_{sust} to U_{crit} (38.4 ± 0.2).

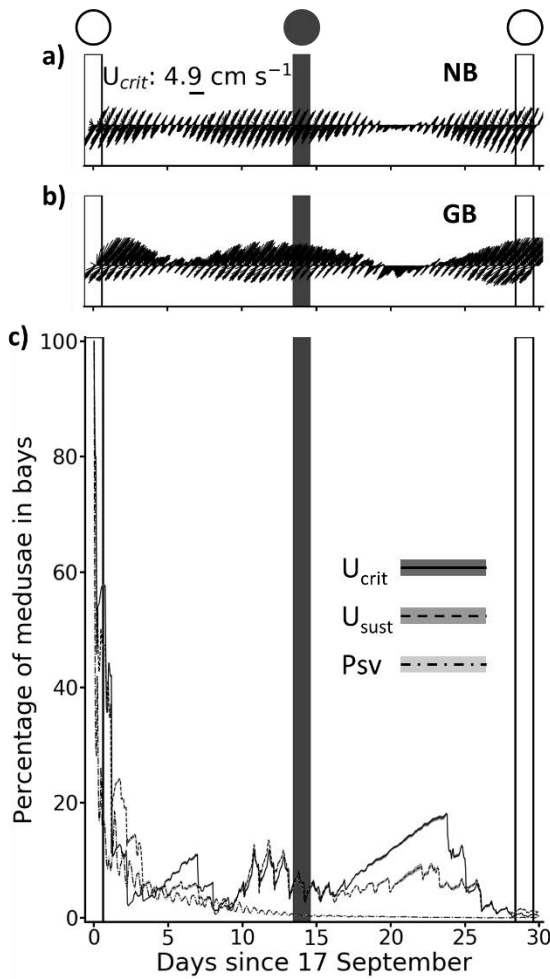


Fig. 4.3. Results of the behavioural retention analysis. The simulated currents experienced by medusae (i.e. half the depth averaged current) at sites in a) Nelly Bay (NB) and b) Geoffrey Bay (GB). The sites are marked in Fig. 4.2. The lengths of the sticks indicate the current speed and the sticks are oriented in the direction the current flowed to. The reference stick in a) shows the stick length for a speed of U_{crit} . c) The average percentage of *Copula sivickisi* medusae remaining in NB and GB through time as simulated with the passive (dashed and dotted line; light grey band) and base models. Base model medusae were modelled to swim at either U_{crit} (solid line; dark grey band) or U_{sust} (dashed line; grey band). The bands underlying each line indicate the range of percentages simulated among the five replicate model runs. The circles at the top of the figure, and the vertical lines running down from them, show when there was a full (white) or new (grey) moon

There were complex interactions between the currents in the bays and the residency of dependent model medusae. Periods of retention, accumulation and loss were simulated in weak, moderate and strong currents. Medusae with the dependent attachment behaviour could only be expatriated from reefal habitat by currents faster than their swim speed, but slower than the current speed cut off. The narrower the range of expatriating currents, the rarer expatriation events were. For example, the greatest retention was recorded in the dependent model scenario with the narrowest range of expatriating currents, where medusae swam at U_{crit} and attached at a cut off of 6 cm s^{-1} (range = $6 - 4.9 = 1.1 \text{ cm s}^{-1}$). In this scenario, there were only two substantial expatriation events during the entire 30 day run. Nearly 18% (17.8 ± 0.9) of the medusae initially seeded in the bays were lost in the consecutive events which occurred between the 15th day and 17th day after release. The medusae remaining in the bays after these events were retained for the duration of the model run. In contrast, there were multiple expatriation events in the first 4 days after release in the scenario with the next narrowest range of expatriating currents (U_{crit} , cut off = 7.5 cm s^{-1} ; range = $7.5 - 4.9 = 2.6 \text{ cm s}^{-1}$). Over half of the medusae (53.3 ± 0.4) were lost from the bays in these events; although, some of the lost medusae moved back into the bays in the following 24 hours. After the initial expatriation events, there were comparatively smaller fluctuations (loss and reaccumulation) in the number of simulated medusae remaining in the bays. Nearly half of the medusae initially seeded in the bays remained at the end of the 30 day run. There was more between replicate variability in the dependent model runs compared to the continuous model runs. The greatest difference between the upper and lower bounds at any time in the base model runs was 1.0%. In contrast, the difference between bounds in the dependent model scenarios was generally an order of magnitude greater, although it rarely exceeded 10%.

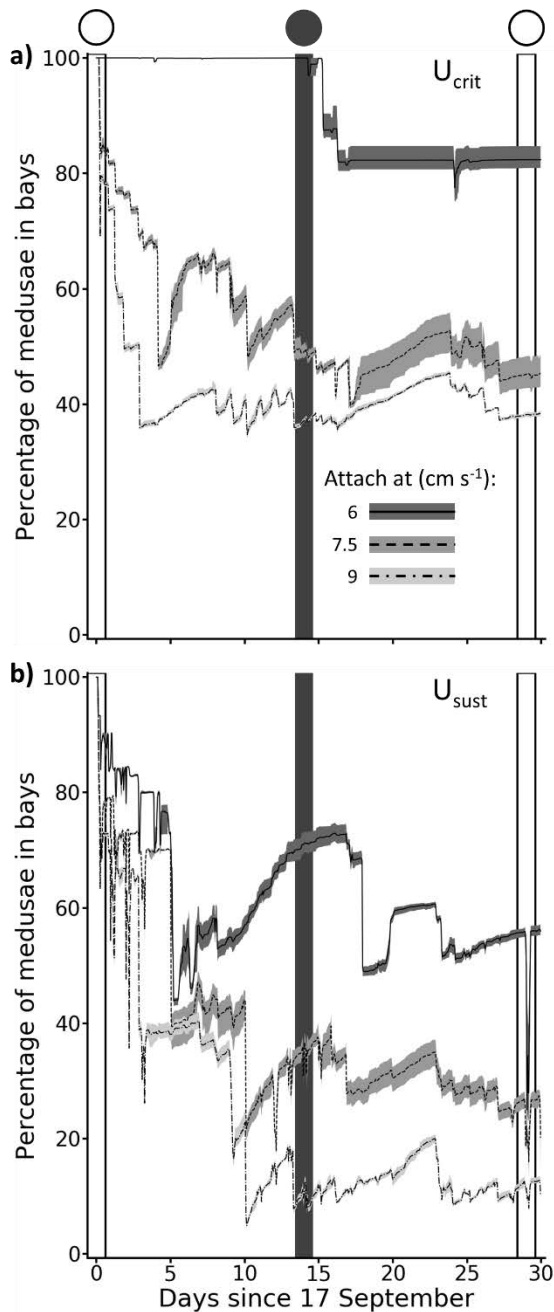


Fig. 4.4. Results of the behavioural retention analysis. The average percentage of *Copula sivickisi* medusae remaining in Nelly Bay and Geoffrey Bay through time as simulated with the dependent model. Model medusae were modelled to swim at either a) U_{crit} or b) U_{sust} , and to attach to habitat at current speed cut offs of 6 (solid line; dark grey band), 7.5 (dashed line; grey band), and 9 cm s^{-1} (dashed and dotted line; light grey band). The bands underlying each line indicate the range of percentages simulated among the five replicate model runs. The circles at the top of the figure, and the vertical lines running down from them, show when there was a full (white) or new (grey) moon

Population structure

Population extent

The population of *Copula sivickisi* medusae extended along the entire east coast of Magnetic Island (Fig. 4.2, 4.5). The reefal habitat on the east coast was dominated by *Sargassum sp.* algae and coral, and near continuous patches of reef were separated by small areas of sand. The abundance of medusae peaked in Geoffrey Bay, mid-way along the east coast, and Florence Bay, the northern most sampling location. Medusae were 2 to 5 times more abundant at Geoffrey Bay and Florence Bay compared to the other sampled locations on the east coast. *C. sivickisi* medusae were absent from Middle Reef where the habitat was similarly dominated by *Sargassum* and coral.

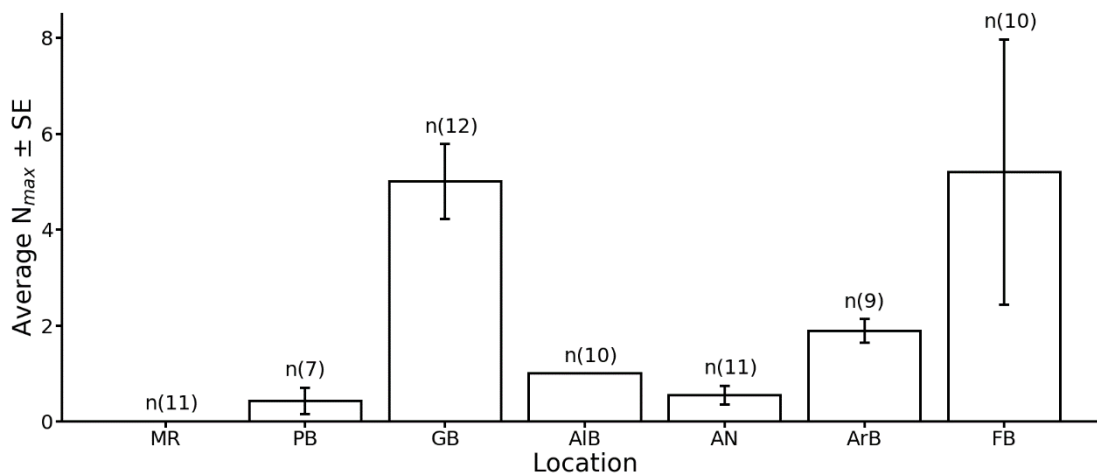


Fig. 4.5. The abundance of *Copula sivickisi* medusae estimated by JCam. The average $N_{max} \pm SE$ is shown by location. Locations are: Middle Reef (MR), Picnic Bay (PB), Geoffrey Bay (GB), Nelly Bay (NB), Alma Bay (AB), Alma North (AN), Arthur Bay (ArB) and Florence Bay (FB; Fig. 4.2). The number of sites averaged per location are indicated; total $n = 70$

Connectivity

The simulated population of *C. sivickisi* on Magnetic Island was well mixed in ecological time. The in-zone retention rate was high, as indicated by the high relative connectivity between identical source and sink locations (top left to bottom right diagonal in matrix; Fig. 4.6, Appendix II Fig. All.3). Inter bay connections were made between adjacent bays, but over small distances. For example, simulated medusae

released from central Nelly Bay were recorded in Geoffrey Bay as adults, in a detection zone 1.1 km to the north east of their initial release location (Fig. 4.7). Adult medusae from central Nelly Bay were also recorded 1.4 km to the south west of their release location, in a detection zone in Picnic Bay.

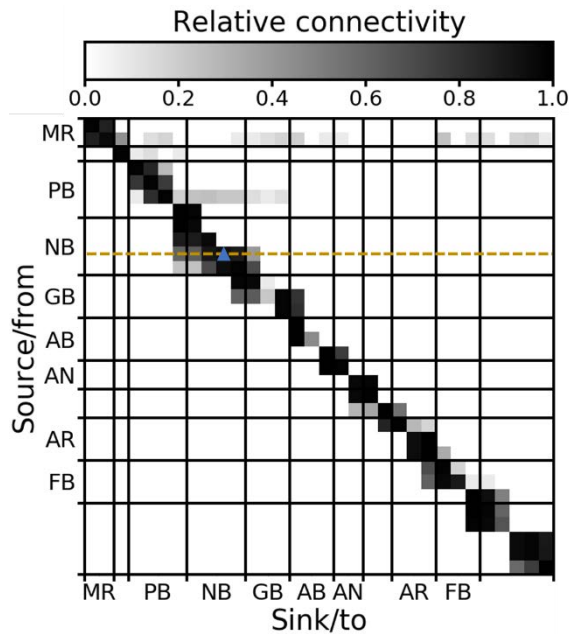


Fig. 4.6. A connectivity matrix showing the relative connectivity between source/from and sink/to detection zones over the entire 2017 medusae season. The detection zones have been pooled by the reefs/bays identified on the x and y axes. Locations are: Middle Reef (MR), Picnic Bay (PB), Geoffrey Bay (GB), Nelly Bay (NB), Alma Bay (AB), Alma North (AN), Arthur Bay (ArB) and Florence Bay (FB; Fig. 4.2). The matrix shows the result from one of five replicate model runs (dependent model, swim speed = $U_{crit} = 4.9 \text{ cm s}^{-1}$, attach at cut off of 6 cm s^{-1}). The yellow dashed line indicates the transect of the connectivity matrices shown in Fig. 4.7, where the blue triangle shows the position of the focal detection zone

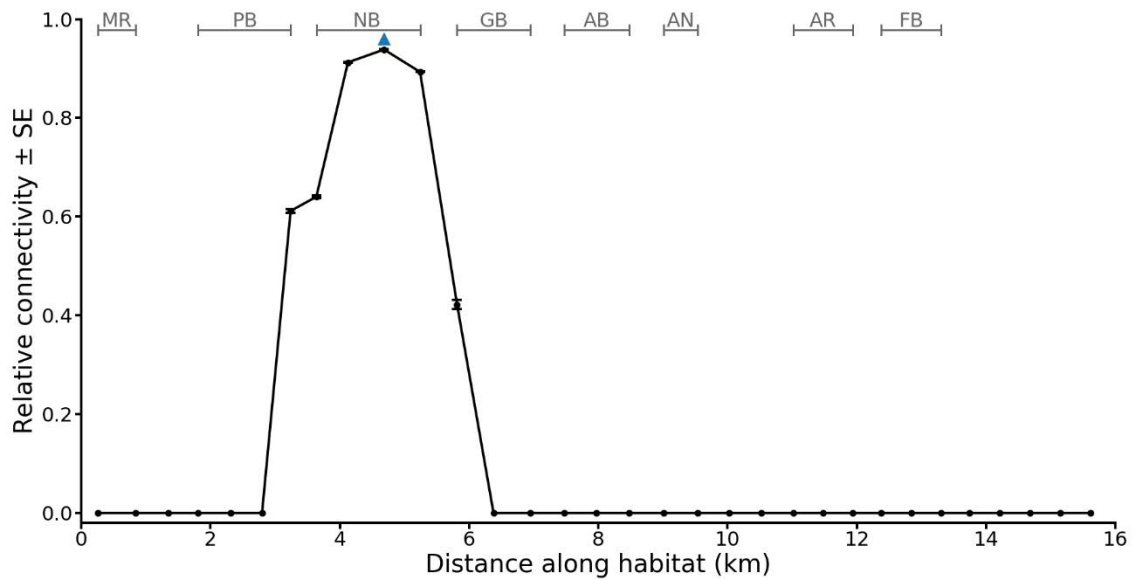


Fig. 4.7. The average relative connectivity \pm SE of the modelled detection zones with a zone in mid Nelly Bay (NB), as indicated in Fig. 4.6. The relative connectivity is plotted with distance along the near continuous habitat band starting from Middle Reef (MR). The position of the focal detection zone is shown by the blue triangle; the connectivity at this position is indicative of the level of within zone retention. The locations/extents of the different reefs/bays are indicated by the identifiers along the top of the figure. Locations are: MR, Picnic Bay (PB), Geoffrey Bay (GB), NB, Alma Bay (AB), Alma North (AN), Arthur Bay (ArB) and Florence Bay (FB; Fig. 4.2). $n = 5$ replicate model runs (dependent model, swim speed = $U_{crit} = 4.9 \text{ cm s}^{-1}$, attach at cut off of 6 cm s^{-1})

Middle Reef did not act as a steppingstone between the simulated island population and any mainland populations. The simulated medusae were rarely exported north-eastward from Middle Reef to Magnetic Island reefs (Fig. 4.6, Appendix II, Fig. All.3). Export in the opposite direction, south-westward from the island to Middle Reef, was almost non-existent.

Further, no direct emigration of *C. sivickisi* medusae from the Magnetic Island population to any mainland populations was modelled. The vast majority of modelled *C. sivickisi* medusae maintained positions on reefal habitat fringing Magnetic Island for the duration of their lives. An average of only 934.0 ± 59.3 medusae (1.3% of all seeded medusae) died in open water, away from the reefs fringing Magnetic Island. No modelled medusae were transported from Magnetic Island reefs to the mainland coast (Fig. 4.8 a). Medusae lost from habitat tended to be advected to the north east, travelling maximum distances of $< 50 \text{ km}$ from Magnetic Island. A few medusae were expatriated to the east south east, and they were transported smaller distances ($< 25 \text{ km}$ from Magnetic Island).

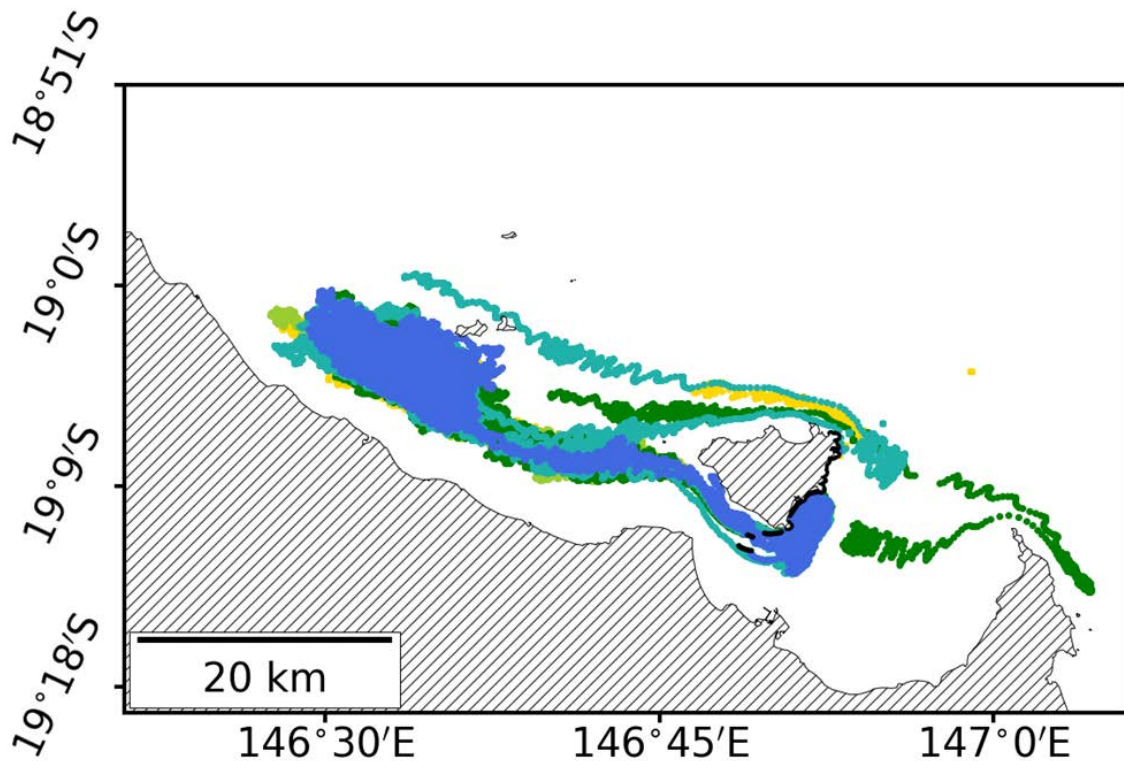


Fig. 4.8. Positions of all adult medusae lost from Magnetic Island habitat over the entire 2017 *Copula sivickisi* medusae season, representing < 1% of the total number of simulated medusae released (dependent model, swim speed = $U_{crit} = 4.9 \text{ cm s}^{-1}$, attach at cut off of 6 cm s^{-1}). The plotted plumes, therefore, show the maximum extent of the export of adult *C. sivickisi* medusae from Magnetic Island. The sequential colours, from yellow to blue, distinguish the results of the five replicate model runs. Land is filled with a hatch pattern and reefs are shown in black

DISCUSSION

The behaviour of *Copula sivickisi* medusae was integral to the maintenance of their restricted distribution on fringing reef habitat. Within a medusae season, it is highly unlikely that ecologically significant numbers of *C. sivickisi* medusae could successfully emigrate from the Magnetic Island population to populations on the mainland.

The importance of behaviour in retention

The behaviour of *C. sivickisi* medusae was critical to maintaining their restricted distribution on fringing reef habitat, in alignment with the predictions of Chapter 3. The documented high retention of medusae on reefal habitat (Chapter 3) was only replicated in the biophysical model when medusae swimming near habitat at night

were modelled to attach to the habitat when the current exceeded a moderate to strong speed cut off (i.e. the dependent model). This suggests that *C. sivickisi* medusae must exhibit some selective activity pattern to maintain their restricted distribution. The modelled current dependent attachment behaviour is realistic given the documented behaviour of *C. sivickisi* medusae in a swim chamber. Over 40 % of the *C. sivickisi* medusae tested in swim trials with step wise increases in flow attached to a side of the swim chamber with the sticky pads on their bells to avoid being pushed back by the flow (Chapter 3). Further, *C. sivickisi* medusae exhibited a strong preference for reefal habitat in the habitat choice experiments conducted by both Schlaefer et al. (Chapter 3) and Garm et al. (2012). There is, however, uncertainty surrounding the true behaviour of *C. sivickisi* medusae in their natural environment given they are nocturnal and have small transparent bodies, and so are extremely difficult to observe in the field. Alternate selective activity strategies could similarly reduce the risk of expatriation. For example, fishes and invertebrates commonly use selective tidal-stream transport to control their horizontal movements. They maintain positions on the bottom until the tide is in a phase that will transport them in their required direction, whereon they ascend to be carried by the tidal current (Forward and Tankersley, 2001). However, catches of *C. sivickisi* medusae in depth stratified plankton tows suggest it is unlikely they utilise selective tidal-stream transport as they were active independent of the state of the tide and never moved up the water column (Chapter 3). Nevertheless, additional laboratory experiment could be performed to clarify how *C. sivickisi* medusae mitigate the risk of expatriation.

Sources of error

The observed behaviours of *C. sivickisi* medusae were modelled with a high level of sophistication. However, models invariably only capture a portion of the variability that exists in natural systems (e.g. ontogenetic, among individual and stochastic variation; Bode et al., 2019). For example, constant average swim speeds were included in this study's biophysical model, and the model results were shown to be sensitive to changes in the swim speed. The variability surrounding these averages, from sources such as medusae varying their swim speed in reaction to external factors (e.g. currents, the presence of prey) and differences in individuals swimming abilities, was not incorporated into the model.

Further, there was uncertainty in specifying some of the physical parameters of the dispersal model. For example, there is considerable uncertainty surrounding the parameterisation of sub-grid scale turbulence models (e.g. the Okubo scheme applied in this study; Okubo 1971). Additionally, a current shear parameter was included to account for the reduced current speeds likely to be encountered near the bottom of the water column. Model medusae were only affected by half of the simulated depth average current. This was conservative given the velocity of a flow can approach zero with increasing proximity to a boundary (e.g. the bottom of the water column; Fischer et al., 1979; Davies and Lawrence, 1994). Three-dimensional hydrodynamic models simulate the current shear with depth, eliminating the need to make assumptions about the current shear. Incorporating more natural variability and moving to three-dimensional models may further understanding in future research. It is also good practice to perform sensitivity analyses to understand how sensitive modelled outcomes are to variations in the model parameterisation (e.g. Critchell and Lambrechts, 2016).

In this chapter, increasing the model complexity by including the dependent attachment behaviour increased the between replicate variability. Importantly, the results were robust as the modelled trends never differed between replicates. Future modelling studies should similarly check that the modelled trends are consistent between replicates to ensure their results do not contain inconsistencies introduced through underseeding (Brickman and Smith, 2002).

Population structure

The observed population of *C. sivickisi* medusae at Magnetic Island was found to extend at least as far as the range of the JCam survey on the island which covered the entire east coast. The population may extend beyond the limits of the survey. The preferred habitat of *C. sivickisi* medusae is fringing reef and the presence of reefs is, therefore, a prerequisite for the presence of *C. sivickisi* (Chapter 3). There is fringing reef on the northern section of the island. However, fringing reef is rare on the west coast where the dominant habitats are shallow sediment flats and seagrass beds (Carter et al., 2016).

The Magnetic Island population of *C. sivickisi* is possibly a robust, genetically distinct stock given the limited potential for export of medusae from the island to the mainland.

Substructural divisions (as described by Kingsford and Battershill, 1998) within the identified stock are likely; the model predicted connected bay-scale local populations with high retention. It is improbable that ecologically significant numbers of *C. sivickisi* medusae from the population on the east coast of Magnetic Island could successfully emigrate to the mainland. There was no evidence that Middle Reef acts as a 'stepping stone' (Slatkin, 1993) between island and mainland *C. sivickisi* populations. *C. sivickisi* medusae were absent from JCam surveys of Middle Reef (Present chapter and Chapter 3) and there was negligible export of medusae from Magnetic Island to Middle Reef. Further, no model medusae directly emigrated from the east coast of Magnetic Island to the mainland. It is exceptionally unlikely that medusae lost from the unmapped north would be transported south/south west to the mainland given the net current in the 2017 *C. sivickisi* medusae season transported a majority of medusae to the north west. Severe storms such as tropical cyclones can drastically increase water turbulence (e.g. Toffoli et al., 2012), and they could, therefore, increase dispersal distances. However, the *C. sivickisi* medusae season at Magnetic Island (September to November) lies mostly outside of the cyclone season (November to May). Further, the turbulence of a severe storm event could physically damage the gelatinous bodies of *C. sivickisi* medusae (Kinsey, 1986) and the fresh water input following a storm could impair the medusae as cubomedusae are sensitive to low salinities (Mooney and Kingsford, 2016b). Additionally, medusae would be more vulnerable to predation in the open water of the crossing, away from the refuge of the structured reefal habitat (Savino and Stein, 1989). The isolation of the Magnetic Island stock suggests that genetically distinct *C. sivickisi* stocks may commonly be differentiable at surprisingly small spatial scales.

In this chapter, I found there was limited potential for simulated medusae from a Magnetic Island source population to emigrate to a mainland sink; however, alternate connectivity hypotheses were not explored. For example, the export of *C. sivickisi* medusae could occur in the opposite direction, from a mainland source to an island sink. This alternate hypothesis is implausible for two reasons: (1) the prevailing direction of current transport is longshore, and (2) the mainland coastal habitat in the vicinity of Magnetic Island is primarily sandy beaches and mud flats which are unsuitable for *C. sivickisi* habitation. Additionally, the 'sticky' earlier life stages of *C. sivickisi* (i.e. the polyps, embryo sacs and planula larvae; Hartwick, 1991b) could disperse by remaining attached to the shedded sporophytes of *Sargassum* algae, as argued in Chapter 3. To survive, the *C. sivickisi* would critically need to metamorphose

into medusae before the *Sargassum* washes onshore and rots, and the medusae would need to find suitable habitat. Similar mechanisms of connectivity have been described for other marine species. For example, floating objects from Ecuador and/or Peru with assemblages of juvenile and adult reef fish have run aground on Gorgona Island hundreds to thousands of kilometres away (Mora et al., 2001).

There is a growing body of evidence that closed populations are more common in marine species than originally suspected. Closed populations separated from adjacent populations at medium spatial scales (tens of kilometres), comparable to the scales of isolation of the Magnetic Island *C. sivickisi* stock, have previously been reported. Populations enclosed in bays at medium spatial scales have been reported in the scyphozoan jellyfish *Catostylus mosaicus* (Pitt and Kingsford, 2000; Dawson, 2005) and in the cubozoan *C. fleckeri* (Chapter 2). For both species, the stock structures were found to be maintained by a combination of retentive currents and strong swimming medusae (Chapter 2; Pitt and Kingsford 2000). Further, the scales of connectivity in some epifaunal species are limited by the short dispersal distances of their lecithotrophic larvae which may only be planktonic for minutes to days (Todd, 1998). For example, the lecithotrophic larvae of the epifaunal mollusc *Adalaria proxima* may be behaviourally adapted to limit dispersion and genetic differences have been found between *A. proxima* populations separated by less than 10 kilometres (Todd et al., 1998).

The modelled limited spatial scales of connectivity in the Magnetic Island *C. sivickisi* population contradict with the currently established cosmopolitan distribution of *C. sivickisi*. *C. sivickisi* are found across the Pacific and in the Indian Ocean (Lewis et al., 2008; Kingsford and Mooney, 2014). It is highly likely that lineages within this distribution have been isolated by vicariance events and have diverged from a common ancestor into incipient (morphologically similar and can interbreed) or cryptic (morphologically similar but cannot interbreed) species. Further, given the findings of this study, it is likely that the expansion of local populations within regions is a slow process. However, even if the genetic flux between lineages was zero (e.g. like between landlocked lakes; Dawson and Hamner, 2005) speciation in cubozoans may be a slow process given the low number of documented species (pers comms). Acevedo et al. (2019) used morphological and genetic tools to compare different populations of the cubozoan *Carybdea marsupialis* from across the Mediterranean, and they concluded that medusae collected from populations separated by hundreds of kilometres represented members of the same species. Work to clarify the taxonomy

of the Class Cubozoa is ongoing (e.g. Lawley et al., 2016; Acevedo et al., 2019), and researchers are currently working to identify incipient or cryptic species classified as *C. sivickisi* (pers comms).

Conclusions

Simulated *C. sivickisi* medusae could maintain their restricted distribution on narrow bands of fringing reef habitat if they selectively attached to habitat to avoid dispersive flows. The population of *C. sivickisi* on Magnetic Island extended along the entire east coast, and likely represented a robust, genetically distinct stock with bay-scale substructure. There was limited potential for simulated medusae from Magnetic Island to connect with mainland populations, either directly or via Middle Reef. The small scales of connectivity (less than 10 kilometres) simulated in the Magnetic Island population suggest that genetic heterogeneity may be common in *C. sivickisi* populations at surprisingly small spatial scales. I predict that incipient or cryptic species may be found within the cosmopolitan distribution of *C. sivickisi*.

CHAPTER SUMMARY

The structures of populations are influenced by the spatial scales of dispersal. The structures of cubozoan jellyfish populations are poorly understood. *Copula sivickisi* are unique among the cubozoans; *C. sivickisi* medusae have sticky pads on their bells which they use to attach to structures. Biophysical modelling was used to investigate the spatial scales of connectivity in a *C. sivickisi* population. Simulated *C. sivickisi* medusae could only maintain their distribution on a narrow band of fringing reef habitat if they avoided dispersive currents by selectively attaching to the habitat with the pads on their bells. This behaviour facilitated the isolation of a *C. sivickisi* population on reefs fringing Magnetic Island, Queensland, Australia, over an entire medusae season (September to November). Population mapping revealed the island population extended along the entire east coast. Within this distribution, there was considerable within bay retention and simulated medusae rarely travelled > 3 km from their source bay. The model island population was, therefore, made up of a collection of connected bay-scale local populations. The few simulated medusae lost from the island habitat were largely advected into open water and away from the mainland coast, which lies <

10 km from the island. Further, there was no evidence that Middle Reef, located in the channel separating the island and the mainland, acted as a steppingstone between populations. The successful emigration of *C. sivickisi* medusae from the island to the mainland is likely a rare event, and so the island population possibly represents a stock that is genetically distinct from any mainland populations. The differentiation of *C. sivickisi* populations within the species cosmopolitan distribution is highly likely given the small scales of connectivity I demonstrated here.

Chapter 5.

General discussion

The medusae of estuarine/coastal cubozoans can orient and maintain positions in structurally complex environments. Their behaviours are guided by an advanced sensory system and driven by their exceptional swimming ability. The spatial scales separating cubozoan stocks (isolated population units) are poorly understood. As stock boundaries and substructure are determined by the movements of organisms, the behaviours of organisms need to be considered in investigations of stock structure. This is especially true for animals which have advanced swimming and orientation abilities, such as cubozoans. Biophysical models can simulate the movements of organisms by considering both the currents and the organisms' behaviour. The technique is particularly well suited to investigating the population structures of mobile species. However, the comprehensive ecological data required to build and apply biophysical models are rare for cubozoans.

The intent of this thesis was to provide accurate biophysical models on the movements of cubozoans. These models were applied to determine the spatial scales separating cubozoan stocks, and to elucidate the substructure within identified stocks. The research focused on two cubozoan species of different sizes that inhabit contrasting environments and have species specific behaviours. Chapter 2 focused on a population of the large, venomous box jellyfish *Chironex fleckeri* inhabiting a semi enclosed estuarine bay (Port Musgrave, Australia). Chapters 3 and 4 focused on a population of the smaller, non-venomous *Copula sivickisi* inhabiting reefs fringing a nearshore island (Magnetic Island, 8 km from the mainland Australian coast) that is exposed to coastal currents. Field and laboratory experiments were run to quantify the behaviour and swimming capabilities of *C. fleckeri* (Chapter 2) and *C. sivickisi* (Chapter 3) medusae. The data were used to build biophysical models which were applied to determine if the *C. fleckeri* population inhabiting the partially closed system (Chapter 2), and the *C. sivickisi* population inhabiting the open system (Chapter 4) represented stocks with local substructure. It was revealed that dispersal was very restricted for both species. The strong swimming and complex behaviours of medusae facilitated the maintenance of their restricted distributions. There was minimal connectivity between population units separated by more than a few kilometres.

INNOVATIVE SOLUTIONS FOR STUDYING CUBOZOANS

Studying cubomedusae requires innovative approaches. Cubomedusae are gelatinous, and their abundance is characteristically highly variable in space and time. These traits make them difficult to study and partially explain why they have been overlooked historically. In this thesis, innovative sampling and modelling techniques were applied to determine the distribution and population structure of cubozoan species. The resultant data are a major contribution to a paradigm shift in our understanding of cubozoan ecology.

The novel underwater Jellyfish Camera units (JCams) presented in this thesis (Chapters 3 and 4) were designed to sample cubomedusae by utilizing their photopositive responses. Lights have previously been deployed near the surface at night to attract cubomedusae to measure their abundance, but with labour intensive monitoring (Kingsford et al., 2012). Llewellyn et al. (2016) used remote monitoring by uniquely positioning lights and cameras above the water to monitor the presence of large cubomedusae (*C. fleckeri* and *Morbakka sp.*) over nearly five years. Valuable data were collected on their seasonality and their ranges of temperature and salinity tolerance. The JCams presented here are innovative for the following reasons: (1) the units use underwater cameras and lights, allowing for the detection of small cubomedusae, and (2) multiple units could be deployed at once because they are compact and inexpensive. The new technology enabled me to measure the abundance of *C. sivickisi* medusae over small to medium spatial scales, providing detailed data on their distribution (Chapters 3 and 4). Such measures of abundance are rare for cubomedusae (Kingsford and Mooney, 2014). Further, little is known about the spatial and temporal abundance patterns of Irukandji species, and JCams could be applied to fill this knowledge gap. Irukandji species can, however, be morphologically similar and the JCam footage may not provide enough detail to distinguish between species. However, when needed, the medusae attracted to the JCam lights can be collected and later identified to species level.

The biophysical models used to simulate the movements of *C. fleckeri* (Chapter 2) and *C. sivickisi* (Chapter 4) medusae in this thesis were, to the authors knowledge, the first published biophysical models of cubozoan species. The models were informed by comprehensive oceanographic and behavioural data and were successfully applied to quantify the dispersal potential of cubomedusae, thereby elucidating their population structure. Biophysical modelling was particularly well suited to estimating patterns of

dispersal in cubozoans. Cubomedusae have a sophisticated sensory system (Nilsson et al., 2005) and associated complex behaviours (Table 1.1), and the behavioural components of the models effectively captured this complexity. The model of *C. fleckeri* movements included up to four unique behaviours (swimming parallel to shore, swimming toward the shore, avoiding beaching, and turning back into bays; Chapter 2), and the *C. sivickisi* model included up to five (diel activity pattern, maintaining positions near the bottom, swimming to habitat, attaching to habitat during the day and attaching to habitat at a current speed cut off; Chapter 4). In contrast, scyphozoans have a less advanced sensory system (Arai, 1997; Coates, 2003); published biophysical models of scyphozoan medusae have either only included a single behaviour (e.g. diel vertical migration, Berline et al. 2013; counter-current horizontal swimming, Fossette et al. 2015), or have simulated the medusae as passive particles (Moon et al., 2010). The behaviours included in the *C. fleckeri* and *C. sivickisi* models were built around swim speed and behaviour data that were expressly collected in field and laboratory experiments (Chapters 2 and 3). While similar data have been collected for other cubozoan species, the detailed data required to build a behavioural model are lacking for most species in the class (Kingsford and Mooney, 2014); although, *Tripedalia cystophora* is a notable exception (e.g. Garm et al., 2011; Garm et al., 2012; Table 1.1). Consequently, species-specific field and laboratory experiments will increase the accuracy of biophysical models for other cubozoan species.

Other emergent technologies have been applied to fill gaps in our knowledge on the class Cubozoa, which has been historically understudied. Understanding the movements of organisms is critical to determining connectivity between populations, and there are limited data on the movements of cubomedusae over large time scales (from hours to the months that constitute a medusa's lifespan). Electronic tags are commonly used to track the movements of organisms over large time scales (Rutz and Hays, 2009). However, this technique has only recently become available for jellyfishes due to the difficulty in attaching tags to the soft bodies of medusae and the challenge of making tags light enough to not impede the swimming of medusae (Fossette et al., 2016). Notably, Gordon and Seymour (2009) attached transmitters to 12 *C. fleckeri* medusae, ranging in size from 9 to 18 cm Inter-Pedalia Distance (IPD), and tracked their movements for up to 38 hours, collecting important data on their habitat usage. Similar studies on other large cubozoan species would be of great utility. However, the movements of tagged cubomedusae have not been tracked for

more than a day or two and tagging is not currently a viable option for smaller medusae (Fossette et al., 2016). Alternatively, the movements of aquatic organisms between different environments (e.g. estuarine and marine habitats) can be tracked by analysing the elemental compositions of their calcified structures, as has been done for fishes (Campana, 1999). Cubomedusae have four sensory clubs (rhopalium), and each is weighted by a calcium sulphate hemihydrate crystal called a statolith. Elemental compositions reflect movements because the replacement of calcium atoms in calcified structures occurs as a function of the environmental conditions (e.g. temperature and salinity; Secor et al., 1995; Bath et al., 2000). A firm understanding of how the environment effects the uptake of elements is required before elemental composition can be used to track movements (Mooney and Kingsford, 2016b). Single factor (temperature; Mooney and Kingsford, 2016b) and orthogonal multi factor (temperature and salinity; Morrissey et al., Appendix III) experiments have been conducted to develop an understanding of how environmental conditions effect the uptake of elements into *C. fleckeri* statoliths. These studies promisingly showed that the elemental chemistry of *C. fleckeri* statoliths was predictably affected by the temperature and salinity of the surrounding water.

The habitats of cubozoan polyps, and therefore the sources of cubozoan medusae, are also largely unknown. Information on the prevalence and distribution of medusae sources is integral to our understanding of cubozoan population structures and dynamics. Innovative solutions are required to locate polyp populations. Cubozoan polyp habitats could be identified by examining the elemental chemistry of statolith cores, which form in the environments of newly metamorphosed medusae (e.g. Mooney and Kingsford, 2012). Alternatively, environmental DNA (eDNA) is a promising avenue of research (Bolte, 2019). Cubomedusae generally appear seasonally (Kingsford and Mooney, 2014). Therefore, the presence of cubozoan DNA in water samples collected when medusae were absent would indicate that the samples were taken in the vicinity of a polyp population (Bolte, 2019).

SWIM SPEED AND BEHAVIOUR

Cubozoan medusae are exceptional swimmers. The burst swim speeds measured for *C. fleckeri* (16.6 cm s⁻¹, Chapter 2) and *C. sivickisi* (12 cm s⁻¹, Chapter 3) medusae were amongst the fastest speeds recorded for any jellyfish species (Table 1.2, Table 2.3). Both *C. fleckeri* and *C. sivickisi* medusae could swim faster than the measured

local current speeds within their structurally complex nearshore/near bottom habitats. The current speeds within these habitats were weakened by current shear (the slackening of a current with proximity to the shore or the bottom; Fischer et al., 1979) and the sticky water effect (retentive current fields generated from the diversion of a current around a structure; Andutta et al., 2012). It is highly likely that other coastal, estuarine and/or reefal cubozoan species also maintain restricted distributions within zones of weakened currents.

C. fleckeri and *C. sivickisi* medusae inhabit structurally complex environments and have associated complex behaviours. Cubozoan medusae have sophisticated visual systems (Nilsson et al., 2005), so it is unsurprising that complex, visually guided behaviours have been reported in numerous species. The obstacle avoidance behaviour documented in *C. fleckeri* medusae in Chapter 2, and previously reported by Kinsey (1986) and Hamner et al. (1995), is beneficial for avoiding coastal obstacles (i.e. rocks and driftwood) and mangrove roots. Similarly, *Tripedalia cystophora* medusae, which live among mangrove roots, exhibited a strong obstacle avoidance in flume tank experiments (Garm et al., 2007). Obstacle avoidance has also been documented in cubozoan species that utilize sand patches in coastal habitats (*Carybdae rastonii*, Matsumoto, 1995; *Chiropsella bronzie*, Garm et al., 2007). In addition to avoiding coastal obstacles, avoiding dark areas such as seagrass and algal beds could help these species maintain positions on sand patches (Matsumoto, 1995). Interestingly, *T. cystophora* medusae had a stronger obstacle avoidance response than *C. bronzie* medusae subjected to the same flume tank experiments (Garm et al., 2007). This difference could be reflective of the greater spatial complexity of the mangroves inhabited by *T. cystophora*, compared to the coasts inhabited by *C. bronzie* (Garm et al., 2007).

C. fleckeri medusae are found near the shore (Gordon and Seymour, 2009; Kingsford and Mooney, 2014), and simulated medusae needed to swim toward the shore to maintain this restricted distribution (Chapter 2). Other coastal cubozoan species may also maintain nearshore distributions by swimming toward the shore; however, the cues cubomedusae use to direct their swimming in the absence of obstacles are largely unknown. In cubomedusae, the weight of the statolith orients the rhopalium so the Upper Lens Eye (ULE) always faces upwards (O'Connor et al., 2009; Garm et al., 2011; Garm et al., 2016), and the ULE's have been linked to orientation. The ULE's of *Chiropsella bronzie* may detect the position of the sun (heliotaxis) and/or moon (lunartaxis), allowing medusae to navigate to or from a beach or to maintain a straight

course while swimming (O'Connor et al., 2009). *C. fleckeri* could likewise use their ULE's to navigate by the sun/moon in embayments and coasts. Heliotaxis (e.g. reef fish larvae, Mouritsen et al., 2013) and lunartaxis (e.g. eels, Cresci et al., 2019) have been documented in a wide range of organisms. *C. fleckeri* medusae also inhabit mangrove channels and mangrove fringed beaches and estuaries (Kingsford and Mooney, 2014). *T. cystophora* detect the mangrove canopy with their ULE's; they orientate via this input to maintain distributions at the edges of mangrove channels (Garm et al., 2011). *C. fleckeri* could similarly orient in mangroves via this mechanism.

Some of the most sophisticated cubozoan behaviours are performed by *C. sivickisi* medusae. Uniquely, *C. sivickisi* medusae have sticky pads on the apex of their bells which allow them to attach to substrates (Hartwick, 1991b). They are also nocturnal (Chapter 3; Hartwick, 1991b; Garm et al., 2012). The eyes of *C. sivickisi* medusae are adapted to low light, and medusae have been observed swimming toward bioluminescent prey in a laboratory experiment (Garm et al., 2016). Simulated *C. sivickisi* medusae avoided being advected from narrow bands of fringing reef by attaching to the reef with the pads on their bells (Chapter 4). However, it is unclear how *C. sivickisi* medusae maintain positions near fringing reef at night given the reef is not luminescent. If they stayed close enough to reefs, they could orient by mechanoreception and random encounters, especially on reefs with dense macroalgae that sways with the current (e.g. *Sargassum* sp.). Alternatively, they could orient to reefs via chemotaxis. Jellyfish have chemosensory proteins on their bells and tentacles. *C. sivickisi* could plausibly smell the material (e.g. mucus and cells) expelled from macroalgae and corals and orient toward it, and thereby toward the source reef. Both mechanoreception (e.g. copepods, Yen et al., 1992; mussels, Amini et al., 2017) and chemotaxis (e.g. benthic invertebrates, Pawlik, 1992; reef fish larvae, Gerlach et al., 2007) are widespread among marine taxa.

POPULATION STRUCTURE

Marine species commonly have bipartite life cycles with meroplanktonic larvae that spend minutes to months in the pelagic zone. There used to be a consensus that currents transport meroplanktonic larvae over large distances, connecting distant adult populations. This paradigm has been challenged over the last two decades, and the populations of many marine species are now considered more closed at much smaller spatial scales than previously thought (e.g. Jones et al., 1999; Cowen et al., 2000;

Almany et al., 2007). However, the paradigm of open populations has persisted for jellyfish species for several reasons. Most jellyfish species are meroplanktonic, with bipartite life cycles. The sessile polyps of meroplanktonic jellyfishes either strobilate ephyrae (Scyphozoa), metamorphose into juvenile medusae (Cubozoa) or laterally bud juveniles (Hydrozoa). The ephyrae of scyphozoans are poor swimmers, and they can be carried hundreds of kilometres by ocean currents (e.g. Barz et al., 2006; Chen et al., 2014). Further, few scyphozoan jellyfishes are holoplanktonic, meaning they are planktonic for their entire life cycle. Genetic studies have found that populations of holoplanktonic jellyfish (e.g. *Pelagia noctiluca* and *Periphylla* spp.) are generally genetically well mixed over thousands of kilometres, although distinct populations have been identified across ocean basins (Stopar et al., 2010; Miller et al., 2012; Glynn et al., 2016; Abboud et al., 2018). Populations that are well mixed over thousands of kilometres have also been identified in meroplanktonic scyphozoan (e.g. *Chrysaora melanaster* in the Bering Sea; Dawson et al., 2015) and cubozoan (e.g. *Alatina alata* has a circumtropical distribution; Lawley et al., 2016) jellyfishes.

Recent evidence is challenging the paradigm of open jellyfish populations, in parallel to the breakdown of the open population paradigm that persisted for other marine taxa. Abboud et al. (2018) investigated genetic structuring in 16 jellyfish taxa at different geographic scales. While they found a lack of genetic structuring in holoplanktonic species across thousands to tens of thousands of kilometres, populations of taxa with bipartite life cycles were often genetically distinct at scales of tens to hundreds of kilometres. Indeed, genetic structuring was identified in meroplanktonic jellyfish populations at spatial scales as small as 3 km (e.g. *Cassiopea* from Indonesia; Abboud et al. 2018). Other studies have similarly found genetic or demographic differences in scyphozoan jellyfish populations separated by tens to hundreds of kilometres (*Aurelia aurita*, Dawson et al., 2015; *Mastigias papua*, Dawson and Hamner, 2005; *Catostylus mosaicus*, Dawson, 2005, Pitt and Kingsford, 2000; *Rhizostoma octopus*, Lee et al., 2013, Glynn et al., 2015). There is also a growing body of evidence that cubozoan stocks are maintained at scales as small as tens of kilometres. Mooney and Kingsford (2016a, 2017) found significant differences in the shapes and elemental chemistry of statoliths from *C. fleckeri* medusae collected from different sites within sampled regions in northern Australia, and sites were only separated by tens of kilometres. The significant differences in statolith shape and chemistry suggested that medusae had experienced different environmental conditions (Secor et al., 1995; Bath et al., 2000; Cadrin, 2010), and potentially a level of genetic isolation (Cadrin, 2010), and were,

therefore, from separate stocks. Further, tagged *C. fleckeri* medusae travelled hundreds of meters to kilometres within a day, but they tended to stay within the coastal or estuarine environments they were tagged in (Gordon and Seymour, 2009). Further, they often travelled along beaches and returned close to the point of release (Gordon and Seymour, 2009). *C. fleckeri* medusae are, therefore, unlikely to emigrate between populations separated by tens of kilometres. In Chapter 2 of this thesis, I found that a *C. fleckeri* population inhabiting Port Musgrave, a semi-enclosed estuarine bay in northern Australia, possibly represents a stock. Port Musgrave is isolated from other estuarine systems by tens of kilometres, in alignment with the scales of *C. fleckeri* stock differentiation suggested by Mooney and Kingsford (2016a, 2017). The first evidence that *C. sivickisi* stocks are maintained at similar scales was provided in Chapters 3 and 4. The population of *C. sivickisi* inhabiting Magnetic Island, which lies approximately 8 km offshore of the mainland Australian coast, was isolated from any mainland populations, suggesting it represents a stock. The isolation of cubozoan stocks at scales of tens of kilometres occurred in habitats with varying levels of physical openness, and with cubomedusae with different swimming capabilities and suites of behaviour. This suggests that the distinction of stocks at scales of tens of kilometres may be widespread among cubozoan species that inhabit coastal, estuarine and reefal environments. Given the new and existing evidence of limited dispersal in jellyfish, and of jellyfish populations that are largely closed, the paradigm that open populations are the norm should be revised.

Different mechanisms worked to isolate the cubozoan stocks in the modelled closed and open systems. The simulated retentive currents in Port Musgrave facilitated the isolation of the bay-scale *C. fleckeri* stock (Chapter 2). In contrast, the currents alone were insufficient to isolate the stock of *C. sivickisi* on the comparatively open Magnetic Island (Chapter 4). Simulated medusae maintained their positions on fringing reefs by behaving to counteract the predicted dispersive currents. Congruently, in both systems, simulated medusae had to swim to maintain stock substructure (i.e. connected local populations) at the small spatial scale of hundreds of meters. These results align with the findings of Wolanski (2017) who, in his treatise on ecological connectivity, compiled examples of the spatial and temporal scales of connectivity across numerous taxa and environments. Wolanski (2017) concluded that as the physical openness of systems increases, population closure increasingly relies on the behaviour of species.

Like adult cubomedusae, the early life history stages of cubozoan species may commonly have limited dispersal potential. Members of the order Carybdeida are all probably ovoviviparous, meaning their eggs are fertilized internally (Bentlage et al., 2010) and, therefore, not dispersed in broadcast spawning's. In most families in the order, the female medusae take up sperm that is released into the water column (Studebaker, 1972; Arneson, 1976). However, in the Family Tripedaliidae which includes *C. sivickisi*, *T. cystophora* and *Tripedalia binata*, the sperm is delivered to the female in courtship behaviours (Werner, 1973; Lewis and Long, 2005; Bentlage et al., 2010). *C. sivickisi* produce sticky embryo sacs which they may selectively attach to reefal habitat (Hartwick, 1991b), and *T. cystophora* (Werner et al., 1971) and *T. binata* (Toshino et al., 2017) release mature, free-swimming planulae larvae. Carybdeida planulae generally settle within 1 to 4 days (e.g. 1-day post hatching, *Malo maxima*, Underwood et al. 2018; 2 to 4 days post release, *T. binata*, Toshino et al. 2017), limiting their exposure to dispersive currents. Fertilization occurs externally in the order Chirodropida; however, the fertilized eggs and planulae of chirodropids may only be affected by currents for a short time. The zygotes and blastula of the chirodropid *C. fleckeri* were negatively buoyant and adhered to surfaces, and planulae emerged within 12 to 24 hours of fertilization and settled within 24 hours (Hartwick, 1991a). Further, the metamorphosis of cubozoan polyps to medusae is more complete than the strobilation of scyphozoan jellyfishes. Either the entire polyp metamorphoses into a single cubomedusa, or only a small regenerative fragment is left over (Straehler-Pohl and Jarms, 2005). Consequently, newly metamorphosed medusae are nearly fully formed (e.g. Werner et al., 1971), in stark contrast to the underdeveloped ephyrae of scyphozoans (e.g. Straehler-Pohl and Jarms, 2010). New medusae range in size from 0.6 to 1.6 mm in Bell Height (BH; Straehler-Pohl and Jarms, 2011) and they would be able to swim competently to counteract dispersive currents soon after metamorphosis. Cubomedusae can grow quickly; *C. sivickisi* medusae nearly tripled in size from 0.9 to 2.7 mm in diameter in the 13 days following metamorphosis (Toshino et al., 2014). Further, cubomedusae as small as 4 mm IPD were found to be competent swimmers in this thesis (Chapter 3). To the authors knowledge, no data on the swimming capabilities of newly metamorphosed medusae have been published, but they have been observed swimming strongly in tanks (Bordehore pers comm).

Stock size impacts population dynamics. As stocks are isolated population units, the dynamics within stocks are governed by internal factors such as growth, mortality and self-recruitment, which are in turn mediated by the surrounding environment (Sinclair,

1988). The abundance of cubomedusae is, therefore, likely influenced by factors at the medium spatial scales of cubozoan stocks, partially explaining why it is characteristically variable. Cubozoan medusae are sensitive to low salinities (Mooney and Kingsford, 2016b), and there is evidence that medusae abundance varies with local rainfall. In three seasons of sampling, *C. fleckeri* medusae were absent or rare in mainland coastal waters in north Queensland, Australia when high riverine discharge reduced the water salinity (Kingsford et al., 2012). Additionally, Llewellyn et al. (2016) monitored the presence of large cubomedusae at a site in north Queensland over nearly five years. The salinity at the site was periodically reduced by monsoonal rains, and medusae from the cubozoans *C. fleckeri* and *Morbakka* spp. were never detected at salinities below 25.2 PSU and 25.4 PSU respectively. Further, the abundance of cubomedusae has been linked to local wind conditions. Gershwin et al. (2014) found that stings from Irukandji species tended to occur when the wind predominantly blew onshore. Although it is questionable if stings experienced by swimmers are an accurate proxy for abundance, this research concluded that Irukandji were more abundant in nearshore waters when they were transported in shore by prevailing onshore winds (Gershwin et al., 2014). Knowledge of the biological and physical factors influencing the abundance of cubozoans is in its infancy.

CONCLUSIONS

Both large (*C. fleckeri*) and small (*C. sivickisi*) cubomedusae were excellent swimmers capable of overcoming local current speeds. Cubozoan stocks were isolated at medium spatial scales (tens of kilometres) in both closed and open systems, although different mechanisms facilitated the isolation. The non-dispersive currents in Port Musgrave, a semi-enclosed estuarine bay, retained a *C. fleckeri* stock within the bay. In contrast, a combination of reduced near shore, near bottom currents and 'sticky' medusae behaviours were required to maintain a *C. sivickisi* stock on Magnetic Island, a relatively open nearshore island. Cubomedusae behaviour was critically important in forming small scale (hundreds of meters) local populations within the stocks identified in both the closed and open environments. *C. fleckeri* medusae had to swim against reduced shallow water currents to maintain nearshore aggregations which constituted local populations. Similarly, *C. sivickisi* medusae had to behave to form local populations on the reefal habitat within the island embayments. Cubomedusae with different swimming capabilities and behaviours, inhabiting physically different systems,

maintained stocks as similar spatial scales. The similarity suggests that coastal, estuarine and reefal cubozoans may commonly maintain stocks at medium spatial scales. The established spatial scales of cubozoan stocks challenge the paradigm that jellyfish have open populations that are genetically well mixed over hundreds to thousands of kilometres.

References

- Abboud SS, Gómez Daglio L, Dawson MN (2018) A global estimate of genetic and geographic differentiation in macromedusae - implications for identifying the causes of jellyfish blooms. *Mar Ecol Prog Ser* 591: 199-216
- Acevedo MJ, Fuentes VL, Olariaga A, Canepa A, Belmar MB, Bordehore C, Calbet A (2013) Maintenance, feeding and growth of *Carybdea marsupialis* (Cnidaria: Cubozoa) in the laboratory. *J Exp Mar Biol Ecol* 439: 84-91
- Acevedo MJ, Straehler-Pohl I, Morandini AC, Stampar SN, Bentlage B, Matsumoto GI, Yanagihara A, Toshino S, Bordehore C, Fuentes VL (2019) Revision of the genus *Carybdea* (Cnidaria: Cubozoa: Carybdeidae): clarifying the identity of its type species *Carybdea marsupialis*. *Zootaxa* 4543: 515-548
- Almany GR, Berumen ML, Thorrold SR, Planes S, Jones GP (2007) Local replenishment of coral reef fish populations in a marine reserve. *Science* 316: 742-744
- Amini S, Kolle S, Petrone L, Ahanotu O, Sunny S, Sutanto CN, Hoon S, Cohen L, Weaver JC, Aizenberg J, Vogel N, Miserez A (2017) Preventing mussel adhesion using lubricant-infused materials. *Science* 357: 668-673
- Andutta FP, Kingsford MJ, Wolanski E (2012) Sticky water enables the retention of larvae in a reef mosaic. *Estuar Coast Shelf Sci* 101: 54-63
- Arai MN (1997) A functional biology of Scyphozoa. Chapman & Hall, 2-6 Boundary Row, London SE1 8HN
- Arneson AC (1976) Life history of *Carybdea alata* Reynaud, 1830 (Cubomedusae). MS thesis, University of Puerto Rico
- Baring RJ, Fairweather PG, Lester RE (2018) Nearshore drift dynamics of natural versus artificial seagrass wrack. *Estuar Coast Shelf Sci* 202: 164-171

- Barz K, Hinrichsen HH, Hirche HJ (2006) Scyphozoa in the Bornholm basin (central Baltic Sea) — the role of advection. *J Mar Syst* 60: 167-176
- Bath GE, Thorrold SR, Jones CM, Campana SE, McLaren JW, Lam JWH (2000) Strontium and barium uptake in aragonitic otoliths of marine fish. *Geochim Cosmochim Acta* 64: 1705-1714
- Beaman RJ (2017) High-resolution depth model for the Great Barrier Reef - 30 m. doi:10.4225/25/5a207b36022d2
- Bentlage B, Cartwright P, Yanagihara AA, Lewis C, Richards GS, Collins AG (2010) Evolution of box jellyfish (Cnidaria: Cubozoa), a group of highly toxic invertebrates. *P R Soc B-Biol Sci* 277: 493-501
- Bentlage B, Peterson AT, Cartwright P (2009) Inferring distributions of chirodropid box-jellyfishes (Cnidaria: Cubozoa) in geographic and ecological space using ecological niche modeling. *Mar Ecol Prog Ser* 384: 121-133
- Berline L, Zakardjian B, Molcard A, Ourmieres Y, Guihou K (2013) Modeling jellyfish *Pelagia noctiluca* transport and stranding in the Ligurian Sea. *Mar Pollut Bull* 70: 90-99
- Black KP, Moran PJ, Hammond LS (1991) Numerical models show coral reefs can be self-seeding. *Mar Ecol Prog Ser* 74: 1-11
- Bode M, Leis JM, Mason LB, Williamson DH, Harrison HB, Choukroun S, Jones GP (2019) Successful validation of a larval dispersal model using genetic parentage data. *PLoS Biol* 17: 13
- Bolte BC (2019) Utility and validation of environmental DNA (eDNA) as a method of detection for the cubozoan, *Copula sivickisi*. BSc (Hon, Marine Biology) thesis, James Cook University
- Brett JR (1964) The respiratory metabolism and swimming performance of young sockeye salmon. *J Fish Res Board Can* 21: 1183-1226

- Brickman D, Smith PC (2002) Lagrangian Stochastic Modeling in Coastal Oceanography. *J Atmos Ocean Technol* 19: 83-99
- Burton RS, Lee B-N (1994) Nuclear and mitochondrial gene genealogies and allozyme polymorphism across a major phylogeographic break in the copepod *Tigriopus californicus*. *Proc Natl Acad Sci USA* 91: 5197-5201
- Buskey EJ (2003) Behavioral adaptations of the cubozoan medusa *Tripedalia cystophora* for feeding on copepod (*Dioithona oculata*) swarms. *Mar Biol* 142: 225-232
- Cadrin S (2010) Stock identification of marine populations. In: Elewa AM (eds) *Morphometrics for Nonmorphometricians' Lecture Notes in Earth Sciences*. Springer, Berlin, pp 219-232
- Campana SE (1999) Chemistry and composition of fish otoliths: pathways, mechanisms and applications. *Mar Ecol Prog Ser* 188: 263-297
- Cappo M, Speare P, De'ath G (2004) Comparison of baited remote underwater video stations (BRUVS) and prawn (shrimp) trawls for assessments of fish biodiversity in inter-reefal areas of the Great Barrier Reef Marine Park. *J Exp Mar Biol Ecol* 302: 123-152
- Carrette T, Alderslade P, Seymour J (2002) Nematocyst ratio and prey in two australian cubomedusans, *Chironex fleckeri* and *Chiropsalmus sp.* *Toxicon* 40: 1547-1551
- Carter AB, Mckenna SA, Rasheed MA, Mckenzie L, Coles RG (2016) Seagrass mapping synthesis: A resource for coastal management in the Great Barrier Reef World Heritage Area. In: Report to the National Environmental Science Programme. Reef and Rainforest Research Centre Limited, Cairns
- Chen K, Ciannelli L, Decker MB, Ladd C, Cheng W, Zhou Z, Chan KS (2014) Reconstructing source-sink dynamics in a population with a pelagic dispersal phase. *PLOS ONE* 9: e95316

- Chevalier C, Pagano M, Corbin D, Arfi R (2014) The salinity responses of tropical estuaries to changes in freshwater discharge, tidal mixing and geomorphology: case study of the man-affected Senegal River Estuary (West Africa). *Mar Freshw Res* 65: 987-1002
- Chin A, Heupel MR, Simpfendorfer CA, Tobin AJ (2013) Ontogenetic movements of juvenile blacktip reef sharks: evidence of dispersal and connectivity between coastal habitats and coral reefs. *Aquat Conserv* 23: 468-474
- Coates MM (2003) Visual ecology and functional morphology of Cubozoa (Cnidaria). *Comp Biol* 43: 542-548
- Coates MC, Theobald JC (2003) Optimal visual parameters for a cubozoan jellyfish in the mangrove environment. *Integr Comp Biol* 43: 1016
- Cochran WG (1954) Some methods for strengthening the common χ^2 tests. *Biometrics* 10: 417-451
- Cohen J (1988) *Statistical power analysis for the behavioral sciences*. Routledge, New York
- Colin SP, Costello JH, Katija K, Seymour J, Kiefer K (2013) Propulsion in cubomedusae: mechanisms and utility. *PLOS ONE* 8: e56393
- Courtney R, Browning S, Seymour J (2016) Early life history of the 'Irukandji' jellyfish *Carukia barnesi*. *PLOS ONE* 11: 13
- Cowen RK, Lwiza KMM, Sponaugle S, Paris CB, Olson DB (2000) Connectivity of marine populations: Open or closed? *Science* 287: 857-859
- Cresci A, Durif CM, Paris CB, Thompson CRS, Shema S, Skiftesvik AB, Browman HI (2019) The relationship between the moon cycle and the orientation of glass eels (*Anguilla anguilla*) at sea. *R Soc Open Sci* 6: 15

- Critchell K, Grech A, Schlaefer J, Andutta, FP, Lambrechts J, Wolanski E, Hamann M (2015) Modelling the fate of marine debris along a complex shoreline: Lessons from the Great Barrier Reef. *Estuar Coast Shelf Sci* 167: 414-426
- Critchell K, Lambrechts J (2016) Modelling accumulation of marine plastics in the coastal zone; what are the dominant physical processes? *Estuar Coast Shelf Sci* 171: 111-122
- Davies AM, Lawrence J (1994) Examining the influence of wind and wind-wave turbulence on tidal currents, using a 3-dimensional hydrodynamic model including wave-current interaction. *J Phys Oceanogr* 24: 2441-2460
- Dawson MN (2005) Incipient speciation of *Catostylus mosaicus* (Scyphozoa, Rhizostomeae, Catostylidae), comparative phylogeography and biogeography in southeast Australia. *J Biogeogr* 32: 515-533
- Dawson MN, Ciciel K, Decker MB, Hays GC, Lucas CH, Pitt KA (2015) Population-level perspectives on global change: genetic and demographic analyses indicate various scales, timing, and causes of scyphozoan jellyfish blooms. *Biol Invasions* 17: 851-867
- Dawson MN, Hamner WM (2005) Rapid evolutionary radiation of marine zooplankton in peripheral environments. *Proc Natl Acad Sci USA* 102: 9235-9240
- Dawson MN, Sen Gupta A, England MH (2005) Coupled biophysical global ocean model and molecular genetic analyses identify multiple introductions of cryptogenic species. *Proc Natl Acad Sci USA* 102: 11968-11973
- De Brye B, De Brauwere A, Gourgue O, Karna T, Lambrechts J, Comblen R, Deleersnijder E (2010) A finite-element, multi-scale model of the Scheldt tributaries, river, estuary and ROFI. *Coast Eng* 57: 850-863
- Durlak JA (2009) How to select, calculate, and interpret effect sizes. *J Pediatr Psychol* 34: 917-928
- Fenner PJ (2005) Dangerous Australian box jellyfish. *SPUMS J* 35: 76-83

- Fischer HB, List EJ, Koh RCY, Imberger J, Brooks NH (1979) Mixing in Inland and Coastal Waters. Academic Press Inc., 111 Fifth Avenue, New York, New York 10003
- Fisher R, Wilson SK (2004) Maximum sustainable swimming speeds of late-stage larvae of nine species of reef fishes. *J Exp Mar Biol Ecol* 312: 171-186
- Forward RB, Tankersley RA (2001) Selective tidal-stream transport of marine animals In: Gibson RB, Barnes M, Atkinson RJA (eds) *Oceanography and Marine Biology*, Vol 39. Taylor & Francis Ltd, London, p 305-353
- Fossette S, Gleiss AC, Chalumeau J, Bastian T and others (2015) Current-oriented swimming by jellyfish and its role in bloom maintenance. *Curr Biol* 25: 342-347
- Fossette S, Katija K, Goldbogen JA, Bograd S and others (2016) How to tag a jellyfish? A methodological review and guidelines to successful jellyfish tagging. *J Plankton Res* 38: 1347-1363
- Freiwald J (2012) Movement of adult temperate reef fishes off the west coast of North America. *Can J Fish Aquat Sci* 69: 1362-1374
- Garm A, Bielecki J (2008) Swim pacemakers in box jellyfish are modulated by the visual input. *J Comp Physiol A* 194: 641-651
- Garm A, Bielecki J, Petie R, Nilsson DE (2012) Opposite patterns of diurnal activity in the box jellyfish *Tripedalia cystophora* and *Copula sivickisi*. *Biol Bull* 222: 35-45
- Garm A, Bielecki J, Petie R, Nilsson DE (2016) Hunting in bioluminescent light: vision in the nocturnal box jellyfish *Copula sivickisi*. *Front Physiol* 7: 9
- Garm A, Hedal I, Islin M, Gurska D (2013) Pattern- and contrastdependent visual response in the box jellyfish *Tripedalia cystophora*. *J Exp Biol* 216: 4520-4529
- Garm A, O'Connor M, Parkefelt L, Nilsson DE (2007) Visually guided obstacle avoidance in the box jellyfish *Tripedalia cystophora* and *Chiropsella bronzie*. *J Exp Biol* 210: 3616-3623

- Garm A, Oskarsson M, Nilsson DE (2011) Box jellyfish use terrestrial visual cues for navigation. *Curr Biol* 21: 798-803
- Gemmell BJ, Costello JH, Colin SP, Stewart CJ, Dabiri JO, Tafti D, Priya S (2013) Passive energy recapture in jellyfish contributes to propulsive advantage over other metazoans. *Proc Natl Acad Sci USA* 110: 17904-17909
- Gemmell BJ, Colin SP, Costello JH (2018) Widespread utilization of passive energy recapture in swimming medusae. *J Exp Biol* 221: 5
- Gerlach G, Atema J, Kingsford MJ, Black KP, Miller-Sims V (2007) Smelling home can prevent dispersal of reef fish larvae. *Proc Natl Acad Sci USA* 104: 858-863
- Gershwin LA, Condie SA, Mansbridge JV, Richardson AJ (2014) Dangerous jellyfish blooms are predictable. *J R Soc Interface* 11
- Gershwin LA, De Nardi M, Winkel KD, Fenner PJ (2010) Marine stingers: review of an under-recognized global coastal management issue. *Coast Manage* 38: 22-41
- Glynn F, Houghton JDR, Bastian T, Doyle TK, Fuentes V, Lilley MKS, Provan J (2016) High-resolution genetic analysis reveals extensive gene flow within the jellyfish *Pelagia noctiluca* (Scyphozoa) in the North Atlantic and Mediterranean Sea. *Biol J Linn Soc* 117: 252-263
- Glynn F, Houghton JDR, Provan J (2015) Population genetic analyses reveal distinct geographical blooms of the jellyfish *Rhizostoma octopus* (Scyphozoa). *Biol J Linn Soc* 116: 582-592
- Golbuu Y, Gouezo M, Kurihara H, Rehm L, Wolanski E (2016) Long-term isolation and local adaptation in Palau's Nikko Bay help corals thrive in acidic waters. *Coral Reefs* 35: 909-918
- Gordon MR, Seymour JE (2009) Quantifying movement of the tropical Australian cubozoan *Chironex fleckeri* using acoustic telemetry. *Hydrobiologia* 616: 87-97

- Gordon M, Seymour J (2012) Growth, development and temporal variation in the onset of six *Chironex fleckeri* medusae seasons: a contribution to understanding jellyfish ecology. PLOS ONE 7: e31277
- Grech A, Wolter J, Coles R, McKenzie L, Rasheed M, Thomas C, Waycott M, Hanert E (2016) Spatial patterns of seagrass dispersal and settlement. Divers Distrib 22: 1150-1162
- Hamner WM, Jones MS, Hamner PP (1995) Swimming, feeding, circulation and vision in the Australian box jellyfish, *Chironex fleckeri* (Cnidaria: Cubozoa). Mar Freshw Res 46: 985-990
- Hartwick RF (1991a) Distributional ecology and behavior of the early life stages of the box-jellyfish *Chironex fleckeri*. Hydrobiologia 216: 181-188
- Hartwick RF (1991b) Observations on the anatomy, behaviour, reproduction and life cycle of the cubozoan *Carybdea sivickisi*. Hydrobiologia 216: 171-179
- Herzfeld M, Andrewartha J, Baird M, Brinkman R, Furnas M, Gillibrand P, Hener M, Joehnk KD, Jones E, McKinnon D, Margevlashvili N, Mongin M, Oke P, Rizwi F, Robson B, Seaton S, Skerratt J, Tonin H, Wild-Allen K (2016) eReefs Marine Modelling: Final Report. Hobart, Tasmania
- Hinrichsen HH, Dickey-Collas M, Huret M, Peck MA, Vikebo FB (2011) Evaluating the suitability of coupled biophysical models for fishery management. ICES J Mar Sci 68: 1478-1487
- Hixon MA, Beets JP (1993) Predation, prey refuges, and the structure of coral-reef fish assemblages. Ecol Monogr 63: 77-101
- Hrycik JM, Chasse J, Ruddick BR, Taggart CT (2013) Dispersal kernel estimation: A comparison of empirical and modelled particle dispersion in a coastal marine system. Estuar Coast Shelf Sci 133: 11-22

- Johnson DR, Perry HM, Graham WM (2005) Using nowcast model currents to explore transport of non-indigenous jellyfish into the Gulf of Mexico. *Mar Ecol Prog Ser* 305: 139-146
- Jones GP, Milicich MJ, Emslie MJ, Lunow C (1999) Self-recruitment in a coral reef fish population. *Nature* 402: 802-804
- Katija K, Colin SP, Costello JH, Jiang HS (2015) Ontogenetic propulsive transitions by *Sarsia tubulosa* medusae. *J Exp Biol* 218: 2333-2343
- Kessler WS, Cravatte S (2013) Mean circulation of the Coral Sea. *J Geophys. Res-Oceans* 118: 6385-6410
- Kingsford MJ (1992) Drift algae and small fish in coastal waters of northeastern New Zealand. *Mar Ecol Prog Ser* 80: 41-55
- Kingsford MJ (1993) Biotic and abiotic structure in the pelagic environment—importance to small fishes. *Bull Mar Sci* 53: 393-415
- Kingsford MJ, Battershill CN (eds) (1998) *Studying temperate marine environments: a handbook for ecologists*. University of Canterbury Press, Christchurch
- Kingsford MJ, Choat JH (1985) The fauna associated with drift algae captured with a plankton-mesh purse seine net. *Limnol Oceanogr* 30: 618-630
- Kingsford MJ, Mooney CJ (2014) The ecology of box jellyfishes (Cubozoa). In: Pitt KA, Lucas CH (eds) *Jellyfish Blooms*. Springer, Dordrecht, p 267-302
- Kingsford MJ, Pitt KA, Gillanders BM (2000) Management of jellyfish fisheries, with special reference to the order Rhizostomeae. *Oceanogr Mar Biol Annu Rev* 38: 85-156
- Kingsford MJ, Seymour JE, O'Callaghan MD (2012) Abundance patterns of cubozoans on and near the Great Barrier Reef. *Hydrobiologia* 690: 257-268

- Kinsey BE (1986) Barnes on box jellyfish. Sir George Fisher Centre for Tropical Marine Studies, James Cook University
- Kovach AI, Breton TS, Enterline C, Berlinsky DL (2013) Identifying the spatial scale of population structure in anadromous rainbow smelt (*Osmerus mordax*). Fish Res 141: 95-106
- Lambrechts J, Hanert E, Deleersnijder E, Bernard PE, Legat V, Rémacle JF, Wolanski E (2008) A multi-scale model of the hydrodynamics of the whole Great Barrier Reef. Estuar Coast Shelf Sci 79: 143-151
- Larson RJ (1992) Riding Langmuir circulations and swimming in circles: a novel form of clustering behavior by the scyphomedusa *Linuche unguiculata*. Mar Biol 112: 229-235
- Lawley JW, Ames CL, Bentlage B, Yanagihara A, Goodwill R, Kayal E, Hurwitz K, Collins AG (2016) Box jellyfish *Alatina alata* has a circumtropical distribution. Biol Bull 231: 152-169
- Lee K, Bae BS, Kim IO, Yoon WD (2010) Measurement of swimming speed of giant jellyfish *Nemopilema nomurai* using acoustics and visualization analysis. Fish Sci 76: 893-899
- Lee PLM, Dawson MN, Neill SP, Robins PE, Houghton JDR, Doyle TK, Hays GC (2013) Identification of genetically and oceanographically distinct blooms of jellyfish. J R Soc Interface 10
- Lewis C, Long TAF (2005) Courtship and reproduction in *Carybdaea sivickisi* (Cnidaria: Cubozoa). Mar Biol 147: 477-483
- Lewis C, Kubota S, Migotto AE, Collins AG (2008) Sexually dimorphic cubomedusa *Carybdea sivickisi* (Cnidaria: Cubozoa) in Seto. Wakayama, Japan
- Llewellyn LE, Bainbridge S, Page G, O'Callaghan MD, Kingsford MJ (2016) StingerCam: a tool for ecologists and stakeholders to detect the presence of venomous tropical jellyfish. Limnol Oceanogr Methods 14: 649-657

- Luick JL, Mason L, Hardy T, Furnas MJ (2007) Circulation in the Great Barrier Reef Lagoon using numerical tracers and in situ data. *Cont Shelf Res* 27: 757-778
- Mantel N, Haenszel W (1959) Statistical aspects of the analysis of data from retrospective studies of disease. *J Natl Cancer Inst* 22: 719-748
- Matsumoto GI (1995) Observations on the anatomy and behaviour of the cubozoan *Carybdea rastonii* Haacke. *Mar Freshw Behav Physiol* 26: 139-148
- Matuschek H, Kliegl R, Vasishth S, Baayen H, Bates D (2017) Balancing type I error and power in linear mixed models. *J Mem Lang* 94: 305-315
- Mayr E (1954) Change of genetic environment and evolution. In: Huxley J, Hardy AC, Ford EB (eds) *Evolution as a process*. Allen and Unwin, London, pp 157–180
- McDonald JH (2014) *Handbook of biological statistics*, 3rd edn. Sparky House Publishing, Baltimore, MD
- Miller BJ, Von Der Heyden S, Gibbons MJ (2012) Significant population genetic structuring of the holoplanktic scyphozoan *Pelagia noctiluca* in the Atlantic. *Ocean Afr J Mar Sci* 34: 425-430
- Moon JH, Pang IC, Yang JY, Yoon WD (2010) Behavior of the giant jellyfish *Nemopilema nomurai* in the East China Sea and East/Japan Sea during the summer of 2005: a numerical model approach using a particletracking experiment. *J Mar Syst* 80: 101-114
- Mooney CJ, Kingsford MJ (2012) Sources and movements of *Chironex fleckeri* medusae using statolith elemental chemistry. *Hydrobiologia* 690: 269-277
- Mooney CJ, Kingsford MJ (2016a) Discriminating populations of medusae (*Chironex fleckeri*, Cubozoa) using statolith microchemistry. *Mar Freshw Res* 68: 1144-1152
- Mooney CJ, Kingsford MJ (2016b) The influence of salinity on box jellyfish (*Chironex fleckeri*, Cubozoa) statolith elemental chemistry. *Mar Biol* 163: 103

- Mooney CJ, Kingsford MJ (2017) Statolith morphometrics as a tool to distinguish among populations of three cubozoan species. *Hydrobiologia* 787: 111-121
- Mora C, Francisco V, Zapata FA (2001) Dispersal of juvenile and adult reef fishes associated with floating objects and their recruitment into Gorgona Island reefs, Colombia. *Bull Mar Sci* 68: 557-561
- Moriarty PE, Andrews KS, Harvey CJ, Kawase M (2012) Vertical and horizontal movement patterns of scyphozoan jellyfish in a fjord-like estuary. *Mar Ecol Prog Ser* 455: 1-12
- Mouritsen H, Atema J, Kingsford MJ, Gerlach G (2013) Sun compass orientation helps coral reef fish larvae return to their natal reef. *PLoS One* 8
- Nilsson DE, Gislén L, Coates MM, Skogh C, Garm A (2005) Advanced optics in a jellyfish eye. *Nature* 435: 201-205
- O'Connor M, Garm A, Nilsson DE (2009) Structure and optics of the eyes of the box jellyfish *Chiropsella bronzie*. *J Comp Physiol A -Neuroethol Sens Neural Behav Physiol* 195: 557-569
- Okubo A (1971) Oceanic diffusion diagrams. *Deep-Sea Res* 18: 789-802
- Paris CB, Cowen RK, Lwiza KMM, Wang DP, Olson DB (2002) Multivariate objective analysis of the coastal circulation of Barbados, West Indies: implication for larval transport. *Deep Sea Res I* 49: 1363-1386
- Pawlik JR (1992) Chemical ecology of the settlement of benthic marine-invertebrates. *Oceanogr Mar Biol* 30: 273-335
- Pham Van C, De Brie B, Deleersnijder E, Houtink AJF, Sassi M, Spinewine B, Hidayat H, Soares-Frazão S (2016) Simulations of the flow in the Mahakam river–lake–delta system, Indonesia. *Environ Fluid Mech* 16: 603-633

- Pitt KA, Kingsford MJ (2000) Geographic separation of stocks of the edible jellyfish *Catostylus mosaicus* (Rhizostomeae) in New South Wales, Australia. *Mar Ecol Prog Ser* 196: 143-155
- R Core Team (2017) R: a language and environment for statistical computing. R Foundation for Statistical Computing, Vienna
- Ricker WE (1975) Computation and interpretation of biological statistics of fish populations. *Bull Fish Res Board Can* 191: 1-382
- Roughgarden J, Iwasa Y, Baxter C (1985) Demographic theory for an open marine population with space-limited recruitment. *Ecology* 66: 54-67
- Rutz C, Hays GC (2009) New frontiers in biologging science. *Biol Lett* 5: 289-292
- Savino JF, Stein RA (1989) Behavior of fish predators and their prey: habitat choice between open water and dense vegetation. *Environ Biol Fishes* 24: 287-293
- Scheltema RS (1988) Initial evidence for the transport of teleplanic larvae of benthic invertebrates across the East Pacific barrier. *Biol Bull* 174: 145-152
- Schroth W, Jarms G, Streit B, Schierwater B (2002) Speciation and phylogeography in the cosmopolitan marine moon jelly, *Aurelia* sp. *BMC Evolut Biol* 2:1
- Secor DH, Hendersonarzapalo A, Piccoli PM (1995) Can otolith microchemistry chart patterns of migration and habitat utilization in anadromous fishes. *J Exp Mar Biol Ecol* 192: 15-33
- Shanks AL, Graham WM (1987) Orientated swimming in the jellyfish *Stomolopus meleagris* L. Agassiz (Scyphozoa, Rhizostomida). *J Exp Mar Biol Ecol* 108: 159-169
- Shorten M, Davenport J, Seymour JE, Cross MC, Carrette TJ, Woodward G, Cross TE (2005) Kinematic analysis of swimming in Australian box jellyfish, *Chiropsalmus* sp. and *Chironex fleckeri* (Cubozoa, Cnidaria: Chirodopidae). *J Zool* 267: 371-380

- Simpson SD, Piercy JJB, King J, Codling EA (2013) Modelling larval dispersal and behaviour of coral reef fishes. *Ecol Complex* 16: 68-76
- Sinclair M (1988) *Marine populations: an essay on population regulation and speciation*. University of Washington Press, Seattle, WA
- Slatkin M (1993) Isolation by distance in equilibrium and non-equilibrium populations. *Evolution* 47: 264-279
- Spagnol S, Wolanski E, Deleersnijder E, Brinkman R, McAllister F, Cushman-Roisin B, Hanert E (2002) An error frequently made in the evaluation of advective transport in two-dimensional Lagrangian models of advection-diffusion in coral reef waters. *Mar Ecol Prog Ser* 235: 299-302
- Stewart SE (1996) Field behavior of *Tripedalia cystophora* (class Cubozoa). *Mar Freshw Behav Physiol* 27: 175-188
- Stobutzki IC, Bellwood DR (1994) An analysis of the sustained swimming abilities of presettlement and postsettlement coralreef fishes. *J Exp Mar Biol Ecol* 175: 275-286
- Stopar K, Ramsak A, Trontelj P, Malej A (2010) Lack of genetic structure in the jellyfish *Pelagia noctiluca* (Cnidaria: Scyphozoa: Semaestomeae) across European seas. *Mol Phylogenet Evol* 57: 417-428
- Straehler-Pohl I, Jarms G (2005) Life cycle of *Carybdea marsupialis* Linnaeus, 1758 (Cubozoa, Carybdeidae) reveals metamorphosis to be a modified strobilation. *Mar Biol* 147: 1271-1277
- Straehler-Pohl I, Jarms G (2010) Identification key for young ephyrae: a first step for early detection of jellyfish blooms. *Hydrobiologia* 645: 3-21
- Straehler-Pohl I, Jarms G (2011) Morphology and life cycle of *Carybdea morandinii*, sp nov (Cnidaria), a cubozoan with zooxanthellae and peculiar polyp anatomy. *Zootaxa* 2755: 36-56

- Studebaker JP (1972) Development of the cubomedusa, *Carybdea marsupialis*. MS thesis, University of Puerto Rico
- Swearer SE, Trembl EA, Shima JS (2019) A review of biophysical models of marine larval dispersal. *Oceanogr Mar Biol Annu Rev* 57: 325-356
- Todd CD (1998) Larval supply and recruitment of benthic invertebrates: do larvae always disperse as much as we believe? *Hydrobiologia* 375-76: 1-21
- Todd CD, Lambert WJ, Thorpe JP (1998) The genetic structure of intertidal populations of two species of nudibranch molluscs with planktotrophic and pelagic lecithotrophic larval stages: are pelagic larvae "for" dispersal? *J Exp Mar Biol Ecol* 228: 1-28
- Toffoli A, McConochie J, Ghantous M, Loffredo L, Babanin AV (2012) The effect of wave-induced turbulence on the ocean mixed layer during tropical cyclones: Field observations on the Australian North-West Shelf. *J Geophys. Res-Oceans* 117: C00J24
- Toshino S, Miyake H, Iwanaga S (2014) Development of *Copula sivickisi* (Stiasny, 1926) (Cnidaria: Cubozoa: Carybdeidae: Tripedaliidae) collected from the Ryukyu Archipelago, southern Japan. *Plankton Benthos Res* 9: 32
- Toshino S, Miyake H, Shibata H (2015) *Meteorona kishinouyei*, a new family, genus and species (Cnidaria, Cubozoa, Chirodropida) from Japanese Waters. *ZooKeys* 503: 1-21
- Toshino S, Miyake H, Srinui K, Luangoon N, Muthuwan V, Sawatpeera S, Honda S, Shibata H (2017) Development of *Tripedalia binata* Moore, 1988 (Cubozoa: Carybdeida: Tripedaliidae) collected from the eastern Gulf of Thailand with implications for the phylogeny of the Cubozoa. *Hydrobiologia* 792: 37-51
- Underwood AH, Straehler-Pohl I, Carrette TJ, Sleeman J, Seymour JE (2018) Early life history and metamorphosis in *Malo maxima* Gershwin, 2005 (Carukiidae, Cubozoa, Cnidaria). *Plankton Benthos Res* 13: 143-153

- van Walraven L, Driessen F, van Bleijswijk J, Bol A and others (2016) Where are the polyps? Molecular identification, distribution and population differentiation of *Aurelia aurita* jellyfish polyps in the southern North Sea area. *Mar Biol* 163: 172
- Wei H, Deng LJ, Wang YH, Zhao L, Li X, Zhang F (2015) Giant jellyfish *Nemopilema nomurai* gathering in the Yellow Sea — a numerical study. *J Mar Syst* 144: 107-116
- Werner B (1973) Spermatozeugmen und Paarungsverhalten bei *Tripedalia cystophora* (Cubomedusae). *Mar Biol* 18: 212-217
- Werner B, Cutress CE, Studebaker JP (1971) Life cycle of *Tripedalia cystophora* conant (Cubomedusae). *Nature* 232: 582-583
- Williamson DH, Harrison HB, Almany GR, Berumen ML, Bode M, Bonin MC, Choukroun S, Doherty PJ, Frisch AJ, Saenz-Agudelo P, Jones GP (2016) Large-scale, multidirectional larval connectivity among coral reef fish populations in the Great Barrier Reef Marine Park. *Mol Ecol* 25: 6039-6054
- Wolanski E (1986) An evaporation-driven salinity maximum zone in Australian tropical estuaries. *Estuar Coast Shelf Sci* 22: 415-424
- Wolanski E (1992) Hydrodynamics of mangrove swamps and their coastal waters. *Hydrobiologia* 247: 141-161
- Wolanski E (1993) Water circulation in the Gulf of Carpentaria. *J Mar Syst* 4: 401-420
- Wolanski E (1994) Physical oceanographic processes of the Great Barrier Reef. CRC Press, Boca Raton, FL
- Wolanski E (2007) Estuarine ecohydrology. Elsevier, Amsterdam
- Wolanski E (2017) Bounded and unbounded boundaries – Untangling mechanisms for estuarine-marine ecological connectivity: scales of m to 10,000 km—a review. *Estuar Coast Shelf Sci* 198:378-392

- Wolanski E, Elliott M (2015) Estuarine ecohydrology, 2nd edn: an introduction. Elsevier, Amsterdam
- Wolanski E, Kingsford MJ (2014) Oceanographic and behavioural assumptions in models of the fate of coral and coral reef fish larvae. J R Soc Interface 11: 20140209
- Wu LJ, Xu JL (2016) Ensemble trajectory simulation of large jellyfish in the Yellow and Bohai Sea. In: Demetrescu I, Oh K, Kaushik NK, Butu A, Othman F (eds) 2016 3rd Int Conf on Chemical and Biological Sciences. MATEC Web of Conferences 60: 02006
- Yen J, Lenz PH, Gassie DV, Hartline DK (1992) Mechanoreception in marine copepods - electrophysiological studies on the 1st antennae. J Plankton Res 14: 495-512

Appendix I.

Chapter 2 supplement

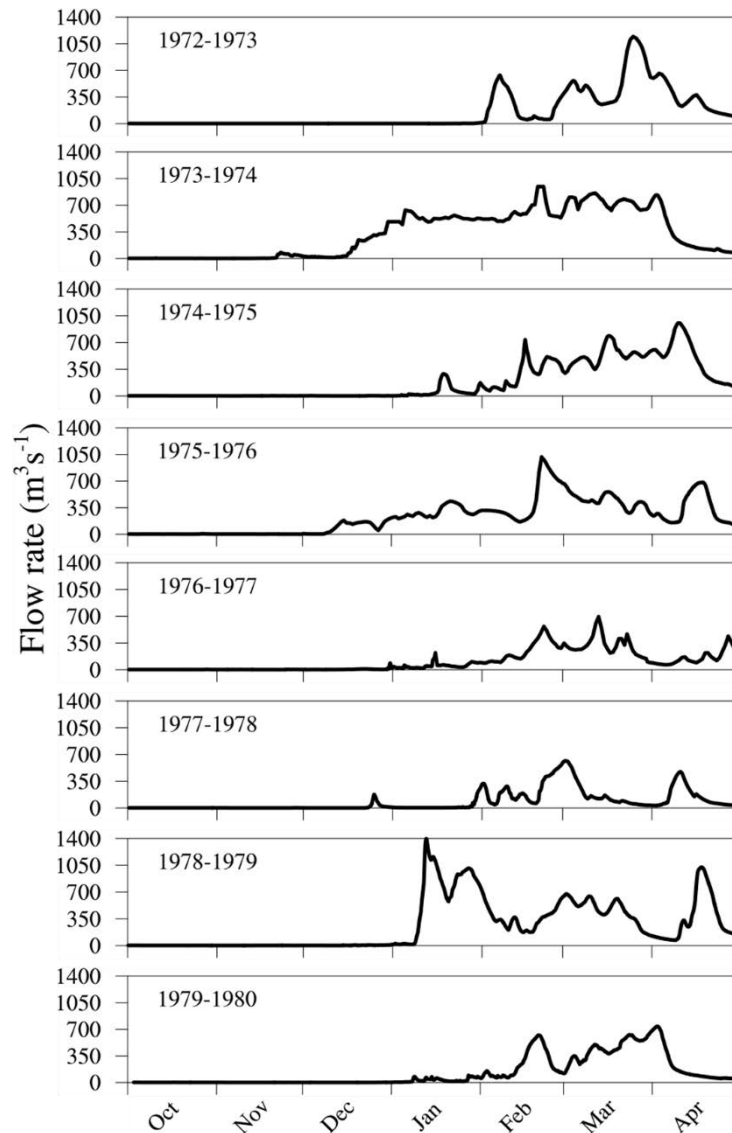


Fig. AI.1. The flow rate recorded at Jacks Camp ($12^{\circ}24'32.5''S$, $142^{\circ}18'16.9''E$), approximately 102 km from the mouth of the Wenlock river, in 16 consecutive *Chironex fleckeri* medusae seasons, from 1972-1973 to 1987-1988. Where data are missing, none were available.

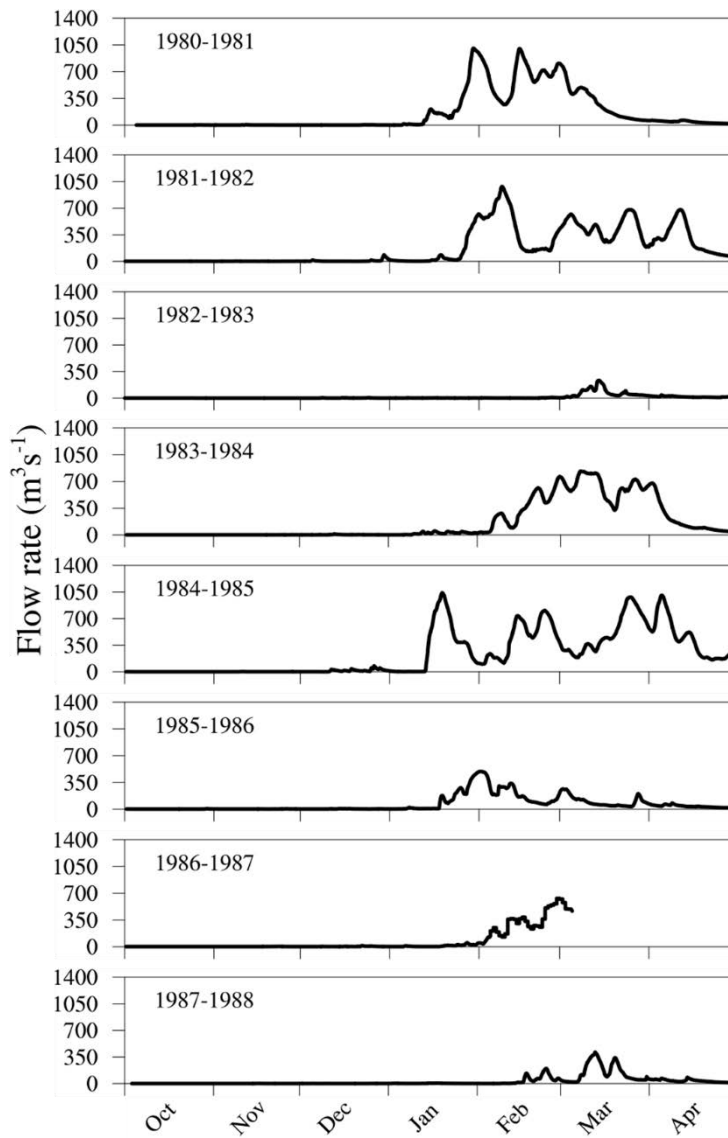


Fig. A1.1. Continued. The flow rate recorded at Jacks Camp (12°24'32.5"S, 142°18'16.9"E), approximately 102 km from the mouth of the Wenlock river, in 16 consecutive *Chironex fleckeri* medusae seasons, from 1972-1973 to 1987-1988. Where data are missing, none were available.

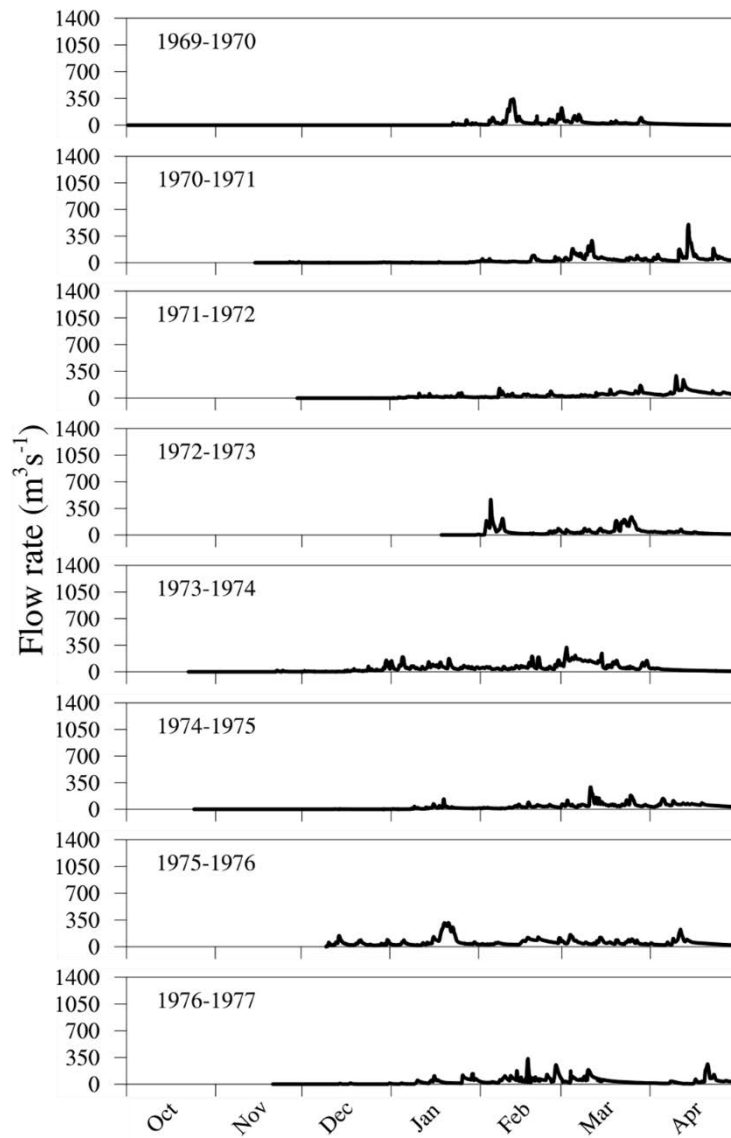


Fig. AI.2. The flow rate recorded at Bertiehaugh (12°07'37.4"S, 142°22'31.6"E), approximately 55 km from the mouth of the Ducie river, in 19 consecutive *Chironex fleckeri* medusae seasons, from 1969-1970 to 1987-1988. Where data are missing, none were available.

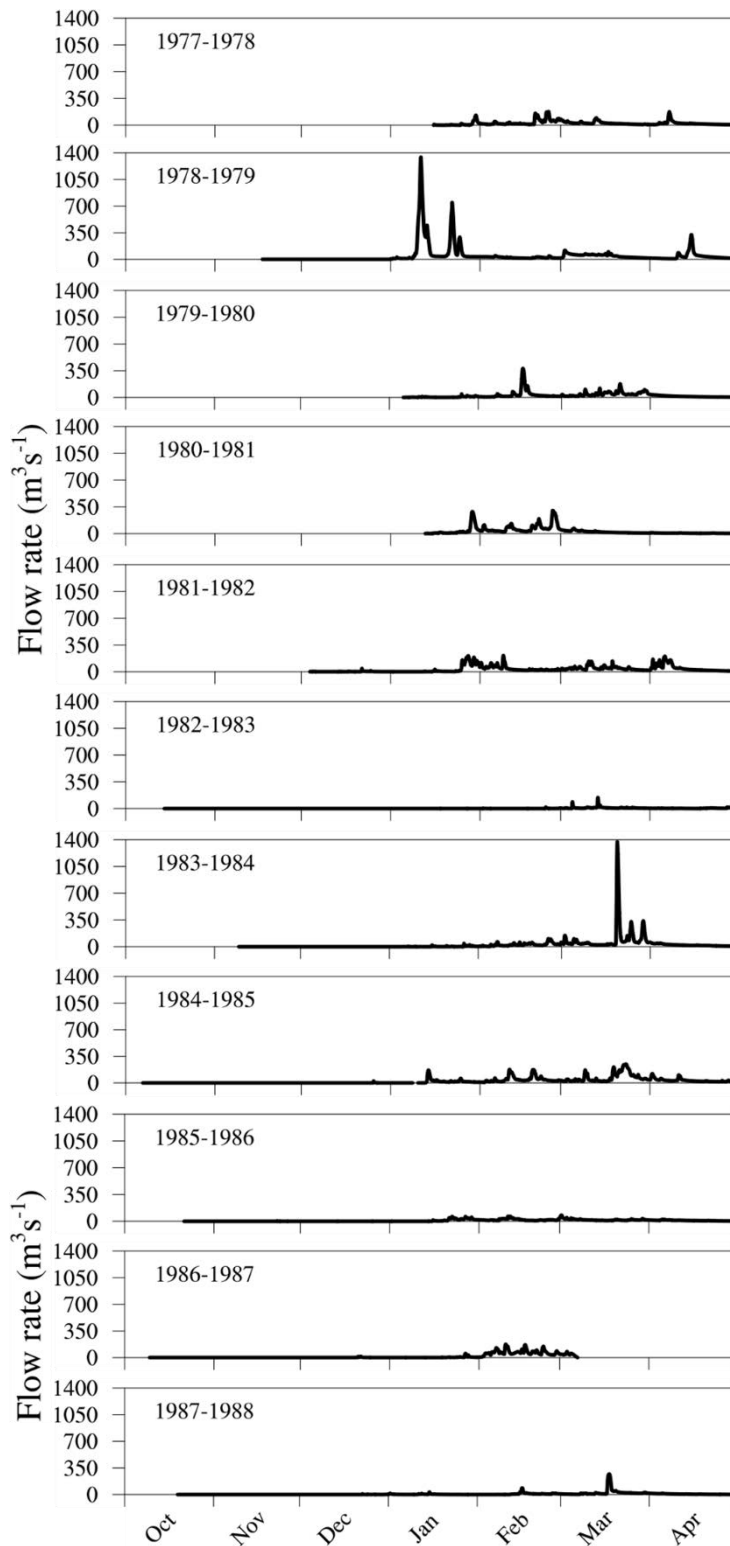


Fig. A1.2. Continued. The flow rate recorded at Bertiehaugh ($12^{\circ}07'37.4''\text{S}$, $142^{\circ}22'31.6''\text{E}$), approximately 55 km from the mouth of the Ducie river, in 19 consecutive *Chironex fleckeri* medusae seasons, from 1969-1970 to 1987-1988. Where data are missing, none were available.

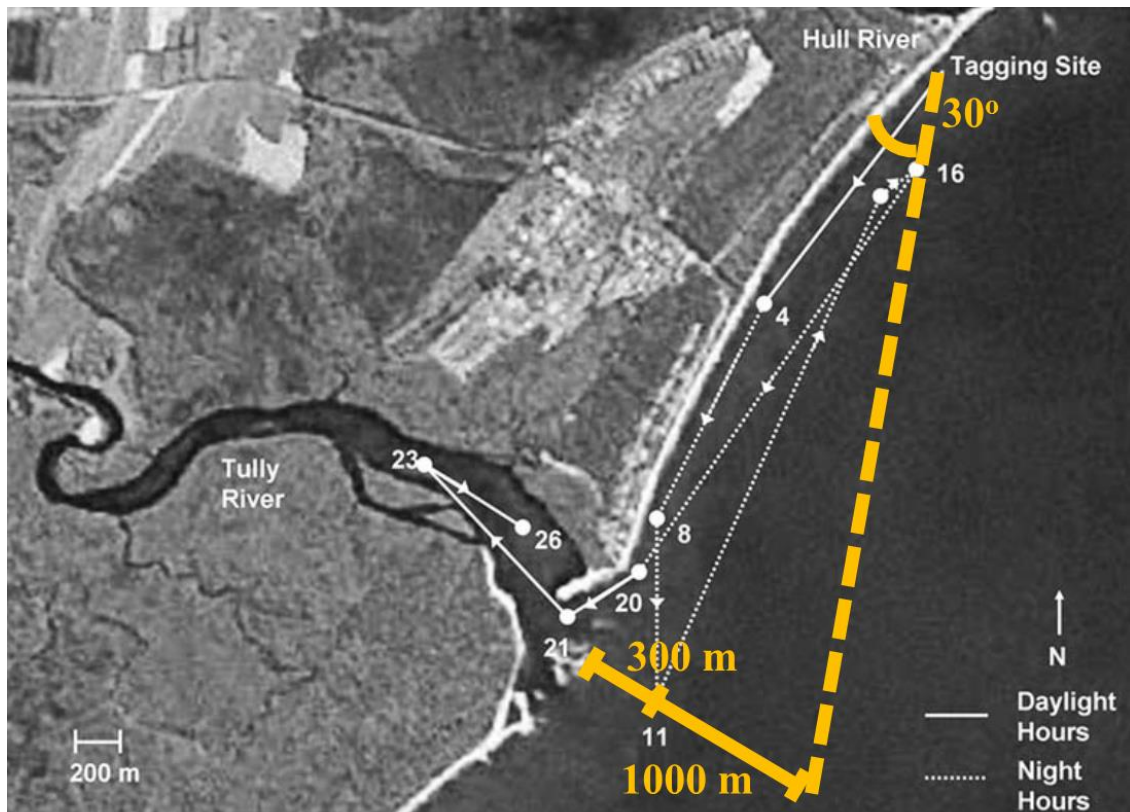


Fig. A1.3. The observed movements of a *Chironex fleckeri* medusa tracked by Gordon and Seymour (2009) over a 26 hour period, at Tully, QLD, Australia, are shown by the white dotted and solid lines. The white numbers indicate the hours since the initial tagging. The area enclosed by the shore line and the yellow dashed line shows the likely dispersion of a passive medusa, based on modelling from Hrycik et al. (2013). The approximate maximum distances from shore are shown for each of the scenarios. Adapted from Gordon and Seymour (2009).

REFERENCES

- Gordon MR, Seymour JE (2009) Quantifying movement of the tropical Australian cubozoan *Chironex fleckeri* using acoustic telemetry. *Hydrobiologia* 616:87-97
- Hrycik JM, Chasse J, Ruddick BR, Taggart CT (2013) Dispersal kernel estimation: A comparison of empirical and modelled particle dispersion in a coastal marine system. *Estuar Coast Shelf Sci* 133:11-22

Appendix II.

Chapter 4 supplement

SUPPLEMENTARY METHODS. BIOPHYSICAL MODEL

Bathymetry correction

The Second-generation Louvain-la-Neuve Ice-ocean Model (SLIM; Lambrechts et al. 2008) bathymetry was derived from an open source high resolution (30 m) depth model of the Great Barrier Reef (GBR; Beaman 2017). The high-resolution bathymetry was averaged/smoothed to a 100 m resolution with QGIS (version 2.18.16). Erroneous deep holes interspersed near shore waters in Beaman (2017), and these holes had to be corrected before the smoothed bathymetry could be used in the SLIM model (Fig. All.1). The bathymetry was corrected in a stepwise process. The holes and their surrounds were manually located and filled with an identifier (Fig. All.1b) using the `serval` plugin (version 0.8.1) in QGIS. The `linspace` function in python (python version 3.6.6, numpy version 1.13.3) was used to fill the lines in the identified regions with evenly spaced numbers, spaced between the bathymetry values of the raster cells directly adjacent to the ends of the lines. The lines were filled in a pre-defined direction i.e. along the horizontal, along the vertical, along the left to right descending diagonal or along the right to left descending diagonal. Each filled cell was also assigned a weighting based on its proximity to the nearest line end. This process was repeated in different directions until all hole identified cells were filled. Cells filled in the successive iterations were assigned less weighting. For example, the cells filled in the second iteration were given less weighting than the cells filled in the first. Multiple corrected bathymetry variants were generated, differing by the direction the lines were filled in first. The variants were averaged based on the weightings assigned to the filled raster cells. The final corrected bathymetry was generated by smoothing the averaged bathymetry with a gaussian filter (`gaussian blur` function in python module `cv2` version 3.2.0; Fig. All.1c).

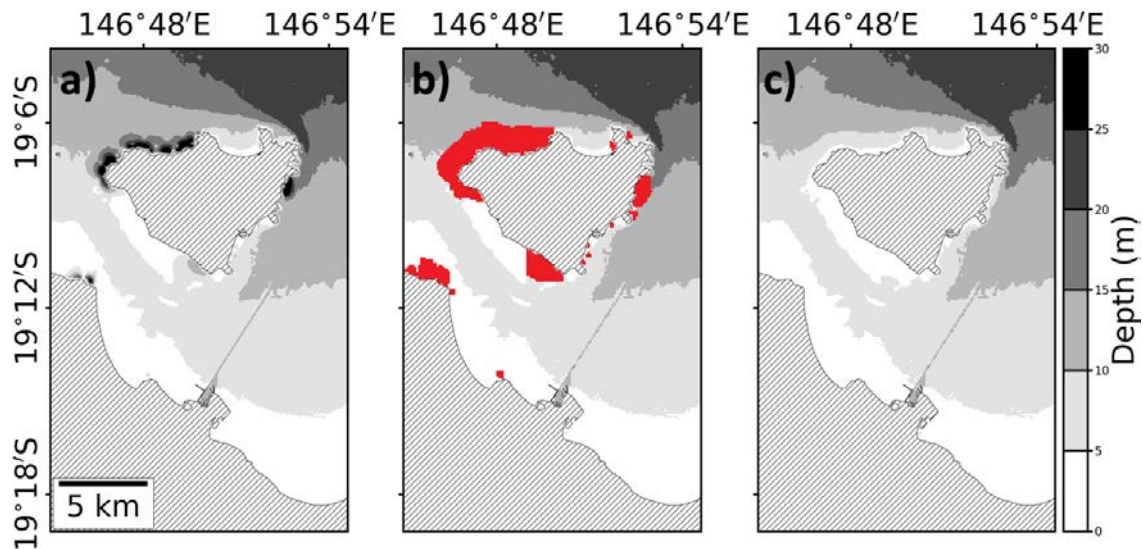


Fig. All.1. The bathymetry correction in the Townsville/Magnetic Island region, Queensland, Australia. a) the raw bathymetry from Beaman (2017) with visible nearshore holes. b) the identified holes and surrounds (red area). c) the corrected bathymetry. The color bar indicates the depth (m). Depths > 25 m are shown in black. Land is filled in a hatch pattern

Hydrodynamic model validation

The tide and currents simulated by SLIM were validated against measured tide and current data. The tidal data were open source and downloaded from Maritime Safety Queensland (Queensland Government). The current meter data were sourced from the Australian Government's National Environmental Science Program - Tropical Water Quality Hub Project 2.1.5 (<https://nesptropical.edu.au/index.php/round-2-projects/project-2-1-5/>). Specifically, I compared the measured and simulated: (1) tidal anomalies at the port of Townsville, and (2) zonal (west to east) and meridional (south to north) current components at Geoffrey Bay, Middle Reef, Orchard Rocks and Cleveland Bay (Fig. 4.1b). These comparisons were made over the periods of both the 2016 behavioural retention analysis (one month, 17 September to 17 October 2016) and the 2017 connectivity analysis (four months, 2 September to 28 December 2017). The SLIM outputs were modelled as linear functions of the corresponding measurements in linear regression analyses to quantify how closely the simulated data matched the measured data. The regressions were performed using the statsmodels (version 0.10.1) python package. All x-y plots of the related simulated and measured data sets showed linear relationships with approximately elliptical clouds of data. This indicated that the regression assumptions of linearity, homogeneity, and normally distributed residuals were met.

SLIM accurately reproduced the tides in the Magnetic Island region (Fig. 4.1b, Table All.1, Fig. All.2a b). The tidal anomalies simulated at the port of Townsville in the 2016 behavioural retention analysis and in the 2017 connectivity analysis both closely matched the anomalies measured at the port over the periods of the analyses (2016: Fig. All.2a and Fig. All.2b [$y \sim x$]; 2016 and 2017: $m \sim 1$, $c \sim 0$ and $RMSE \sim 0$).

The currents simulated at Magnetic Island and in the surrounding region matched current meter measurements (Fig. 4.1b, Table All.1, Fig. All.2c d e f). The currents simulated at Geoffrey Bay were well represented in SLIM. Although the zonal (west-east; U) and meridional (south-north; V) components of the currents simulated in 2016 tended to be greater than the measured components, the trends were captured well (Fig. All.2c d e f, RMSE range: 0.24 to 0.26). As the flood (negative U and V) and ebb (positive U and V) tidal current peaks were both slightly overestimated, the simulated net tidal transport would have closely matched the real tidal transport. The measured trends in the U and V current components at Geoffrey Bay were captured equally well in SLIM in 2017 (RMSE range: 0.23 to 0.27); although, U went from being slight overestimated to being slightly underestimated ($m < 1$). The simulated U component at Middle Reef was somewhat inflated in both 2016 and 2017 ($m > 1$), and the V component was generally weaker than measured ($m < 1$); however, the trends were captured effectively (RMSE range: 0.16 to 0.26). At Orchard Rocks, the U and V current components were both slightly underestimated in 2016 ($m < 1$) but the overall fit was good (RMSE range: 0.13 to 0.15). The currents measured at a site in Cleveland Bay were well represented in the model (RMSE range: 0.11 to 0.24); although, the U component could be underestimated ($m < 1$) and the V component could be overestimated ($m > 1$).

Table All.1. SLIM validation. SLIM data have been compared with measured data (Fig. 4.1b) over the one-month period of the behavioural retention analysis (17 September to 17 October **2016**) and over the four-month period of the connectivity analysis (2 September to 28 December **2017**). Metrics of the accuracy of the tidal anomaly (**TA**) simulated at the port of Townsville (**POT**) and of the currents simulated at Geoffrey Bay (**GB**), Middle Reef (**MR**), Orchard Rocks (**OR**) and Cleveland Bay (**CB**) are presented. The currents have been broken up into their zonal (**U**, west to east) and meridional (**V**, south to north) components. Linear regression lines of the form $y = mx + c$ have been generated, where the SLIM outputs (y) are modelled as a function of the measured values (x). **m** is the slope of the regression line and **c** is the y-axis intercept. In a perfect model $m = 1$ and $c = 0$. The normalised root mean square error (**RMSE**, i.e. the standard deviation of the residuals) has also been presented for each regression line. The closer the RMSE is to 0, the better the fit of the SLIM output with the corresponding measured data. The number of measurements taken by the instruments during each period are indicated (**n**). Where cells are blacked out, no measured data were available

		2016				2017			
		m	c	RMSE	n	m	c	RMSE	n
TA	POT	1.03	-0.04	0.03	4321	1.03	-0.11	0.04	13530
U	GB	1.39	1.05×10^{-3}	0.26	1859	0.87	0.02	0.27	13766
	MR	1.34	0.01	0.20	4321	2.00	-0.04	0.26	13587
	OR	0.59	-2.75×10^{-3}	0.15	4321				
	CB	0.54	-8.79×10^{-3}	0.15	4321	0.59	-4.04×10^{-3}	0.11	5689
V	GB	1.13	0.04	0.24	1859	1.21	0.02	0.23	13766
	MR	0.60	0.01	0.16	4321	0.60	0.01	0.17	13587
	OR	0.61	-7.96×10^{-4}	0.13	4321				
	CB	1.32	0.01	0.24	4321	1.21	0.02	0.15	5689

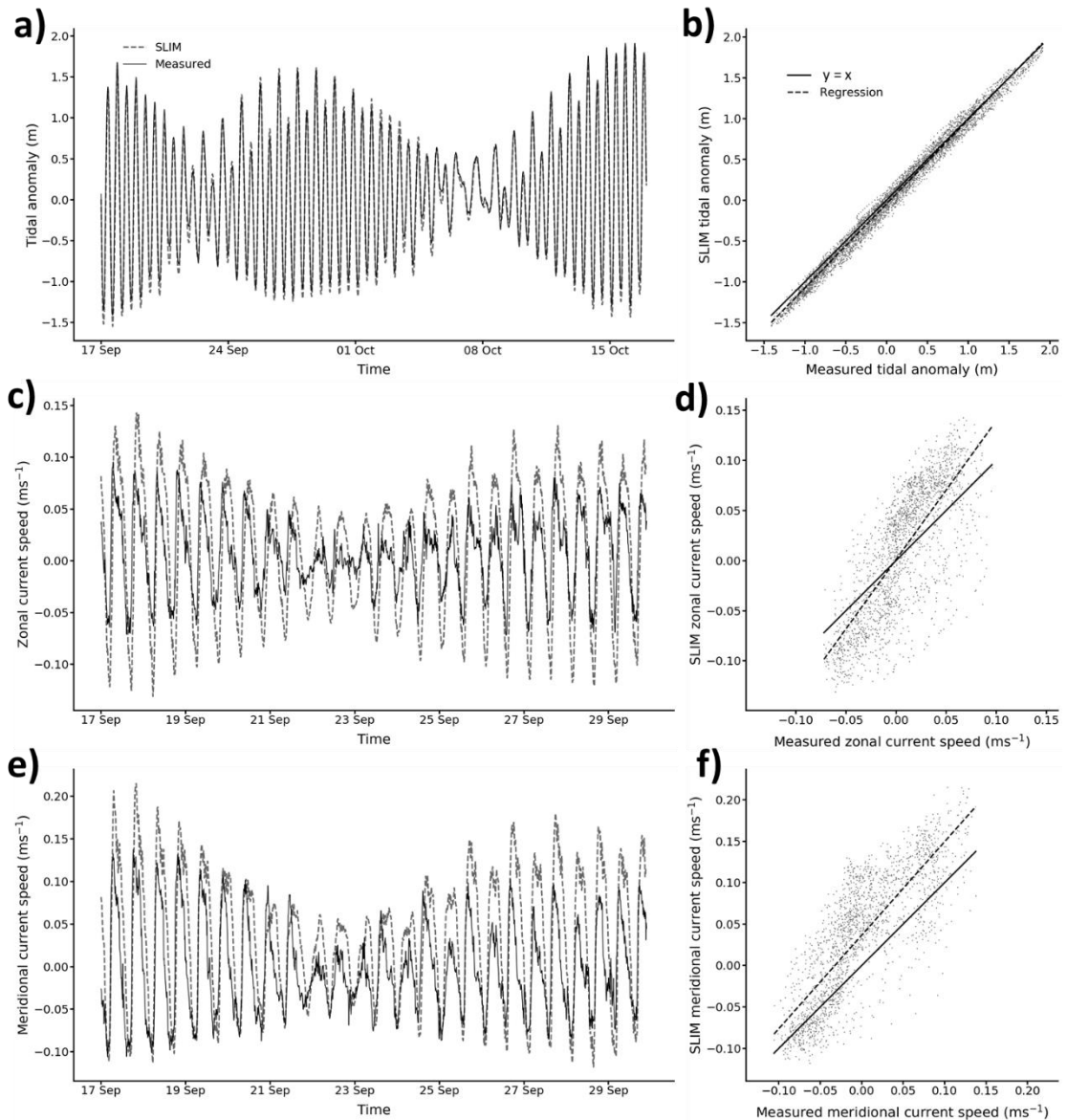


Fig. AII.2. Visualisation of the SLIM validation. a) time series and b) x-y plot comparing the measured and simulated tidal anomalies at the port of Townsville. Data are shown for the full period of the behavioural retention analysis (17 September to 17 October 2016). c) time series and d) x-y plot comparing the measured and simulated zonal (west to east) components of the currents at Geoffrey Bay. Data are shown for the period of the behavioural retention analysis for which current meter data were available (17 September to 30 September 2016). e) time series and f) x-y plot comparing the measured and simulated meridional (south to north) components of the currents at Geoffrey Bay. Data are shown over the same time period as the zonal components. In all time series, the measured data are shown with a solid black line, and the SLIM data are shown with a dashed grey line. In all x-y plots, the regression line of the SLIM data (y) modelled as a function of the measured data (x) is shown as a black dashed line and compared to a solid black identity line ($y = x$). The locations of the measuring instruments are shown in Fig. 4.1b

Behavioural model setup

The base and dependent behavioural models are described in detail in Chapter 4 (Materials and methods, Behavioural retention, Biophysical model). The behavioural models were set up based on the results of Chapter 3, and on behaviours documented by Garm et al. (2012). The inclusion of each component of the model is justified in Table All.2.

Table All.2. Descriptions of the behaviours included in the base (B) and dependent (D) models of *Copula sivickisi* medusae behaviour, accompanied by justifications for their inclusion.

Description of modelled behaviour	Model	Justification (reference)
Nocturnal	B & D	In tank experiments, the level of activity in <i>Copula sivickisi</i> medusae increased from day to night, coinciding with a reduction in their level of inactivity (Chapter 3, Garm et al. 2012). <i>C. sivickisi</i> medusae have been sampled with plankton nets during the day and at night in their natural environment and have been almost entirely absent from the daytime samples (Chapter 3, Garm et al. 2012).
'On habitat' within 100 m of the habitat midline and 'off habitat' beyond this zone	B & D	The distribution of <i>C. sivickisi</i> medusae was mapped at a fine spatial scale in Nelly Bay and Geoffrey Bay at Magnetic Island. Medusae were most abundant at sites on a dense band of fringing reef habitat dominated by <i>Sargassum sp.</i> algae and coral. Medusae were also abundant at sites with high to moderate habitat availability, within 110 m of the dense band (Chapter 3).
Attach to habitat (daytime)	B & D	Numerous <i>C. sivickisi</i> medusae were observed attaching to <i>Sargassum sp.</i> algae in a habitat choice experiment, and a single medusa was filmed attaching to sargassum in its natural environment (Chapter 3). <i>C. sivickisi</i> medusae attached to coral and algal species in another habitat choice experiment (Garm et al. 2012).

Table All.2. Continued.

Description of modelled behaviour	Model	Justification (reference)
Maintain positions near the bottom of the water column	B & D	Moderate numbers of <i>C. sivickisi</i> medusae were collected in near bottom plankton tows at night, and no medusae were collected in the nighttime surface tows (Chapter 3).
Swim to habitat midline	B & D	<i>C. sivickisi</i> medusae displayed a strong preference for <i>Sargassum sp.</i> algae (Chapter 3) and coral underside (Garm et al. 2012) over other available habitats in habitat choice experiments.
Attach to habitat (night time) when the current speed exceeds a predefined cut off	D only	In swim trials with stepwise increasing currents, 17 of 41 medusae (more than 40%) attached to the side of the tank to avoid being pushed back by the current (Chapter 3).

SUPPLEMENTARY RESULTS - POPULATION STRUCTURE (CONNECTIVITY)

There was little variability in the inter bay/reef connectivity simulated in the replicate connectivity analysis model runs (Fig. All.3). The matrices from the replicate runs similarly show: high in-zone retention of *C. sivickisi* medusae in the bays of the east coast of Magnetic Island, connectivity with adjacent bays over small distances, negligible export of medusae from the island population to Middle Reef, and limited export in the opposite direction (from Middle Reef to Magnetic Island).

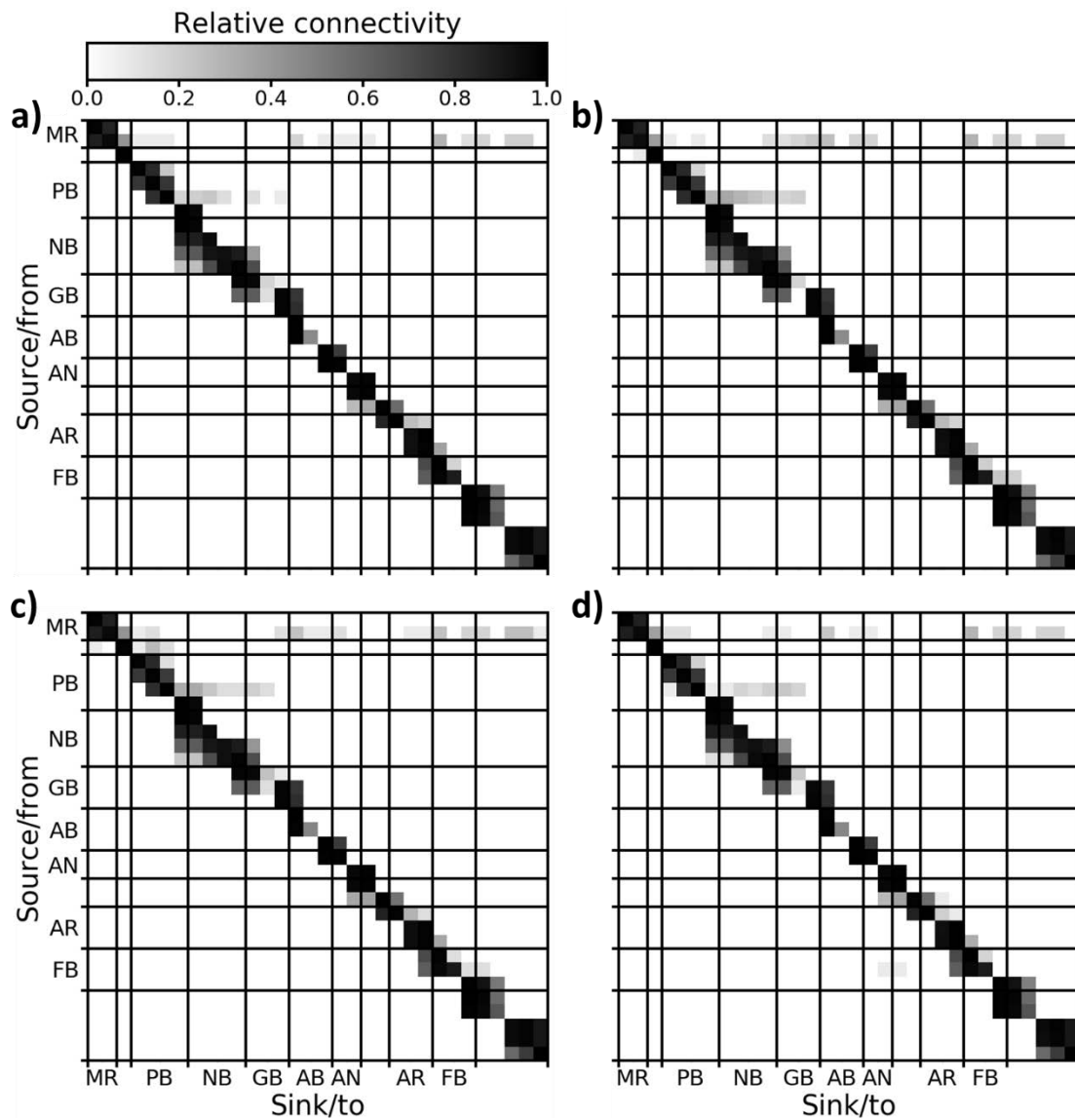


Fig. All.3. a) to d) Connectivity matrices showing the relative connectivity between source/from and sink/to detection zones over the entire 2017 *Copula sivickisi* medusae season at Magnetic Island, Queensland, Australia. The matrices show the results of the four replicate model runs that were not presented in Chapter 4 (dependent model, swim speed = $U_{crit} = 4.9 \text{ cm s}^{-1}$, attach at cut off of 6 cm s^{-1}). The detection zones have been pooled by the reefs/bays identified on the x and y axes. Locations are: Middle Reef (MR), Picnic Bay (PB), Geoffrey Bay (GB), Nelly Bay (NB), Alma Bay (AB), Alma North (AN), Arthur Bay (ArB) and Florence Bay (FB; Fig. 4.2)

REFERENCES

Beaman RJ (2017) High-resolution depth model for the Great Barrier Reef - 30 m.
doi:10.4225/25/5a207b36022d2

Garm A, Bielecki J, Petie R, Nilsson DE (2012) Opposite patterns of diurnal activity in the box jellyfish *Tripedalia cystophora* and *Copula sivickisi*. *Biol Bull* 222:35-45

Lambrechts J, Hanert E, Deleersnijder E, Bernard P-E, Legat V, Remacle J-F, Wolanski E (2008) A multi-scale model of the hydrodynamics of the whole Great Barrier Reef. *Estuar Coast Shelf Sci* 79:143-151.

Appendix III.

Experimental validation of the relationships between cubozoan statolith elemental chemistry and salinity and temperature

Morrissey SJ, **Schlaefer JA**, Kingsford MJ (2020) Experimental validation of the relationships between cubozoan statolith elemental chemistry and salinity and temperature. J Exp Mar Biol Ecol 527. <https://doi.org/10.1016/j.jembe.2020.151375>

ABSTRACT

Knowledge surrounding the movements of jellyfish is limited, but elemental chemistry has the potential to elucidate these movements. The objective of this study was to experimentally validate elemental chemistry as a technique which may provide insight into the movements of cubozoans. The approach used a laboratory experiment on the well-known cubozoan species *Chironex fleckeri*, examining the relationship between statolith elemental chemistry and temperature and salinity. Strong evidence was found that statolith Sr:Ca varied with temperature and that this was independent of variation in salinity. Sr:Ca ratios in saltwater varied little with variation in temperature or salinity. Accordingly, a physiological mechanism within *C. fleckeri* must have affected statolith Sr:Ca, causing it to vary with temperature. Based on the experimental data from this study and correlative evidence that Sr:Ca varied with temperature in another cubozoan, *Copula sivickisi*, we provide robust evidence that statolith Sr:Ca can be utilised as a proxy for temperature and may be applicable to other species of cubozoans. Ba:Ca in statoliths was found to vary with both temperature and salinity. As a result, it was determined that Ba:Ca profiles in statoliths have the potential to help resolve jellyfish movements in some circumstances. The use of elemental chemistry to elucidate horizontal or vertical movements of cubozoan species has significant potential and application.

INTRODUCTION

Knowledge on the movements of marine organisms is critical for understanding species ecology, and for the effective management and conservation of marine species (Elsdon and Gillanders, 2003; Gillanders et al., 2003). Additionally, as the robustness of stocks within metapopulations depends on immigration and emigration (Sinclair and Iles, 1989), knowledge surrounding movements is critical for understanding the population dynamics of species. Analysing the elemental chemistry of hard, calcified structures in aquatic species can give a detailed time frame of the movements of individuals if there is some knowledge on the periodicity with which the increments on the structures are deposited (Campana, 1999; Thorrold et al., 2002). The elemental composition of hard calcified structures can be used to reconstruct environmental conditions and movements.

Calcified structures can be used to reconstruct environmental conditions and movements of individuals through use of their contained elemental chemistry. Some trace elements, from surrounding sea waters, are incorporated into these structures through substitution for calcium in the calcium-matrix of the structures (Campana, 1999). The deposition and chronological record of these trace elements is unaltered as these hard-calcified structures are metabolically inert (Campana, 1999). Hence, the contained elemental chemistry is representative of waters experienced by individuals through their lives and these structures act as elemental records (Campana, 1999; Elsdon and Gillanders, 2003). Further, variations in the chemistry of these structures can represent shifts by individuals between environments (Arkhipkin et al., 2004). Accordingly, there is the potential for these chemical records to fill knowledge gaps surrounding the palaeoenvironment and the complex ecology of marine organisms (Campana, 1999; Weber, 1973). The use of this method to do so has been successful (Beck et al., 1992; de Villiers et al., 1994; McCulloch et al., 1994; Shen et al., 1996).

A number of assumptions underly the use of hard calcified structures to reconstruct environmental conditions and movements of species. They include the following; 1) material deposited is metabolically inert after deposition, 2) the physical and chemical environment influences the rate of trace element incorporation and 3) ontogenetic changes in the structure's elemental composition does not exist (Campana, 1999; Campana and Thorrold, 2001; Kalish, 1989; Secor et al., 1995). Studies on otolith elemental chemistry have revealed that elements influenced by physiological regulation likely do not meet the second assumption (Proctor et al., 1995; Thresher, 1994), however, elements such as strontium, barium, manganese, magnesium, lead and iron

meet both the first and second assumption as these elements referenced to calcium have significant effects on otolith elemental composition with changing temperature (Dove, 1997; Farrell and Campana, 1996; Fowler et al., 1995). As a result of this, most studies utilise these elements to interpret the environmental conditions faced by individuals throughout their lives (Gillanders et al., 2003).

The elements of focus for this study were strontium and barium. Numerous studies have examined the potential use of these elements as an environmental proxy for both temperature and salinity. Strontium has been examined more extensively than barium in past literature (Thorrold et al., 1998). Specifically, the use of strontium as an environmental proxy for temperature (Beck et al., 1992; Coutant and Chen, 1993; de Villiers et al., 1994; Halden et al., 1995; Kalish, 1990; Limburg, 1995; Mazloumi et al., 2017; McCulloch et al., 1994; Otake and Uchida, 1998; Secor et al., 1995; Shen et al., 1996). Numerous studies have examined the relationship and use of otolith elemental Sr:Ca and Ba:Ca as an environmental proxy for both temperature and salinity. Studies examining these relationships have reported varying strengths and directions. Positive relationships (Arai et al., 1995; Bath et al., 2000; Elsdon and Gillanders, 2002; Fowler et al., 1995; Hoff and Fuiman, 1995; Kalish, 1989; Kawakami et al., 1998; Mugiya and Tanaka, 1995; Secor et al., 1995; Tzeng, 1996; Yamashita et al., 2000), negative relationships (Elsdon and Gillanders, 2002; Radtke, 1990; Secor et al., 1995; Townsend et al., 1995) and no relationships at all (Bath et al., 2000; Chesney et al., 1998; Elsdon and Gillanders, 2002; Fowler et al., 1995; Gallahar and Kingsford, 1996; Hoff and Fuiman, 1995; Kawakami et al., 1998; Tzeng, 1996; Yamashita et al., 2000) have been reported. It appears that for fish otoliths, these relationships are species specific (Elsdon and Gillanders, 2003). As a result of this, laboratory experiments must be undertaken to determine the relationships between elemental fingerprints and environmental variation for each species studied.

The use of this method to elucidate the movements of individuals has considerable potential for studying cubozoan movements. This method overcomes the challenges associated with individual based methods such as tagging and would have higher success as most species are generally short lived. This method has only recently been utilised to examine cubozoan statoliths (Kingsford and Mooney, 2014; Mooney and Kingsford, 2012; Mooney and Kingsford, 2016). A study by Mooney and Kingsford (2012) examined the elemental chemistry of *Chironex fleckeri* statoliths to determine whether the anecdotal paradigm, that *C. fleckeri* medusa metamorphose from sessile polyps in estuaries and then migrate into coastal waters, was true. This study examined

Sr:Ca within the statoliths, from the core to edge, and used this elemental ratio as a proxy of salinity to elucidate the movements of the species. They concluded that *C. fleckeri* likely originate from both estuarine and coastal waters. A later experimental study again by Mooney and Kingsford (2016) looked further into the use of elemental chemistry as a means to elucidate the movements of cubozoans. A laboratory experiment was undertaken to establish how the elemental chemistry of *C. fleckeri* statoliths was affected by salinity. This study revealed that, with the exception of manganese, elements within the statoliths did not vary over the range of salinities tested (20-35ppt) and hence salinity did not have an effect upon the elemental chemistry of cubozoan statoliths. The findings from this experimental study suggested that the patterns observed in the statoliths from Mooney and Kingsford's previous study (2012) were likely influenced by temperature. An a-posteriori comparison of Sr:Ca and water temperature was undertaken by Mooney and Kingsford (2016) to examine whether temperature had an influence and a strong positive relationship was detected. The relationship between temperature and Sr:Ca within the aragonite structures of a number of taxa vary greatly, and despite the positive relationship found between temperature and Sr:Ca Mooney and Kingsford's 2012 study was only correlative. Consequently, a laboratory experiment was required to definitively determine whether a relationship exists between Sr:Ca and temperature for cubozoan statoliths. The determination of such a relationship, particularly one that is independent of salinity, would be of great benefit for determining jellyfish movements among different thermal environments.

The objective of this study was to investigate and validate the relationship between statolith elemental chemistry and environmental variation. Specifically, this was undertaken through: (1) experimentally testing *C. fleckeri* medusa in orthogonal combinations of controlled temperature and salinity within their known tolerance range and, the resultant elemental chemistry was measured in the medusa's statoliths, (2) testing seawater for variation in Me:Ca ratios and (3) using an *in-situ* approach to determine the relationship between temperature and elemental ratios in another species of cubozoan, *Copula sivickisi*.

MATERIALS AND METHODS

Experimental Design

C. fleckeri medusae were collected at Port Musgrave, North Queensland (11.99°S 141.91°E). Sampling of these medusae was undertaken in December of both the 2015 and 2016 jellyfish season. Medusae were located through visually searching surface waters and were captured using buckets. These medusae were then transported to Weipa, Queensland, where the experiment was undertaken. Medusae were held in 9L buckets with waters maintained at two different salinities, 22ppt and 34ppt, and three different temperatures, 20, 25 and 30°C. An orthogonal experiment design was utilised so that each of the temperature treatments were paired with the two different salinities, hence there were six combinations of temperature and salinity. Four medusa were held per temperature and salinity treatment, so 24 medusa were held in total. The medusae were acclimated in the treatment conditions for a day before being held for a minimum of four days. Seawater was used for the 34ppt treatment. Water for the 22ppt treatment was made by diluting seawater with filtered freshwater. The freshwater was filtered using two 5-µm pure tec® impregnated carbon filter cartridges to reduce chlorine, sediments, pesticides, herbicides and other chemicals. To maintain the experimental temperatures, the replicate buckets were partially submerged in shallow pools with waters circulating through Aqua Medic Titan 2000 cooling units. Half water changes were performed daily. The salinity of the treatment water was monitored daily with a refractometer. There was minimal evaporation, the salinity remained within 1ppt of the target salinity for each treatment. During the experiment, the temperature was monitored with a glass thermometer to ensure it remained within two degrees of the target temperature for each treatment. Additionally, the treatment temperatures were measured every five or ten minutes for the duration of the experiment with Tinytag TG-3100 data logger. The salinities which the medusae were exposed to represent the full salinity range that can be tolerated by *C. fleckeri* medusae (Mooney and Kingsford, 2016). *C. fleckeri* medusae have been observed inhabiting the approximate temperature range covered by the experimental water temperatures (21.7°C to 31.6°C; (Llewellyn et al., 2016). Individual medusa which died short of the minimum four days were replaced (only 5 medusas were replaced). Throughout this period, the medusae were fed frozen prawns less than 2cm long. At the end of the four-day minimum period, the four rhopalium of each medusa were extracted and preserved in 100% ethanol. Based on the width of daily rings (6 microns) the experimental period represented about 24 microns of statolith growth. Daily increments have been

validated in Cubozoa (Haack and Kingsford pers. comm.). Two water samples per treatment were also taken daily during the experiment in order to be able to compare the elements available in the water with what was laid down in the statoliths.

Correlative Approach

C. sivickisi medusae were collected from Geoffrey Bay, Magnetic Island near Townsville Queensland. Sampling of the medusae occurred on a weekly basis from the 25th of September till the 30th of October 2017. Sampling was undertaken at night as *C. sivickisi* undertake diurnal migrations where they spend their time on the benthos during the day and in the water column during the night (Garm et al., 2007). Medusae were attracted to a submerged LED light source (2000 Lumens) and captured with a net. Medusae were then transported in seawater back to the laboratory and preserved in 100% ethanol within three hours of capture. A Tinytag TG-3100 data logger was deployed in Geoffrey Bay, it recorded the water temperature every 70 minutes over the entire sampling period. The logger allowed for direct correlation between the elemental chemistry of statoliths from the collected medusae and the water temperature. The water temperature increased by 2°C during the sampling period. Temperatures were pooled into the following categories, 25.5°C to 26.5°C = 26°C, 26.5°C to 27.5°C = 27°C, 27.5°C to 28.5°C = 28°C.

Statolith Preparation

The statoliths of *C. fleckeri* and *C. sivickisi* were firstly extracted from the four rhopalium of each individual. Two fine needles were used to tease out the statolith from the rhopalial niche under a Leica WILD M3Z dissection microscope. The statoliths were then moved and stored in 1.5ml eppendorf tubes in 100% ethanol. One statolith from each individual was then mounted onto separate glass slides as follows. Firstly, a glass slide was placed onto a hot plate and Crystal Bond adhesive was applied when the slide reached an appropriate temperature. The slide was then lowered onto a statolith from above so that the adhesive attached to the specimen. Fine needles were then used to manipulate and move the statoliths into the appropriate position, proximal face up (cleavage vertical), before the Crystal Bond adhesive set. The Crystal Bond adhesive was spread evenly on the end of each slide to provide an even surface for easier

polishing. Following extraction and mounting, each statolith was polished using 0.3µm lapping film until it was sectioned and had a smooth surface where the structures concentric rings could be observed through an Olympus CX31 compound microscope. The increment width of each statolith was measured from images taken through a Lecia DMLB UV microscope using the Lecia Application Suite software. The slides which contained the polished statoliths were then cut down to approximately 10mm in size and were attached to 50mm glass slides via Crystal Bond adhesive as this allowed for more samples to be analysed via the LA-ICPMS (Mooney and Kingsford, 2016).

LA-ICPMS Operating Procedure for Experimental and Correlative Statoliths

LA-ICPMS analyses were undertaken at the Advanced Analytical Centre (AAC) at James Cook University (JCU). A Teledyne Analyte G2 laser system and iCAP RQ ICPMS were utilised for this study. The statoliths were placed in a vacuum chamber on an automated X-Y sample stage and a mix of helium and argon gas moved the ablated material from the chamber to the ICPMS. LA-ICPMS has a number of parameters which need to be addressed to detect elemental signatures. These parameters include, carrier gas flow rate, energy (fluence), mask size, repetition rate, shot count and attenuator reading. A pilot study was undertaken to determine the settings of these parameters for *C. sivickisi* and *C. fleckeri*. Different levels of each parameter, specifically energy and mask size, were tested to find the optimum settings which allowed for the detection of isotopes with ICPMS for each of the targeted elements (i.e. Sr and Ba) without destroying the delicate samples. The optimum settings for *C. fleckeri* were an energy of 1.5J/cm² and a mask size of 16µm, and for *C. sivickisi* they were an energy of 1.5J/cm² and a mask size of 50 µm.

The *C. fleckeri* statoliths were lasered using a step repeat cleaning procedure followed by an analysis transect along the edge of the statolith which corresponded to the experimental area. Medusae were held in treatments for four days. With a mask size of 16 microns per sample spot, this easily fitted within the estimated experimental area of 24 microns. The *C. sivickisi* statoliths were lasered with a single spot as the individuals caught were young, approximately 6-7 days old, and hence the elemental fingerprints of the statoliths would represent the chemistry of the water near the time of capture.

To calibrate the ICPMS, the reference materials NIST 610 (National Institute of Standards and Technology) and NIST 612 were utilised. The levels of elements in these

reference materials are known and are accurate for Ba and Sr. The process of calibrating the ICPMS was undertaken prior to lasering and following lasering of the statoliths via lasering the NIST reference materials using a line of spots laser track.

SO-ICPMS Operating Procedure for Experimental Water

Solution based inductively coupled plasma mass spectrometry (SO-ICPMS) analyses were undertaken upon the water samples from the *C. fleckeri* experiment. The analyses were conducted at the AAC at JCU. The SO-ICPMS operating procedure was undertaken as per Mooney and Kingsford (2016). A Varian 820-MS ICPMS using H₂ as a collision reaction interface (CRI) gas was utilised for the trace element analysis. For this, water samples were diluted 10-fold and multi-element standard solutions were used to calibrate the ICPMS. Twenty ppb of yttrium and indium were used as internal standards to control for instrumental drift and matrix effects. For quality control and to remove backgrounds from all analysed samples a CASS-4 sea water Certified Reference Material (CRM) was analysed every 20 samples. A Varian Liberty Series II ICP-OES was utilised for major element analysis after the trace element analysis had been undertaken. A series of multi-element standard solution were used to calibrate the instrument. A 1 ppm independent standard was also used as the quality control sample.

Data and Statistical Analysis

To analyse the data and to test hypotheses, the isotopic count data from the LA-ICPMS was converted to elemental ratios. This was undertaken by converting the raw elemental count data to parts per million (ppm; based on atomic weight) and then to $\mu\text{mol/mol}$ values as per convention (Woodhead et al., 2007). The detectable isotopes used were as follows: Sr⁸⁸, Ba¹³⁸, Ca⁴³, Ca⁴⁴. These values were then ratioed appropriately (Sr:Ca and Ba:Ca). Water chemistry data was also converted in this manner so it could be compared to the elemental chemistry of the cubozoan statoliths. The elemental signatures were ratioed to calcium because the exact amount of CaSO₄ removed by the laser cannot be determined. The calcium signal was consistent among all spot samples. We used Partition coefficients (D_{Me}) to determine relationships between elemental ratios in water with that of the statoliths. Partition coefficients (D_{Me}) were calculated by dividing the elemental calcium ratio found in the statoliths by the elemental calcium ratio

measured in the experimental waters (Morse and Bender, 1990). Where values of D_{Me} increased in the statoliths while those for sea water remained unchanged we interpreted that as an organism induced retention of a metal (Campana, 1999).

For the *C. fleckeri* experiment, two-way orthogonal Analyses of Variance (ANOVA) were undertaken for both the statolith Sr:Ca and Ba:Ca ratios. The orthogonal analyses were performed to test for differences in the ratios among the temperature treatments (fixed) and the salinity treatments (fixed), and to determine if temperature and salinity interacted to affect the ratios. An SNK post-hoc test was undertaken in addition to the ANOVA's to determine specifically which treatments were significantly different. A one-way ANOVA was performed to test for differences in the Ba:Ca ratios before and after the experiment for both the experimental water treatments. A two-way ANOVA was not undertaken as it was not necessary to look at the differences in the Ba:Ca ratio between temperatures in the two experimental water types. Prior to all analyses the data were checked for heterogeneity of variance with a Levene's test and they were checked for normality to ensure they did meet the assumption of ANOVA that the data are normally distributed (Underwood, 1997). For *C. sivickisi*, a one-way ANOVA was undertaken for the Sr:Ca ratios to test for significant differences existed among the three sea surface temperatures identified across the collection period of the species. All statistical analyses were undertaken using SYSTAT 13 for windows.

RESULTS

Experimental Chemistry of Seawater

Sr:Ca levels within the experimental water were similar regardless of temperature and salinity treatments (Fig. AIII.1). The Sr:Ca ratio of the water was consistent throughout the experiment with values of $\sim 9 \mu\text{mol/mol}$ found both before and at the end of the experiment. This was true for all orthogonal combinations of temperature and salinity.

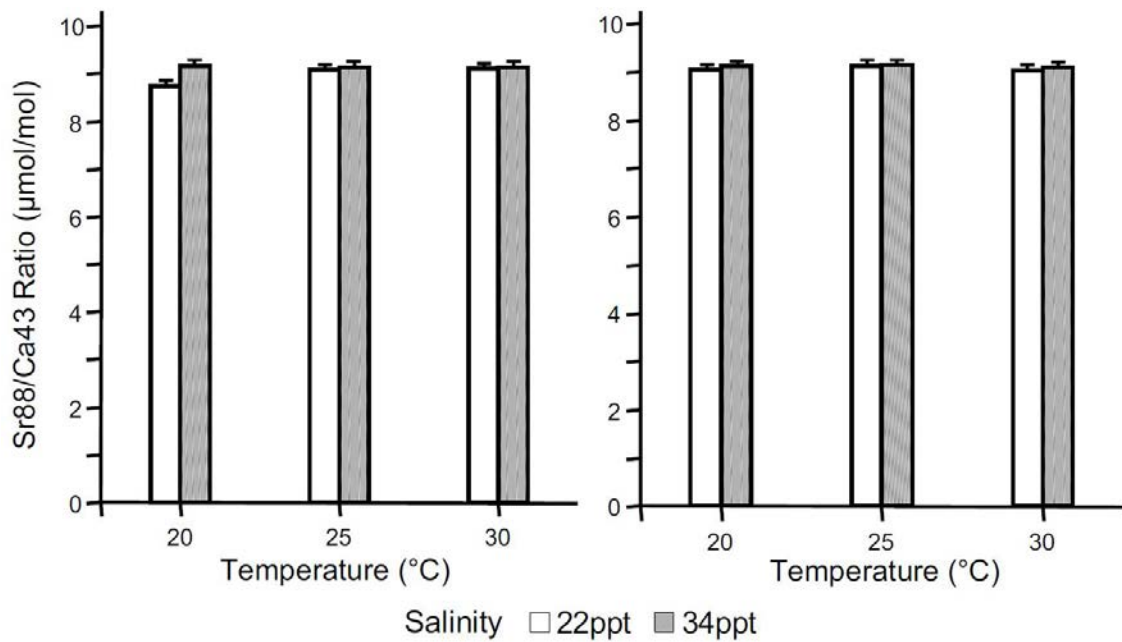


Fig. AIII.1: Mean elemental Sr:Ca ratio ($\mu\text{mol/mol}$), +1SE, in experimental water for three fixed temperatures and two salinity treatments, before experiment (a) and after experiment (b).

Ba:Ca levels within the experimental water differed between salinity treatments (Fig. AIII.2). Ba:Ca within the water for the 34ppt treatments was consistently about half of that in the 22ppt treatments. An overall decline in the Ba:Ca levels within the experimental waters was also observed for all three temperature treatments after the experiment was undertaken despite this decline not being significant ($F_{(2,6)}=0.75$, $p < 0.05$; $F_{(2,6)}=0.47$, $p < 0.05$) (Table AIII.1).

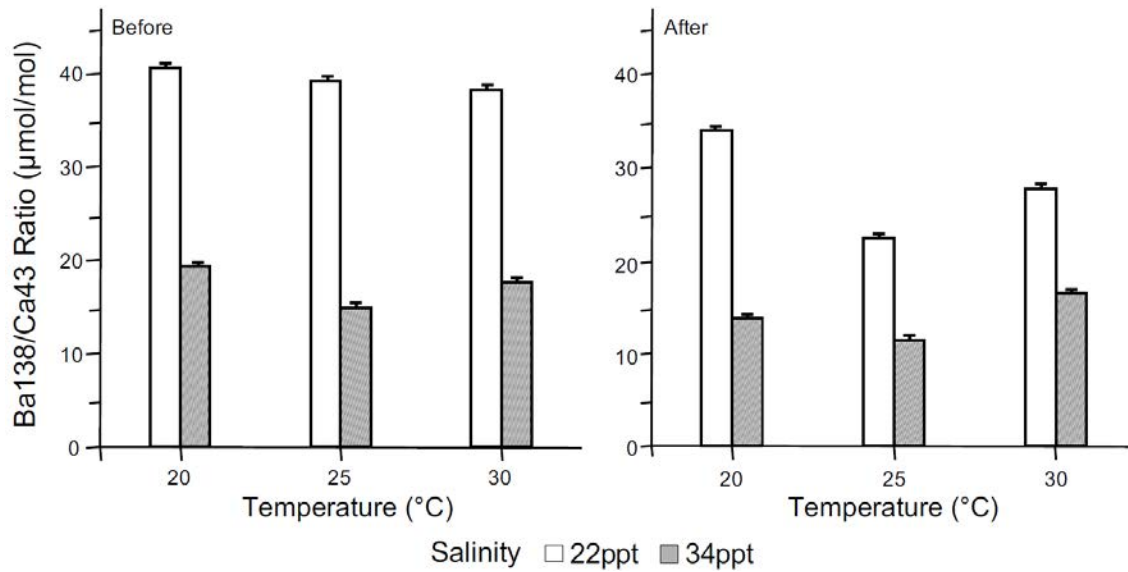


Fig. AIII.2: Mean element Ba:Ca ratio ($\mu\text{mol/mol}$), +1SE, in experimental water for three fixed temperatures and two salinity treatments, before experiment (a) and after experiment (b).

Influence of Temperature and Salinity on Elemental Isotopes within *Chironex fleckeri* Statoliths

There were significant increases in statolith Sr:Ca with temperature and this pattern was unaffected by salinity (Fig. AIII.3). This pattern resulted in a significant effect for temperature and there was no interaction between temperature and salinity (Table AIII.1). The Sr:Ca ratios ranged from 1.79 $\mu\text{mol/mol}$ at 20°C for the 22ppt salinity treatment to 3.33 $\mu\text{mol/mol}$ at 30°C for the 34ppt salinity treatment. The effect of salinity on mean Sr:Ca ratios at different temperatures was inconsistent in rank, but this pattern was weak as no interaction was detected. The within treatment error was low with standard errors ranging from 4.5-13% of the mean. The temperature related uptake of Sr into the bassinite statoliths contrasted with the Sr:Ca ratios in water as no differences were detected among temperature treatments for water.

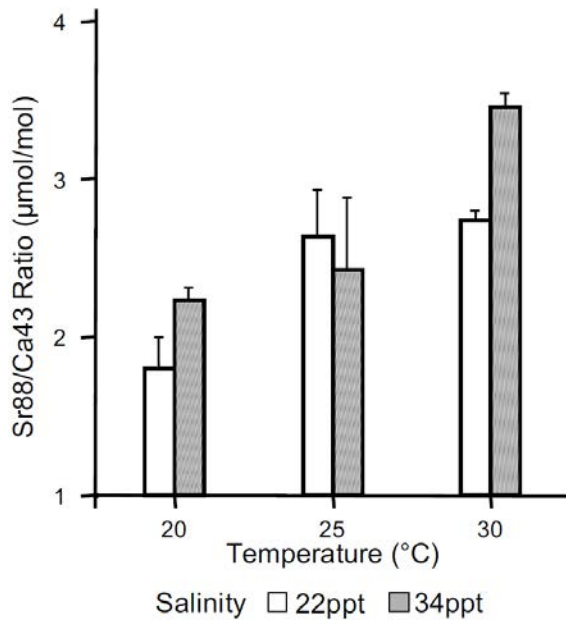


Fig. AIII.3: Mean Sr:Ca ratio ($\mu\text{mol/mol}$), +1SE, in *Chironex fleckeri* statoliths for three fixed temperatures and two salinity treatments.

Temperature and salinity affected the Ba:Ca ratio within the statoliths (Fig. AIII.4). Only main effects were significant and there was no interaction between temperature and salinity (Table AIII.1). Ba:Ca ratios were consistently lower by magnitudes of 2 (2°C), 2.5 (25°C), and 3.7 (30°C) in the water of highest salinity. The temperature effect was stepwise where 20°C and 25°C treatments were similar, while Ba:Ca at 30°C was clearly lower by magnitudes of 1.9 (22ppt) and 3.5 (34ppt) (SNK $20^{\circ}\text{C} = 25^{\circ}\text{C} \neq 30^{\circ}\text{C}$) in both salinity treatments. The within treatment error was low with standard errors ranging from 14-21% of the mean. The lowest values of statolith Ba:Ca were found in statoliths at 34ppt, similar to the results of water samples. In contrast, the temperature related uptake of Ba into the bassinite statoliths contrasted with the Ba:Ca ratios in waters as the water Ba:Ca was found to be lowest in the 25°C treatments.

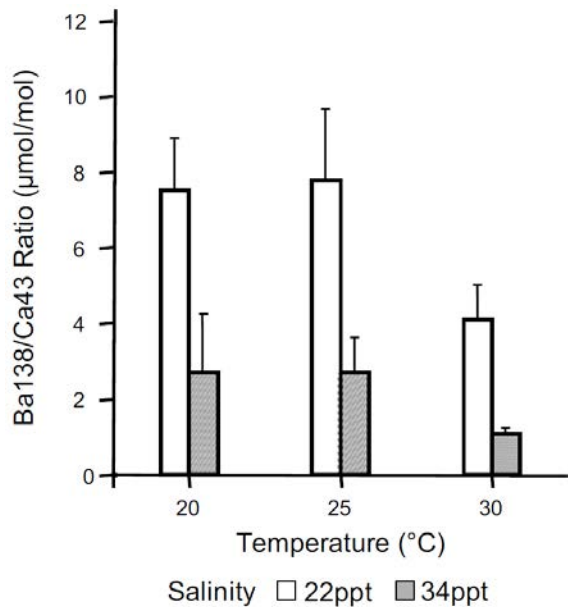


Fig. AIII.4: Mean Ba:Ca ratio ($\mu\text{mol/mol}$), +1SE, in *Chironex fleckeri* statoliths for three temperature and two salinity treatments.

Table AIII.1: Two-way ANOVA, *Chironex fleckeri* among temperature, among salinity and interaction between temperature and salinity, $n = 4$ jellyfish (ns = not significant, * denotes $p < 0.05$, ** denotes $p < 0.01$, *** denotes $p < 0.001$); Levene's, $F = 1.476$, $p = 0.246$, ns.

Source	df	Sr:Ca		Ba:Ca	
		MS	F	MS	F
Salinity	1	59.75	3.611	11090.3	25.603 ***
Temperature	2	234.34	14.16 ***	1782.20	4.114 **
Salinity x Temperature	2	45.22	2.734	249.98	0.577
Residual	18	16.54		433.16	

Partition Coefficients

The partition coefficients largely reflected the Me statolith: water relationships found in the statoliths. D_{Sr} increased with temperature for both salinities which follows the relationship in the statoliths (Fig. AIII.5). D_{Ba} , however, didn't follow the stepwise relationship observed in the statoliths and peaked at 25°C. Both D_{Sr} and D_{Ba} both did not vary between salinity treatments.

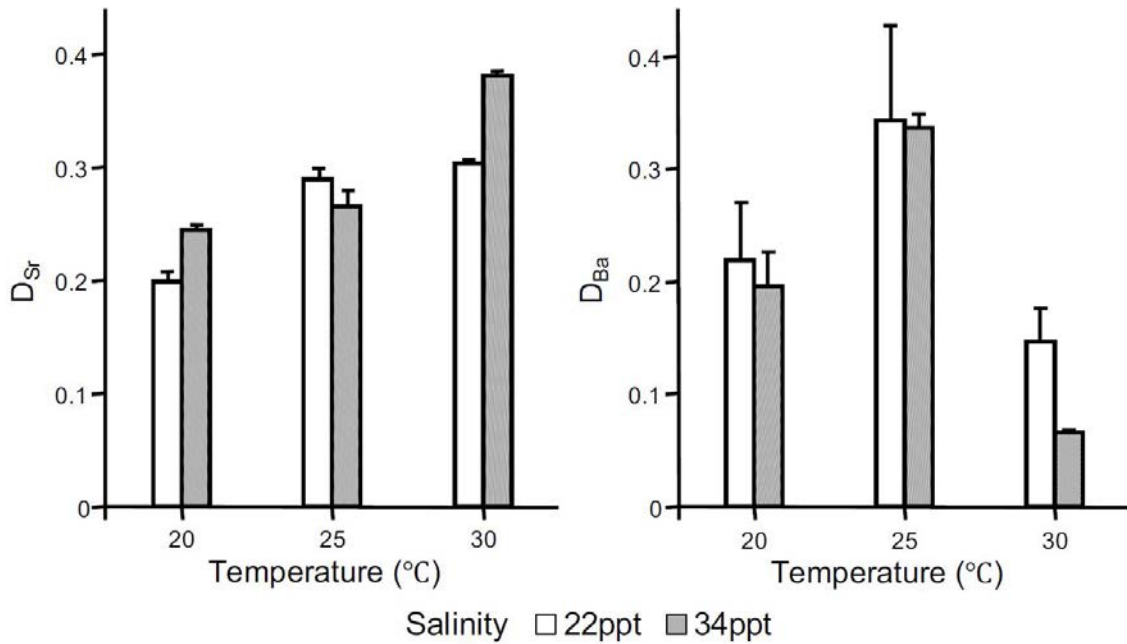


Fig. AIII.5: Mean element Ca⁻¹ ratios (μmol/mol), +1SE, for D_{Me} for three temperature and two salinity treatments.

Correlation between Temperature and the Elemental Fingerprints of *Copula sivickisi* Statoliths

There was a strong and significant relationship for Sr:Ca in the statoliths of *C. sivickisi* to increase (magnitude of 1.2 times each degree Celsius) with temperature (ANOVA, F_{2,10} df = 13.96, p = 0.01; Fig. AIII.6). This trend was apparent despite the relatively narrow 2°C difference (minimum temperature 26°C, maximum temperature 28.3°C) found at Magnetic island over the sampling period.

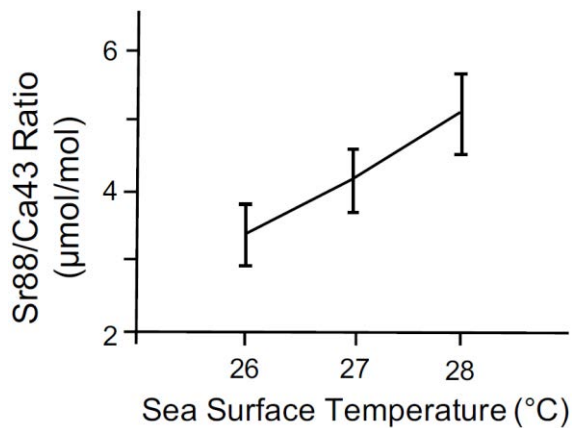


Fig. AIII.6: Mean Sr:Ca ratio ($\mu\text{mol/mol}$), +1SE, in *Copula sivickisi* statoliths for three sea surface temperatures ($^{\circ}\text{C}$), $n = 5$ for 26°C , $n = 5$ for 27°C , $n = 3$ for 28°C . $25.5^{\circ}\text{C} - 26.5^{\circ}\text{C}$ was pooled to 26°C , $26.5^{\circ}\text{C} - 27.5^{\circ}\text{C}$ was pooled to 27°C and $27.5^{\circ}\text{C} - 28.5^{\circ}\text{C}$ was pooled to 28°C .

DISCUSSION

The present study provides strong experimental evidence that Sr:Ca in the statoliths of cubozoans increases with temperature and that this is independent of variation in salinity. This result supports the correlative study of Mooney and Kingsford (2016), where they found a significant positive correlation between Sr:Ca and temperature in the statoliths of wild *C. fleckeri*. The lowest Sr:Ca ratios were found at approximately 26°C and the highest Sr:Ca ratios were found at approximately 31°C (Mooney and Kingsford, 2016). Additionally, strontium within the *C. sivickisi* statoliths analysed in the present study was more abundant in individuals which were collected from waters with higher sea surface temperatures. The relationship between Sr:Ca and temperature within cubozoan statoliths does not appear to be species dependent and therefore is likely to have broad applicability to the Cubozoa. Further, the relationship between statolith Sr:Ca and temperature may be similar in jellyfishes from other taxa with calcium sulphate statoliths. However, the statoliths of Scyphozoan jellyfishes grow differently to cubozoans as follows. Cubozoans have a single statolith in each rhopalium, while the statocysts of Scyphozoans contain tens to hundreds of small crystal-like statolith (Sötje et al., 2017). Accordingly, elucidating the temperatures experienced by medusae in scyphozoans examining their statolith elemental chemistry may be more complicated than in cubozoan jellyfishes.

Other cnidarian taxa have also shown strong relationships between Sr:Ca and temperature. Numerous studies examining the relationship between Sr:Ca and

temperature in the aragonite skeletons of corals have identified strong positive relationships (Alibert and McCulloch, 1997; Beck et al., 1992; de Villiers et al., 1994; McCulloch et al., 1994; Shen et al., 1996). A study by Shen et al. (1996), examined the use of Sr:Ca as a proxy for temperature variation and found a strong positive relationship between the two factors within *Porites* corals. Hence the relationship found in this study for cubozoans is similar to the relationship identified in another member of the Cnidaria despite the different elemental compositions of coral skeletons (calcium carbonate) and cubozoan statoliths (calcium sulphate). Studies have also utilised the relationship between Sr:Ca and temperature to determine the sea surface temperatures that corals have experienced over their lives (Beck et al., 1992). Similar analyses could be performed to reconstruct the temperatures experienced by *C. fleckeri* medusae throughout their lives. Notably, the relationship between Sr:Ca and temperature for phyla, other than the cnidaria, however, has been found to vary in magnitude and direction (positive or negative) (Bath et al., 2000; Gallahar and Kingsford, 1996; Secor et al., 1995). Further, it has been demonstrated for some taxa experimentally that Sr:Ca can co-vary with salinity and temperature (Arai et al., 1995; Fowler et al., 1995; Kalish, 1989; Limburg, 1996). Other factors can also affect Me:Ca relationships. For example, sex hormones in the blood of fish (Campana, 1999) and diet (Kalish, 1991; Sanchez-Jerez et al., 2002) can alter deposition patterns. Hence, laboratory experiments are the only way to definitively determine relationships between Sr:Ca and temperature in cubozoan statoliths. In the present study, the *C. fleckeri* medusae were fed the same diet throughout the experiment, so changes in diet could not have influenced our findings. Additionally, jellyfish absorb elements by simple diffusion. There is not the same complexity of a circulatory systems with multiple membranous filters to the semi-circular canals and endolymph that effect the uptake of elements into fish otoliths (Campana, 1999). At least for *C. fleckeri*, variation in temperature appears to be the primary factor in determining Sr:Ca ratios.

This study determined that salinity, referring to the underlying water chemistry associated with differing salinities, did not influence the Sr:Ca ratio in *C. fleckeri* statoliths. Salinities have been found to influence Sr:Ca in otolith elemental chemistry (McCulloch et al., 2005; Phillis et al., 2011; Tabouret et al., 2010), but the salinities were generally much lower than those *C. fleckeri* medusae can tolerate and survive. Sr:Ca ratios are generally influenced by salinities below 12ppt (McCulloch et al., 2005; Phillis et al., 2011; Tabouret et al., 2010). Mooney and Kingsford (2016) demonstrated experimentally that the Sr:Ca ratios within *C. fleckeri* statoliths were unaffected by

salinities within the range medusae could tolerate, in accordance with the results of the present study.

In contrast to the findings for Sr:Ca, both temperature and salinity influenced the Ba:Ca ratios within the statoliths of *C. fleckeri*. Ba:Ca decreased as temperature increased hence an inverse relationship, it should be noted however that this was largely due to a 'stepped' drop in Ba:Ca from 25-30°C. In the present study, statolith Ba:Ca was found to decrease with increasing salinity, independent of the temperature treatment. This is likely due to Ba:Ca being lower in the higher salinity experimental water which is typically observed in estuaries. Contrastingly, Mooney and Kingsford (2016) found a strong trend for D_{Ba} and Ba/Ca of statoliths to increase with salinity demonstrating a greater, albeit not significant, uptake at higher salinities in the statoliths, and, the temperature varied by less than 0.5°C between their salinity treatments so it is unlikely that the results of their experiment were confounded by temperature. The relationship found in the present study between Ba:Ca and salinity showed lower Ba in waters of higher salinity, contrasting the findings of Mooney and Kingsford (2016). The Ba:Ca ratios in the experimental waters for the 34ppt treatments were approximately half of the Ba:Ca ratios in the waters for 22ppt treatments. Freshwater was used to dilute seawater to create the 22ppt experimental water. The addition of this fresh water could have altered levels of Ba but there was no such suggestion for Sr:Ca. It is known that the mouths of estuaries contain high concentrations of Ba (Hanor and Chan, 1977). This occurs through ligands, which are transported via freshwater, breaking down and releasing free Ba ions as they come into contact with saltwater (Hanor and Chan, 1977). It is possible that the freshwater used to dilute the seawater for the creation of the 22ppt experimental water had clay in it, and hence ligands, which resulted in the release of free Ba ions within the experimental water.

There is potential for statolith Ba:Ca to be used to determine the movements of cubozoans. As Ba:Ca ratios varied with temperature and salinity, reconstructing the movements of medusae between water masses in nearshore waters would not be possible as the two factors would be confounded. However, the analysis of the statolith Ba:Ca ratio could potentially help to elucidate vertical movements. Well away from land and the influence of freshwater, Ba can vary greatly with depth (Walther et al., 2013). Ba distribution through the water column is influenced by biological processes causing it to be depleted in surface waters and higher in deep waters (Bruland and Lohan, 2006). Hence, the Ba:Ca ratio could complement reconstructions of vertical movements where both Sr:Ca and Ba:Ca would vary with temperature and depth.

In conclusion, we provided evidence that Sr:Ca ratios within cubozoan statoliths can be utilised as a proxy for temperature. A laboratory experiment on *C. fleckeri* demonstrated that Sr:Ca ratios varied with temperature and that this was independent of water salinity. Additionally, a correlation was found between temperature and Sr:Ca ratios in *C. sivickisi* statoliths. The Ba:Ca ratios in *C. fleckeri* statoliths were affected by variation in both temperature and salinity. Despite this, Ba:Ca profiles in statoliths also have the potential to help resolve jellyfish movements in some circumstances. The elemental chemistry of statoliths, therefore, provides a tool to further understand the complex ecology and movements of cubozoans. Potentially, the relationships between environmental variables and statolith elemental chemistry could be utilised to determine the ambient water temperatures experienced by individuals over the duration of their lives as they make excursions through water masses of different temperatures, be they horizontal or with depth. Future implications of these findings would allow for a better understanding of cubozoan population dynamics and population models.

REFERENCES

- Alibert, C., McCulloch, M.T., 1997. Strontium/calcium ratios in modern Porites corals from the Great Barrier Reef as a proxy for sea surface temperature: calibration of the thermometer and monitoring of ENSO. *Paleoceanography* 12, 345-363.
- Arai, N., Sakamoto, W., Maeda, K., 1995. Analysis of trace elements in otoliths of red sea bream *Pagrus major*. *Fisheries science* 61, 43-47.
- Arkhipkin, A.I., Campana, S.E., FitzGerald, J., Thorrold, S.R., 2004. Spatial and temporal variation in elemental signatures of statoliths from the Patagonian longfin squid (*Loligo gahi*). *Canadian Journal of Fisheries and Aquatic Sciences* 61, 1212-1224.
- Bath, G.E., Thorrold, S.R., Jones, C.M., Campana, S.E., McLaren, J.W., Lam, J.W., 2000. Strontium and barium uptake in aragonitic otoliths of marine fish. *Geochimica et cosmochimica acta* 64, 1705-1714.
- Beck, J.W., Edwards, R.L., Ito, E., Taylor, F.W., Recy, J., Rougerie, F., Joannot, P., Henin, C., 1992. Sea-surface temperature from coral skeletal strontium/calcium ratios. *Science* 257, 644-647.

- Bruland, K., Lohan, M., 2006. Controls of trace metals in seawater. *The oceans and marine geochemistry* 6, 23-47.
- Campana, S.E., 1999. Chemistry and composition of fish otoliths: pathways, mechanisms and applications. *Marine Ecology Progress Series* 188, 263-297.
- Campana, S.E., Thorrold, S.R., 2001. Otoliths, increments, and elements: keys to a comprehensive understanding of fish populations? *Canadian Journal of Fisheries and Aquatic Sciences* 58, 30-38.
- Chesney, E.J., McKee, B.M., Blanchard, T., Chan, L.-H., 1998. Chemistry of otoliths from juvenile menhaden *Brevoortia patronus*: evaluating strontium, strontium:calcium and strontium isotope ratios as environmental indicators. *Marine Ecology Progress Series* 171, 261-273.
- Coutant, C.C., Chen, C., 1993. Strontium microstructure in scales of freshwater and estuarine striped bass (*Morone saxatilis*) detected by laser ablation mass spectrometry. *Canadian Journal of Fisheries and Aquatic Sciences* 50, 1318-1323.
- de Villiers, S., Shen, G.T., Nelson, B.K., 1994. The SrCa-temperature relationship in coralline aragonite: Influence of variability in (SrCa) seawater and skeletal growth parameters. *Geochimica et Cosmochimica Acta* 58, 197-208.
- Dove, S.G., 1997. The incorporation of trace metals into the eye lenses and otoliths of fish. University of Sydney.
- Elsdon, T.S., Gillanders, B.M., 2002. Interactive effects of temperature and salinity on otolith chemistry: challenges for determining environmental histories of fish. *Canadian Journal of Fisheries and Aquatic Sciences* 59, 1796-1808.
- Elsdon, T.S., Gillanders, B.M., 2003. Reconstructing migratory patterns of fish based on environmental influences on otolith chemistry. *Reviews in Fish Biology and Fisheries* 13, 217-235.
- Farrell, J., Campana, S.E., 1996. Regulation of calcium and strontium deposition on the otoliths of juvenile tilapia, *Oreochromis niloticus*. *Comparative Biochemistry and Physiology Part A: Physiology* 115, 103-109.
- Fowler, A.J., Campana, S.E., Thorrold, S.R., Jones, C.M., 1995. Experimental assessment of the effect of temperature and salinity on elemental composition

- of otoliths using solution-based ICPMS. *Canadian Journal of Fisheries and Aquatic Sciences* 52, 1421-1430.
- Gallahar, N., Kingsford, M., 1996. Factors influencing Sr/Ca ratios in otoliths of *Girella elevata*: an experimental investigation. *Journal of Fish Biology* 48, 174-186.
- Garm, A., Coates, M., Gad, R., Seymour, J., Nilsson, D.-E., 2007. The lens eyes of the box jellyfish *Tripedalia cystophora* and *Chiropsalmus* sp. are slow and color-blind. *Journal of Comparative Physiology A* 193, 547-557.
- Gillanders, B.M., Able, K.W., Brown, J.A., Eggleston, D.B., Sheridan, P.F., 2003. Evidence of connectivity between juvenile and adult habitats for mobile marine fauna: an important component of nurseries. *Marine Ecology Progress Series* 247, 281-295.
- Halden, N.M., Babaluk, J.A., Campbell, J.L., Teesdale, W.J., 1995. Scanning proton microprobe analysis of strontium in an arctic charr, *Salvelinus alpinus*, otolith: implications for the interpretation of anadromy. *Environmental Biology of Fishes* 43, 333-339.
- Hanor, J.S., Chan, L.-H., 1977. Non-conservative behavior of barium during mixing of Mississippi River and Gulf of Mexico waters. *Earth and Planetary Science Letters* 37, 242-250.
- Hoff, G.R., Fuiman, L.A., 1995. Environmentally induced variation in elemental composition of red drum (*Sciaenops ocellatus*) otoliths. *Bulletin of Marine Science* 56, 578-591.
- Kalish, J., 1990. Use of otolith microchemistry to distinguish the progeny of sympatric anadromous and non-anadromous salmonids. *Fish. Bull. (Wash. DC)* 88, 657-666.
- Kalish, J.M., 1989. Otolith microchemistry: validation of the effects of physiology, age and environment on otolith composition. *Journal of Experimental Marine Biology and Ecology* 132, 151-178.
- Kalish, J.M., 1991. ^{13}C and ^{18}O isotopic disequilibria in fish otoliths: metabolic and kinetic effects. *Marine Ecology Progress Series* 75, 191-203.
- Kawakami, Y., Mochioka, N., Morishita, K., Tajima, T., Nakagawa, H., Toh, H., Nakazono, A., 1998. Factors influencing otolith strontium/calcium ratios in *Anguilla japonica* elvers. *Environmental Biology of Fishes* 52, 299-303.

- Kingsford, M.J., Mooney, C.J., 2014. The ecology of box jellyfishes (Cubozoa), Jellyfish blooms. Springer, pp. 267-302.
- Limburg, K.E., 1995. Otolith strontium traces environmental history of subyearling American shad *Alosa sapidissima*. Marine Ecology Progress Series, 25-35.
- Limburg, K.E., 1996. Growth and migration of 0-year American shad (*Alosa sapidissima*) in the Hudson River estuary: otolith microstructural analysis. Canadian Journal of Fisheries and Aquatic Sciences 53, 220-238.
- Llewellyn, L., Bainbridge, S., Page, G., O'Callaghan, M., Kingsford, M., 2016. StingerCam: A tool for ecologists and stakeholders to detect the presence of venomous tropical jellyfish. Limnology and Oceanography: Methods 14, 649-657.
- Mazloumi, N., Doubleday, Z., Gillanders, B., 2017. The effects of temperature and salinity on otolith chemistry of King George whiting. Fisheries Research 196, 66-74.
- McCulloch, M., Cappo, M., Aumend, J., Müller, W., 2005. Tracing the life history of individual barramundi using laser ablation MC-ICP-MS Sr-isotopic and Sr/Ba ratios in otoliths. Marine and Freshwater Research 56, 637-644.
- McCulloch, M.T., Gagan, M.K., Mortimer, G.E., Chivas, A.R., Isdale, P.J., 1994. A high-resolution Sr/Ca and $\delta^{18}\text{O}$ coral record from the Great Barrier Reef, Australia, and the 1982–1983 El Niño. Geochimica et Cosmochimica Acta 58, 2747-2754.
- Mooney, C., Kingsford, M., 2012. Sources and movements of *Chironex fleckeri* medusae using statolith elemental chemistry, Jellyfish Blooms IV. Springer, pp. 269-277.
- Mooney, C.J., Kingsford, M.J., 2016. The influence of salinity on box jellyfish (*Chironex fleckeri*, Cubozoa) statolith elemental chemistry. Marine biology 163, 103.
- Morse, J.W., Bender, M.L., 1990. Partition coefficients in calcite: Examination of factors influencing the validity of experimental results and their application to natural systems. Chemical Geology 82, 265-277.
- Mugiya, Y., Tanaka, S., 1995. Incorporation of water-borne strontium into otoliths and its turnover in the goldfish *Carassius auratus*: effects of strontium concentrations, temperature, and 17β -estradiol. Fisheries science 61, 29-35.

- Otake, T., Uchida, K., 1998. Application of otolith microchemistry for distinguishing between amphidromous and non-amphidromous stocked ayu, *Plecoglossus altivelis*. *Fisheries science* 64, 517-521.
- Phillis, C.C., Ostrach, D.J., Ingram, B.L., Weber, P.K., 2011. Evaluating otolith Sr/Ca as a tool for reconstructing estuarine habitat use. *Canadian Journal of Fisheries and Aquatic Sciences* 68, 360-373.
- Proctor, C., Thresher, R., Gunn, J., Mills, D., Harrowfield, I., Sie, S., 1995. Stock structure of the southern bluefin tuna *Thunnus maccoyii*: an investigation based on probe microanalysis of otolith composition. *Marine Biology* 122, 511-526.
- Radtke, R., 1990. Strontium: calcium concentration ratios in otoliths of herring larvae as indicators of environmental histories. *Environ. Biol. Fish.* 27, 51-61.
- Sanchez-Jerez, P., Gillanders, B., Kingsford, M., 2002. Spatial variability of trace elements in fish otoliths: comparison with dietary items and habitat constituents in seagrass meadows. *Journal of Fish Biology* 61, 801-821.
- Secor, D.H., Henderson-Arzapalo, A., Piccoli, P., 1995. Can otolith microchemistry chart patterns of migration and habitat utilization in anadromous fishes? *Journal of Experimental Marine Biology and Ecology* 192, 15-33.
- Shen, C.-C., Lee, T., Chen, C.-Y., Wang, C.-H., Dai, C.-F., Li, L.-A., 1996. The calibration of D [Sr/Ca] versus sea surface temperature relationship for *Porites* corals. *Geochimica et Cosmochimica Acta* 60, 3849-3858.
- Sinclair, M., Iles, T., 1989. Population regulation and speciation in the oceans. *ICES Journal of Marine Science* 45, 165-175.
- Sötje, I., Dishon, T., Hoffmann, F., Holst, S., 2017. New methods of morphometric analyses on scyphozoan jellyfish statoliths including the first direct evidence for statolith growth using calcein as a fluorescent marker. *Microscopy and Microanalysis* 23, 553-568.
- Tabouret, H., Bareille, G., Claverie, F., Pécheyran, C., Prouzet, P., Donard, O., 2010. Simultaneous use of strontium: calcium and barium: calcium ratios in otoliths as markers of habitat: Application to the European eel (*Anguilla anguilla*) in the Adour basin, South West France. *Marine Environmental Research* 70, 35-45.

- Thorrold, S.R., Jones, C.M., Campana, S.E., McLaren, J.W., Lam, J.W., 1998. Trace element signatures in otoliths record natal river of juvenile American shad (*Alosa sapidissima*). *Limnology and Oceanography* 43, 1826-1835.
- Thorrold, S.R., Jones, G.P., Hellberg, M.E., Burton, R.S., Swearer, S.E., Neigel, J.E., Morgan, S.G., Warner, R.R., 2002. Quantifying larval retention and connectivity in marine populations with artificial and natural markers. *Bulletin of Marine Science* 70, 291-308.
- Thresher, R., 1994. An evaluation of electron-probe microanalysis of otoliths for stock delineation and identification of nursery areas in a southern temperature groundfish, *Nemadactylus macropterus* (Cheilodactylidae). *Fish. Bull.* 92, 817-840.
- Townsend, D., Radtke, R.L., Malone, D.P., Wallinga, J.P., 1995. Use of otolith strontium: calcium ratios for hindcasting larval cod *Gadus morhua* distributions relative to water masses on Georges Bank. *Marine Ecology-Progress Series* 119, 37.
- Tzeng, W.-N., 1996. Effects of salinity and ontogenetic movements on strontium: calcium ratios in the otoliths of the Japanese eel, *Anguilla japonica* Temminck and Schlegel. *Journal of Experimental Marine Biology and Ecology* 199, 111-122.
- Underwood, A.J., 1997. *Experiments in ecology: their logical design and interpretation using analysis of variance*. Cambridge University Press.
- Walther, B.D., Kingsford, M.J., McCulloch, M.T., 2013. Environmental records from Great Barrier Reef corals: Inshore versus offshore drivers. *PloS one* 8, e77091.
- Weber, J.N., 1973. Incorporation of strontium into reef coral skeletal carbonate. *Geochimica et Cosmochimica Acta* 37, 2173-2190.
- Woodhead, J.D., Hellstrom, J., Hergt, J.M., Greig, A., Maas, R., 2007. Isotopic and elemental imaging of geological materials by laser ablation inductively coupled plasma-mass spectrometry. *Geostandards and Geoanalytical Research* 31, 331-343.
- Yamashita, Y., Otake, T., Yamada, H., 2000. Relative contributions from exposed inshore and estuarine nursery grounds to the recruitment of stone flounder,

Platichthys bicoloratus, estimated using otolith Sr: Ca ratios. Fisheries
Oceanography 9, 316-327.